INERTIAL CONFINEMENT FUSION

Lawrence Livermore National Laboratory

UCRL-LR-105820-00/01

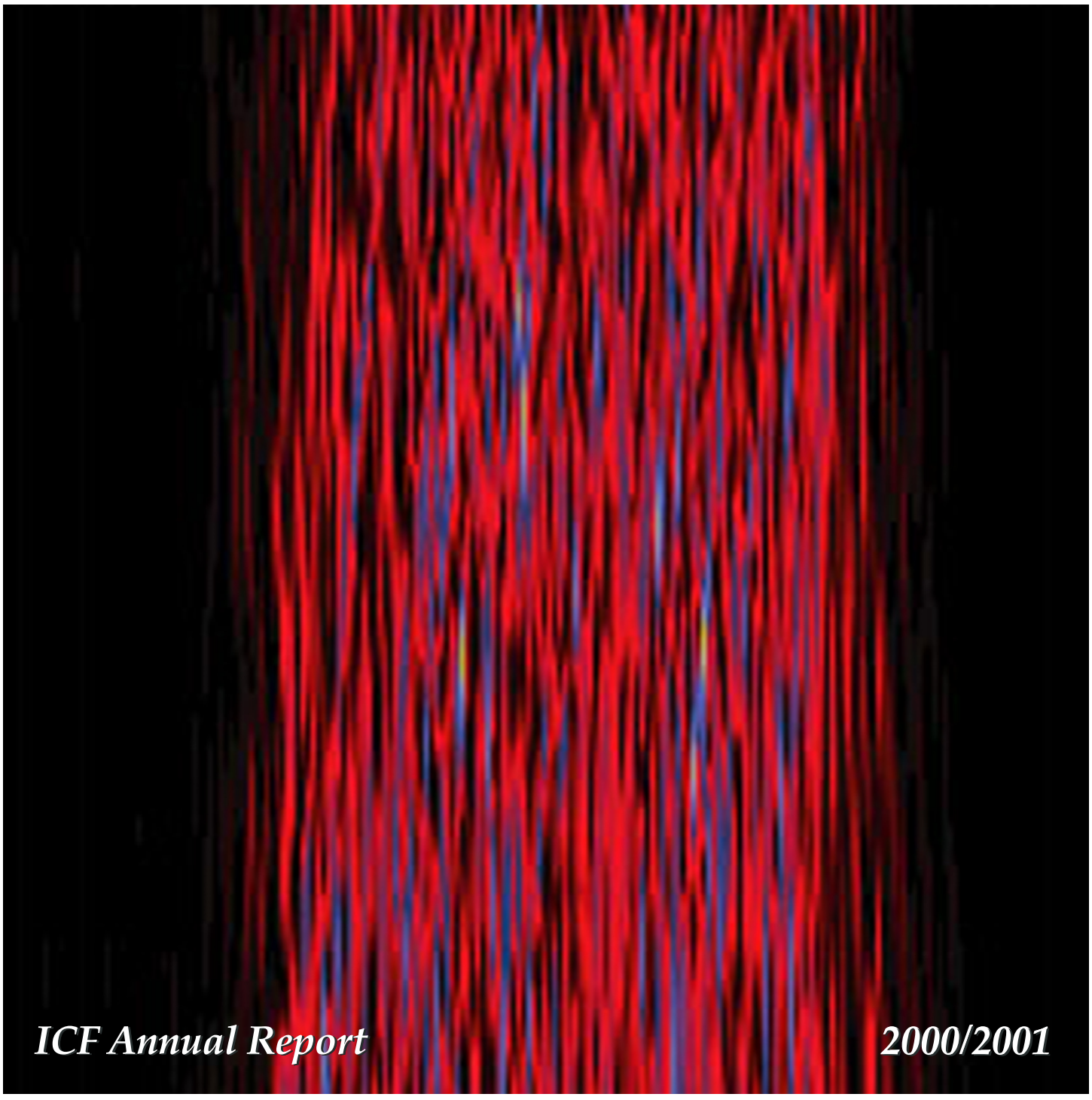

ICF Annual Report *2000/2001*

The Cover:

The figure shows the result of calculations using the pF3D code of a beam propagating through a 1-mm-long underdense plasma. The simulated beam is a full-size Nova $f/8$ beam with a kinoform phase plate (KPP). The plasma ramps from 2 to 20% of the critical density for 3ω light from bottom to top. The beam also propagates from bottom to top. The image is a slice through the center of the beam. The color contours represent the beam intensity, with red being the most intense. The beam modulation is representative of the propagation of a KPP beam through plasma (see p. 13).

On the Web:

http://www.llnl.gov/nif/icf/icf.html

This document was prepared as an account of work sponsored by an agency of the United States Government. Neither the United States Government nor the University of California nor any of their employees makes any warranty, express or implied, or assumes any legal liability or responsibility for the accuracy, completeness, or usefulness of any information, apparatus, product, or process disclosed, or represents that its use would not infringe privately owned rights. Reference herein to any specific commercial product, process, or service by trade name, trademark, manufacturer, or otherwise, does not necessarily constitute or imply its endorsement, recommendation, or favoring by the United States Government or the University of California. The views and opinions of authors expressed herein do not necessarily state or reflect those of the United States Government or the University of California and shall not be used for advertising or product endorsement purposes.

UCRL-LR-105820-00/01
October 1999–September 2000 and
October 2000–September 2001

Printed in the United States of America
Available from
National Technical Information Service
U.S. Department of Commerce
5285 Port Royal Road
Springfield, Virginia 22161
Price codes: printed copy A03, microfiche A01.

This work was performed under the auspices of the U.S. Department of Energy by University of California Lawrence Livermore National Laboratory under Contract No. W–7405–Eng–48.

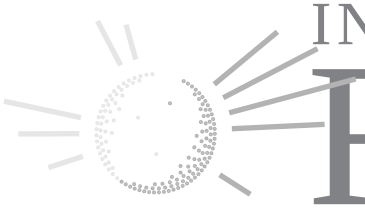

INERTIAL CONFINEMENT

FUSION

2000/2001 ICF Annual Report

MS Date
July 2003

Lawrence Livermore
National Laboratory

UCRL-LR-105820-00/01

FOREWORD

The 2000–2001 *ICF Annual Report* provides documentation of the achievements of the Lawrence Livermore National Laboratory (LLNL) Inertial Confinement Fusion (ICF) Program by a summary of activity that is a narrative of important results for the fiscal years 2000 and 2001. This *Annual Report* is also on the Web at http://www.llnl.gov/nif/icf/icf.html.

The underlying theme for LLNL's ICF Program research continues to be defined within DOE's Defense Programs Stockpile Stewardship missions and goals. In support of these missions and goals, the ICF Program advances scientific and technology development in major interrelated areas related to ignition, including target theory and design, target experiments, target fabrication, and cryogenic systems. The ICF Program also provides experimental support for studies in high-energy-density physics in support of stockpile stewardship.

While in pursuit of its goal of demonstrating thermonuclear fusion ignition and energy gain in the laboratory, the ICF Program also partially supports the necessary research base for the possible long-term application of inertial fusion energy for civilian power production. ICF technologies continue to have spin-off applications for additional government and industrial use.

The LLNL ICF Program is only one, though the largest, part of the National ICF Program. The program is also executed at Los Alamos National Laboratory, Sandia National Laboratories, the University of Rochester, and the Naval Research Laboratory. General Atomics, Inc., develops and provides many of the targets for the above experimental facilities.

Questions and comments relating to the technical content of the journal should be addressed to the ICF Program Office, Lawrence Livermore National Laboratory, P.O. Box 808, Livermore, CA 94551.

Bruce Hammel
ICF Program Leader

Al Miguel
Publication Editor

ACKNOWLEDGMENTS

We thank the many authors and their coauthors who contributed to this *Annual Report*. We are grateful for their willingness to take time from busy schedules to write the articles that describe their work. We thank Roy Johnson for his careful classification reviews. We also thank the administrative staff for typing manuscripts, arranging meetings, and offering other invaluable assistance.

We thank Innovative Business and Information Services (IBIS) editor Al Miguel for editing and managing the production cycle; designer Stacy Bookless for coordinating art work, laying out this document, and designing the cover; and artists Clayton Dahlen, Cyndi Brandt, Damien Jemison, Leonard Walton, Nancy Rutter, and Lori Dempsey for providing expertise in graphic design.

We appreciate the support of Michael Gallardo, the Government Printing Office coordinator, who worked with the Government Printing Office to obtain high-quality printing; Mary Nijhuis of IBIS's Publications Services for coordinating the review of this report; Amanda Fisher of Document Services for managing its distribution; and the talents and dedication of the ICF Program staff in producing this *Annual Report*.

Bruce Hammel
ICF Program Leader

UCRL-LR-105820-00/01

CONTENTS

INTRODUCTION

For 2000 and 2001, the ICF Program consisted of two major components, the Ignition Program and the High Energy Density Physics (HEDP) Program. The goal of the Ignition Program is to demonstrate fusion ignition in the laboratory by inertial confinement. The HEDP Program performs experiments on the various laser and pulsed-power facilities in support of the National Nuclear Security Administration's (NNSA's) Stockpile Stewardship Program.

After the closure of the Nova laser at Lawrence Livermore National Laboratory (LLNL) in 1999, the experimental program transitioned its focus to the OMEGA laser at the University of Rochester's Laboratory for Laser Energetics (LLE). The combined Program elements performed around 300 shots per year at this facility. In addition, support experiments were done at the Janus laser at LLNL, the Trident laser at Los Alamos National Laboratory (LANL), the HELEN laser at the Atomic Weapons Establishment (AWE) in the United Kingdom, and the Vulcan laser at the Rutherford-Appleton Laboratory in the United Kingdom. The modeling and theory element of the programs also improved its capabilities with the addition of the ASCI White machine at LLNL's Advanced Simulations and Computing (ASCI) Program, allowing larger and faster simulations of problems than previously attainable.

In addition, the ICF Program continued its record of excellence as highlighted by the numerous awards, patents, and publications detailed in Appendices A and B. Employees associated with the ICF Program received over 150 patents and coauthored over 250 publications. Several members of the Program received prestigious awards, including Mordicai Rosen who received a Teller Fellowship and John Lindl who received the Fusion Power Associated Leadership Award.

Accomplishments in 2000 and 2001 for the Ignition Program are summarized in Section 1. The Ignition Program has four major elements corresponding to the four divisions of the indirect-drive ignition plan of the NNSA's National Ignition Program (NIF). The four elements are hohlraum energetics and laser–plasma interactions, drive symmetry, shock timing and capsule optimization, and ignition experiments. Ignition experiments have three components consisting of ignition target design, ignition diagnostic development, and ignition target development. Together these make up the seven chapters in Section 1.

The hohlraum energetics and laser–plasma interactions element of the Ignition Program develops the understanding of laser–plasma interactions and coupling of laser light to x-rays to optimize the efficiency of NIF hohlraums for ignition target designs. In 2000 and 2001, this element continued experiments and theory of laser–plasma instabilities in large-scale, underdense plasmas. Experiments showed that stimu-

lated Raman scattering and stimulated Brillouin scattering are both in the highly saturated regime. Modeling using the pF3D code developed at LLNL predicted the data trends using postulated nonlinear saturation models. Research continues on developing a better physical understanding of these nonlinear saturation processes. The modeling effort was significantly enhanced with the ASCI White machine, allowing propagation calculations of the entire NIF beam in the underdense plasma for the first time. Experiments were performed in hohlraums investigating the effect of material mixtures that may be more efficient than the standard Au hohlraums presently used. Improvements in target modeling also continued with the inclusion of magnetic fields in LASNEX simulations. LASNEX modeling including magnetic fields improved agreement with measurements of the underdense plasma electron temperature by reducing heat transport to the underdense plasma outside of the laser irradiation volume. Modeling efforts began investigating options for ignition targets using 2ω light at NIF. NIF can potentially produce significantly more energy with 2ω light than with 3ω light. Modeling indicates that a significantly larger target design parameter space would be available if laser backscatter and hot electron production can be controlled. Experiments began in 2001 using the HELEN laser at AWE to study laser coupling with 2ω light.

The symmetry element of the Ignition Program develops the understanding to accurately control and measure the x-ray flux asymmetries on the capsule in a hohlraum. In 2000 and 2001, experiments at OMEGA and modeling efforts investigated various techniques for measuring flux symmetry on capsules for tuning NIF symmetry. Techniques were demonstrated for use at various times during the implosion, and requirements were refined for NIF symmetry diagnostics. Implosion experiments were also done during this period on OMEGA. Having more beams than Nova, OMEGA can obtain better symmetry than Nova and more closely approximate the NIF geometry. The OMEGA implosion experiments demonstrated improved implosion performance in higher convergence than obtained in Nova experiments. Results from implosion experiments without argon in the capsule obtained better agreement with modeling than previous experiments with argon doping in the fuel.

The shock timing and capsule optimization element of the Ignition Program optimizes the match of available drive pulses and ablator designs to obtain proper shock coalescence with adequate implosion stability and efficiency. A series of sensitivity calculations were done to determine the robustness of the ignition designs. The timing sensitivity of the fourth shock in the ignition pulse was completed during this period, after a timing sensitivity study of the first three shocks in 1999 was done. Sensitivity studies also investigated the robustness of the various designs to equation of state and opacity models and assumed drive spectra. Experiments at OMEGA addressed a number of ablator issues. Indirect-drive halfraums were used to measure the x-ray burnthrough in beryllium and polyimide ablators and shock timing in beryllium ablators. Rayleigh–Taylor instability growth and the effects of preheat were studied in polyimide ablators. OMEGA experiments were also done to develop techniques for optimizing ablators on NIF. The accuracy obtainable using backlit implosions for measuring burnthrough rates was evaluated and determined to be promising. Activation of the VISAR diagnostic was begun at OMEGA to measure shock timing.

Ignition target design efforts were directed toward better understanding of the performance of the suite of existing ignition target designs. A comprehensive evaluation of capsule sensitivity to Rayleigh–Taylor instability demonstrated that it is a strong function of absorbed energy, drive temperature, and ablator material. Preignition cryogenic implosion designs were investigated using 96 beams in a symmetric NIF geometry to perform preignition experiments to optimize ignition designs before NIF completion. Work on hohlraum coupling efficiency suggested that energy available for imploding capsules with indirect drive could be substantially larger. Beryllium capsule designs driven at 250 eV with absorbed energy up

to 600 kJ were begun. Design work was done on polystyrene capsules absorbing more energy than the point design, showing that increased absorbed energy can improve its robustness. Also, a number of issues concerning design details were evaluated computationally. These included sensitivity to the central gas density, fill holes in beryllium capsules, and low-mode out of roundness. 3D simulations using HYDRA continued to investigate symmetry requirements. Finally, calculated neutron spectra were evaluated to identify potential ignition diagnostics. Measurement of down-scattered neutrons was shown to be a promising method for measuring the total ρr at ignition.

Techniques for ignition diagnostics are based on neutron, charged particle, and x-ray emission from the fuel and post-shot analysis of target debris. In 2000 and 2001, calculations were done of the neutron background at OMEGA and that expected at NIF for evaluation of neutron diagnostic measurements. Techniques for measuring down-scattered neutrons were evaluated. These included use of the Medusa time-of-flight spectrometer at OMEGA, development of chemical vapor deposition diamond detectors, and gated scintillator-fiber detectors. A gas sampling system was developed and is being installed at OMEGA to test its use on radiochemistry diagnosis of implosions. A technique for taking multispectral x-ray images of imploded capsules was demonstrated on OMEGA. Bubble detector options were evaluated for neutron imaging detectors. In collaboration with LANL, development of a gamma ray diagnostic continued for testing at OMEGA to measure the fusion reaction time history.

Ignition target development in 2000 and 2001 focused on developing fuel capsules corresponding to present designs and on developing methods to form, characterize, and control the cryogenic fuel layers. All capsule fabrication techniques, except machined beryllium, rely upon coating a spherical plastic mandrel with the ablator material. During this reporting period, fabrication of mandrel shells at sizes required for NIF was demonstrated with sphericity and surface finish at, or better, than NIF specifications. Previously, it was demonstrated that polyimide capsules of the design thickness could be fabricated, but the surface quality was poor. During this period, it was shown that the surface finish could be improved significantly, although not yet to NIF requirements, by suspending the capsule in an atmosphere containing vapor solvent. Also, several important properties such as burst strength, hydrogen permeability, density, and optical transmission properties of polyimide shells were measured. Progress also continued on developing beryllium capsules having various additives, using the process of physical vapor deposition on mandrels. Most ignition target designs have a cryogenic fuel layer coating the inside of the capsule. Cooling the DT fuel below the freezing point of the gas phase forms cryogenic fuel layers. Internal heat causes the layer to become symmetric in a process called “beta layering.” During this period, a number of experiments were done to understand the beta layering process at various cooling rates and end-point temperatures, as well as the stability of these layers after formation. Also, experiments for studying methods for enhancing the process using infrared light were begun. Research began to understand how to implement beta layering and enhanced beta layering using infrared light in hohlraum targets. Finally, a new cryogenic system was delivered, and activation to test filling and layering of indirect-drive targets was begun.

Accomplishments in 2000 and 2001 for the HEDP Program are summarized in Section 2. These accomplishments represent only the unclassified portion of the HEDP Program. The principal activities were directed toward developing techniques and capabilities for OMEGA and NIF experiments. Techniques were investigated for studying hydrodynamics in spherical implosions on OMEGA. The effects of mix at the pusher fuel interface were studied in experiments designed to be sensitive to this effect. Also, x-ray backlighting was used to study mix at this interface with specially designed targets. A number of experiments were done related to studying energy dynamics in indirect targets. These included studying radiation transport in underdense materials by

imaging both self-emission and backlighting. Experiments were done using a variety of radiation transport geometries to understand their effects. Dependence of hohlraum performance on wall conditions was also investigated. Capabilities for NIF hydrodynamics experiments require improvements in resolution and fidelity. Several pinhole geometries were tested to improve resolution and signal to noise. Performance of gated imaging detectors was improved by changing the recording medium from film to charge-coupled device arrays. Removing the small-scale noise by characterization and flat fielding the data also enhanced the image quality. Other imaging techniques such as dual color radiography and fluorescence anisotropy for measuring micron-scale features were also investigated. The physics of materials at high density can be extremely complex and their properties difficult to diagnose. During this period, experiments demonstrated a technique to use x-ray Thomson scattering to measure electron temperature in dense, bulk-heated beryllium.

In summary, progress has been made in a number of areas in the Ignition and HEDP Programs. This progress has led to improved understanding, taking us closer to the goals of ignition and more general understanding of high-energy-density physics. Also, important techniques continue to be developed for the better use of NIF when it becomes operational. This report summarizes this work for the years 2000 and 2001.

SECTION 1

IGNITION TARGET PHYSICS EXPERIMENTS THEORY AND MODELING

HOHLRAUM ENERGETICS AND LASER–PLASMA INTERACTIONS

S. H. Glenzer

The production of soft x-rays and x-ray–driven capsule implosions on the National Ignition Facility (NIF) depends on the efficient coupling of laser light to the target. The use of large gas-filled hohlraums (~1 cm) and long laser pulse lengths (~20 ns) results in the production of large-scale underdense plasmas through which the laser beams will propagate on their way to the hohlraum wall, where the laser beams are converted into soft x-rays.

In fiscal years 2000 (FY00) and 2001 (FY01), we have developed theoretical modeling of the laser beam propagation through underdense plasmas and have verified calculations of laser beam absorption and intensity profile modification with experiments. On the other hand, the stimulated scattering processes in these plasmas like stimulated Brillouin scattering (SBS) and stimulated Raman scattering (SRS) are not as well understood. These instabilities drive ion-acoustic and electron plasma waves to large amplitudes through the laser beam itself and scatter the laser light back, reducing the laser power available for the production of soft x-rays. Experiments and modeling in this period have shown that the amplitudes of these waves are saturated. Moreover, progress on understanding the nonlinear saturation mechanisms has been made indicating that a predictive design capability may be possible to find the optimum laser-target coupling regime on NIF. An additional method to improve the total soft x-ray production on NIF might be the use of hohlraum walls made of high-Z mixtures. Experiments have begun in this period comparing the soft x-ray production of various mixtures with standard gold hohlraums.

Hohlraum Energetics

Significant experimental and theoretical progress in FY00 and FY01 has indicated that a predictive capability of the laser–plasma interaction (LPI) target physics may be in our reach for designing the performance of NIF experiments. Efficient conversion of laser light to soft x-rays, hard x-rays, or shocks is important for all NIF users (in particular, for the indirect-drive ignition targets or high-gain implosions). The conversion efficiency can be reduced by instabilities such as SBS and SRS that scatter the incident laser light before it can couple into the target. Furthermore, SRS can produce hot electrons that can preheat the ignition capsule. Control of LPI using laser beam-smoothing techniques, such as smoothing by spectral dispersion (SSD), has been demonstrated in Nova experiments,[1, 2] but the extrapolation to predict NIF target performance requires understanding of the nonlinear saturation[3, 4] of the instabilities expected on NIF.

In FY00, our capability to calculate laser beam propagation in underdense plasmas has improved to a level where the interaction of whole NIF-like laser beams with mm-scale plasmas can be simulated.

Various experiments in this period studying the laser beam self-smoothing,[5] filamentation,[6] and collisional absorption[7] have increased our confidence in calculating laser beam intensity profiles deep into long–scale-length plasmas. However, the comparison of the calculated ion wave amplitude and the associated SBS losses with Nova gasbag experiments have clearly demonstrated the need for including nonlinear saturation models that limit the wave amplitude in the simulations.[8]

In FY01, a first successful attempt to develop a first-principle understanding of the saturation mechanisms with Thomson scattering experiments[9] on the Trident laser facility at Los Alamos National Laboratory (LANL) has revealed that ion trapping plays an important role in low-Z plasmas, such as those produced in the gas plasma inside an ignition hohlraum.[10] This important finding has led to extensive analytic modeling and supporting particle in cell (PIC) simulations with BZOHAR, which indicate that ion-acoustic frequency shifts generated by ion trapping may quantitatively account for the saturation of the ion waves in SBS[11] and crossed-beam energy transfer experiments.[12] This model has resulted in the first successful quantitative calculation of SBS backscattering losses.

The nonlinear ion wave response is also important in the studies of crossing laser beam effects on the University of Rochester's Laboratory for Laser Energetics OMEGA laser. The experiments show significant energy transfer in plasmas with Mach-1 flow and are designed to help in developing a mitigation strategy for this process on NIF. For electron plasma waves that are participating in the SRS backscattering process, progress has been made studying the decay of the primary electron plasma wave into a secondary plasma wave and an ion-acoustic wave.[13] The existence of this so-called Langmuir decay instability (LDI) in high-temperature plasmas has been observed in FY00 as a potential saturation mechanism for SRS.

To further test our LPI modeling capability and to obtain quantitative measurements of these nonlinear saturation processes for SBS and SRS, we are presently developing a Thomson scattering capability at the OMEGA laser facility. Initially, the Thomson scattering probe beam will operate at 527 nm (2ω) and may also be employed to assess the interaction of 2ω laser beams with large–scale-length plasmas. These studies have been motivated by detailed design calculations in this period that have indicated that it may be possible to couple 1 MJ of energy to a fusion capsule for high-gain ignition on NIF. These predictions take advantage of the higher laser damage threshold for 2ω laser light resulting in an increased laser output relative to NIF's 3ω performance as well as of advanced hohlraum wall materials (i.e., "cocktails"). The latter are under investigation at the OMEGA laser. Experiments have shown enhanced soft x-ray reemission at energies around 450 eV when compared to pure gold hohlraums consistent with LASNEX predictions indicating that improved hohlraum performance may be possible.

Developing a Basis for Optimizing Laser Beam Smoothing for NIF

Experiments to study laser self-smoothing and beam propagation in large-scale plasmas were conducted at the Vulcan laser facility at the Rutherford Appleton Laboratory, UK. An incident laser with a wavelength of 527 nm was passed through a mask creating an intensity pattern in the near field. The beam was then focused with an $f/10$ optic and propagated transversely to the density gradient of a preformed exploding foil plasma. The transmitted light was collected with a second $f/10$ optic. The measured transmitted near-field intensity was then compared to the incident near-field intensity, allowing a detailed test of our beam profile modeling capability using the code pF3D.

A series of shots were performed to investigate the effects of varying probe energy, plasma length (0.5–3 mm), and probe smoothing (random phase plate [RPP] and no RPP) on the plasma-induced self-smoothing. The plasma density was inferred from the SRS spectra—ranging from 4% to 8% of the 2ω critical density, n_{cr}. The electron temperature was measured with Thomson scattering to be T_e = 500 eV.

These measurements provide critical input into the pF3D simulations, which include the mask, the RPP (if present), and the beam phase in the near field.

The simulations reproduced many of the features and trends observed in the experiment. First, with low probe energy (2.5 J incident), neither the simulations nor the experiment shows significant self-smoothing effects. On the other hand, at high probe intensities (10^{15} W cm^{-2}), most of the incident light undergoes scattering in the focal region. For example, we observe that for the non-RPP case, the average intensity within the masked regions is approximately equal to the unmasked in both simulation and experiment. However, the edges of the mask remain distinct. We understand this in that the high spatial frequencies represented by these edges correspond to the fringes of the focal spot, where the intensity is too low for the speckle self-focusing and forward Brillouin scatter mechanisms responsible for plasma-induced self-smoothing to take effect. As can be seen qualitatively in Figure 1, these features are well reproduced by the pF3D modeling. A quantitative comparison that uses the Fourier analysis of the transmitted light has demonstrated the need for refined heat transport models that affect laser beam filamentation and self-smoothing. These models are presently being developed in collaboration with scientists at the University of Alberta, Canada, and will be tested against these data.

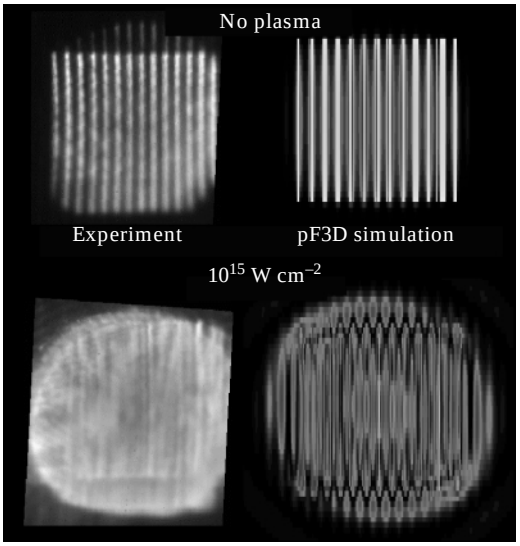

FIGURE 1. Experimental and simulated transmitted near-field images for the no-plasma case and for a high-intensity laser shot through a 1-mm-long CH plasma. In the simulation, half of the energy is scattered outside the originally unmasked area into the masked areas (and outside the *f*/10 cone where it was unmeasured). Nevertheless, the edges of the mask remain very distinct. (NIF-0602-05262pb01)

In another series of experiments performed at the Helen Laser Facility, UK, we have explored the interaction of a single high-energy 2ω laser beam with underdense gas targets. These experiments with gasbags and small, gas-filled gold containers were intended to develop an ability to control laser scattering losses by SBS and SRS, as well as the hot-electron production with 2ω laser beams. The Au containers filled with C_5H_{12} showed that by going to fairly extreme conditions, $n_e \sim n_{cr}/4$ and $I = 6 \times 10^{15}$ W cm^{-2}, it is possible to convert up to 20% of the laser energy to hot electrons. However, by decreasing the intensity and/or density, this conversion fraction can readily be reduced to below 10%. Gasbags filled with C_5H_{12} produced hot electrons with a similar efficiency as the containers, up to the highest density explored (~0.15 n_{cr}). A very exciting result came from gasbags filled with CO_2 and C_5H_{12}. Changing to CO_2 from C_5H_{12} caused both the Raman backscattering and the hot electron fraction to drop precipitously, presumably because of the decrease in ion Landau damping.

This finding is consistent with the Nova gasbag experiments that have shown saturated SBS losses and saturated ion-acoustic wave amplitudes but negligible SRS with a CO_2 fill. Under these conditions, the LDI may prevent the growth of SRS. The Nova experiments[4] supporting this physical picture are discussed below. The single-beam Helen experiments described in this section clearly indicate that it may be possible to control hot electron production at 2ω by judicious choice of materials, in addition to density and intensity. The range of different targets included underdense gasbags filled with C_5H_{12}, gasbags filled with CO_2, Kr jets, and C_5H_{12}-filled Au containers heated by a single laser beam equipped with and without phase plates. The data

set, taken as a whole, shows that at 2ω it is possible to make changes that greatly change the backscattering losses. Figure 2 shows the time-integrated SRS reflectivity from the various targets. It shows that on Helen, SRS can be controlled by gas selection, by using jet plasmas (gradient) vs gasbag, and by beam smoothing.

A similar chart for SBS (Figure 3) shows that for some conditions this instability appears to be anticorrelated to SRS (C_5H_{12} vs $CO_{2)}$. This behavior may help us to suppress backscattering losses by choosing materials with low ion wave damping to suppress SRS and apply laser beam smoothing with phase plate and spectral dispersion to directly reduce SBS. Also interesting is the very low total SRS and SBS reflectivity from the Kr jet. Whether this is due to the gradient, the material, or something else is presently under investigation.

In FY01, we also have completed the interpretation of Nova experiments that have shown strong anomalous absorption of a 2ω laser beam in a highly ionized gold plasma.[7] By varying the laser power of a 2ω probe beam over four orders of magnitude, we have observed that laser absorption begins to deviate from predictions of an inverse bremsstrahlung absorption model for intensities of $I \geq 10^{14}$ W cm^{-2}. By further increasing the (vacuum) laser intensity of the probe beam to $I = 8 \times 10^{15}$ W^{-2} cm, the absorption rises to a maximum measured value of 50%. Simultaneously, the electron temperature of the plasma rises from T_e = 900 eV to 2 keV. Both these parameters are measured independently; the absorption with a full-aperture detector for the transmitted laser light and the temperature with Thomson scattering.

The experimental observations are successfully explained in terms of anomalous processes involving ion-acoustic turbulence which is excited by the heat-flux–driven return current instability. Ion-acoustic turbulence in inertial confinement fusion (ICF) plasmas has been predicted to be an important process influencing the laser light absorption, thermal transport, and growth and saturation of scattering instabilities.[14] In spite of the previous work, ion-acoustic turbulence has been poorly characterized in laser-produced plasmas. In collaboration with the University of Alberta and the Institute for Laser Science and Applications at LLNL, we have developed a new absorption model that includes these theories of anomalous absorption and thermal transport. This model provides good agreement with the experiment and is thus one of the most convincing evidences so far for the ion-acoustic turbulence.

Figure 4 shows the laser beam absorption for various 2ω probe beam intensities. The comparison of the experimental data with calculations from two models shows that inverse bremsstrahlung absorption is not sufficient to explain the measurements (squares). Good agreement can be seen by

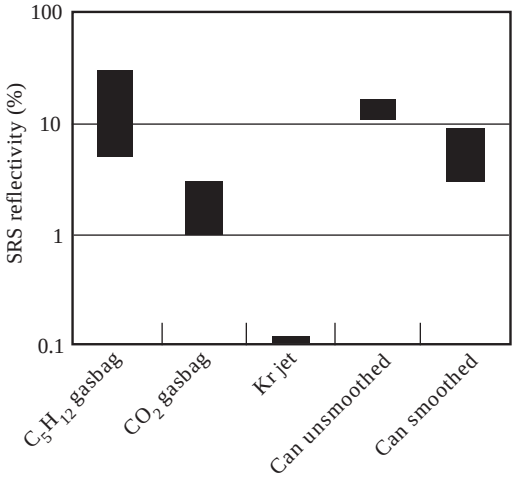

FIGURE 2. Experimental SRS reflectivity from a 2ω laser beam interacting with various underdense gas targets. The SRS reflectivity decreases by an order of magnitude by only changing the gas fill in the experiment. (NIF-0602-05263pb01)

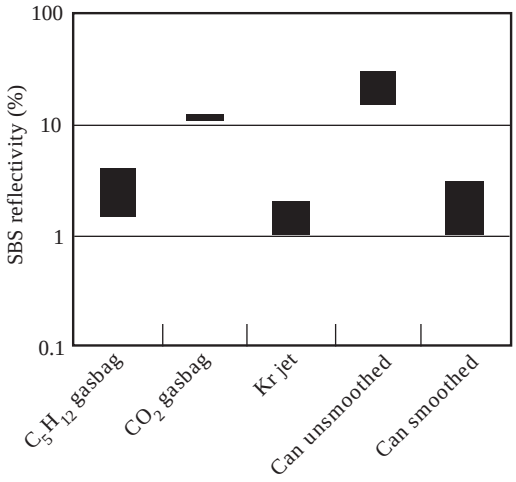

FIGURE 3. Experimental SBS reflectivity from a 2ω laser beam interacting with various underdense gas targets. The SBS reflectivity increases significantly in CO_2 where SRS is shown to decrease. (NIF-0602-05264pb01)

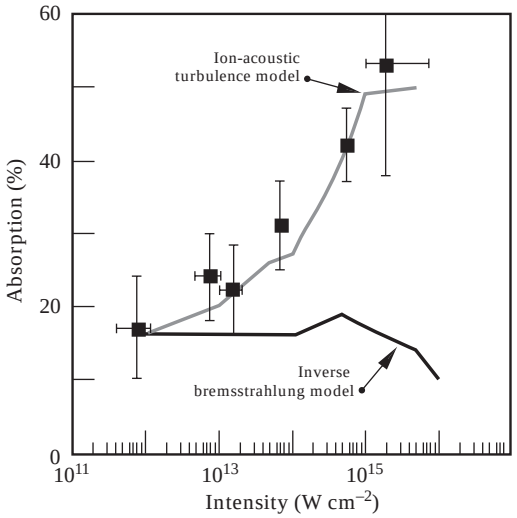

FIGURE 4. Experimental absorption from a 2ω laser beam in a highly ionized Au plasma. The large absorption can be modeled by ion-acoustic turbulence.
(NIF-0602-05265pb01)

including ion-acoustic turbulence leading to an enhanced collisionality and therefore to an enhanced laser beam absorption with increasing laser intensity. Similarly, we also find improved agreement of the ion-acoustic turbulence model with the electron temperature in the plasma as measured with Thomson scattering (not shown). This study introduces modeling of the ion-acoustic turbulence on the scale of a single laser hot spot, thus motivating the development of a reduced model for our laser–plasma interaction code to better take into account transport and interaction physics in large-scale underdense plasmas created by randomized laser beams.

Predictive Capability of Laser–Plasma Interactions

Modeling Developments

The parallel code pF3D is being developed to predict the backscattering losses, transmission, spreading, and deflection of NIF laser beams in ignition plasmas. Presently, pF3D contains physics modules that model light propagation, nonlinear 3D Eulerian hydrodynamics, and linearized nonlocal heat conduction so that the simulations take into account important processes such as filamentation, beam bending, and forward SBS. In addition, major progress has been made by including SBS and SRS backscattering processes into pF3D. The new routines have been tested and verified against the old code in small-scale calculations, and new diagnostics has been added to quantify the levels of the Langmuir and ion-acoustic waves and of the backscattered (Raman and Brillouin) light. Present computational capabilities have allowed the simulation of plasmas with the dimensions of 720 μm × 720 μm × 1010 μm, which is approaching the size of a NIF beam (with the SBS and SRS backscattering models included).

Resolving the evolution of the SBS / SRS backscatter requires a time step reduction of approximately 50, compared to simulations which modeled only filamentation and forward SBS. The resulting run times would have made full-beam SBS / SRS backscatter simulations impractical without significant algorithmic improvement. This motivated our work on subcycling the light propagation calculations and further domain decomposition in the direction of laser propagation. The former reduces the amount of calculations per hydrodynamic time step; the latter allows a greater degree of efficient parallelism and scalability to larger numbers of processors as bigger machines become available. Run time decreases close to linearly with the number of subdomains in the laser direction.

As an example, our October 1999 milestone run propagating a Nova beam through 1.1 mm of 0.1 n_{cr} plasma with only filamentation / forward SBS physics ran at a rate of 1.7 ps / hr on 128 CPUs of the ASCI Blue / SKY machines. Our October 2001 milestone simulation of the same beam and plasma conditions, but including the new SBS / SRS backscatter packages and algorithmic improvement, ran at 0.8 ps / hr on 160 CPUs of ASCI Blue / SKY. Beyond the major capability addition of modeling SBS and SRS, we

have made numerous other code improvements:

- The Bychenkov et al. model of nonlocal transport has been added as an additional option to our original model.
- Kinetic dispersion relations for multispecies ion-acoustic waves and Langmuir waves have been implemented by table lookup.
- Simple nonlinear saturation models for SBS and SRS based on increasing the ion wave or Langmuir wave damping above the two-ion decay or LDI thresholds, respectively, were implemented.
- We have added a very extensive set of run time and postprocessing diagnostics to the code.
- We have added the ability to import and design RPP and kinoform phase plate (KPP) beams for whole beam and letterbox simulations.

Simulations using pF3D in its current form have been extremely useful for interpreting experiments and as a tool for theoretical laser–plasma interaction physics studies. The simulations have indicated that plasma self-smoothing and filamentation of the laser beams are important effects that need to be modeled to better design laser smoothing concepts, such as RPPs. However, nonlinear saturation models will need to be added in the future to obtain a predictive capability. This topic is presently the focus of much activity in this area and is further described below. The pF3D code has already drawn considerable attention in the community and has been used by a number of outside groups including Princeton University, the University of Alberta, Canada, and the Commissariat à l'Energie Atomique (CEA), France.

For example, in collaboration with CEA, a model was added for increasing the damping of Langmuir waves in the presence of large amplitude ion-acoustic waves, such as those driven by SBS backscattering. The model calculates the effect of reducing the strength of SRS when the ion-acoustic wave driven by SBS is large enough and when SRS and SBS occur in the same spatial location. This mechanism is different from the effect already known where the SBS and SRS compete directly for the laser power in a speckle. Simulations that include this model might help us to provide insight in the anticorrelation between SRS and SBS observed in many experiments.

The code pF3D has also been applied to simulate for the first time the propagation and backscattering of full-sized Nova $f/8$ KPP beams through a 1-mm-long plasma (Figure 5). The 1024*512*640 zone mesh is the same as was used in the milestone runs of more than two years ago with only filamentation and forward SBS physics. However, since that time we have added SRS and SBS backscatter physics, many diagnostics, and other code improvements as described above. A C_5H_{12} plasma was modeled that was 1 mm long with a density ramping linearly from 0.02 to 0.2 of critical, at a temperature of 3 keV, with a transverse flow at 2×10^7 cm/s. The Nova

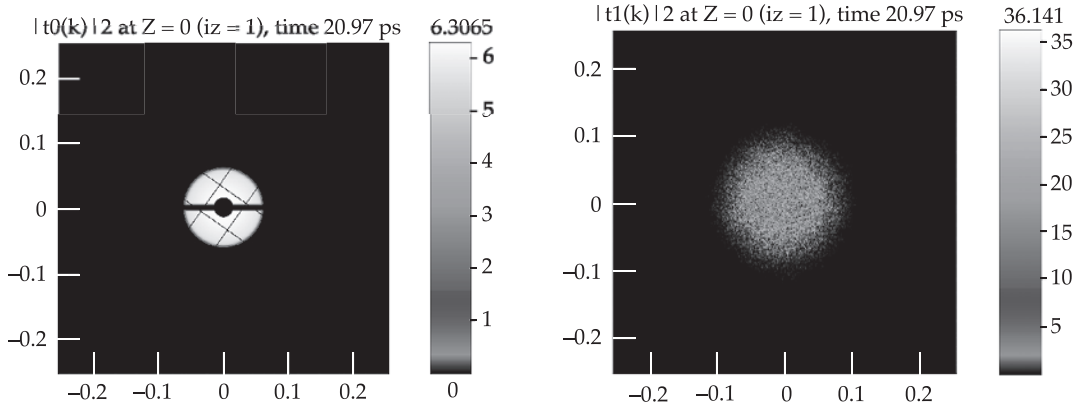

FIGURE 5. Calculated Nova near-field images of the incident laser light (left) and the back-reflected SBS light (right) at the entrance plane of the simulation at 21 ps. (NIF-0602-05266pb01)

beam had 2 TW of power, focused into an elliptical spot with the aid of the KPP.[15]

The instantaneous reflectivity is as high as 75% (20% time average). These high values are obtained because the SBS gain in the absence of longitudinal velocity gradients is very high. Most of the light is reflected back into the lens cone. The SRS reflectivity is negligible; suppressed by the density gradient and the strong SBS. Beam spreading was likewise suppressed by the strong SBS reflectivity. A second simulation, shown in Figure 6, uses a logarithmic density ramp from 2% to 20% n_{cr} to suppress backward SRS and a transverse flow to look at beam steering in the presence of backward SBS.

In this period, pF3D was also used to study the 2ω/3ω scaling of filamentation in smoothed beams (Figure 7). It is well established that potentially deleterious laser–plasma interactions, such as filamentation, beam spray, beam bending, and stimulated Raman and Brillouin backscattering, increase as the incident laser wavelength increases. Nevertheless, since more power and energy may be available from NIF at 2ω than at 3ω, it is worth looking more closely at the trade-off: more incident power and energy vs more problematic laser–plasma interactions.

As the first step in this quantification, a series of simulations of the interaction of an RPP-smoothed laser beam with a uniform slab of plasma was performed describing adequately thermal and ponderomotive filamentation and forward SBS. Simulations including models of backward SRS and SBS will follow in the next phase. The modeling propagated 2ω

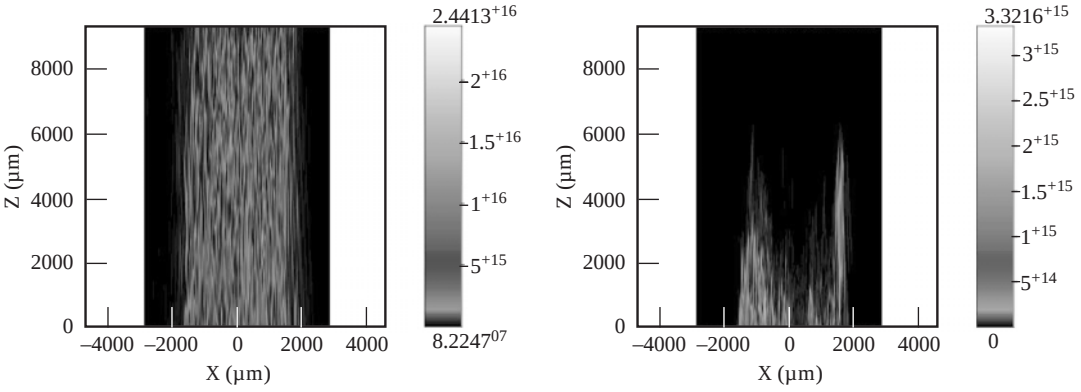

FIGURE 6. Calculated slice through the laser intensity vs the longer transverse (X) direction and the laser propagation (Z) direction (left). Note that the beam shows deflection in the positive X direction. A similar slice through the backscattered SBS light (right) at a time when there was approximately 40% reflectivity.
(NIF-0602-05267pb01)

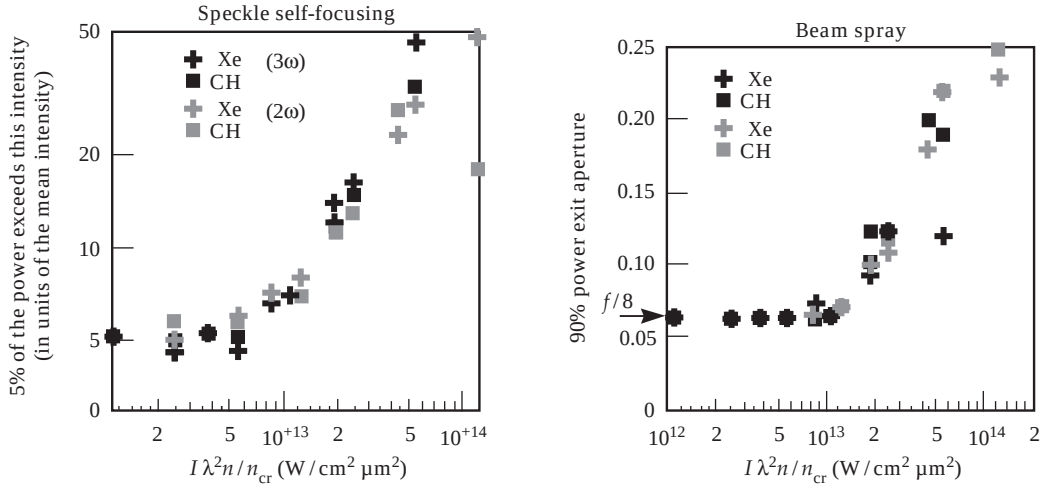

FIGURE 7. Scaling of self-focusing showing I_5/I_{av} against $I\lambda^2 n/n_{cr}$ (left) and scaling of beam spray (right). The latter shows the calculated cone angle in which 90% of the exiting laser power of the original *f*/8 beam is contained vs the same $I\lambda^2 n/n_{cr}$ parameter. The data show a rapid increase beyond $I\lambda^2 n/n_{cr} = 10$.[13]
(NIF-0602-05268pb01)

and 3ω beams through uniform slabs of CH and Xe plasmas with electron and ion temperatures of 3 and 1 keV respectively. The slabs were $192\lambda \times 192\lambda$ by 2400λ in size, containing about 500 speckles in the cross section, which is sufficient to provide adequate statistics for the high-intensity tail of the speckle distribution, which is the first to self-focus. The same random phases for the $f/8$ square RPP were used for each simulation to facilitate comparison between the runs. The electron densities were varied from 0.044 to 0.225 of the corresponding critical density, and intensities were varied from 2×10^{14} to 2×10^{15} W/cm^2. The simulations were run for 24 ps with a smooth 7-ps rise time, at which point the simulations appeared to have reached a statistical macroscopic steady state. Two phenomena are of particular concern: self-focusing of the higher intensity speckles (which is exacerbating stimulated laser backscattering) and beam spray (which can affect radiation symmetry in hohlraums).

The expected scaling parameter for both ponderomotive filamentation and forward SBS is $I\lambda^2 n/n_{cr}$. Here I is the averaged laser intensity, λ the wavelength of the incident laser light, and n/n_{cr} the ratio of the electron density over the critical density for which the laser light cannot propagate in the plasma.

For both processes we find that the data lie largely on a single curve, indicating that thermal effects are playing a minor role, even in xenon. The scaling of the onset of filamentation and forward SBS at $I\lambda^2 n/n_{cr} = 10^{13}$ is thus reasonably well characterized. The influence of backscattering losses and the scaling with smoothing by spectral dispersion bandwidth (of which more may be available on NIF at 2ω) is the subject of further study.

Nonlinear Saturation Experiments

Nova experiments and modeling in FY00 have observed for the first time that ion-acoustic wave amplitudes are saturated for conditions similar to those anticipated in future ignition experiments.

For these measurements, we have applied ultraviolet Thomson scattering of a 263-nm probe beam in well-characterized large scale-length gasbag plasmas with an electron temperature of T_e = 3 keV. The temporally resolved Thomson scattering spectra have shown simultaneously the scattering from thermal electrostatic fluctuations and ion-acoustic waves that have been excited to large amplitudes by SBS from a kilojoule interaction beam at 351 nm (cf. Figure 8). By varying the intensity, I, of the interaction beam, we have observed that the ion-acoustic waves saturate for $I > 5 \times 10^{14}$ W cm^{-2}. These results of the local Thomson scattering measurements are also consistent with the observed SBS reflectivity that shows saturation at the 30% level for these interaction beam intensities.

The experiments have been compared with calculations using the laser-plasma interaction code pF3D. Simulating the propagation and SBS of the 3ω interaction beam through the whole length of the gasbag plasma, we find that 30% SBS corresponds to an ion wave amplitude of $\delta n/n_e = 2 \times 10^{-3}$ (normalized to the electron density, n_e). Without nonlinear damping, the simulations show 100% reflectivity and ion-acoustic fluctuations in the Thomson scattering volume that return to the thermal level after a short initial burst, both in

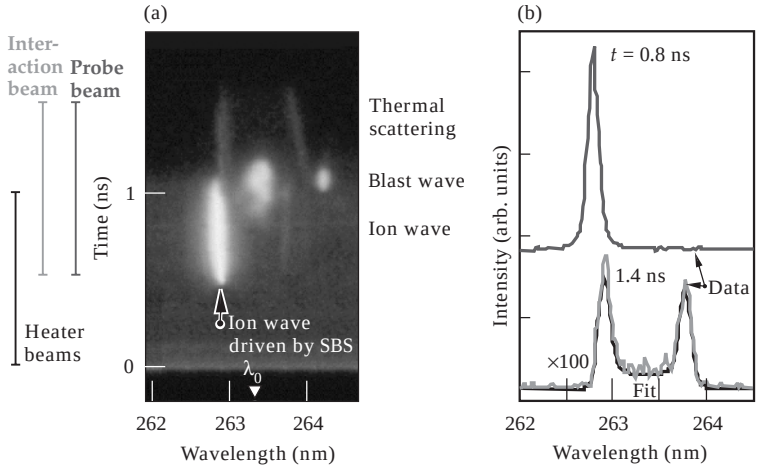

FIGURE 8. (a) Time-resolved Thomson scattering spectrum showing coherent scattering on ion waves driven by SBS, scattering on the blast wave, and thermal incoherent scattering at late times. The time sequence of the laser beams is indicated on the left. (b) Lineouts at t = 0.8 ns and t = 1.4 ns. The earlier lineout shows 2 orders of magnitude enhanced scattering compared to the spectrum at later times. The fits of the theoretical Thomson scattering form factor for a gas fill of CO_2 plus 1% Ar gives T_e = 3 keV at 0.8 ns and T_e = 2.5 keV and T_i = 1.7 keV at 1.4 ns. (NIF-0602-05269pb01)

contradiction with experimental data. Only by including a nonlinear damping model that is based on secondary decay of the primary ion-acoustic wave into two ion waves, do we observe results that are consistent with the experiments. Choosing a maximum ion wave amplitude that scales with ion wave decay is particularly motivated by the fact that CO_2 plasmas approach low ion wave damping conditions (similar to high-Z plasmas like Xe or Au) for which other nonlinear effects are less important. For example, the ion wave fluctuation level observed in these experiments is significantly smaller than the threshold for ion trapping, i.e., $\delta n / n_e = 0.2$.

Figure 9 shows that by using a nonlinear scaling, both SBS reflectivity and Thomson scattering data can be reproduced. The remaining small discrepancies might be explained by uncertainties in the absolute measured scattering power introduced by the Cassegrain telescope (alignment and incomplete sampling). However, the model assumed that two-ion wave decay occurs at a threshold lower than suggested by theoretical linear calculations. This indicates that either our theory of the two-ion wave decay instability is insufficient, or that other nonlinear mechanisms need to be included.

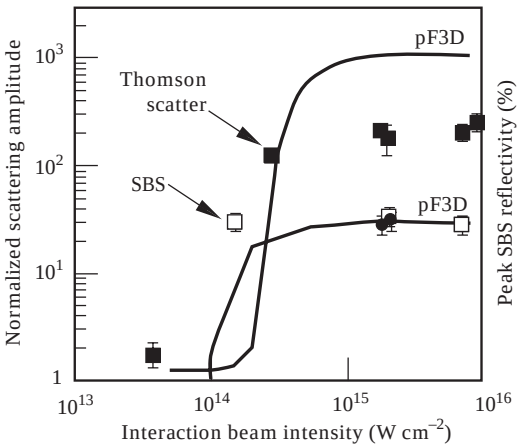

FIGURE 9. Scattering amplitude of the blue-shifted ion-acoustic wave normalized to the intensity of the red-shifted thermal peak (solid squares) for various beam intensities. Amplitudes are for t = 0.8 ns. SBS reflectivity data are obtained with and without RPPs (solid circles and open squares, respectively) and is observed to saturate at the 30% level. The curves represent the modeling. (NIF-0602-05270pb01)

These experiments provide the first experimental evidence that the SBS instability is saturated in ICF plasmas. Our findings further indicate that laser scattering losses in future ignition experiments on the NIF might be reduced by controlling the plasma conditions together with the nonlinear wave saturation processes. Moreover, these Nova gasbag experiments have clearly shown the limits of our present modeling capability. It is obvious that a first-principle understanding of the saturation process will be required to obtain a predictive modeling capability. We are planning to address the nonlinear wave physics of the high-temperature, low–ion-wave damping plasmas that primarily occur in the high-Z wall plasma of an ignition hohlraum in the immediate future using the Thomson scattering capability that we are presently implementing on the OMEGA laser facility. In FY01, experiments on the Trident laser have already begun to investigate the ion wave saturation physics of highly damped systems such as Be or He that will occur in the low-Z gas plasma of the large-scale interior fillings of ignition hohlraums.

We performed further experiments on saturation at the Trident laser facility, utilizing a new, very accurate Thomson scattering technique, which characterizes plasma conditions and the amplitudes of ion-acoustic waves in two-ion-species plasmas. Figure 10 shows the red- and blue-shifted ion-acoustic wave spectra with and without excitation by the SBS

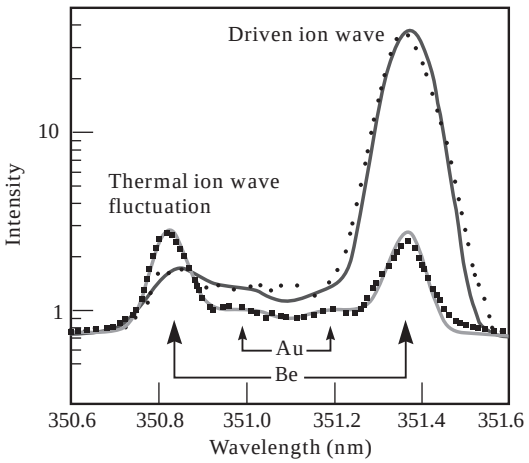

FIGURE 10. Thomson scattering spectra from two–ion-species plasmas (10% Au, 90% Be) show increased damping of the blue-shifted Be mode as well as the driven red-shifted ion wave when exciting SBS with an interaction beam of 3.5 × 10^{15} W cm^{-2} (gray circles). The data shown as black squares are taken without the interaction beam. (NIF-0602-05271pb01)

instability.[9] A wealth of information is obtained from these data; the red-shifted peaks show the nonthermal excitation, which only affects the lighter element, while the blue-shifted peaks measure the resultant thermal changes. We observe up to a twofold increase of the ion temperature when exciting ion-acoustic waves to large amplitudes by SBS. The ion temperature increase and its correlation with SBS reflectivity measurements are the first direct quantitative evidence of hot ions created by ion trapping in laser plasmas.

The experiment has been modeled assuming a 1-mm-long slab of homogeneous plasma (preformed to $n_e = 10^{20}\text{cm}^{-3}$, $T_e = 430$ eV, 140 eV $< T_i <$ 250 eV as measured with Thomson scattering), and a 527-nm interaction beam with intensities ranging from 10^{15} to 4×10^{15} W cm^{-2}. The interaction beam was not smoothed and had a focal spot diameter of ~60 μm. Solving the kinetic dispersion relation for the 10% Au to 90% Be mix shows the presence of a fast, weakly damped mode (with a normalized Landau damping $\nu/\omega_a = 0.05$) and a slow, heavily damped mode ($\nu/\omega_a = 0.3$). The linear gain calculations are in agreement with the Thomson scattering spectra of the driven SBS acoustic waves, which show only one red-shifted peak: the gain for the fast (Be-like) mode is $G \sim 200$, while there is almost no amplification of the slow mode ($G_{SBS} \propto 1/\nu$). The frequency of the acoustic wave is well reproduced.

While linear theory explains the shape of the spectrum, it predicts a reflectivity of $R_{SBS} \sim 100\%$ for such a large gain; thus one needs to invoke nonlinear saturation processes. The observation of an increase in T_i when the SBS acoustic wave is driven (see the increased damping of the blue Be-like peak in Figure 10 and also Figure 12 below) suggests the presence of trapped Be ions. Indeed, with $Z_{Be}T_e/T_i \sim 10$, there is a large population of Be ions at the phase velocity of the acoustic wave. Trapping reduces the ionic part of the Landau damping (by flattening the distribution function of Be ions at the phase velocity), leading to a minimum value $\nu/\omega_a \sim 0.015$, and modifies the dispersion relation for the acoustic waves, detuning the 3-wave coupling of the SBS instability. The resulting nonlinear frequency shift reduces the expected reflectivity from $R_{SBS} \sim 100\%$ (linear theory) to be of the order of 10%, in agreement with the experimental measurements. Furthermore, the scaling of R_{SBS} with the percentage of gold impurities is well reproduced: as gold ions are added, the phase velocity of the fast mode decreases, more Be ions are trapped, giving a larger frequency shift and a lower reflectivity (Figure 11).

This model can further be validated estimating the increase in T_i due to SBS.

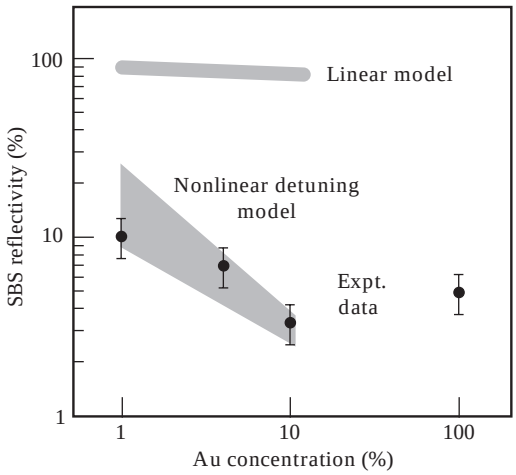

FIGURE 11. SBS reflectivity for various two–ion-species plasmas (from 1% Au, 99% Be to 10% Au, 90% Be mix) showing excellent agreement with the nonlinear modeling that is based on ion trapping. (NIF-0602-05272pb01)

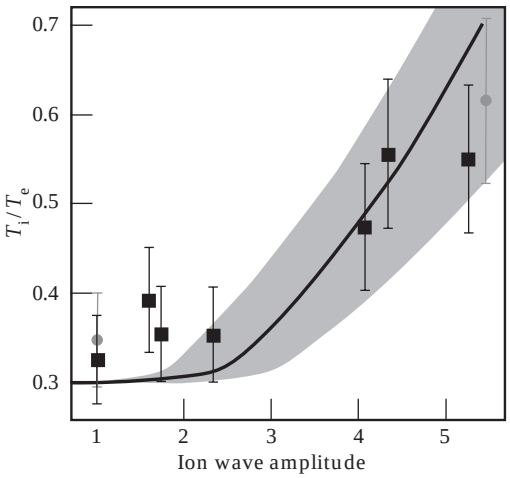

FIGURE 12. Ion-to-electron temperature ratio in the Thomson scattering volume as function of the amplitude of the driven SBS acoustic wave. Because no absolute measurement of the ion wave amplitude is available, the theoretical ratio is matched with the experimental ratio for a high-amplitude/high-reflectivity data point. (NIF-0602-05273pb01)

Balancing the energy flux deposited into the acoustic waves (from the Manley-Rowe relations) with a free-streaming heat flux carried by Be ions gives T_i in the Thomson scattering volume. The scaling seen in the experiments is well reproduced by this model (Figure 12).

The combined data set of the Thomson scattering and reflectivity measurements provide the strongest evidence so far for ion trapping and frequency detuning as the dominant SBS saturation mechanism in low-Z plasmas. The model is in excellent agreement with the experimental SBS data without using multipliers, indicating that it will be an important part of a predictive code capability. Full physics particle simulations are presently being used to benchmark this simple analytical model, developing it into a standard tool in pF3D. Figure 11, on the other hand, also shows that saturation in high-Z plasma is still not understood. No sophisticated modeling is presently available that can be compared to the data point for 100% Au, and future studies will need to address these conditions for the calculation of the reflectivity from the hohlraum wall plasma on NIF.

Crossing Laser Beams

In FY01, the energy transfer between crossing beams has been thoroughly investigated with experiments as well as with theory and simulations. In the past, modeling was limited to transverse flows that are constant in space and time at a given axial position. However, in the OMEGA experiments performed in this period and in the NIF targets they emulate, a spatial flow gradient is present so that the flow is significantly different from sonic in most of the crossing beam region. To address this problem and begin to model the OMEGA experiments, we have performed 2D simulations that include transverse flow gradients, and we compared the results with theoretical scaling.

Because pF3D cannot presently handle nonperiodic transverse boundary conditions, we used the ALPS code to simulate the energy exchange between crossing laser beams. In addition to the energy exchange, these simulations take into account a density gradient that varies exponentially through the crossing beam region with the same scale length as the flow gradient. The density at the sonic point was 0.1 n_{cr}. The simulations further include refraction of the light in the density gradient and beam deflection by the transverse flow as well as the energy exchange by forward SBS. Figure 13 shows two examples of the crossing laser beam simulations. They clearly show the decrease in power transfer and increase of beam steering when increasing the gradient in the plasma. While a good understanding of the beam steering aspect has been established previously, we have developed in this period the calculations of the absolute power transfer and tested the

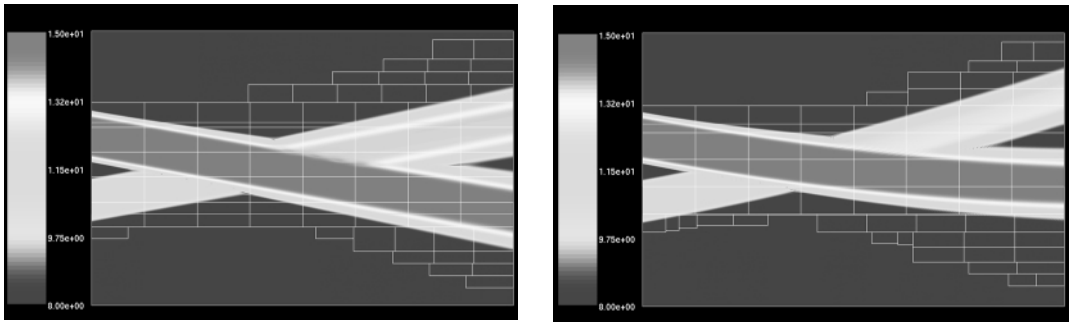

FIGURE 13. Two-dimensional simulations of crossing beams for a case with weak gradients (left) and for strong gradients (right). The flow is increasing in magnitude from bottom to top; thus, the beam moving upwards gains energy. The beams are incident from the left. Because of the gradients, the beams refract towards lower density (upwards), which changes the angle between the beams and the axial position at which they cross.
(NIF-0602-05274pb01)

results by comparing these simulations against theory.

We have further begun to compare these simulations to the presently ongoing experiments. For this purpose, we will need to include nonlinear saturation of the ion-acoustic wave because the gain for power transfer is proportional to the ion wave damping. An initial attempt to provide a quantitative comparison with the experiments is shown in Figure 14. The experiments measure the amplification of a probe beam in an exploding foil plasma with the presence of a pump beam.

We observed the threshold for resonant energy transfer at 10^{14} W/cm^2. The spectra of the transmitted light are not shifted, indicating that contributions to probe beam transmission from forward scattering and refraction of the heater beam are negligible, and the measured amplification is entirely due to interaction between the two beams. Because the exploding foils produced CH plasmas in the large ion wave damping regime, the same nonlinear frequency detuning model as for the Trident experiments was used. The modeling performed for the electron densities of the experiments, i.e., 0.03 n_{cr} and of 0.064 n_{cr}, shows agreement with the measured amplification for an interaction length of L_x = 75 mm. The goal of these scaling studies with the plasma parameters is to establish a physics base for selecting the optimum frequency shift for two-color operation on NIF to suppress power transfer in ICF experiments.

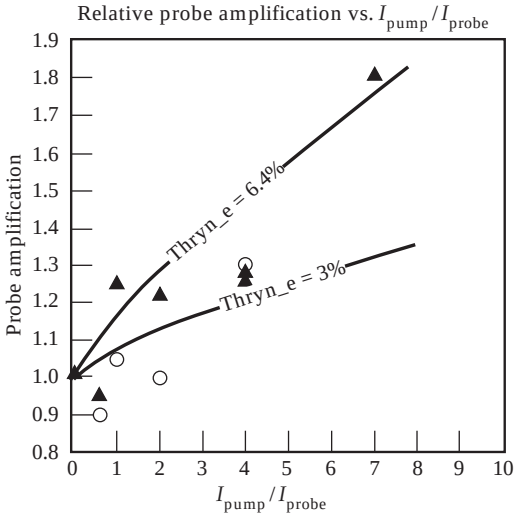

FIGURE 14. Experimental and modeled amplification of the probe beam for various pump laser intensities. The amplification is defined as the probe laser transmission normalized to a shot without the pump laser. (NIF-0602-05275pb01)

Energetics Measurement Capability for Soft X-Rays and Scattered Light

Based on ICF, High Energy Density Science (HEDS), and Physical Data Research Program (PDRP) needs for characterizing underdense plasmas and understanding 2ω laser–plasma interactions, an existing OMEGA beamline is being modified to act as a high-energy 2ω or 4ω probe. This project represents a collaboration between LLNL NIF Programs target physicists and engineers and the University of Rochester's Laboratory for Laser Energetics (LLE) target and laser scientists and engineers, with some funding assistance from the Physics and Advanced Technologies (PAT) Directorate.

The project redirects the 2ω laser light of an existing beam (Beam 25) to port P9 at the OMEGA target chamber using a kinematic mirror. The first goal is to provide for 2ω Thomson scattering and laser–plasma interaction experiments by late spring of FY02. This capability is scheduled to be upgraded to 4ω Thomson scattering by inserting a KDP quadrupler (plus rotator) into the beamline. The present performance goals are ~450 J in 1 ns at 2ω, and ~100 J in 1 ns at 4ω in a ~100-μm focal spot. The initial Thomson scattering collection system will use a ten-inch manipulator, TIM-2, providing 101° scattering. A 2ω FABS (Full Aperture Backscattering Station) will be built in addition to the existing 3ω FABS. A transmission diagnostic is being planned as well. A schematic of the setup is shown in Figure 15.

In addition to optical measurement capabilities, we are investigating soft and hard x-ray imaging detectors using a photo conductive detector (PCD) array. Experiments at the Janus laser facility were performed to evaluate the performance characteristics of a prototype 4 × 4 diamond PCD array when exposed to x-rays inside a target chamber. A gold foil target was irradiated by the Janus laser to produce soft x-rays. The laser pulse energy was varied between 1 J and 55 J, while the pulse length was switched

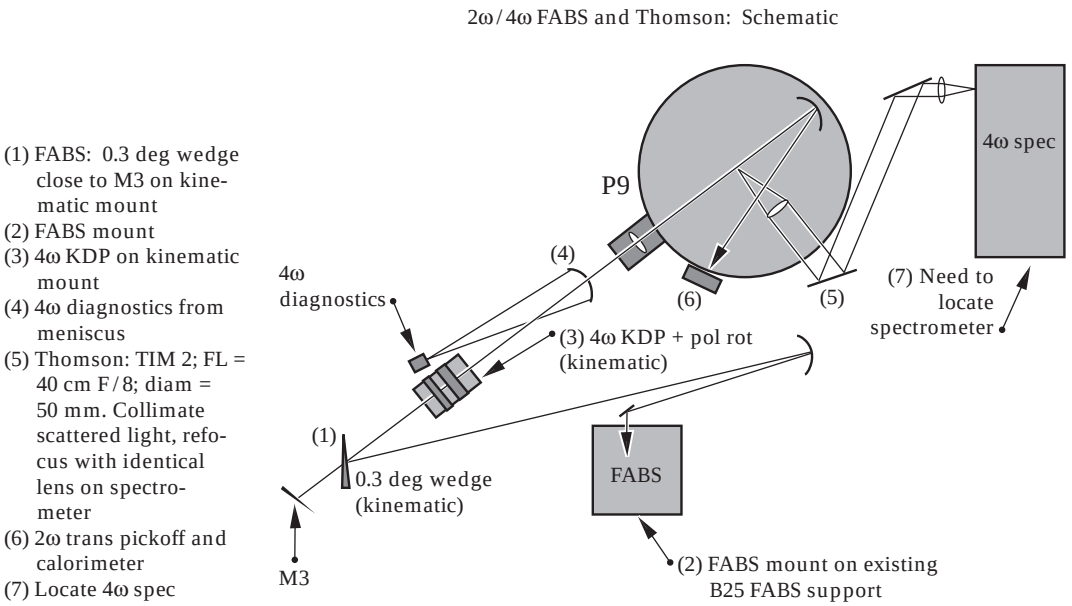

FIGURE 15. Schematic of the Thomson scattering probe beam capability at the OMEGA laser facility. (NIF-0602-05276pb01)

between 1 ns and 8 ns. The spot size at the target was estimated to be 60 μm diam. A linear response of the array was observed in these experiments, which motivated us to test a 20×20 array in the next step. The latter may be used to image the laser entrance hole (LEH) of a hohlraum through a pinhole so that the soft x-ray production will be measured while measuring and accounting for diagnostic hole closure effects.

This potential diagnostic might be particularly important for future drive experiments on the NIF because of the ongoing uncertainties about the usefulness of the DMX, a time-resolved broadband soft x-ray spectrometer, for drive measurements. It appears that the diodes used in DMX become contaminated when used in laser experiments at OMEGA so that DMX has given a factor of two less sensitivity than Dante. Until the DMX contamination and calibration issues are resolved, Dante will remain our core soft x-ray drive diagnostic.

Scaling of Magnetic Fields in Hohlraum Plasmas

The radiation-hydrodynamics code LASNEX has been used to build a picture of magnetic field generation, saturation, and impact on the hohlraum environment. In previous periods, we have shown that the electron temperature measurements in the low-Z gas plasma of Nova hohlraums are not consistent with standard LASNEX simulations that predict a rather isotropic temperature distribution in this area.[16] However, by including magnetic fields into the modeling, significant electron heat transport inhibition occurs in the gas plasma leading to strong temperature gradients in the LEH region in good agreement with the Thomson scattering measurements that show peak T_e values of 5 keV. In this period we have further measured T_e and the ionization distribution in the high-Z Au plasma and observed that radiation-hydrodynamic simulations are consistent with our experimental findings. These studies have motivated us to investigate the scaling to smaller scale hohlraums as a way to study high-energy-density systems that will be produced on NIF.

The hohlraum scaling simulations began by revisiting the Nova scale 1 experiment, and subsequently increasing the energy density to scale ¾ and scale ½. In addition, we have implemented a new B-field source term into LASNEX arising from momentum deposition in the plasma by the laser beam itself. LASNEX predicts a magnetic field of ~1 MG, which has the dramatic effect of inhibiting electron transport near the LEHs. The consequence is that electron temperatures are up to

~2× of those calculated without B-fields. The saturation mechanism appears to be consistent with convection of the field away from the gold wall where it is generated via $\nabla n \times \nabla T$. This occurs over the first few hundred picoseconds, at which time the field has already approached ~1 MG. The gold wall is largely nonmagnetized as expected, whereas the gas is highly magnetized with $1 < \omega\tau < 10$, where ω is the electron cyclotron frequency and τ is the electron–ion collision time. The mean free path of the thermal electrons is typically ~100 μm, whereas that for the heat carriers it is ~80× larger, which is very much greater than the size of the hohlraum. The magnetic field serves to reduce this to about the Larmor radius, which is ~0.5 mm and comparable to the scale of the hohlraum. This strongly suggests a magnetized nonlocal transport treatment is necessary. A more formal assessment based on the departure of the electron distribution from a Maxwellian confirms this.

Results for the scale ¾ hohlraums show that the demarcation between magnetized gas and nonmagnetized gold wall plasma is even more obvious. Despite larger electron temperatures, a slightly larger B-field means that the degree to which linear transport breaks down is not obviously worse than in the scale 1. At this time it has not been possible to complete the simulations for the scale ½ hohlraums. This is due to the difficulty of modeling the Righi-Leduc heat flow parallel to the temperature gradient, and may arise from an instability that is a consequence of the model equations rather than nature. The Righi-Leduc heat flow, however, is real and a significant effect even in the scale 1 hohlraum. Including the magnetic field source term due to deposition of laser beam momentum has a relatively small but noticeable effect in the simulations, because these neglect self-focusing and filamentation. The very much higher intensities in laser filaments can drive fields via inverse bremsstrahlung to values comparable to those from the $\nabla n \times \nabla T$ source term. In addition, instabilities in filaments have much shorter deposition lengths than the inverse bremsstrahlung absorption length and consequently have the potential to drive very large magnetic fields locally. Since this is most likely to occur in the LEH plasma where the laser intensity is highest, these fields are likely to further reduce the already inhibited heat flow due to the $\nabla n \times \nabla T$ driven fields. The consequence of this effect is presently studied.

Experiments at the Nova laser used scale 1 hohlraums heated with ten 3ω (351 nm) laser beams with a total energy of 27 kJ. They also applied kinoform phase plates to smooth the laser beams and employed shaped laser pulses of 2.4-ns duration with a 7-TW foot reaching 17-TW peak power at 1.6 ns (pulse shape No. 22: PS22). The hohlraums were filled with 1 atm of propane (C_3H_8) to tamp the hohlraum wall plasma, and the diagnostic and LEHs have been covered with 0.35-μm-thick polyimide. The radiation-hydrodynamic model-

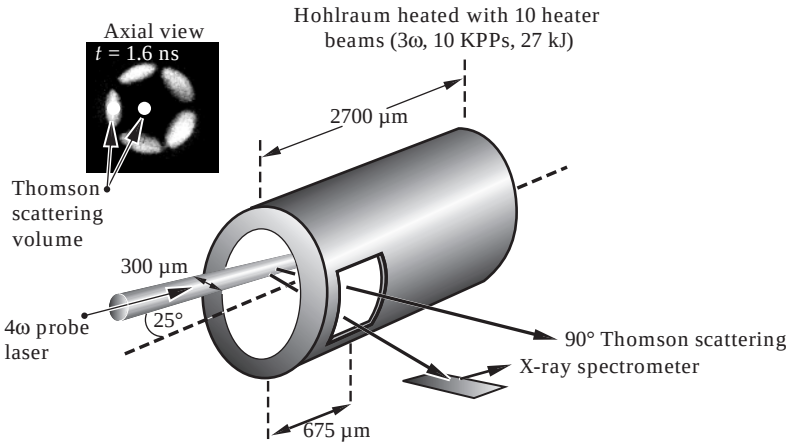

FIGURE 16. Schematic of the x-ray spectroscopy and Thomson scattering experiment that measures T_e and Z of the hohlraum wall plasma. (NIF-0602-05277pb01)

ing shows that the C_3H_8 gas fill slows down the Au blowoff plasma resulting in a fairly homogeneous Au plasma close to the hohlraum walls.

A flat crystal x-ray spectrometer has been employed to measure the Au M-shell 5-3 transitions through a diagnostic hole cut in the side of the hohlraum. The same hole was used to simultaneously measure the hohlraum electron temperature in the gold and in the gas plasma with 4ω Thomson scattering (cf. Figure 16). The locations of the Thomson scattering volume is indicated on the gated 2D x-ray image that shows the emission of the Au blowoff plasma with $E > 2$ keV at 1.6 ns. Measurements were performed inside the high-Z Au blowoff plasma and in the low-Z gas plasma.

Figure 17 compares the measured plasma parameters with non-LTE radiation-hydrodynamic LASNEX modeling. Two calculations have been performed. The first one uses a standard flux-limited heat transfer model while the second calculation includes a self-consistent calculation of magnetic fields and their effects on electron thermal transport. For both models, the comparison with the experimental plasma parameters shows good agreement in the Au plasma. However, in the gas plasma, Thomson scattering shows that T_e decreases, which is more consistent with the magnetic field modeling that calculates low temperatures in this region inside the hohlraum. In the gas plasma the flux-limited model predicts isotropic temperatures not in agreement with the Thomson scattering measurements. However, the soft x-ray radiation field in hohlraums is essentially determined by the conditions in the Au plasma. We find that both models calculate nearly the same radiation temperature, which agrees with the PCD data of these experiments.[17] These measurements explain why in previous periods we have successfully modeled the hohlraum radiation temperatures with LASNEX but have been less successful in predicting the hohlraum electron temperatures. The modeling that includes magnetic fields will be important for studying the laser–plasma interactions in hohlraums and might also play an important role for higher energy density systems as described above.

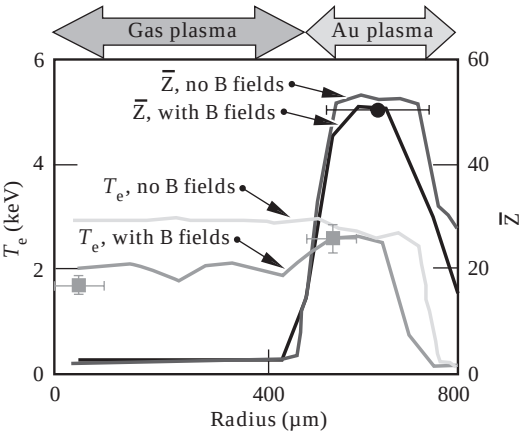

FIGURE 17. Comparison of the measured microscopic plasma parameters with LASNEX modeling at $t = 1.6$ ns; T_e (squares) and Z (circle). (NIF-0602-05278pb01)

Upper Limits to Capsule-Absorbed Energy on NIF

With the assumption that laser backscattering and hot electron production can be controlled at 2ω, a number of LASNEX simulations have indicated exciting options for ignition targets on NIF. One of the most attractive features of 2ω is found in the assumption that green light would allow operation at a significantly higher fluence than blue. Taking the maximum NIF 1ω energy to be about 5 MJ with 11/7 amplifier configuration, and multiplying by the possible 2ω conversion and transport efficiencies, ~70–80%, leads to approximately 3.5–4 MJ of green light incident upon a target. This level corresponds to a fluence of 14–16 J/cm^2 at the final optics, which will probably produce acceptable low damage. With that much energy we see that NIF might be able to drive some very energetic ignition capsules, even with relatively low coupling efficiency.

If we further assume that ~3.4 MJ of x-rays will be available to drive a 250-eV capsule, then simple scaling shows that at a standard case-to-capsule ratio (square root of the ratio of hohlraum area/capsule area) we could drive a capsule that absorbs more than 900 kJ of energy. Figure 18 shows the results of the simulations indicating the significantly increased capsule-absorbed

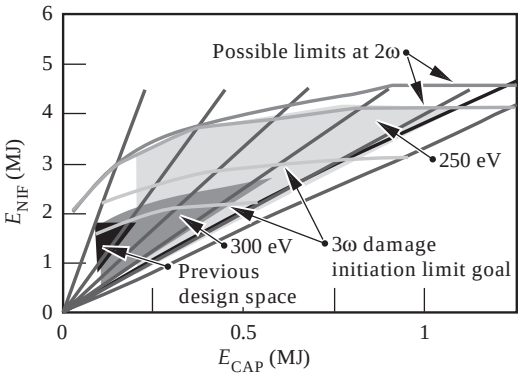

FIGURE 18. Capsule-absorbed energy for 2ω and 3ω operation on NIF. (NIF-0602-05279pb01)

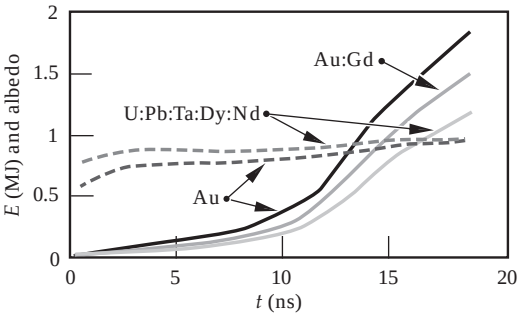

FIGURE 19. Calculated hohlraum wall loss (solid curves) and albedo (dashed curves) for ignition designs on NIF. The mixture materials clearly show a reduced loss. The minimum possible loss at the end of the pulse is represented by the Dyson limit and is 800 kJ for these conditions. (NIF-0602-05280pb01)

energy for 2ω operation on NIF. These simulations provide a strong motivation to further investigate the option of 2ω operation on NIF. Future work will need to assess laser backscattering losses, the soft x-ray conversion efficiency,[18] and the diagnostic capabilities at 2ω.

Another way to increase the performance of NIF hohlraums is to employ cocktail instead of pure gold hohlraums. LASNEX simulations have found a significant decrease in wall losses using a variety of four and five material mixtures. Figure 19 shows wall loss vs time for three different materials exposed to a 250-eV peak drive ignition pulse. The losses plotted correspond to the area of a scale 5.55 Nova hohlraum made out of the indicated materials. The lowest wall absorption plotted, about ⅔ of gold, is not at all a unique result. In fact, a variety of cocktail mixtures have provided a similar improvement. Cocktails have also the advantage that they increase the albedo. At early times there can be a very significant increase in albedo, which not only saves energy but also serves to reduce the hot-spot:wall emission ratio. This, in turn, should reduce both intrinsic asymmetry and random asymmetry due to laser beam power imbalance.

Experiments at the OMEGA laser have been performed to evaluate the performance of cocktail materials. For this purpose, the soft x-ray reemission of the indirectly driven back wall of half hohlraums of varying size has been measured. The back wall was split into two halves. One half was a standard Au plate and the other half was the cocktail material. From LASNEX calculations it was expected that the reemission of the cocktail material would be a factor of 1.3 higher than for the Au plate at the smallest scale hohlraum in the 450-eV energy band that was studied. Initially, such an increase has not been observed in experiments that have used Nova scale ½ half hohlraums. Very recently, however, we have shown that the cocktail reemission increases at higher radiation temperature, i.e., with decreasing hohlraum size. Additional experiments have also compared the radiation temperatures from gold vs cocktail Nova scale ¾ hohlraums that were heated with 40 beams at the OMEGA laser facility. These experiments show that cocktail hohlraums have about the same total soft x-ray production as gold hohlraums but a factor of two smaller M-band emission that could be a source of preheat in ignition experiments (cf. Figure 20). It is remarkable that the cocktail hohlraums achieved this performance although a significant amount of the laser power was lost due to SBS and SRS backscattering.

Notes and References

1. S. H. Glenzer, L. J. Suter, R. E. Turner, B. J. MacGowan, K. G. Estabrook, M. A. Blain, S. N. Dixit, B. A. Hammel, R. L. Kauffman, R. K. Kirkwood, O. L. Landen, J. D. Moody, T. O. Orzechowski, D. M. Pennington, G. F. Stone,

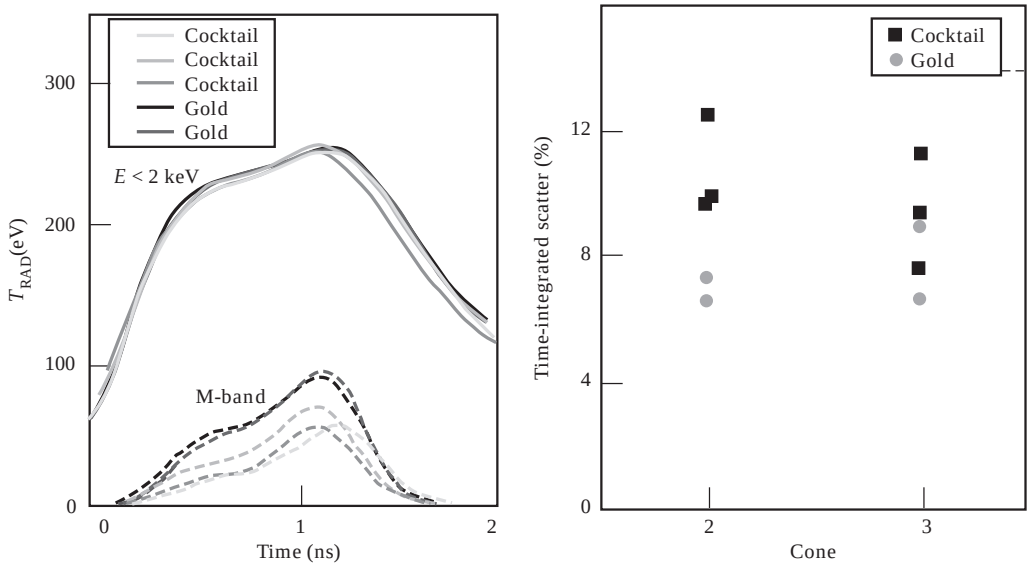

FIGURE 20. Measured radiation temperature (radiation energy of $E = 0–2$ keV) and M-band emission ($E > 2$ keV) for cocktail and gold hohlraums as function of time (left). The total time-integrated scattering losses from SBS and SRS for the laser beams in Cone 2 and Cone 3 (right). No data are available for Cone 1.
(NIF-0602-05281pb01)

and T. L. Weiland, *Energetics of Inertial Confinement Fusion Hohlraum Plasmas*, Lawrence Livermore National Laboratory, Livermore, CA, UCRL-JC-129236; also in *Phys. Rev. Lett.* 80, 2845–2848 (1998).

2. J. D. Moody, B. J. MacGowan, J. E. Rothenberg, R. L. Berger, L. Divol, S. H. Glenzer, R. K. Kirkwood, E. A. Williams, and P. E. Young, *Backscatter Reduction Using Combined Spatial, Temporal, and Polarization Beam Smoothing in a Long Scale-Length Laser-Plasma*, Lawrence Livermore National Laboratory, Livermore, CA, UCRL-JC-139843; also in *Phys. Rev. Lett.* 86, 2810–2813 (2001).
3. R. K. Kirkwood, D. S. Montgomery, B. B. Afeyan, J. D. Moody, B. J. MacGowan, S. H. Glenzer, W. L. Kruer, K. G. Estabrook, K. B. Wharton, E. A. Williams, and R. L. Berger, *Observation of the Nonlinear Saturation of Langmuir Waves Driven by Ponderomotive Force in a Large Scale Plasma*, Lawrence Livermore National Laboratory, Livermore, CA, UCRL-JC-128298; also in *Phys. Rev. Lett.* 83, 2965-2968 (1999).
4. L. Divol, *Workshop on SBS/SRS Nonlinear Saturation*, April 3–5, Wente vineyard, Proceedings, Lawrence Livermore National Laboratory, Livermore, CA, UCRL-JC-148983-SUM.
5. J. D. Moody, B. J. MacGowan, S. H. Glenzer, R. K. Kirkwood, W. L. Kruer, D. S. Montgomery, A. J. Schmitt, E. A. Williams, and G. F. Stone, *First Measurements of Short Scale-Length Density Fluctuations in a Large Laser-Plasma*, Lawrence Livermore National Laboratory, Livermore, CA, UCRL-JC-133035; also in *Phys. Rev. Lett.* 83, 1783–1786 (1999).
6. J. D. Moody, B. J. MacGowan, S. H. Glenzer, R. K. Kirkwood, W. L. Kruer, D. S. Montgomery, A. J. Schmitt, E. A. Williams, and G. F. Stone, *Experimental Investigation of Short Wavelength Density Fluctuations in Laser-Produced Plasmas*, Lawrence Livermore National Laboratory, Livermore, CA, UCRL-JC-136401 Rev 1; also in *Phys. Plasmas* 7, 2114–2125 (2000).
7. S. H. Glenzer, W. Rozmus, V. Y. Bychenkov, J. D. Moody, J. Albritton, R. L. Berger, A. Brantov, M. E. Foord, B. J. MacGowan, R. K. Kirkwood, H. A. Baldis, and E. A. Williams, *Anomalous Absorption of High-Energy Green Laser Light in High-Z Plasmas*, Lawrence Livermore National Laboratory, Livermore, CA, UCRL-JC-145287; also in *Phys. Rev. Lett.* 88, 235002 (2002).
8. S. H. Glenzer, L. M. Divol, R. L. Berger, C. Geddes, R. K. Kirkwood, J. D. Moody, E. A. Williams, and P. E. Young, *Thomson Scattering Measurements of Saturated Ion Waves in Laser Fusion Plasmas,* Lawrence Livermore National Laboratory, Livermore, CA, UCRL-JC-140588; also in *Phys. Rev. Lett.* 86, 2565–2568 (2001).
9. D. H. Froula, L. Divol, and S. H. Glenzer, *Measurements of Nonlinear Growth of Ion-Acoustic Waves in Two-Ion-Species Plasmas with Thomson Scattering*, Lawrence Livermore National Laboratory, Livermore, CA, UCRL-JC-145688; also in *Phys. Rev. Lett.* 8704, 045002-045005 (2002).
10. B. J. MacGowan, B. B. Afeyan, C. A. Back, R. L. Berger, G. Bonnaud, M. Casanova, B. I. Cohen, D. E. Desenne, D. F. Dubois, A. G. Dulieu, K. G. Estabrook, J. C. Fernandez, S. H. Glenzer, D. E. Hinkel, D. H. Kalantar, R. L. Kauffman, R. K. Kirkwood, W. L. Kruer, A. B. Langdon, B. F. Lasinski, D. S. Montgomery, J. D. Moody, D. H. Munro, L. V. Powers, H. A. Rose, C. Rouseaux, R. E. Turner, B. H. Wilde, S. C. Wilks, and E. A. Williams, *Laser Plasma Interactions in Ignition-Scale Hohlraum Plasmas*, Lawrence Livermore National Laboratory, Livermore, CA, UCRL-JC-121499 Rev 1; also in *Phys. Plasmas* 3, 2029–2040 (1996).
11. D. H. Froula, L. Divol, H. A. Baldis, R. L. Berger, D. G. Braun, B. I. Cohen, R. P. Johnson, D. S.

Montgomery, E. A. Williams, and S. H. Glenzer, *Observation of Ion Heating by Stimulated-Brillouin-Scattering-Driven Ion-Acoustic Waves Using Thomson Scattering*, Lawrence Livermore National Laboratory, Livermore, CA, UCRL-JC-145885; also in *Phys. Plasmas* 9, 4709–4718 (2002).

12. R. K. Kirkwood, J. D. Moody, A. B. Langdon, B. I. Cohen, E. A. Williams, M. R. Dorr, J. A. Hittinger, R. L. Berger, P. E. Young, L. J. Suter, L. Divol, S. H. Glenzer, O. L. Landen, and W. Seka, *Observation of Saturation of Energy Transfer between Copropagating Beams in a Flowing Plasma*, Lawrence Livermore National Laboratory, Livermore, CA, UCRL-JC-148550; also in *Phys. Rev. Lett.* 89, 215003 (2002).
13. R. K. Kirkwood, B. B. Afeyan, C. A. Back, D. E. Desenne, K. G. Estabrook, S. H. Glenzer, H. N. Kornblum, B. F. Lasinski, B. J. MacGowan, D. S. Montgomery, J. D. Moody, R. Wallace, and E. A. Williams, *Effect of Ion Wave Damping on Stimulated Raman Scattering in High-Z Laser-Produced Plasmas*, Lawrence Livermore National Laboratory, Livermore, CA, UCRL-JC-124019 Rev 1; also in *Phys. Rev. Lett.* 77, 2706–2709 (1996).
14. W. Rosmuz, V. T. Tikhonchuk, V. Y. Bychenkov, and C. E. Capjack, "Enhanced Ion-Acoustic Fluctuations in Laser-Produced Plasmas," *Phys. Rev. E* 50, 4005–2016 (1994).
15. S. N. Dixit, M. D. Feit, M. D. Perry, and H. T. Powell, *Designing Fully Continuous Phase Screens for Tailoring Focal-Plane Irradiance Profiles*, Lawrence Livermore National Laboratory, Livermore, CA, UCRL-JC-123842 Rev 1; also in *Opt. Lett.* 21, 1715–1717 (1996).
16. S. H. Glenzer, W. E. Alley, K. G. Estabrook, J. S. De Groot, M. G. Haines, J. H. Hammer, J.-P. Jadaud, B. J. MacGowan, J. D. Moody, W. Rozmus, L. J. Suter, T. L. Weiland, and E. A. Williams, *Thomson Scattering from Laser Plasmas*, Lawrence Livermore National Laboratory, Livermore, CA, UCRL-JC-131357; also in *Phys. Plasmas* 6, 2117–2128 (1999).
17. S. H. Glenzer, K. B. Fournier, B. G. Wilson, R. W. Lee, and L. J. Suter, *Ionization Balance in Inertial Confinement Fusion Hohlraums*, Lawrence Livermore National Laboratory, Livermore, CA, UCRL-JC-139505 Rev 1; also in *Phys. Rev. Lett.* 87, 045002 (2001).
18. E. Dattolo, L. Suter, M.-C. Monteil, J.-P. Jadaud, N. Dague, S. Glenzer, R. Turner, D. Juraszek, B. Lasinski, C. Decker, O. Landen, and B. MacGowan, *Status of Our Understanding and Modeling of X-Ray Coupling Efficiency in Laser Heated Hohlraums*, Lawrence Livermore National Laboratory, Livermore, CA, UCRL-JC-137622 Rev 1; also in *Phys. Plasmas* 8, 260–265 (2001).

DRIVE SYMMETRY

O. L. Landen *P. A. Amendt*

D. K. Bradley *O. S. Jones*

S. M. Pollaine *R. E. Turner*

Ignition of future high-convergence implosion targets at NIF will require accurate understanding, control, and measurements of hohlraum flux asymmetries. Several campaigns aimed at measuring, demonstrating, and using symmetry control were pursued at the 60-beam OMEGA facility. First, we have demonstrated 1% time-integrated symmetry measurement accuracy using NIF-scale symmetry diagnostic techniques begun at OMEGA. Second, we have demonstrated near-1D performance for up to convergence-ratio-20 (initial-to-final fuel radius), high-growth-factor implosions by switching to Ar-free fuel and by using the NIF-like multiple-cone capability available at OMEGA. This allows us to bridge the gap between understanding the performance of hydrodynamically equivalent Nova convergence-ratio-10 implosions and NIF convergence-ratio >30 implosions. Third, we have NIF designs for the principal target-mounted pinhole imaging techniques now used for symmetry studies based on extrapolations from recent OMEGA demonstrations. Finally, we are beginning a detailed computational investigation of the fidelity of various surrogate capsule symmetry techniques at NIF-scale.

Detecting with 1% Accuracy Hohlraum Asymmetry Modes at NIF-Scale

An experimental campaign investigating diagnosis and control of higher order mode hohlraum asymmetries during the foot of the NIF ignition drive continued in FY00 and 01 at the OMEGA laser facility. The design and experimental methodology continue to evolve. First, we have switched to slightly smaller Nova Scale 2.1 hohlraums (3.3 vs 4.8-mm-diam by 5.6 vs 8-mm-long), which emulate the full NIF foot 90-eV temperature (vs 70 eV for the larger earlier hohlraums). [See Figure 1.] Flux asymmetries decomposed into Legendre modes are

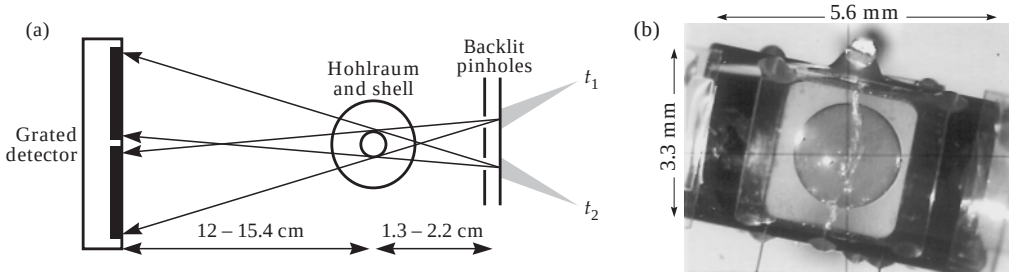

FIGURE 1. (a) Experimental setup for point projection backlighting of thin shells. (b) Picture of hohlraum with Ge-doped thin plastic shell, without Au-coated patches.
(NIF-0602-05245pb01)

inferred from the out-of-round distortions observed on backlit 1.6-mm-diam Ge-doped thin plastic shells. A shell-to-hohlraum radius ratio of ≈0.5 has been chosen to amplify the imprinting of higher order mode distortions (e.g., P_6) on the shell (see Figure 2). Calculations predict values of a_2 through a_6 between 4 to 10 µm should be observed after 6 ns for the backlit shells. This is a 2× improvement in sensitivity over previous Nova Scale 3 designs, principally because of the higher drive temperature (T_r = 90 vs 70 eV) accessible leading to a greater distance ($\sim T_r^{1.75}$) traveled by the shell. Second, preshot radiographs are taken (see Figure 3) using an x-ray source to account for any preexisting asymmetries, with typically only a_2 present at the 1-µm level. Also shown in the figure are examples of two 4.7-keV gated radiographs taken 3.4 ns (Figure 3b) and 7.4 ns (Figure 3c) into the drive. A plot of radius vs polar angle after summing four quadrants of an analyzed limb image is shown in Figure 4 for a 15-µm shell after 6 ns of drive. Over-plotted are fits using even Legendre modes only with and without mode 6 included, showing a much better fit with the inclusion of mode 6. Another example of analyzed data for all modes (even and odd) is shown in Figure 5 for a 15-µm shell, which has traveled 200 µm after 6 ns of drive. Overplotted are the results of 2D simulations, which are in reasonable agreement on this shot with the measured even mode distortions. Translating the distortions to average flux asymmetry using the equality $a_n / a_0 = P_n / P_0$, we can infer from the error bars that we have demonstrated 1% accuracy in detecting flux asymmetries.

However, all shots still show the presence of significant levels of odd modes, which are not intrinsic to a 2D symmetric hohlraum illumination. A likely source of odd modes is believed to be due to hohlraum misalignment at the level of 50 µm. Future shots will place the hohlraum at target chamber center to improve alignment accuracy and repeatability. A second potential source of odd modes is beam-to-beam energy imbalances. This has recently been mitigated by a factor of ≈√2 by doubling the number of beams on at any given time by switching from the previous 6-ns staggered beam configuration to a 3.5-ns nonstaggered configuration. This also has the advantage of making the lowest intrinsic azimuthal asymmetry m = 6 rather than m = 3.

We have also begun to study the symmetry and drive implications for roughened hohlraums required for symmetrizing IR smoothing of the cryogenic capsule fuel

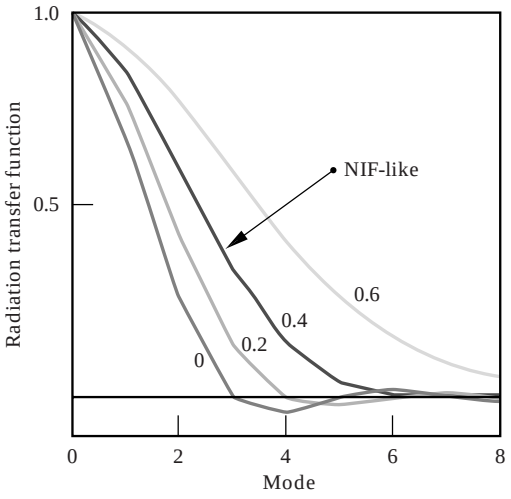

FIGURE 2. Radiation transfer function between case and capsule vs Legendre mode number for various capsule-to-case radii ratios. A transfer function value of 1 corresponds to no smoothing.
(NIF-0602-05246pb01)

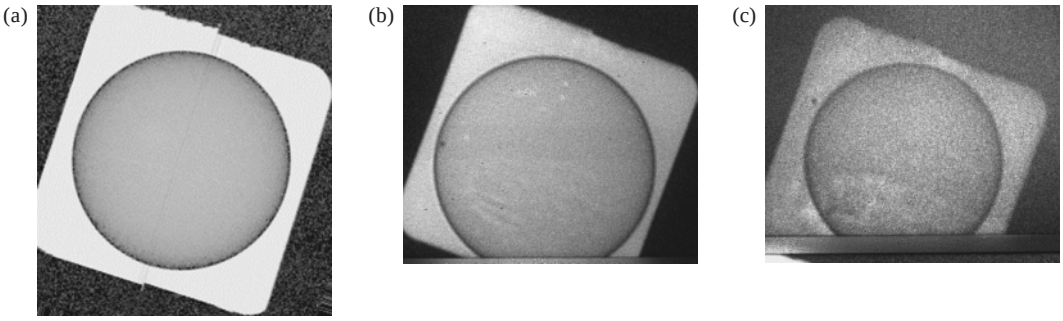

FIGURE 3. Radiographs of 14-µm-thick Ge-doped CH shell in hohlraum: (a) preshot dc radiograph at 2.3 keV, (b) gated 4.7-keV radiograph 3.4 ns into drive, and (c) gated 4.7-keV radiograph 7.4 ns into drive.
(NIF-0602-05247pb01)

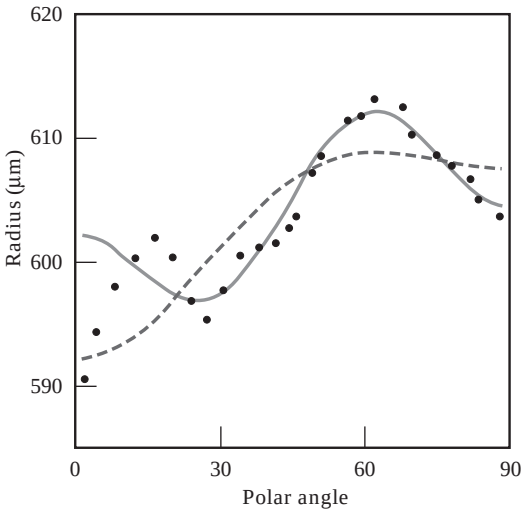

FIGURE 4. Measured (dots) and Legendre-fitted (curves) radius vs polar angle for 15-μm shell 6 ns into drive. Solid and dashed fits are with and without mode 6 (both include modes 0, 2, and 4).
(NIF-0602-05248pb01)

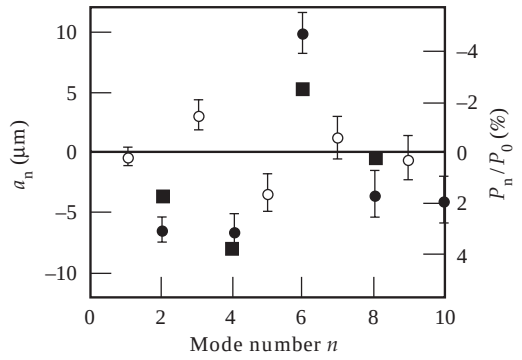

FIGURE 5. Measured (circles) and calculated (squares) modal amplitudes vs mode number for 15-μm shell at 6 ns into drive. Closed circles are even modes; open circles, odd modes. On right axis is average inferred flux asymmetry, showing 1% accuracy achieved.
(NIF-0602-05249pb01)

on NIF. It has been suggested that the roughened hohlraums have both a lower albedo and enhanced laser spot emission at early times before the roughness has time to smooth out. Since our backlit thin shell technique is most sensitive to the conditions inside the hohlraum just after shock breakout in the thin shell, we have studied the effects of the roughened hohlraums by looking at two cases: one where short-scale roughness is expected to smooth out before shock breakout in the capsule, and one where longer-scale roughness is expected to remain after shock breakout. We shot hohlraums with imposed sawtooth modulations: two with 60-μm period and two with 10-μm period, each with a modulation amplitude-to-wavelength ratio of 0.5. From 2D LASNEX simulations including wall surface roughness, we expected a change from 0% to +6% P_2 asymmetry imprinted on the thin shells at shock breakout when switching from smooth to the longer wavelength roughness hohlraums, consistent with reduced albedo for rougher hohlraums. By contrast, from the data we inferred a change in P_2 asymmetry imposed from 3.5% to –1% ± 1%. However, 3D viewfactor simulations using the exact beam energies reproduced this opposite trend in P_2 asymmetry swing (from 3% to –2.5%). Since the 3D viewfactor simulations ignored roughness, we conclude that roughened hohlraums in the experiment led to only a +1 ± 1% increase in P_2 flux asymmetry. Other diagnostics on the shots included a photo conductive detector (PCD) and the Commissariat a l´Energie Atomique (CEA) diode array for drive measurements, which unexpectedly did not show any significant (<5% flux) differences between the rough and smooth cases. Simulations predicted a 20% and 15% decrease in flux at 1 ns and 3.5 ns respectively for roughened hohlraums attributed to increased hohlraum wall surface area. The drive discrepancy is currently attributed to possibly better than calculated conversion efficiency in roughened hohlraums offsetting increased surface area losses.

Analytic work on thin shell implosion dynamics was completed and published.[1, 2] Except at very early times during the implosion, the response of the shell acceleration g to the ablation pressure P_r is not exactly linear due to variations in time of the shell areal density. Expressed in terms of a power law $g \sim P_r^c$, where $c = 1$ represents linear behavior, c rises to 1.3 for shells converged by 50%. Fortunately, the greatest sensitivity of the shell is to asymmetries occurring right after shock breakout before

the shell has converged appreciably and when c is <1.2. The thin shell technique can be compromised by initial variations in the shell areal density. For example, an initial 0.5% sixth-order Legendre variation in shell thickness can lead to an ≈4 μm a_6 by the time a 1-mm-radius shell has converged to half of its initial radius, comparable in magnitude to the distortions likely from intrinsic flux asymmetries we are trying to isolate. Thus, carefully characterizing the initial thickness uniformity of the thin shells fielded on OMEGA and eventually NIF is essential for maintaining integrity of the experiments as a measure of flux asymmetry. We have employed spectral interferometry for providing the sub-μm accuracy needed. Measurements on shell thickness show as much as 0.5 μm P_1 offset, as much as 0.1 μm P_2, and negligible (<.03 μm) thickness variations in higher modes. Since these represent <0.2% higher order shell thickness variations for the 15-μm shell used, we expect <0.25-μm higher order distortions after 130-μm shell travel, much less than the measurement error bars or data. The use of thin shells as a means of measuring drive near target center has also been examined through calculations. Comparison of radiation-hydrodynamics simulations and an analytical model shows good agreement and indicates some promise as a viable drive diagnostic. Finally, simulations have shown that the flux asymmetry modes n of importance (n <10) grow secularly in time and are amenable to a simple 1D rocket model analysis.

For future experimental series, several improvements are planned. First, using a 1-μm Gd patch rather than 0.5-μm Au along the line-of-sight should provide 3× lower opacity to the Ti backlighter radiation while matching the Au low-temperature albedo. To avoid Gd oxidation and cracking, we are considering thin (0.1-μm) Au-lined Gd. Thinner Au patches (0.25-μm each) which have 2.5× more transmission at 4.75 keV also appear to be an option again since the thin shells are most sensitive to early-time albedo (t < 2 ns). In either case, these alternate patches should also reduce the additional source of noise on images due to nonuniform transmission resulting from Rayleigh–Taylor unstable patch acceleration. Second, we will switch from a 6-fold to a 10-fold azimuthal geometry for the inner cone to further mitigate azimuthal asymmetries. This will also have the advantage of providing a Dante view through the laser entrance hole (LEH) for better drive measurements. Third, the power ratio between the inner and outer beams will be optimized to minimize both P_2 and P_4 for better isolation of the effects of P_6. Finally, shots varying the case-to-shell radius ratio and/or beam pointing to change the level of P_6 asymmetry will be designed for FY02 shots to begin P_6 symmetry control and check the fidelity of the surrogate backlit shell.

Scaling Current Drive Asymmetry Measurement Techniques to NIF-Size

A first pass at the experimental geometry for symmetry diagnosis on NIF was completed for the various ramp-up stages of NIF (4-fold 2-cone, 8-fold 2-cone, and full NIF). Two principal classes of experiments were considered, backlighting of foamballs and shells, and imaging self-emission from imploded capsules.[3] In each case the present OMEGA setup was scaled to full NIF operation[4] with the constraints of maintaining or improving the number of photons/resolution element while avoiding debris damage to the instrument.

For the scaled backlit foam ball point projection geometry[5, 6, 7] (see Figure 6), Table 1 shows that the fluence/resolution element can be maintained between OMEGA and NIF by using a single 3-TW NIF beam per backlighter point source. The strategy here has been to maximize the distance between point backlighter and hohlraum (set by the extent of NIF laser beam travel [±2.5–3 cm]). This allows us to increase detector standoff distance and hence survivability for a given magnification, and to avoid large angular field-of-views which are distorted by the nonuniform angular sensitivity of microchannel plates (MCPs)[8] used as detectors. We expect further improvements in backlighter fluence by eventually switching to more efficient underdense emitters,[9] which have been demonstrated up to 13 keV.

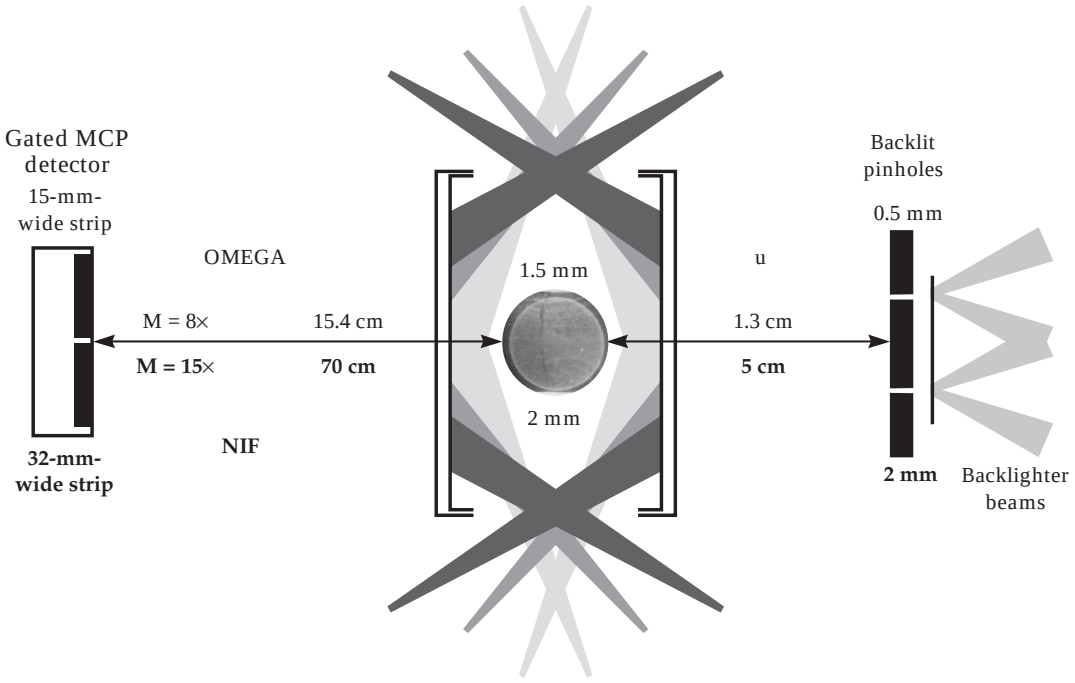

FIGURE 6. OMEGA (upper half) and proposed scaled NIF experimental parameters (lower half) for backlighting foam ball or shell. (NIF-0602-05250pb01)

TABLE 1. Comparison of photon fluxes at backlit pinhole in OMEGA vs proposed NIF configuration.

Facility	P_B (GW)	u (cm)	Flux at hohlraum center $\sim P_L / 4\pi u^2$
OMEGA	200	1.3	9.4
NIF (1 beam)	3000	5	9.5

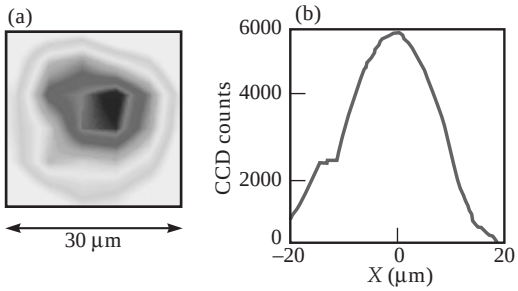

FIGURE 7. (a) 100× magnification, 5 µm-resolution, 4-keV x-ray image of imploded core taken using target-mounted pinhole array at 4 mm to capsule. (b) Horizontal lineout showing low noise due to high collection efficiency. (NIF-0602-05251pb01)

For core imaging, the strategy has been to maximize collection efficiency by minimizing pinhole distance while allowing for 10× larger magnifications than had been used before (100× vs 10×). Successful 4-mm distant target-mounted 5-µm pinhole imaging has been demonstrated at OMEGA (see Figure 7). We note the noticeable a_4 asymmetry on the core image, now easily discerned because of the ultrahigh magnifica-tion, large collection solid angle, and use of charge-coupled device (CCD) recording medium rather than noisier film.[10] Scaling to NIF leads to 1 cm-distant target-mounted pinholes (see Figure 8).

In addition to simple geometric scaling, we have iterated on the choice of back lighter orientations and diagnostic instrument manipulator (DIM) detector locations as the NIF ramp-up plan has evolved. Finally, a typical NIF backlit shell or foam ball experimental setup describing all target dimensions, orientations, and materials was distributed to NIF Mission Support staff for detailed evaluation of debris issues. In particular, typical 50-mg target-mounted pinholes were calculated to be acceptable sources of shrapnel and debris, especially since located on the waist where there is no final NIF optics.

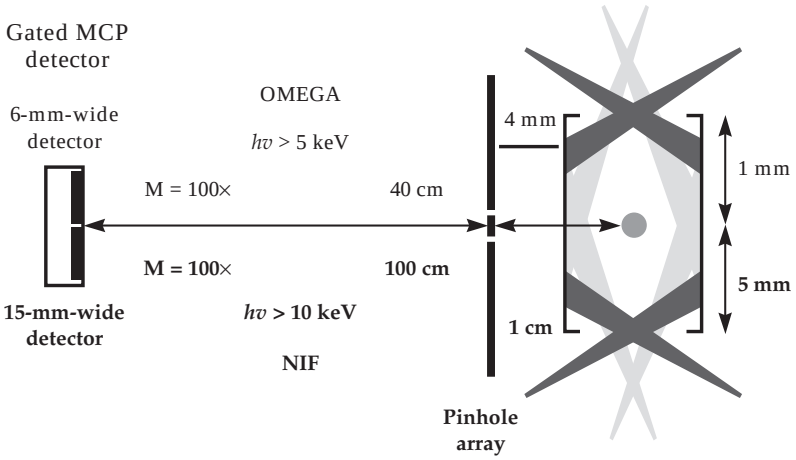

FIGURE 8. OMEGA (upper half) and proposed scaled NIF experimental geometry (lower half) for high-magnification x-ray imaging of imploded cores using target-mounted pinholes. (NIF-0602-05252pb01)

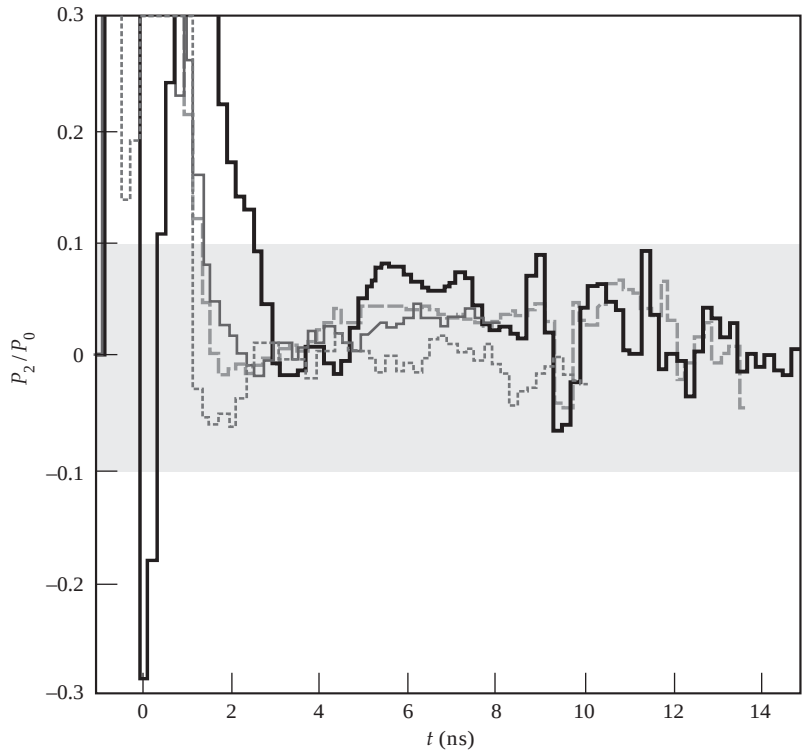

FIGURE 9. Second Legendre ablation pressure asymmetry in NIF ignition hohlraum inferred from distortions of igniting Br-doped capsule (thick solid line), 0.1 g/cm^3 SiO_2 foamball (thin solid line), 0.3 g/cm^3 SiO_2 foamball (long dashed line) and 15-µm-thick Ge-doped shell (short dashed line). Dashed area corresponds to ±10% P_2 variation, tolerable over any 2-ns interval. (NIF-0602-05253pb01)

Viability of Backlit Foam Ball and Shell Techniques for Assessing Asymmetry throughout NIF Ignition Hohlraum Drive

Simulations checking the degree of surrogacy of thin shells and foam balls under a NIF-like symmetry condition allowing for ignition have begun. The simulated symmetry histories of a 0.25% Br-doped NIF-scale CH capsule have been compared with those from same initial size foam ball and thin-shell capsule in gas-filled NIF hohlraums. Figure 9 compares the inferred P_2 asymmetry at the NIF ignition capsule compared to three surrogates. We note that all the surrogates match the P_2 time history witnessed by the igniting capsule to within the ignition-tolerable ±10% P_2 swings over any 2-ns interval. This suggests fidelity of these surrogates would be sufficient to validate tolerable levels of P_2 asymmetry. Next year, more simulations testing surrogacy for untuned cases will be conducted, for both foam balls and thin shells of various thicknesses.

Near-1D Performance from High-Convergence Implosions with Dopant-Free Fuel

A campaign of moderate and high-convergence, high–growth-factor implosions continued at OMEGA using a NIF- or LMJ-like multiple-cone[11] 40-beam hohlraum illumination geometry[12] (see Figure 10). The goal is to demonstrate improved implosion performance as a consequence of having improved symmetry over previous Nova hohlraums illuminated by a single cone per side and just 10 beams,[13, 14] and over previous OMEGA hohlraums driven by staggered sets of beams.[15] The major accomplishment over the last two years has been demonstrating close to calculated performance for the higher convergence targets by removing the Ar x-ray tracers used in the fuel.

The majority of the OMEGA implosions were driven by a 6:1 contrast, 2.5-ns-long pulse (PS26) (see Figure 11a) in Scale 1

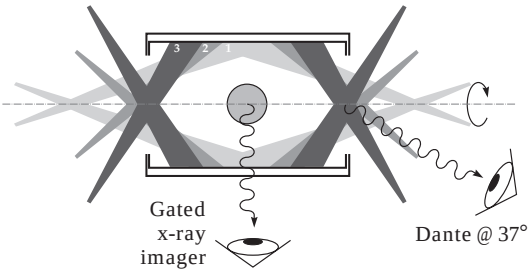

FIGURE 10. Hohlraum illumination geometry at OMEGA with important lines-of-sight shown.
(NIF-0602-05254pb01)

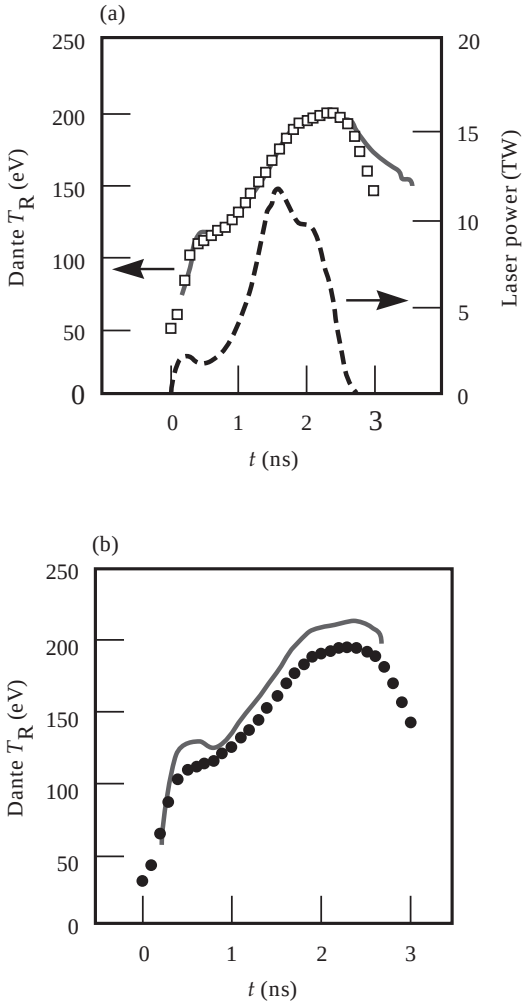

FIGURE 11. (a) Measured (squares) and calculated (solid line) gold hohlraum drive temperature as measured through LEH by Dante. Also plotted is laser power profile (dashed line). (b) Measured (closed circles) and calculated (solid line) cocktail hohlraum drive temperature as measured through LEH by Dante.
(NIF-0602-05255pb01)

(2.5-mm-long by 1.6-mm-diam) Au hohlraums. The beam-to-beam energy balance was good, 4–5%. The peak drive temperature as measured through the LEH was 200 eV. The full drive history is in excellent agreement with simulations including the latest Dante recalibrations and without assuming any significant (>10%) backscatter losses (see Figure 11a).

Capsule ablators consist of smooth 1% Ge-doped plastic, with surface roughness between 0.01 and 0.03 μm rms. The capsules were filled with D_2 and on some shots, an additional 0.05-0.25 atm Ar for providing brighter core x-ray images. The convergence ratio was progressively increased by reducing the initial capsule fill from 50 atm to 5 atm D_2. The final cores were imaged in emission at 4 keV with 21×, 5-μm, 70-ps resolution. As a further proof of understanding the drive, we note that the measured and calculated peak x-ray emission times at stagnation are also in agreement (see Figure 12). The measured x-ray core shapes were close to round with residual distortions only 20% different from those calculated by LASNEX, translating to <2% offset between the experimentally inferred and calculated time-integrated P_2 asymmetry (see Figure 13).

Figure 14 compares the measured neutron yield from Ar-filled and Ar-free implosions normalized to postshot simulations of

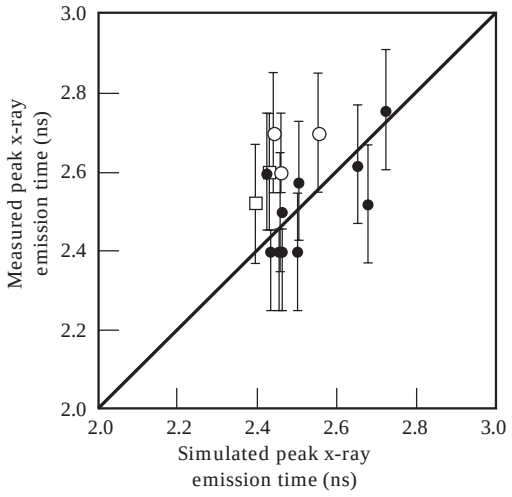

FIGURE 12. Measured vs calculated peak x-ray emission time of implosions. (NIF-0602-05256pb01)

clean yields for both 50 atm and 10 atm fill implosions. We note that just adding 0.5% Ar leads to a 2× greater degradation in yield than expected from simulations. Specifically, simulations predict a 2× yield degradation from adding 0.5% Ar while the results show on average a 4× degradation with 100% data scatter (from 8×10^8 to 2×10^8 neutrons). By contrast, we find that the 10 atm-fill implosions without Ar are performing consistently at close to 40% of 2D clean yield. Figure 15 plots the measured Ar-free yields vs inferred convergence normalized to 2D simulations. When the effects of mix are included, the measured 50 atm (10 atm) fill yields reach 100% (70%) of calculated, respectively. This is to be contrasted with the 40% of calculated achieved at Nova for 50 atm fill capsules. The measured and calculated convergence ratios inferred from the secondary to primary yield ratio are plotted in Figure 16, showing a systematic offset.

Two 10 atm, D_2 fill Ar-free implosions were also shot in a U / Nb / Dy-based "cocktail" hohlraum predicted to yield a 15-eV

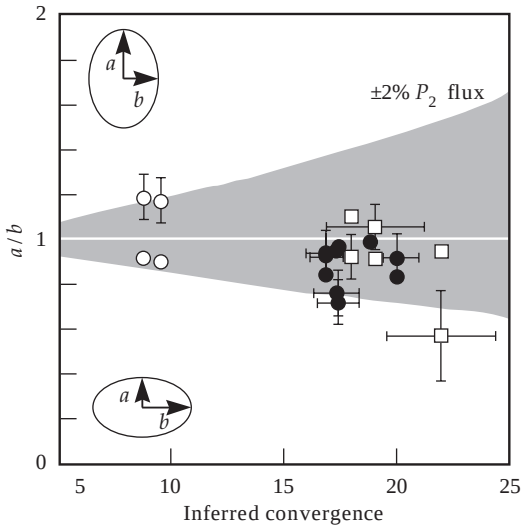

FIGURE 13. Measured and calculated core ellipticities vs inferred convergence ratio for capsules with 50 atm (open circles), 10 atm (closed circles), and 5 atm (open squares) initial D_2 fill. Symbols with error bars are data and other symbols are post-shot simulation results. Gray area denotes distortions expected for <2% average P_2 flux asymmetry.
(NIF-0602-05257pb01)

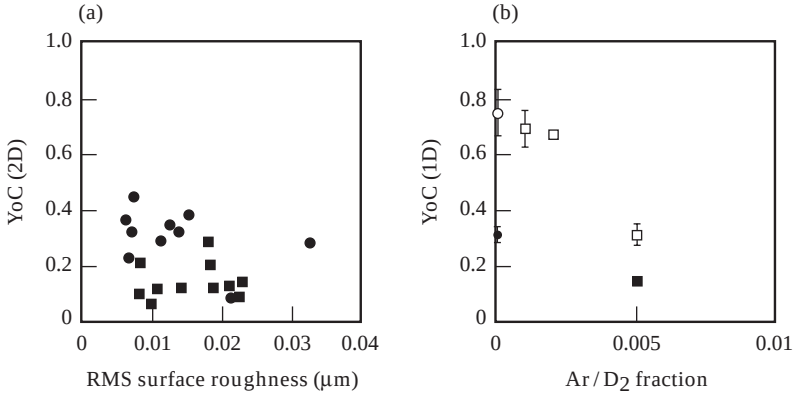

FIGURE 14. (a) Ratio of measured to clean 2D calculated yield as a function of initial surface roughness ratio for 10 atm D_2 fill capsules with 0.05 atm Ar (squares) and without Ar (circles). (b) Ratio of measured to clean 1D calculated yield as a function of Ar to D_2 fill initial fraction capsules for 50 atm D_2 fill (open symbols) and 10 atm D_2 fill (closed symbols).
(NIF-0602-05258pb01)

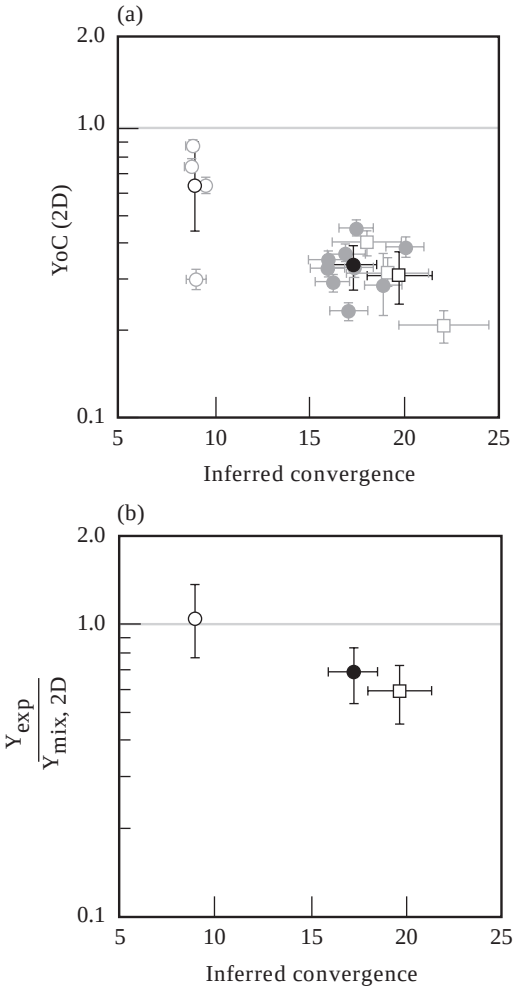

FIGURE 15. a) Ratio of measured to clean 2D calculated yield as a function of inferred convergence ratio. (b) Ratio of measured to 2D calculated yield including mix as a function of inferred convergence ratio. Open circles, closed circles, and open square represent Ar-free 50 atm, 10 atm, and 5 atm initial D_2 fill, respectively. Gray symbols are individual shots and black symbols are averages.
(NIF-0602-05259pb01)

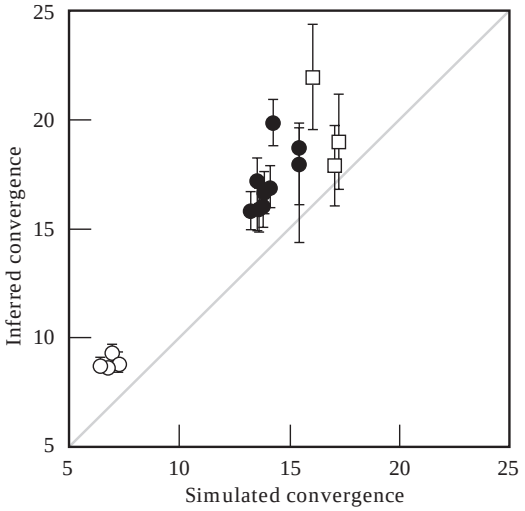

FIGURE 16. Measured vs calculated convergence ratio inferred from the ratio of measured secondary to primary neutron yield. Open circles, closed circles, and open squares represent Ar-free 50 atm, 10 atm, and 5 atm initial D_2 fill, respectively. (NIF-0602-05260pb01)

higher peak drive temperature and 200-ps shorter implosion times due to increased albedo. In fact, the measured temperature was very similar to the gold hohlraum case (see Figure 11b). Moreover, the measured primary neutron yields for implosions in Au and cocktail hohlraums were identical within the 30% scatter and the measured peak x-ray emission times were identical to the ±50 ps level. Figure 17 does show a measurable difference in core image ellipticity (a/b) between implosions in Au and cocktail hohlraums. However, the 40% average difference in these core ellipticities translates to only an ≈2% difference in pole-to-equator flux asymmetry. These results suggest that the increased albedo for cocktail hohlraums as measured as part of the Hohlraum Energetics Project may be offset by reduced laser absorption or x-ray conversion efficiency. The solution for such a problem would be to use Au-lined cocktail hohlraums, to be tested in FY02.

The other issues remaining are the tendencies for the simulations to overpredict YoC performance by a factor-of-two in the presence of argon and the near factor-of-two underprediction in DT/DD neutron ratio for the higher fill, lower convergence targets. With regard to the first discrepancy, we have begun to explore better models of radiative cooling by Ar and, in particular, the atomic kinetics and line-transfer properties[16, 17] of mid-Z dopants at relevant 1-keV temperatures. With regard to the second discrepancy, we are comparing the measured and calculated secondary neutron yield spectrum, which could provide a correction to the inferred areal density and, hence, convergence.

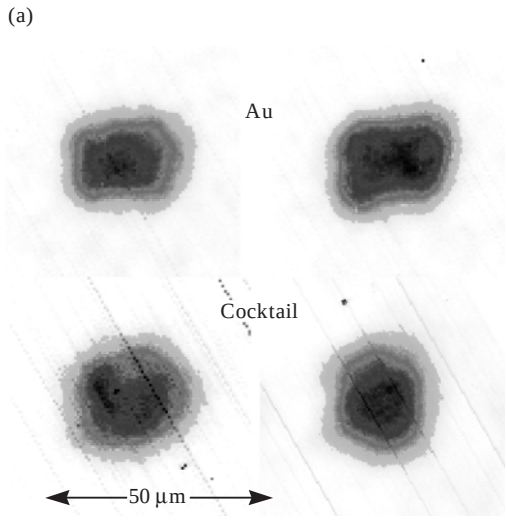

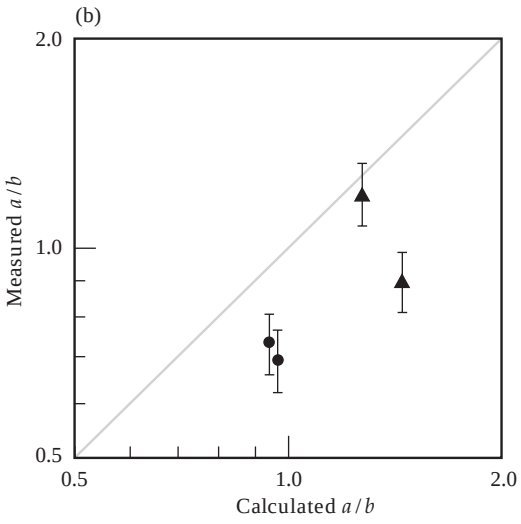

FIGURE 17. (a) Comparison of 24× magnification, 5-µm, 40-ps resolution core x-ray images from 10 atm D_2 fill implosions in two Au and two cocktail hohlraums. (b) Measured vs calculated core ellipticities for implosions in gold (circles) and cocktail (triangles) hohlraums. (NIF-0602-05261pb01)

Notes and References

1. S. M. Pollaine, D. K. Bradley, O. L. Landen, R. J. Wallace, O. S. Jones, P. A. Amendt, L. J. Suter, and R. E. Turner, "National Ignition Facility-scale Hohlraum Asymmetry Studies by Thin Shell Radiography," *Phys. Plasmas* 8, 2357–2364 (2001).
2. P. A. Amendt, A. I. Shestakov, O. L. Landen, S. M. Pollaine, D. K. Bradley, L. J. Suter, and R. E. Turner, "Implosion Target Surrogacy Studies on OMEGA for the NIF: Backlit Thin Shells," *Phys. Plasmas* 8, 2908–2917 (2001).
3. O. L. Landen, D. K. Bradley, S. M. Pollaine, P. A. Amendt, S. G. Glendinning, O. S. Jones, L. J. Suter, R. E. Turner, R. J. Wallace, B. A. Hammel, N. D. Delamater, J. Wallace, G. Magelssen, and P. Gobby, "Indirect-Drive Time-Dependent Symmetry Diagnosis at NIF-Scale," in *Proc. of Inertial Fusion Science and Applications* 99, C. Labaune, W. J. Hogan, and K. A. Tanaka, Eds. (Elsevier, Paris, 2000), p. 174.
4. J. D. Lindl, P. A. Amendt, N. D. Delamater, S. G. Glendinning, S. W. Haan, O. L. Landen, T. J. Murphy, L. J. Suter, et al., "Review of the National Ignition Facility Target Designs and the Nova Technical Contract on Indirect Drive ICF (Including Recent Extensions to the OMEGA Laser)," submitted to *Phys. Plasmas*.
5. D. K. Bradley, O. L. Landen, A. B. Bullock, S. G. Glendinning, and R. E. Turner, "Efficient, 1-100 keV X-ray Radiography with High Spatial and Temporal Resolution," *Opt. Lett*. 27, 134–136 (2002).
6. O. L. Landen, D. R. Farley, S. G. Glendinning, et al., "X-ray Backlighting for the National Ignition Facility," *Rev. Sci. Instrum*. 72, 627 (2001).
7. A. B. Bullock, O. L. Landen, and D. K. Bradley, "10 and 5 μm Pinhole-Assisted Point-Projection Backlit Imaging for the National Ignition Facility," *Rev. Sci. Instrum*. 72, 690 (2001).
8. O. L. Landen, A. Lobban, T. Tutt, et al., "Angular Sensitivity of Gated Microchannel Plate Framing Cameras," *Rev. Sci. Instrum*. 72, 709 (2001).
9. C. A. Back, J. Grun, C. Decker, L. J. Suter, J. Davis, O. L. Landen, R. Wallace, W. W. Hsing, J. M. Laming, U. Feldman, M. C. Miller, and C. Wuest , "Efficient Multi-keV Underdense Laser-Produced Plasma Radiators," *Phys. Rev. Lett*. 87, 275003 (2001).
10. R. E. Turner, O. L. Landen, D. K. Bradley, et al., "Comparison of Charge Coupled Device vs Film Readouts for Gated Micro-Channel Plate Cameras," *Rev. Sci. Instrum*. 72, 706 (2001).
11. E. Dattolo, M. C. Monteil, S. Lafitte, et al., "Hohlraum X-Ray Drive Control: an Issue in the Design of LMJ / NIF Targets," in *Proc. of Inertial Fusion Science and Applications 99*, C. Labaune, W. J. Hogan, and K. A. Tanaka, Eds. (Elsevier, Paris, 2000), p. 158
12. O. L. Landen, P. A. Amendt, R. E. Turner, D. K. Bradley, L. J. Suter, R. J. Wallace, and B. A. Hammel, "High Convergence Implosion Symmetry in Cylindrical Hohlraums," in *Proc. of Inertial Fusion Science and Applications 99*, C. Labaune, W. J. Hogan, and K. A. Tanaka, Eds. (Elsevier, Paris, 2000), p. 178.
13. M. C. Monteil, F. Colin, S. Lafitte, et al., "Simulations of Radiation Symmetry Experiments at Nova and OMEGA," in *Proc. of Inertial Fusion Science and Applications 99*, C. Labaune, W. J. Hogan, and K. A. Tanaka, Eds. (Elsevier, Paris, 2000), p. 162.
14. N. D. Delamater, E. L. Lindman, G. R. Magelssen, B. H. Failor, T. J. Murphy, A. A. Hauer, P. Gobby, J. B. Moore, V. Gomez, K. Gifford, R. L. Kauffman, O. L. Landen, B. A. Hammel, G. Glendinning, L. V. Powers, L. J. Suter, S. Dixit, R. R. Peterson, and A. L. Richard, "Observation of Reduced Beam Deflection Using Smoothed Beams in Gas-Filled Hohlraum Symmetry Experiments at Nova," *Phys. Plasmas* 7, 1609 (2000).
15. R. E. Turner, P. A. Amendt, O. L. Landen, S. G. Glendinning, et al., "Demonstration of Time Dependent Symmetry Control in Hohlraums by the Use of Drive Beam Staggering," *Phys. of Plasmas* 7, 333 (2000).
16. S. H. Langer, H. A. Scott, M. M. Marinak, and O. L. Landen, "Towards a Complete Model of 3D Line Emission from ICF Capsules: Results from the First 3D Simulations," *J. of Quant. Spectrosc. & Radiat. Transfer* 65, 353 (2000).
17. S. H. Langer, H. A. Scott, M. M. Marinak, and O. L. Landen, "Modeling Titanium Line Emission from ICF Capsules in Three Dimensions," *J. of Quant. Spectrosc. & Radiat. Transfer* 71, 479–492 (2001).

Shock Timing and Capsule Optimization

G. W. Collins *S. W. Haan* *S. G. Glendining* *D. H. Munro*
P. M. Celliers *P. A. Amendt* *D. K. Bradley* *R. D. Olson*

The Shock Timing and Capsule Optimization effort will determine the best match of available drive pulse shapes and ablator designs (material compositions and dimensions) that give proper coalescence of shocks with adequate implosion stability and efficiency. To achieve ignition on the NIF, the laser energy must be applied in a precise temporal pulse shape in order to avoid sending shocks that are too strong or too weak through the DT fuel. If the shocks are too closely spaced, they overtake one another within the DT ice; if too widely spaced, the DT ice unloads to low density between shocks. In either case, the DT fuel winds up too hot too soon to achieve the required density for ignition. To set the pulse shape for an ignition capsule, we will first approximate the pulse shape through a series of radiation hydrodynamics simulations, varying the timing of the steps in laser power until the capsule ignites robustly in the simulation. Preliminary estimates suggest the relative timing between shocks need to be tuned to within 200 ps (this represents about 2% in foot shock velocity and within 5% in foot radiation drive). In addition to tuning the shocks in the fuel, we must ensure the fuel is not excessively preheated. To this end, another key objective is to ensure the ablator in an ignition capsule does not burn through. Finally, the capsule must have adequate stability. That is the final constraint on the drive, capsule composition, and capsule dimension.

Because of uncertainties in the overall laser-hohlraum-capsule coupling, the optimal laser pulse shape, and resulting shock timing, must be determined experimentally on NIF. In preparation for NIF campaigns, current experiments are developing diagnostics for shock tuning, detecting ablator burnthrough, and testing capsule stability. In addition, other experiments are testing our predictive capability with the top ablator candidates through a series of integrated experiments (Rayleigh–Taylor [R-T], burnthrough, and shock breakout). Sensitivity studies and integrated experiments determine what fundamental experiments are needed to test specific physics packages used in the hydrodynamic computer code LASNEX. To date simulations have placed more accurate requirements on shock timing and burnthrough diagnostics and have guided improvements in physics packages used in LASNEX for ignition capsule design.

The current experimental approach for timing shocks includes a series of planar face-on VISAR (velocity interferometer) measurements of the shock velocity in the fuel, planar side-on high-resolution radiography measurements of the interface and shock velocities of the fuel, and convergent side-on fuel-pusher interface velocity measurements (Figure 1a). During the early stages of NIF, we will use single-sided hohlraum drive to set the early part of the pulse shape and to debug diagnostics. An example target design for single-sided illumination is shown in Figure 1b. Our ablation rate shot plan includes a series of planar shock breakout and burnthrough

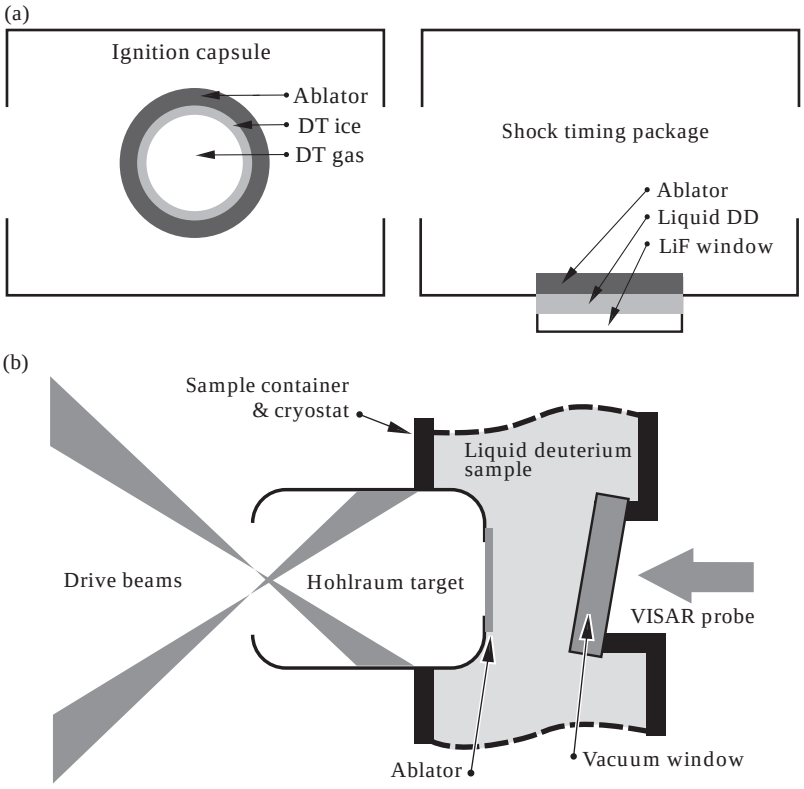

FIGURE 1. (a) Convergent and planar target designs for shock timing. (b) Single-sided hohlraum drive for early NIF experiments. LiF anvil might be inserted at a known distance inside target to ensure we are tracking the shock front in the deuterium.
(NIF-0602-05283pb01)

measurements early in time and then finishing with convergent experiments that detect when the ablation front is reaching a tracer layer in the ablator. Finally, to check target stability, we have planned a series of convergent R-T experiments. Our progress is described in order of our implementation plan, which includes: Sensitivity Studies, Ablator Characterization, and the Shock Timing and Capsule Optimization Diagnostic Development.

Sensitivity Studies

Sensitivity of the 300-eV Capsule Designs to the Fourth Shock Timing

In fiscal year 1999 (FY99), sensitivity studies established requirements for timing the first three shocks of NIF ignition capsules. From this we developed a detailed plan for verifying these shocks are tuned.

The fourth shock requirements, however, were not addressed. To set these requirements, were began by tuning the first three shocks (Figure 2) as described in the FY99 *ICF Annual Report* (timed so that first three shocks combine 5 μm below nominal spherical fuel thickness, the fourth shock comes in 500 ps later). Varying the fourth shock in one dimension (1D) (Figure 3) gives the requirement of timing of ±300 ps and drive to about ±15 eV. The timing required to achieve low entropy depends weakly on shock strength. Capsule performance degrades by the entropy being too large if the timing is early or late by 300 ps, by burning through if the peak temperature is high by 15 eV, and by the velocity being too low if the peak temperature is low by 15 eV. For these reasons, we now plan on measuring velocity through backlit implosions and bang time; burnthrough will be measured separately with doped backlit implosions.

It turns out that deceleration R-T is the tightest constraint on timing the fourth shock. Based on fall line penetration, the

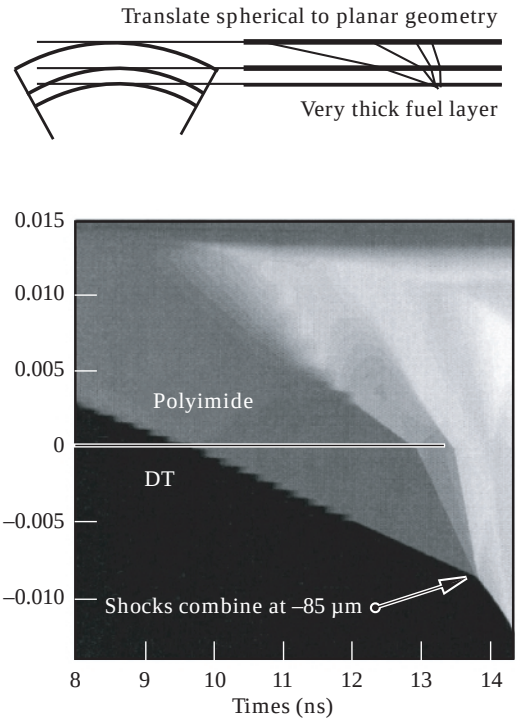

FIGURE 2. Log contours of pressure in planar simulations vs initial position. (NIF-0602-05284pb01)

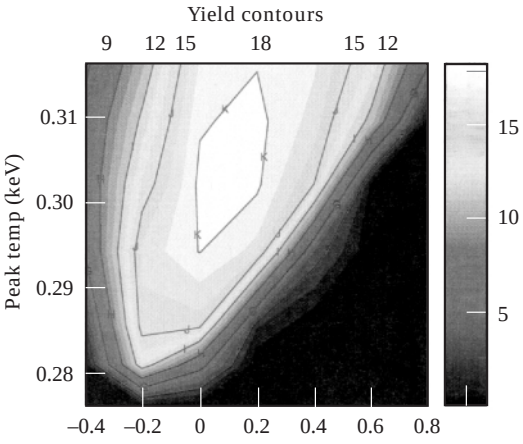

FIGURE 3. Contours of yield vs time and peak temperature of the fourth pulse. (NIF-0602-05285pb01)

requirement for shock timing for the fourth shock is ±150 ps. This is a rather tight constraint since it does not include the accumulation of errors from other aspects of the implosion and thus needs to be understood better.

Sensitivity of the 300-eV Polyimide and Beryllium Capsule Designs to Uncertainties in the EOS, Opacity, and Preheat

Sensitivity studies used a suite of 1D LASNEX calculations covering all 24 combinations of the following: polyimide or beryllium (plus 0.9% copper) ablator, QEOS model or Young[1] tabular for two DT equations of state (EOS), XSN code or opacity server for ablator opacity, and Planckian, nominal gold, or gold with doubled M-band for drive spectrum (Figure 4). The results show that both of Dittrich's designs are extremely robust in 1D. The point designs originally used QEOS, XSN, and gold spectrum to obtain the nominal yield of 18.0 MJ for the polyimide capsule and 18.8 MJ for the beryllium. The smallest yield over the entire set of 24 calculations is 16.2 MJ; the largest is 22.3 MJ. This range of variation is well within the operating space of the capsules.

The pulse shape in this study was not varied; all the capsules were shot with their nominal pulse shapes. Since none of the yield degradations was significant, reoptimizing the pulse shape for each case would not significantly change the overall results. Observable variations typically were as expected: The greater the preheat, the lower the yield, and the yield for the stiffer QEOS DT is always lower than the Young DT. The total yield variation due to preheat from Planckian to 2× gold M-band was about 10% for polyimide and 15% for beryllium. The difference between the two DT EOSs was likewise in the 10 to 15% range. The difference between the two opacity models was smaller for beryllium-copper; the yield changed only about 5% (XSN was lower yield with QEOS, but higher yield with Young tabular EOS). For the polyimide ablators, the effect of the opacity model was comparable to the effect of the EOS model, the change being especially large in combination with QEOS DT. This effect was traced to a bug in the server that creates the opacity tables; we have yet to rerun the faulty calculations in the sensitivity study.

We looked at the Atwood number between the ablator and fuel, and at the

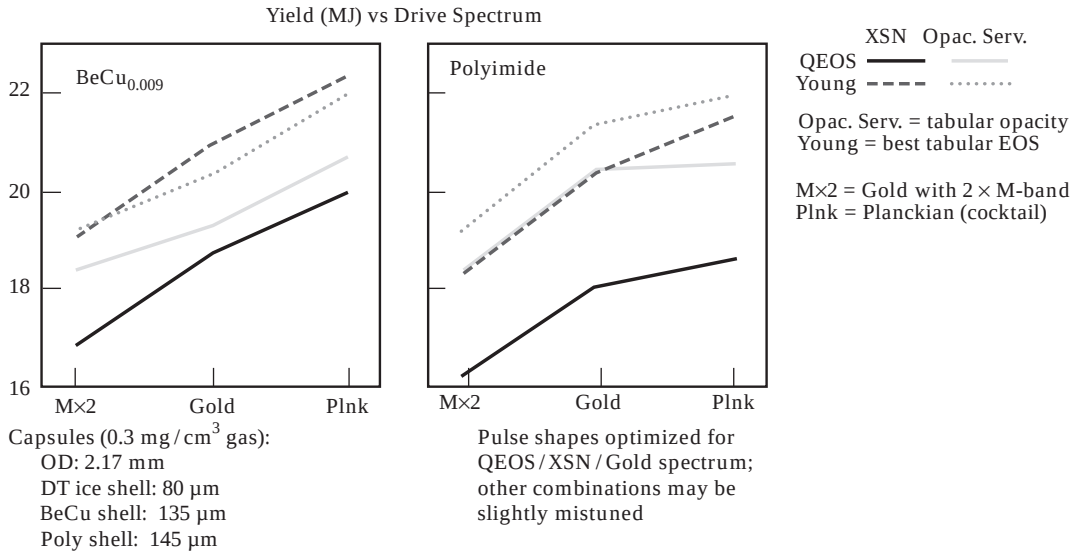

FIGURE 4. Be + 9% Cu and polyimide capsule yield vs drive spectrum (M×2 = gold opacity with twice the gold M-band, Plnk = Planckian spectrum) for different combinations of EOS and opacity models. (NIF-0602-05286apb01)

ablator thickness in order to assess the effect of the parameter variations on capsule stability. This study shows that the only parameter that significantly changes capsule stability is preheat. When these capsules reach half their initial radius, the fuel is denser than the ablator; the ablator thickens rapidly as the drive reaches 300 eV, and the ablation front thickness becomes comparable to the remaining ablator thickness. There is a thickness difference of about a factor of two between the thin shell with Planckian drive and the thick shell with 2× M-band drive. Another factor is the Atwood number; the thicker shells have an even lower density relative to the DT fuel, so the Atwood number is nearly twice as high (0.4) for the high preheat cases as for the low preheat cases (0.2).

A combined error in ablator opacity and flux onto the capsule will be difficult to ascertain experimentally, since we will not know either exactly, and to first order they have similar effects that could cancel. Lower opacity decreases the albedo of the ablator, making it absorb flux more efficiently. To first order the effect of decreased opacity is the same as that of increased flux. For example, an opacity multiplier of 0.5, combined with a flux multiplier of 0.8, results in an implosion with radius vs time history indistinguishable from the nominal implosion. (A slight time dependence in the flux multiplier is necessary to restore optimal pulse shaping.) At this opacity multiplier, the baseline polyimide ignition capsule fails. At opacity multiplier 0.625 (flux multiplier 0.85), the yield is reduced to 12.8 MJ from the nominal 17.5. Hence it would be valuable to be able to observe the effect of an opacity about 25% below nominal. (Future experiments will address how likely it is that the opacity is off this much from nominal.) The failure mode is ablator burnthrough; before ignition is achieved, the ablator becomes hot enough that x-ray preheat ruins the adiabat of the fuel.

Planned ablation rate experiments described below will develop techniques to ensure burnthrough does not occur in a NIF ignition capsule and provide integrated data to test current models. These experiments are in convergent rather than planar geometry. This is because when the same combination of opacity and flux multipliers stated above are used in a planar geometry simulation, there is very little, if any, observable effect. The balance between flux and opacity errors, which is adjusted to be such that the radius vs time history is the same, yields the same ablation rate in planar geometry. Hence a planar experiment cannot give useful data regarding this possible failure mode. In simulations of spherical geometry experiments, such as the backlit doped implosion series currently being explored on

OMEGA at the University of Rochester (UR), N.Y., there is observable impact of the combined opacity–flux multipliers.

In addition to the 1D results described above, a change in the ablation rate has a significant impact on R-T growth, both for NIF capsules and for current polyimide R-T experiments on OMEGA. For NIF capsules, the impact is time dependent, changing the time dependence of the R-T growth.

At intermediate times during the implosion, a multiplier of 0.75 on opacity (with corresponding flux multiplier so that the 1D hydro looks the same) changes the size of the perturbations by a factor of two for perturbations initially on the ablator, and by nearly an order of magnitude for perturbations initially on the ice. The net effect at ignition time is smaller: only about 15% for ablator perturbations, and a factor of two for ice perturbations as shown in Figure 5. For ablator perturbations a multiplier larger than unity causes more net R-T, while for ice perturbations a multiplier less than unity causes more net R-T growth. For the OMEGA experiments, a 0.5 multiplier decreases the perturbation growth by a factor of two. So OMEGA polyimide R-T experiments will be a useful constraint on our knowledge of the polyimide opacity, albeit at a lower temperature than NIF capsules.

Finally, beryllium capsule designs show robust performance over a broad energy range and are quite resilient to DT surface roughness. Beryllium, however, early in the implosion, may behave differently than an amorphous plastic as used for the NIF PT design ablator. Several issues are being addressed, such as anisotropy of shock propagation caused by Be anisotropy, opacity variations throughout the ablator perhaps caused by oxygen at grain boundaries or anisotropy of dopant, effect of defects caused by filling process. The first issue appears to be easily handled by ensuring the first shock during an ignition implosion melts the Be. To this end, we are determining the melt transition of Be ablators. Since the turn-on of the drive takes a finite time, a thin plastic coating on the exterior of the Be shell may be needed to delay the shock from entering the Be until the shock strength is high enough to melt it.

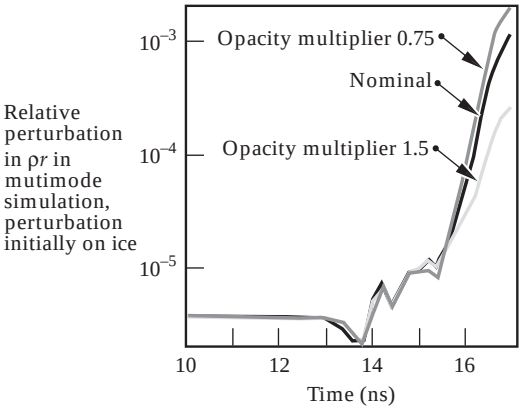

FIGURE 5. Relative Rayleigh–Taylor growth in a NIF capsule for different opacity multipliers (and associated drive multiplier so that the 1D hydro remained the same). (NIF-0602-05286bpb01)

Ablator Characterization Experiments in Halfraum Geometry

Several experiments on OMEGA were used to test our predictive capability with current ignition ablators. These experiments are led by Sandia National Laboratories (SNL) and are performed in collaboration with Los Alamos National Laboratory (LANL), LLNL, and UR. Indirect-drive burnthrough data for both polyimide and pure beryllium were collected in FY00 using a halfraum geometry (Figure 6a). These burnthrough data consisted of x-ray emission at 550 eV measured vs time, as shown in Figure 6b. The two timing fiducial beams shown in this figure provide an accurate time-tie of each pixel in the image to the laser pulse, and allows us to compare the data with the predictions of 2D LASNEX simulations. In FY01 the polyimide data set was expanded to include static x-ray imager (SXI) measurements at 700 eV and the first burnthrough measurements with Be + 0.9% Cu samples at both 550 eV and 700 eV at OMEGA. SXI images for 700-eV burnthrough of Be + 0.9% Cu and polyimide samples are shown in Figure 6c. A reference hole (t = 0) and 2-ns square laser pulses above and below the halfraum (t = 1, 2, 3,

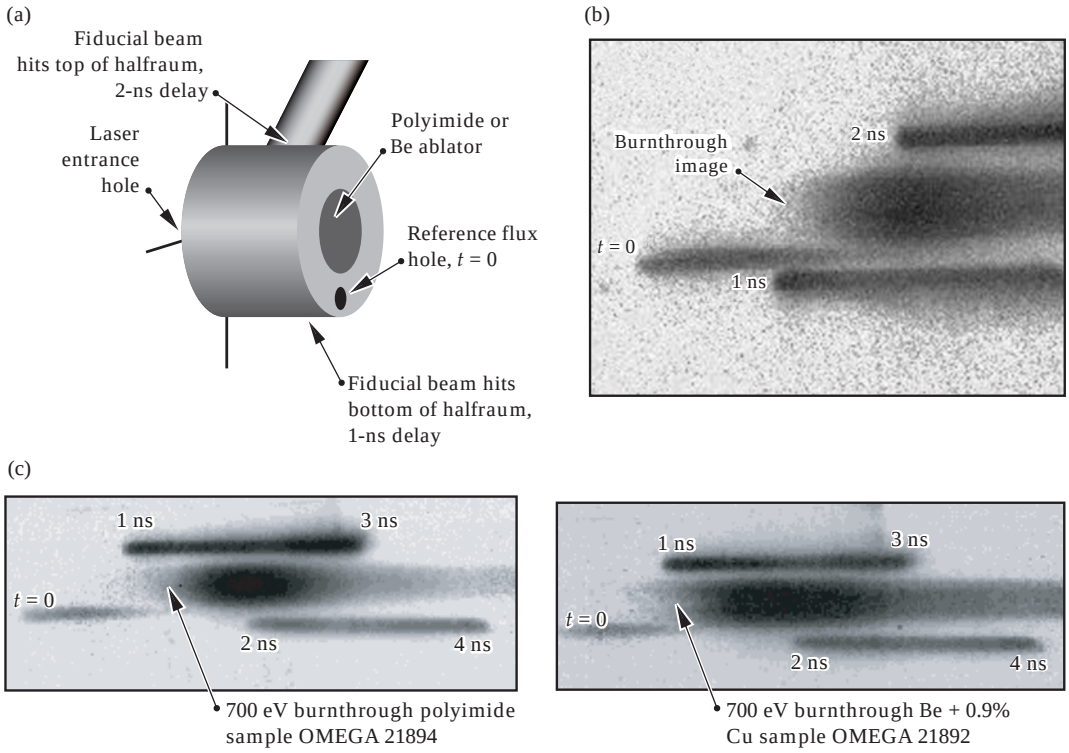

FIGURE 6. (a) Schematic of 1.6-mm-diam, 1.2-mm-long OMEGA halfraum. Fifteen drive beams are delivered in two cones through the laser entrance hole. (b) Streaked image of 550-eV x-rays on OMEGA shot 20162. A detailed lineout through the image indicates that burnthrough of the polyimide sample is within ~200 ps of the integrated preshot prediction with 2D LASNEX. (c) SXI images for 700-eV burnthrough in polyimide and Be + 0.9% Cu ablator samples. A reference hole (t = 0) and 2-ns square laser pulses above and below the halfraum (t = 1, 2, 3, and 4 ns) provide time fiducials for the streaked ablator burnthrough image.

and 4 ns) provide time fiducials for the streaked ablator burnthrough image. This again allows for accurate comparison with integrated 2D LASNEX simulations.

Comparison of LASNEX calculations and measurements of shock propagation in Be + 0.9% Cu is shown in Figure 7. The calculation uses the measured on-target 3ω laser power as input and, via a combination of 2D and 1D calculations, predicts the time-dependent 4.5-eV ultraviolet (UV) emission intensity that would be viewed by the streaked optical pyrometer (SOP) diagnostic.[2] The beryllium ablator shock breakout in OMEGA experiment 19021 is calculated to within ~200 ps. Comparison between LASNEX calculations and measurements for ablator burnthrough in polyimide samples is shown in Figure 8. The calculation uses the measured on-target 3ω laser power as input and predicts the time-dependent 550-eV x-ray emission intensity that would be viewed by the SXI diagnostic. Here, the polyimide burnthrough peak at 550 eV for OMEGA experiment 20162 is calculated to within ~200 ps.

Experimental shock breakout data for a Be + 0.9% Cu wedge, a Be + 0.9% Cu step, and polyimide step sample are all shown in Figure 9. The step samples confirm shock uniformity across the flats during early and late phases of shock breakout. An Au disk-target timing shot performed on the same day provides a time-tie for the fiducials in the SOP data. The Au wall reemission was measured with a soft x-ray framing camera and a photo conductive detector (PCD). These data will allow for an accurate comparison with integrated 2D LASNEX simulations. The wedge geometry provides a time-dependent measurement of shock velocity and will allow us to advance to multishock measurements planned for the upcoming fiscal year. Simulations at both SNL and LLNL model the shock-breakout halfraum experiments on OMEGA quite accurately. For the wedge Be-witness plates, both LLNL and SNL show excellent agreement with shock-breakout and Dante data.

Figure 10 shows the shock breakout position as a function of time for 1D calculations (independently done at both SNL and LLNL) for which the 21890 Dante T_r unfold was used as the drive. The data points represent the local intensity peak for the shock breakout along the length of the wedge.

Figure 11, in addition to the Dante unfold, also shows simulated Dante data that is generated via a postprocessing of a 2D integrated halfraum calculation. The Dante data used here was reduced using the Commissariat a L'Energie Atomique / Laboratoire Utilize de Radiation Electromagnetique (CEA / LURE) calibrations.

Polyimide R-T Growth Measurements vs Drive to Estimate Effects of Preheat on Polyimide

R-T experiments are extremely sensitive to material opacity and drive spectrum and thus are a stringent test of our ability to model NIF ablators. Previous beryllium R-T experiments showed that the opacity used in beryllium capsule designs needed to be changed.[3] We have begun a polyimide R-T campaign on OMEGA. Similar experiments were performed on Nova, but these showed less contrast than expected at all times. This was the result of a high sensitivity to the high-energy part of the backlighter spectrum. Generally the R-T experiments do not depend on this part of the spectrum, but for this particular combination of foil material, spectral filtering, and backlighter spectrum, the backlighter reduced the contrast significantly. Realistic extrapolations of the measured spectrum suggests that the ~4- to 7-keV component of the spectrum reduced the contrast by the observed ~40%. Because R-T growth is so sensitive to the drive, the OMEGA experiments simultaneously

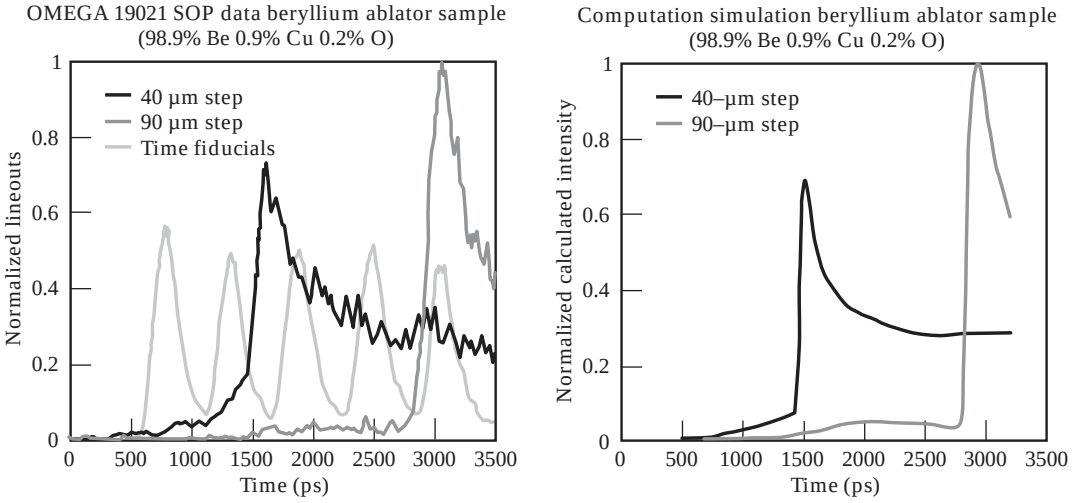

FIGURE 7. The most accurate calculation technique for Be + 0.9% Cu shock propagation uses a 2D integrated halfraum calculation to generate a detailed source for a 1D shock calculation. Lineouts through SOP data for 40-µm and 90-µm Be + 0.9% Cu steps used in OMEGA experiment 19021 are shown on the left. A computational simulation of the same experiment is shown on the right. (NIF-0602-05288apb01)

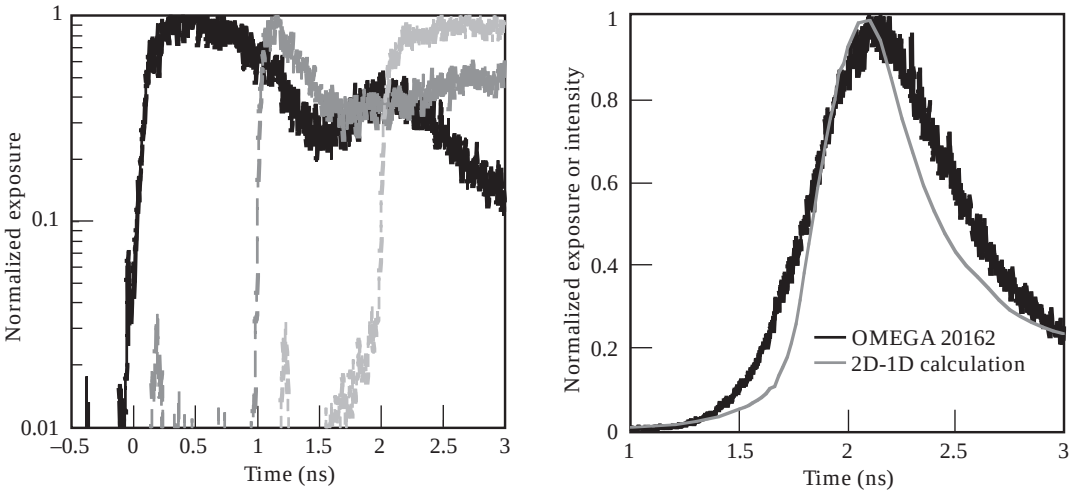

FIGURE 8. Calculation for polyimide ablator burnthrough using a 2D integrated halfraum calculation to generate a source for 1D ablator burnthrough calculation monitoring 550-eV x-ray emission. Lineouts through the SXI data for the 0-, 1-, and 2-ns fiducial pulses for OMEGA experiment 20162 are shown on the left. On the right is an overlay of the lineout through the 550-eV SXI burnthrough data for shot 20162 (black) and a computational simulation (gray). (NIF-0602-05288bpb01)

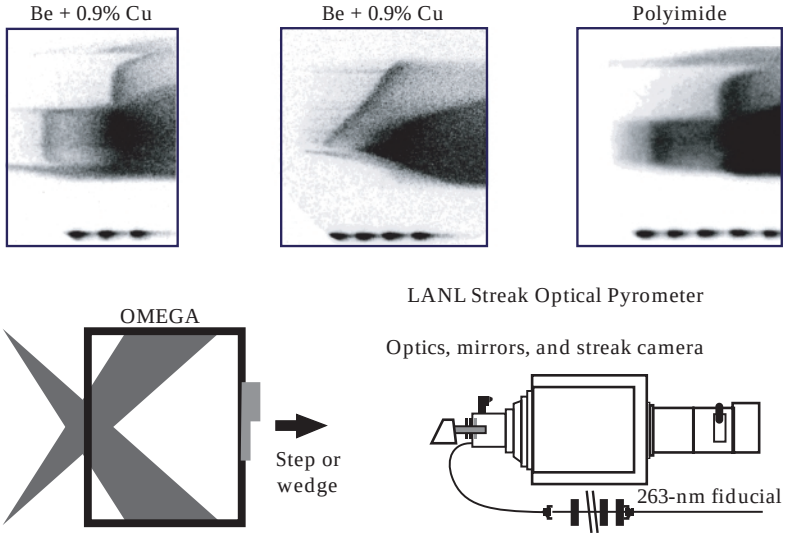

FIGURE 9. Data from the LANL streaked optical pyrometer (SOP) for a Be + 0.9% Cu step, Be + 0.9% Cu wedge, and PI step ablator samples. (NIF-0602-05290pb01)

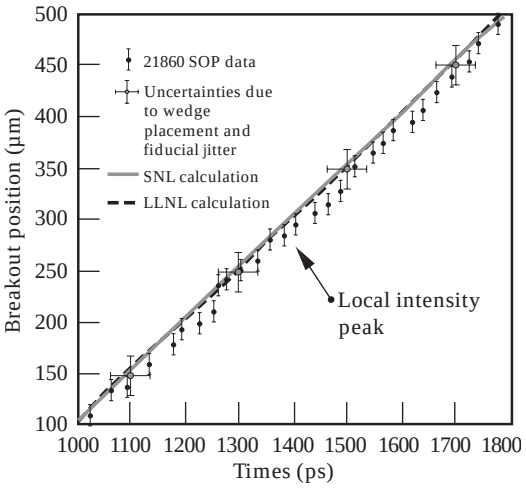

FIGURE 10. SOP wedge data from OMEGA shot 21860 together with calculations from SNL and LLNL. (NIF-0602-05291pb01)

measure Dante, 1D hydro, and R-T growth. The setup is shown in Figure 12a. This is the first time side-on trajectory, face-on modulation growth, initial contrast with the actual backlighter spectrum, and x-ray drive history have been measured simultaneously on each shot. Dante and hohlraum simulations agree quite well as shown in Figure 12b. The postprocessed Dante data (light gray) and simulated Dante are about 10 eV higher than the drive the package sees. This is due to a significant geometrical correction that needs to be added. These experiments revealed good contrast in the side-on images as shown in Figure 12c. Comparison between calculated and measured side-on trajectories is shown in Figure 12d. The hohlraum calculations predict the side-on measurement quite closely. Also shown are trajectories from three different experiments. The face-on images were not collected due to a manufacturing problem in the diagnostic holder.

Later in FY00, four polyimide R-T experiments gave face-on radiographs at three wavelengths, drive temperature, and side-on trajectory. Simulations with the measured laser pulses are shown in Figure 13 for the 30-μm (2-μm initial amplitude), 50-μm (1.6-μm initial amplitude) and 70-μm (1.9-μm initial amplitude) wavelength cases. The measured peak

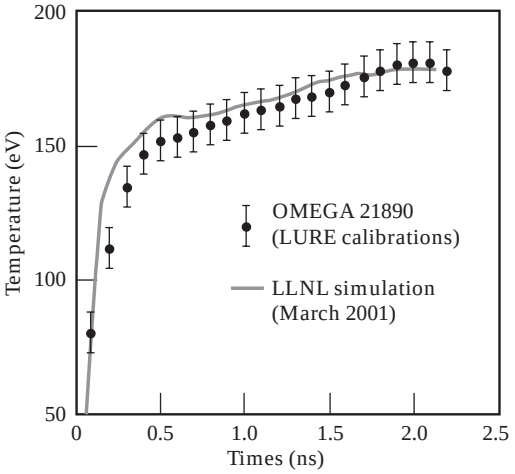

FIGURE 11. Dante data and simulated Dante data generated via postprocessing 2D integrated halfraum calculation. (NIF-0602-05292pb01)

temperature for these experiments was ~150 eV. These data compare well with simulations using OPAL opacities and calculated spectrum.

It appears likely that high-albedo ("cocktail") mixtures will be used for hohlraum walls on NIF ignition capsules. This changes the spectrum of radiation incident on the capsule and can affect the R-T growth. To optimize sensitivity to this, the growth needs to stay in the linear regime for as long as possible (small initial

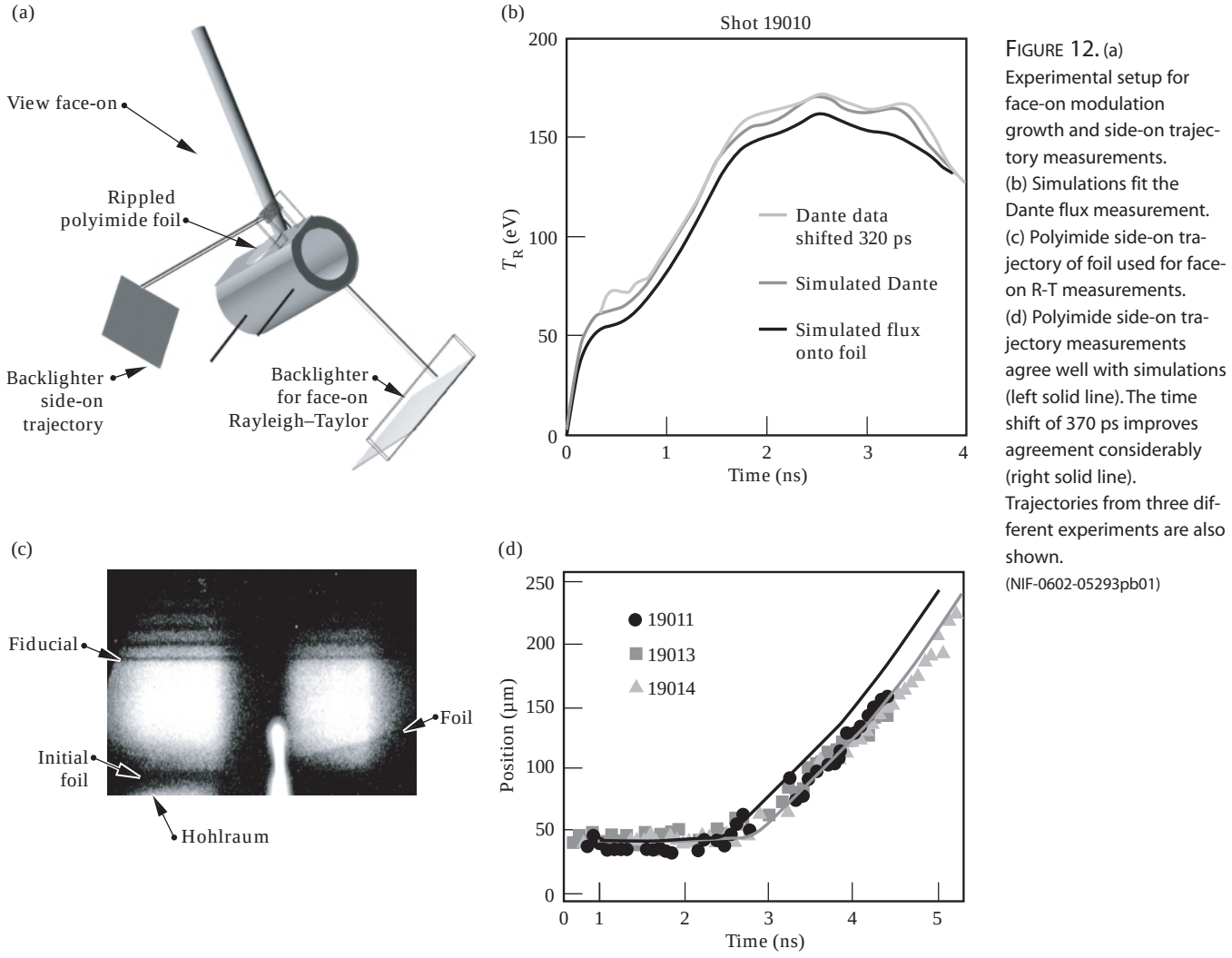

FIGURE 12. (a) Experimental setup for face-on modulation growth and side-on trajectory measurements. (b) Simulations fit the Dante flux measurement. (c) Polyimide side-on trajectory of foil used for face-on R-T measurements. (d) Polyimide side-on trajectory measurements agree well with simulations (left solid line). The time shift of 370 ps improves agreement considerably (right solid line). Trajectories from three different experiments are also shown. (NIF-0602-05293pb01)

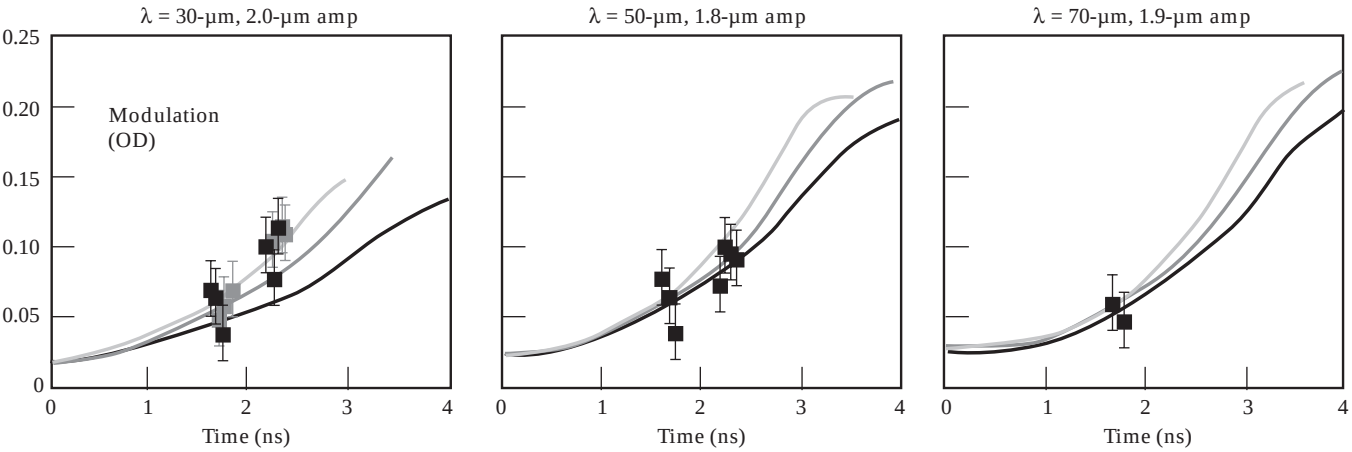

FIGURE 13. Face-on polyimide R-T experiments compared to simulations with a calculated spectrum, Dante drive, XSN opacities (black line), OPAL opacities, drive that matches side-ons and calculated spectrum (gray line), and OPAL opacities with Planckian spectrum (light gray line). (NIF-0602-05294pb01)

amplitude and large growth factors). As a rough estimate of the cocktail spectrum, we used a Planckian radiation source. This is actually a bit more extreme than expected cocktail spectra as shown in Figure 14. The spectral difference increases the growth in a typical simulated foil (50-μm wavelength, 0.5-μm initial amplitude) by a factor of about two. Preheat is noticeably reduced so that the density of the foil is about twice as large with a Planckian source. Hence there is likely to be an observable increase in perturbation growth with a cocktail wall.

One of four R-T experiments with Au hohlraums, similar to those described above albeit with lower initial amplitudes to obtain data more in the linear regime to compare with later cocktail spectra, is shown in Figures 15a and b. Growth was measured using 70-, 50-, and 30-μm wavelengths with initial perturbations amplitudes of 1, 0.5, and 0.5 μm respectively. The diagnostic noise was dramatically reduced in analysis for this round of shots by the use of instrument flat fielding.

The modulations in optical depth as a function of time for three wavelengths measured with low initial amplitudes are shown in Figures 16a–c. Analysis of the growth factors in optical depth gives about ten for the 70-μm data, about 25 for the 50-μm data, and about 20 for the 30-μm data.

We are now prepared to compare these Au hohlraum-driven data with cocktail-driven data. Late in FY01 four R-T experiments were conducted to determine the effect of drive spectra: two hohlraums were cocktails, one gold (shown in Figure 16), and one uranium. The drive data from the gold and cocktail hohlraums are shown below in Figures 17a–c. The M-band emission is shown in Figure 17b and appears to be lower in the two cocktail hohlraums. The laser drive ends at about 3.5 ns; the late time flux seen in the M-band channel is apparently due to the backlighter. The total spectrum at 2.5 ns is shown in Figure 17c; the cocktail hohlraums have enhanced emission near 1.5 keV. The gold hohlraum results are compared with previous (December 2000) results at 50 and 30 μm in Figure 16 and reproduce the previous results reasonably well. The cocktail hohlraum results were at 70 μm and are compared with previous gold hohlraum results in Figure 18. The R-T growth appears to have been enhanced in the cocktail hohlraums. However, the drive in the June 2001 cocktail experiments was significantly lower than in the gold

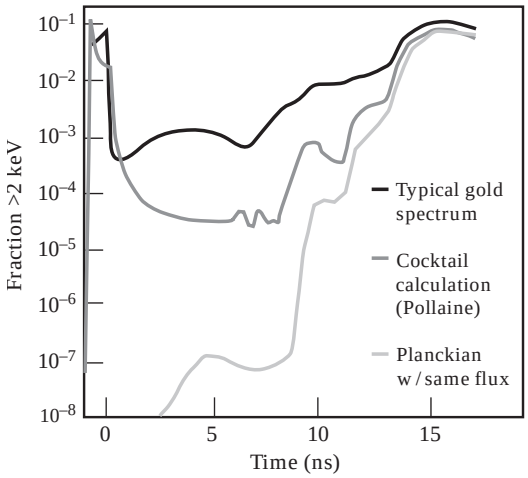

FIGURE 14. Fraction of spectrum above 2 keV for gold, cocktail, and Planckian drive. (NIF-0602-05295pb01)

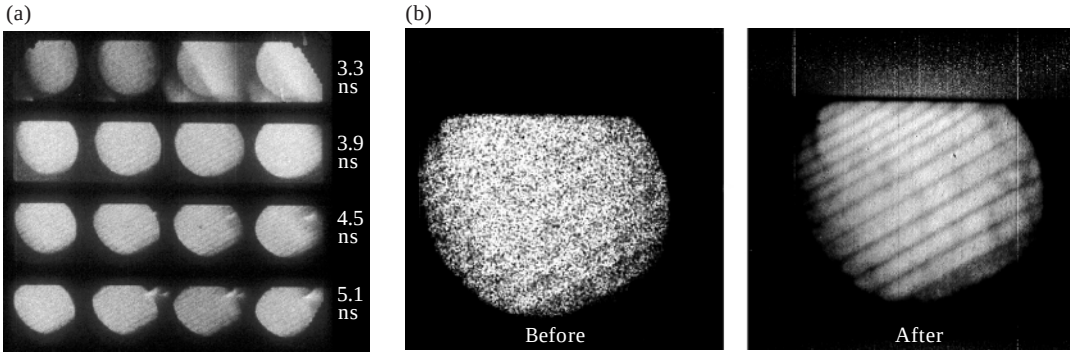

FIGURE 15. (a) Typical data with two wavelengths, $\lambda = 30$ and $\lambda = 50$ μm. (b) Image from data in (a), before and after flat fielding. (NIF-0602-05296pb01)

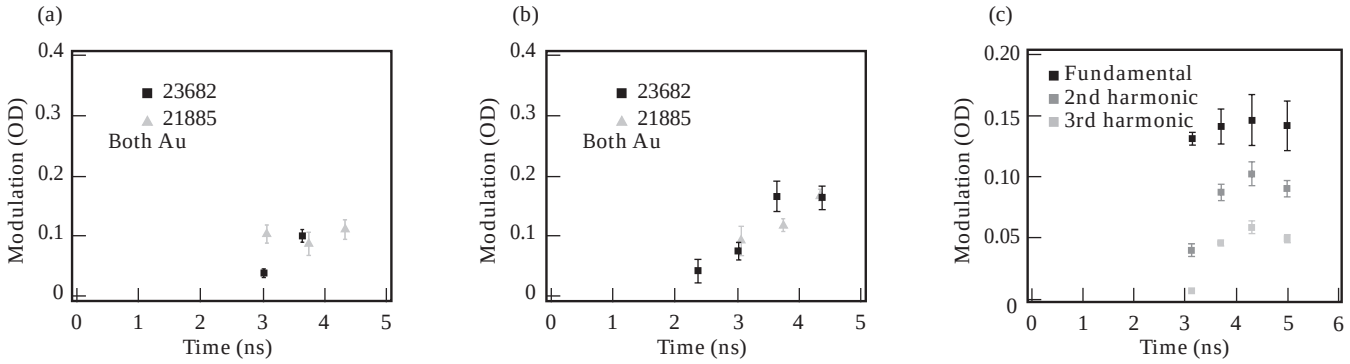

FIGURE 16. (a) R-T growth at 30 µm, June 2001 data (black) compared with December 2000 data (gray). (b) R-T growth at 50 µm, June 2001 data (black) compared with December 2000 data (gray). (c) Shot 21884 (70-µm wavelength) from December 2000. (NIF-0602-05297pb01)

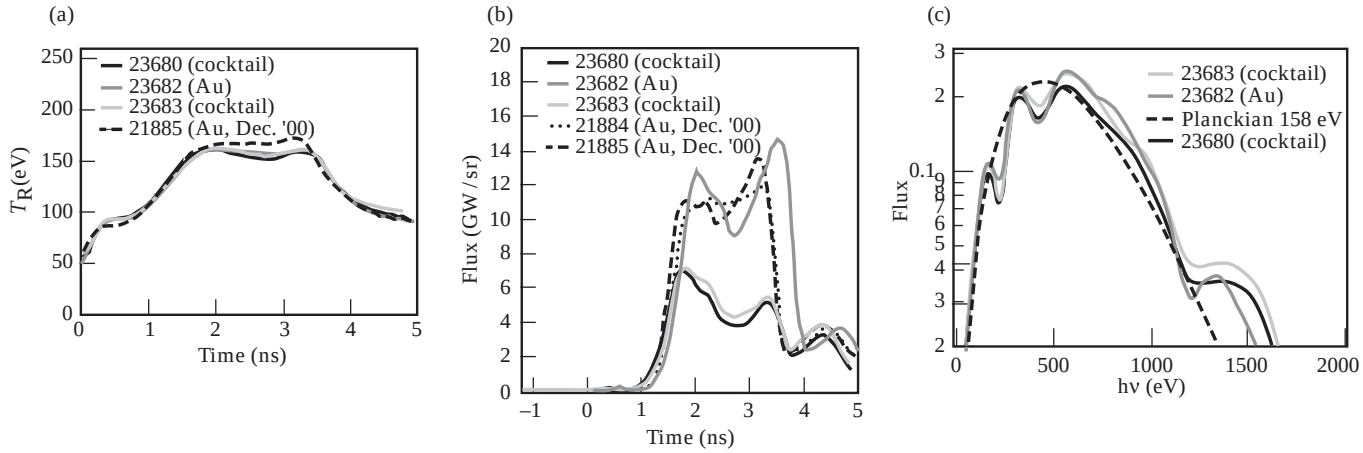

FIGURE 17. (a) Measured Dante T_R vs time for two cocktail and two gold hohlraums. The energy delivered was about 10.8 kJ in the recent experiments and about 10.7 kJ in December. (b) High-energy flux (>2 keV) Dante channel data for two cocktail and two gold hohlraums. (c) X-ray flux as a function of photon energy at 2.5 ns into the drive for two cocktail, one gold hohlraum, and a calculated Planckian. (NIF-0602-05298pb01)

comparison experiments of December 2000 (as seen in Figure 17a). The effect of this change in drive on R-T growth has not been calculated yet.

Using Backlit Implosions to Determine Burnthrough Time

As shown in FY99, a typical 300-eV design burns off ~90 to 95% of the ablator. If the ablator burns off, x-rays preheat the fuel. If the ablator burns off too little, the implosion velocity is reduced. A standard way to measure the ablation rate is by measuring the x-ray emission from a planar foil vs time as described previously. However, using planar measurements on the NIF to ensure we have not burned through is very difficult. There is a change in hydro of a simulated NIF implosion when the burnthrough varies by about 60 ps. For a planar experiment, a variation in peak drive of ~5% (which recall is the same constraint on the fourth shock drive) changes the burnthrough by about 60 ps. These suggest that the planar burnthrough from a planar foil would need to be measured to at least 60 ps if the planar foil burnthrough technique were used to ensure the ignition capsule did not burn through. This, however, does not take into account

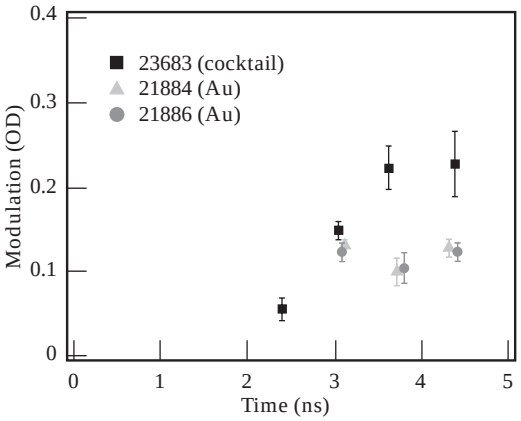

FIGURE 18. R-T growth at 70 µm, June 2001 data (cocktail) compared with December 2000 (Au) data. (NIF-0602-05299pb01)

the difference in flux at the hohlraum center vs the hohlraum wall, effects caused by convergence, or the spectral dependence of the burnthrough. For these reasons, the ablation rate (or more precisely the net material ablated during the implosion) needs to be checked in spherical geometry.

The experimental design we are pursuing to determine if the ablator has burned through in an ignition implosion begins with a heavily doped ablator interior (for example, with germanium). The shell is imaged with a backlighter at a photon energy optimized to see the interface between the doped and undoped regions at the time of interest. There is also the possibility of seeing when the shocks pass from the undoped to doped material—by seeing when the doped material starts to move. This will probably require quite high energies (possibly 12-keV backlighting) and high resolution on the NIF and will be described in detail below. With lower backlighter energy, we would expect to see the more gross motion of the shell and doped layer. First the doped layer will accelerate inward and then, when the ablation front reaches this layer, it will accelerate outward away from the imploding shell. It would give us a good measurement of the ablation rate, in the relevant spherical configuration. This measurement requires less precision and lower backlighter energy—perhaps 5 keV on NIF, with 5% Ge dopant. This concept is being tested on OMEGA, for which a 3- to 5-keV backlighter on a standard OMEGA capsule with a Ti-doped inner layer is clearly observed to turn around as the ablation front reaches it.

Five shots of backlit scale 1 hohlraum implosions were successfully carried out on OMEGA in November 2000 in support of ablator characterization and technique development effort. These PS26 experiments were designed to study the trajectory of the interface between a buried Ti-doped layer and the surrounding CH ablator in the imploding capsule. Simulations indicate that this trajectory shows an inflection point when the ablation surface reaches the doped layer. The experiments used area backlighting along the hohlraum axis at 13× magnification onto an x-ray framing camera filtered by 25-µm Fe to reduce thermal emission from the Au hohlraum plasma. The thin (7 µm) backlighter foils were irradiated by five OMEGA beams overlapped in a 600-µm spot on the side facing away from the hohlraum. Large (20 µm) pinholes and relatively long (180 ps) frame times were used to maximize the signal.

Data were collected for both Fe and V backlighters and for two different ablator thicknesses. The setup is shown in Figure 19. The position of the doped layer was very clear (a 3 to 5× dip in intensity).

Figure 20 shows a comparison between simulation and experiment for a 21.5-µm ablator. There is reasonable agreement in this case for the trajectory of both the minimum-transmission point and the 90% point. For thinner ablators, the agreement for the 90% point was less exact. However, the high signal levels were enough to drive the detector into slight saturation making the 90% transmission point difficult to accurately identify. Analysis of this data is ongoing.

The backlit implosions shown above show great promise, but we must determine if this technique is accurate enough for NIF. The answer is partially given in Figure 21 where shell radius is plotted versus ablator thickness. For a given radius uncertainty of 5 µm, we see this gives an uncertainty in mass ablated of $\Delta M/M \sim 4\%$. For NIF with the ~4× larger capsule radius, $\Delta M/M$ should be 1%, meeting the 2 to 3% NIF requirement in $\delta M/M$.

Shock Timing Technique Development

The VISAR shock measurement technique appears to be very well suited to measuring the strength and timing of the first three shocks in ignition implosions.

As part of our theoretical effort for shock-timing diagnostic development, we completed a paper on the Nova VISAR shock timing experiments.[4] We used two basic types of pulse shapes for the Nova VISAR experiments: 2-ns "square" pulses and 6-ns shaped pulses. While the 2-ns square data matches well with modeling described previously, the PS100 data has been harder to understand. Most of the PS100 shots show only a single shock data, which agrees with simulated shock velocities. Modeling for the three PS100 shots that show a second shock overtaking the first reveals how sensitive the shock overtake depth is to the details of the drive shape. We hope to be able to follow up this Nova VISAR work on OMEGA. In particular, we ought to be able to demonstrate reproducibility of the shock strength at OMEGA, and to extend the Nova results to higher drive. We know from Nova that the VISAR can work with a 150-eV hohlraum behind the ablator. However, for a NIF three-shock timing experiment with a drive pulse that is not truncated until shock

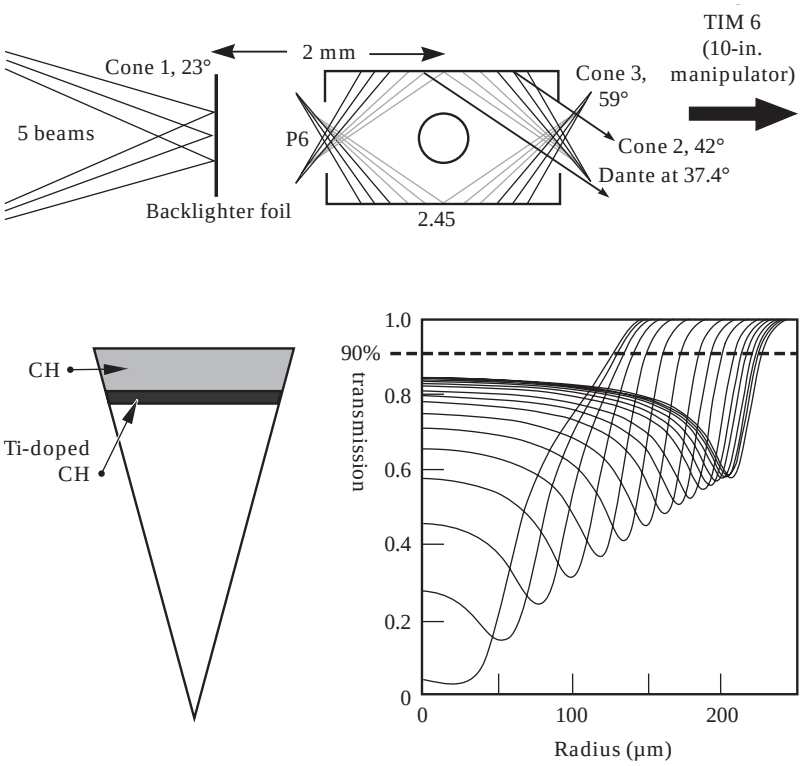

FIGURE 19. Experimental setup for backlit implosion to detect burnthrough. Top figure shows hohlraum and backlighter arrangement. Bottom left shows capsule design. Bottom right shows predicted lineouts through backlit image where detecting 90% transmission should allow adequate sensitivity for determining burnthrough. Simulations indicate that this trajectory shows an inflection point when the ablation surface reaches the doped layer. (NIF-0602-05300pb01)

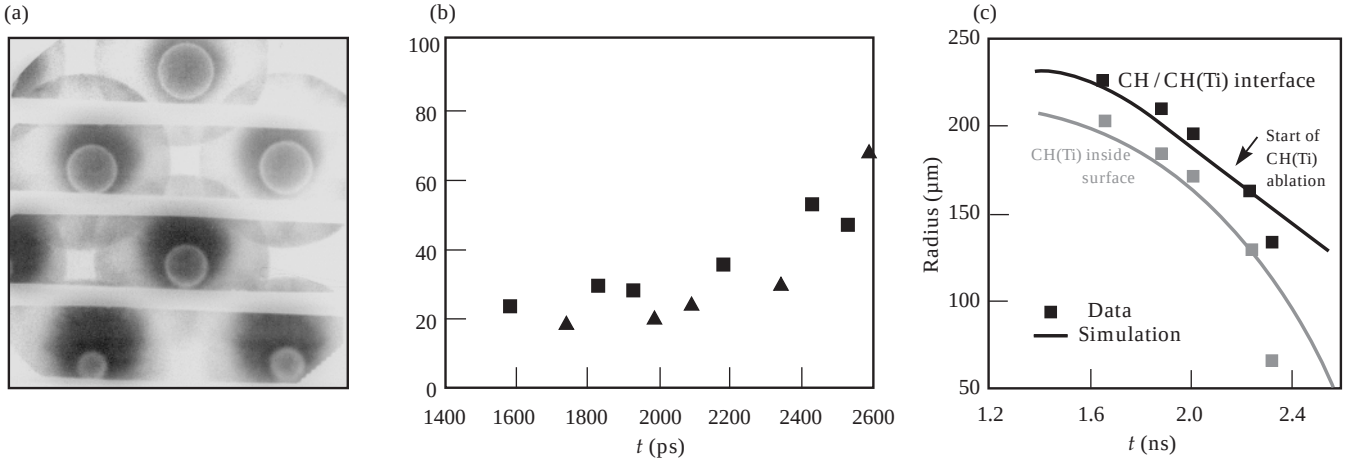

FIGURE 20. (a) Backlit 5.2-keV images of imploding capsule doped with Ti as viewed along hohlraum axis. (b) Separation of 90% transmission point and limb vs time for two shots.. (c) Comparison of measured and calculated position of shell limb and Ti-doped–undoped interface position as a function of time. (NIF-0602-05301pb01)

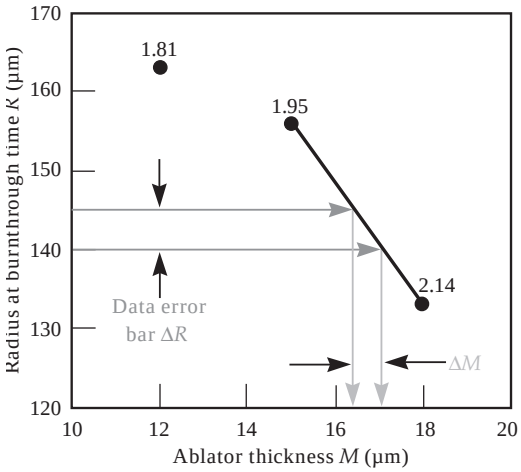

FIGURE 21. Capsule radius vs ablator thickness for OMEGA backlit implosions showing the sensitivity to measure radius of ~5-μm accuracy gives quite high precision in determining relative mass ablation.
(NIF-0602-05302pb01)

coalescence (which may be longer than necessary), the VISAR will need to function against the background of a 250-eV hohlraum.

The fourth shock may require development of a distinct technique primarily because the fourth shock comes late enough in time that there will be substantially more preheat. Both the shock front temperature and high hohlraum radiation temperature may render the VISAR measurement of the shock velocity unreliable. The expected failure mode is that ionization of the cold fuel in front of the shock will cause the refraction index of the cold material to vary with time in a complicated way. Since the VISAR-measured velocity depends directly on this index of refraction, it may be difficult to back out a velocity history, shock trajectory, or even a shock catch-up time for this fourth shock. The precise drive conditions where VISAR begins to fail will be determined in future experiments on OMEGA. For these reasons, we are investigating other techniques for timing the fourth shock. One possibility is to time it simply on the basis of other known experimental parameters: the fourth shock is launched at a time close to the time at which shocks 1 to 3 combine and transits the ablator and fuel very quickly. Since all of these times are within about 1 ns of each other, it is plausible that we could base the timing on simulations and approximate knowledge of the fourth shock speed and initiation time. Whether this is adequate is a topic for further study. As described above, the necessary timing is only weakly dependent on the strength of the fourth shock, changing by only about 100 ps for plausible variations in shock strength. This, combined with the observation that the target can tolerate about ±150-ps variations in timing of this shock, suggests this "dead reckoning" of the fourth shock is plausible.

In order to optimize the fourth shock timing and verify that the flux on the planar, hohlraum wall-mounted, shock timing experiment is the same as that on the capsule, we have developed a convergent geometry shock timing experiment. The concept is to use high-resolution imaging to follow the ablator-fuel interface as shocks passed through. A first test of this technique used a streaked slit camera (SSCA) and a crossed slit arrangement. The targets were scale 1 hohlraums containing a solid CH ball of density 1.05 g/cm^3 and radius 250 μm overcoated with 30 μm of 1.7% (1.8%) Ti-(Cl-) doped CH. The purpose of the doping layer was to mimic the opacity difference between the ablator and fuel layers in a NIF capsule. The diagnostics consisted of the streak camera operated with a 20× snout using either a 5-μm or 10-μm slit, and a 50-μm slit mounted along the hohlraum axis. An example target and data record are shown in Figure 22.

Figure 23 shows our current understanding of these convergent shock-timing experiments. The simulation predicts the first shock reaches the doped layer at about 0.7 ns and the second shock reaches the doped layer near 2 ns. The 1D and 2D simulations differ modestly over the first shock passage, which can be attributed to the effects of flux asymmetry. The 1D and 2D shock speed for the second shock compare well to each other as well as with the data. The data show a strong tendency for the second shock to break out earlier than predicted. Analysis for these data are ongoing as are sensitivity studies to determine the required accuracy for the NIF tuning campaign.

The next phase of this experiment will contain a NIF-like design using a solid CH foam ball of density 0.25 g/cm^3 and radius 250 μm overcoated with 30 μm of 1% Ti-doped CH. A new pulse-shape was devised which generates two well-defined shocks separated by 1 ns. Simulated streaks

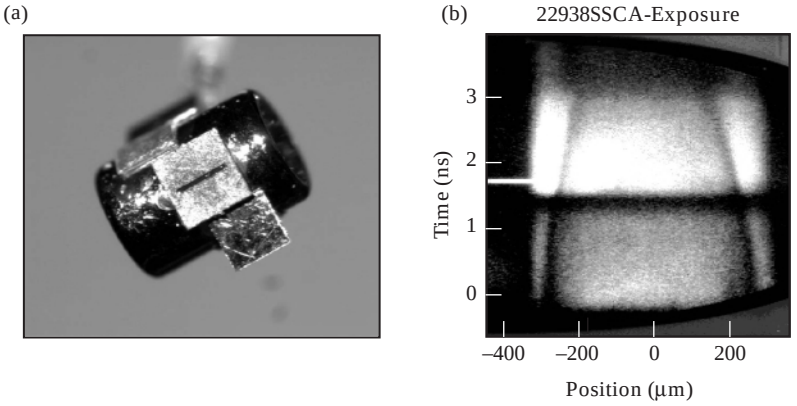

FIGURE 22. (a) Example target and (b) data record for streaked backlit implosion experiment used for timing shocks in convergent geometry. (NIF-0602-05304pb01)

with the expected temporal (5 ps) and spatial resolution (2 μm) clearly show the trajectory of the interface under the influence of the separate shock transits as shown in Figure 24.

To achieve the very high accuracy required for these experiments suggests a need for a KB (Kirkpatrick Baez) high-resolution x-ray microscope. The Laboratory for Laser Energetics (LLE) at UR is building a KB design that revolves around an advanced x-ray streak camera, called PJx, with high resolution and high dynamic range. They plan to implement a 6× KB optic operating at a 2.1° grazing angle. The KB optic will be coated with Ir and is optimized to operate around 1.5 to 2 keV. Their KB optic is expected to resolve down to 5 μm, which is sufficient for their application but not for ours. The most interesting aspect of their system is the performance of the streak camera. They expect to achieve a point spread function in the camera image that is equivalent to ~18 μm at the slit plane. This is at least 5× better than that achieved with the LLNL-Kentech system that was fielded on Nova 10-beam. If this performance is demonstrated, it would eliminate the need for very high magnification. For example, it would be possible to achieve 1-μm object plane resolution using a 20× KB system coupled to this camera. This presents a significant advantage because such a system could be designed to fit entirely within a ten-inch manipulator (TIM) housing and, therefore, become a modular system with minimal impact on the facility.

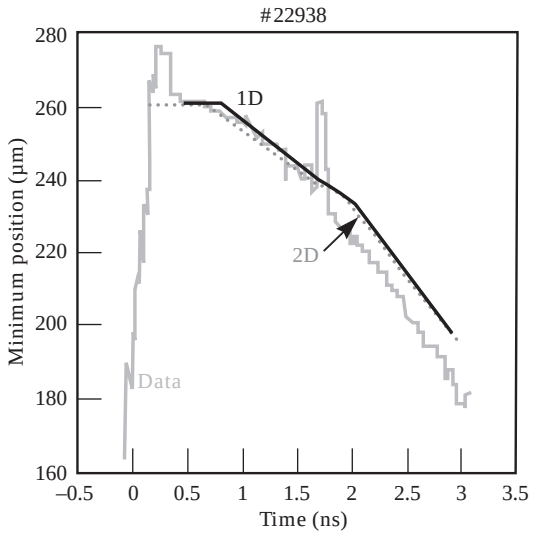

FIGURE 23. Calculated and measured transmission minimum from backlit implosion. (NIF-0602-05305pb01)

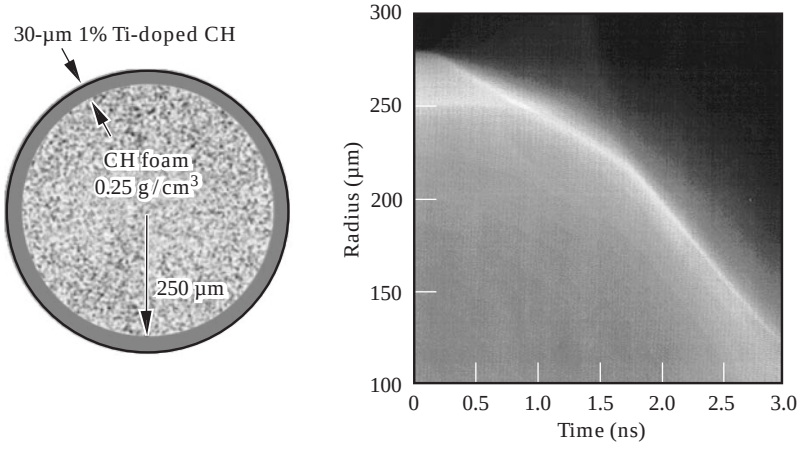

FIGURE 24. NIF-like backlit implosion design for tracking shocks. (NIF-0602-05307pb01)

Presently, we are exploring options that involve making use of the LLE advanced PJx design. The LLNL effort would concentrate on designing a high-resolution KB optic operating at 4 to 6 keV that is coupled to the LLE streak camera.

An analysis of the backlighter intensity required to produce adequate photon statistics in the recorded image showed that at least 10^{-6} sr collection angle is required to produce high-quality data. Analysis of various possible design options (streaked slits or pinholes) reveals that a KB is the only option available that can achieve the required collection solid angle and reach the needed spatial resolution simultaneously. The optic is designed to have sufficient collection to provide a high dynamic range signal for tracking shell motion in backlit implosion experiments and shock trajectories in EOS experiments.

The primary constraint involved in mounting the KB onto the LLE PJx is the 650-mm cathode-to-target distance. A design has been worked out for a 12× magnification, 50-mm-working-distance optic that will project a 500-µm field of view onto the 6-mm slit. The cathode plane point spread function on the LLE camera is expected to be ~18 µm, so the KB optic will be designed to operate at an object plane resolution between 1 and 2 µm to match this (cathode plane point spread from 12 to 24 µm).

The resolution and the collection angle of the KB optic will be controlled by a slit aperture placed approximately 33 mm downstream of the first mirror. The baseline design will use a 150-µm slit, which allows for a collection angle of ~1.3 µsr (including mirror reflection losses), and an object plane resolution of 2 µm. The resolution can be improved at the expense of signal level by reducing the aperture, or vice versa. Backlighter materials being considered are Sc, Ti or V, which emit in the 4- to 6-keV range.

Notes and References

1. *ICF Annual Report (1999)*, Lawrence Livermore National Laboratory, Livermore, CA, UCRL-LR-105820-99, p.19.
2. R. L. Kauffman, *Phys. Rev. Lett*. 73, 2320–2323 (1994).
3. M. M. Marinak et al., *Phys. of Plasmas,* 9 (8), 3567–3572 (2002).
4. D. Munro et al., *Phys. of Plasmas,* 8 (5), 2245–2250 (2001).

IGNITION TARGET DESIGN

S. W. Haan *P. A. Amendt* *T. R. Dittrich*
M. C. Herrmann *O. S. Jones* *M. M. Marinak*
D. H. Munro *S. M. Pollaine* *G. L. Strobel*
L. J. Suter

While the basic ignition target design remains unchanged, effort continues on a wide variety of detailed issues: target fabrication planning, diagnostic development, defining issues for the experimental program, and continuing to optimize our use of the NIF laser. This section describes the various projects worked on in these areas.

There are several ignition capsules being considered, using various drive temperatures and ablator materials. Current designs are shown in Figure 1. This figure includes all of the designs that have been considered, and results for most of them will be described. (Two are not described in more detail. The double-shell design is a speculative noncryogenic design.[1] Modeling of the Rayleigh–Taylor [R-T] instabilities in this target is very difficult, requiring turbulent mix modeling. The thick-fuel design is relevant as an extreme case for target-fabrication planning purposes.) For each design a range of scales is possible, depending on how much energy ends up being available to the hohlraum, and on the hohlraum-to-capsule coupling efficiency. A range of scales is indicated for each capsule, and pertinent results will be described in more detail.

Overview of R-T Simulations

Many of the results described here amount to comparing R-T instability growth for various capsules and fielding scenarios. It is useful to overplot a large number of these results in order to facilitate comparison; our approach in this section is first to present this summary plot and describe the basic assumptions that went into making it, and then incorporate many of the results described in more detail below into this overview plot. Hence many details about the plot will be discussed as appropriate below.

Given a capsule design, we evaluate its R-T susceptibility by doing a series of two dimensional (2D) simulations, generating a plot as shown in Figure 2. (This plot is for a scale 1.25 250-eV capsule.) All of the simulations described here assume that the surface has roughness with spherical harmonic amplitudes given by:

$$R_{lm} = 10 / l^{1.5} + 0.08 / \left[(l / 60)^{0.7} + (l / 1200)^4 \right] (nm) \ , \qquad (1)$$

where R_{lm} is the spherical harmonic amplitude in nm, with normalization such that the rms in interval (l_1,l_2) is

$$\sigma = \sqrt{\frac{1}{4\pi} \sum_{l=l_1}^{l_2} (2l+1) |R_{lm}|^2} \ . \qquad (2)$$

The index m is inactive, since surfaces are presumed isotropic. This surface, which is based on characterization of a

Nova capsule, is then used with various multipliers until failure is seen. The rms reported here is the sum over all modes and is 10.3 nm for the spectrum with no multiplier. This is a nominal spectrum that for modes $l > 30$ is the same as the spectrum sometimes called the "NIF standard." Typical capsules have larger perturbation amplitudes at low modes, which we treat explicitly as described in a separate section below. For 2D simulations all of the power in a given l-mode is combined into that 2D mode.

From results such as those shown in Figure 2 we extract a "cliff," defined as the surface roughness that produces 50% yield degradation. This can then be plotted as shown in Figure 3, where we plot the "cliff" roughness versus absorbed energy. The allowable roughness, also

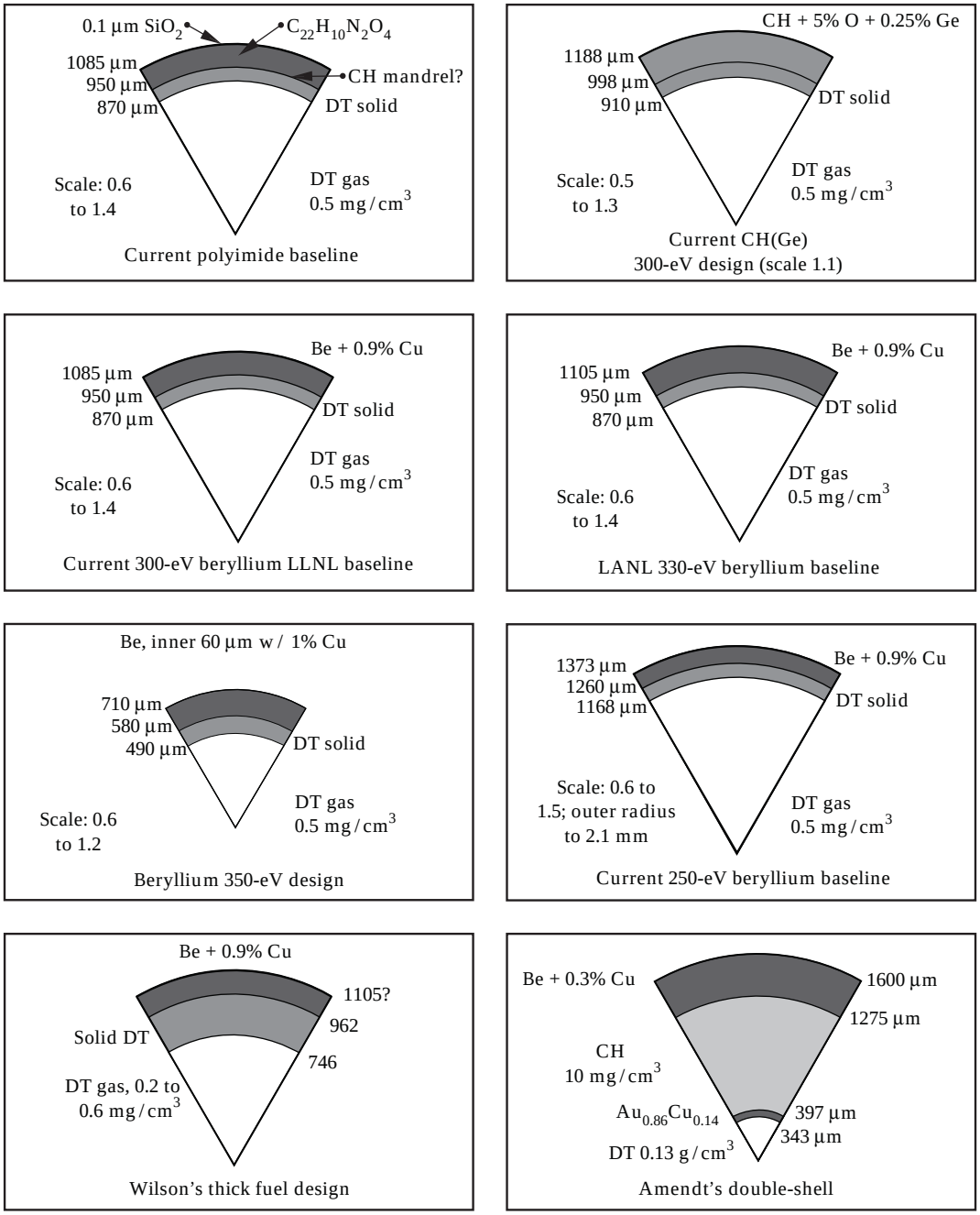

FIGURE 1. Possible ignition capsules being considered for the NIF. All designs currently being considered are shown. For each capsule an indicated range of scales is of interest, depending on the laser power and energy and the hohlraum-to-capsule coupling efficiency. Except in the one case indicated, the indicated dimensions are scale 1.0. (NIF-0602-05232)

indicated in the figure, can be taken to be ⅓ of the perturbation that causes 50% yield degradation. This leaves margin for other perturbations and sources of error, such as ice roughness, hohlraum asymmetry, low-mode target imperfections, errors in pulse shaping, and other errors in the modeling. Note that most of these effects add in quadrature, so a ⅓-of-cliff specification leaves room for eight other equivalent sources of perturbation. It is evident from Figure 3 that the R-T sensitivity is a strong function of all three parameters: absorbed energy, drive temperature, and ablator material. Various targets in Figure 3 will be described in detail below.

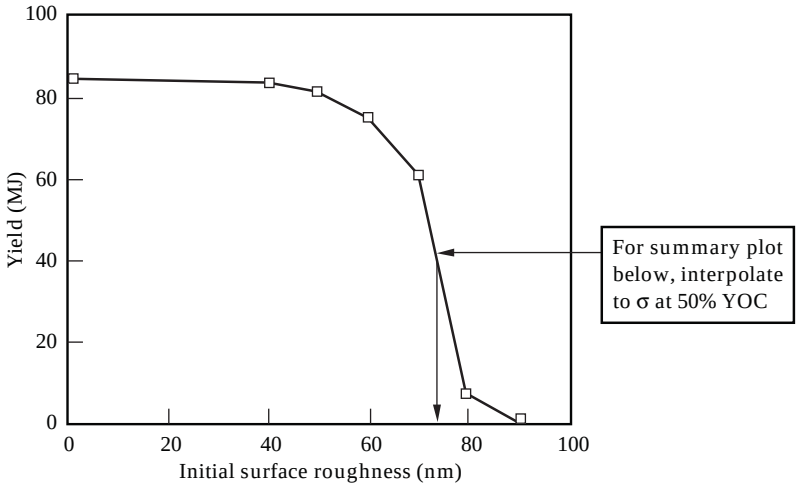

FIGURE 2. Results of two-dimensional simulations of scale 1.25 Cu-doped beryllium target. YOC is the ratio of observed yield to the theoretical clean (no mix) yield. (NIF-0602-05233)

Preignition Cryogenic Implosions

As NIF is being built, there will be a significant period of time during which part of the laser will be available for experiments. To ascertain the value of experiments that might be done during such a time, we examined the design of preignition cryogenic implosion experiments, using fewer than 192 beams.

Designs have been simulated at a scale appropriate for preignition experiments using 96 beams in a symmetric configuration. These use 140-TW peak power and 355-kJ absorbed third harmonic laser energy. The capsules and the pulse shape are scaled from the full-NIF targets by a factor of 0.6. These designs utilize a mixture of materials in the hohlraum wall (to maximize hohlraum efficiency) and polyimide ablators. They do not ignite, typically giving a few 10s of kJ of yield. Their implosion characteristics are very similar to scales of full-size ignition targets, in that almost all aspects of the hydrodynamics can be made arbitrarily close to exact hydrodynamic scales of the ignition targets (until the latter ignite). Completed design work includes:

- Integrated calculations ensuring the hohlraum energetics and adequate symmetry in two dimensions.
- Three-dimensional (3D) viewfactor calculations to ensure adequate symmetry with 96 beams. Both the intrinsic asymmetry and the power balance are worse with 96 beams, but the higher albedo of the mixed-material wall improves the symmetry back to levels similar to the full-scale gold-wall hohlraum.
- A full set of R-T simulations. With ice perturbations, the capsules still give 10s of kJ of yield with 0.5-μm rms perturbations. Perturbations beyond about 1-μm rms would severely disrupt the implosion. The ablator surface will need to be about 15 nm rms or better in order to get performance above 10% of the full clean yield. These tight surface specifications are to be expected of the hydrodynamics scales, since the full-scale target requires roughness of about 30 nm.

Design work has also been done on noncryogenic high-performance implosions that might be done during the construction phase of NIF. Such targets can reproduce the acceleration-phase hydrodynamics of the ignition targets, if it is possible to fabricate them with a beryllium layer inside of a polyimide layer. The beryllium couples less to preheat and stays at higher density than the ablator, in

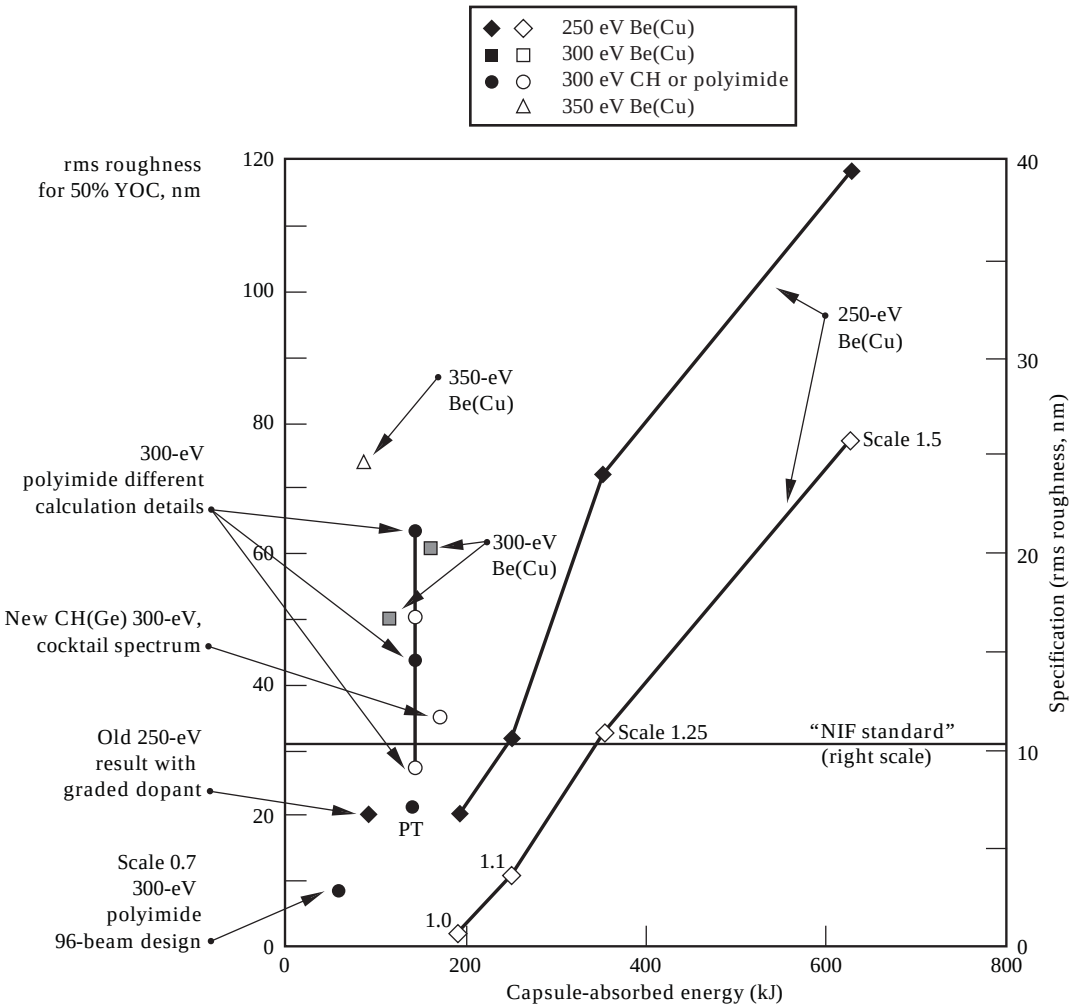

FIGURE 3. Surface roughness requirements (right-hand axis) for various targets vs capsule-absorbed energy. The solid curves are for 250-eV capsules uniformly doped with 0.9% Cu. The left-hand axis shows the results of a series of 2D simulations that were used to locate the surface roughness at which the yield is degraded by 50%. The requirement is taken to be ⅓ of this value. All calculations assume the standard spectrum for the perturbation as described in the text. Solid symbols are 0.3 mg/cm^3 DT gas, and open are 0.5 mg/cm^3. (NIF-0602-05234)

a similar fashion to how the DT fuel in an ignition capsule can be at higher density than the ablator. Without the beryllium layer the acceleration-phase hydrodynamics is similar only at early times, before a density mismatch is created in the ignition target by the differential preheat in the ablator and cryogenic fuel. Backlit imaging of the partially imploded shell would provide valuable confirmation of our ability to model the acceleration-phase R-T growth. The deceleration-phase hydrodynamics is qualitatively different for any noncryogenic target than for a cryogenic ignition target, which is a serious disadvantage to a noncryogenic target.

The experimental observables for subscale implosions are based on the same diagnostics planned for possible failed ignition implosions, although the signals are somewhat weaker than full-scale targets. These include neutron spectra and x-ray images, which will provide detailed information about the imploded configuration. As described below, some neutron diagnostics actually work slightly better for the subscale implosions, since they have smaller column density and charged-particle stopping is less of an issue.

Work at slightly larger scales has indicated that ignition begins at about scale 0.7 in one dimension, but specifications for such a target are impossibly tight. Ablator surface would have to be smoother than 10 nm, and the ice smoother than 0.3 μm. This point is shown in Figure 3, at 53-kJ absorbed energy and 8-nm roughness cliff. A scale at which ignition begins to look

plausible is 0.9, at which a beryllium capsule can tolerate 50-nm ablator roughness or 1.5-μm ice roughness. This point is also shown in Figure 3. Such a target could conceivably be driven with 96 beams, although to do so would require that all parts of the laser and target work extremely well, with no margin for either the laser or target physics.

Large 250-eV Capsules

Work on the hohlraum coupling efficiency suggests that the energy available to be absorbed by the capsule may be somewhat larger, at 250-eV hohlraum temperature, than had been previously assumed. This raises the issue of how much the R-T and symmetry requirements might be loosened as the energy increases. Hence work was done on beryllium-ablator designs, driven at 250 eV, at absorbed energies up to a suggested maximum of 600 kJ.

In order to ensure the best possible scaled designs, we reoptimized the existing 250-eV designs, which are at 190 kJ absorbed. We systematically compared existing 250-eV designs at this scale. Designs have been done over the years with various dopants, dopant concentration profiles, dimensions, and drive pulse shapes. There is quite a large variation possible in the target parameters. For example, designs perform fairly well with the aspect ratio of the beryllium shell as low as 8 and as high as 12, with various dopant profiles. For this study we systematically varied the dimensions of one design, while keeping the absorbed energy and dopant fixed. Interestingly, the region of parameter space in which this target performs does not connect with the other designs, implying that to completely understand the parameter space we need to include variations in dopant and drive pulse shape.

A 250-eV target was systematically optimized subject to the constraints that the absorbed energy was fixed at 190 kJ, and that the dopant was uniform. Optimization was done over fuel thickness, ablator thickness, and the concentration of copper in the ablator. (The one remaining free parameter, the outer radius, was varied to maintain the absorbed energy.) With central gas density 0.3 mg/cm^3, the parameter space of good performance is quite a bit larger than with 0.5 mg/cm^3. The target giving the highest yield with 0.5 mg/cm^3 gas density was selected as the optimum design. This is the design shown in Figure 1. It is striking that this design, while similar to existing designs with uniform dopant concentration, has significantly higher aspect ratio than existing designs that use graded dopant layers. Hence it is clear that grading the dopant changes the design space significantly, and it will be important in the future to consider systematically designs with graded dopants. At any rate, to establish performance with uniform dopants, this design was then scaled to various absorbed energies. At the largest scale (600 kJ, scale 1.5), the flux during the foot of the profile had to be increased in order to keep the pulse length below approximately 22 ns. The copper dopant was reduced, roughly as 1/scale, as the target was scaled.

Two-dimensional simulations were done at four scales to determine the susceptibility to R-T (and, in some cases, to drive asymmetry as reported below). These results are the solid lines in Figure 3, for the two central gas densities. It is evident that at the smaller scales it will be very challenging to meet the surface roughness requirements. A "NIF standard" surface roughness is adequate at absorbed energy above about 250 kJ with central gas density 0.3 mg/cm^3, and above about 320 kJ with central gas density0.5 mg/cm^3.

We have not systematically varied the ice roughness in simulations of this target, but did check two cases: at scale 1.1, with 0.5 mg/cm^3 central gas, a 1.5-μm ice rms gave simulated yield of 80% of clean; and at scale 1.5, with 0.5 mg/cm^3 central gas, a 3-μm ice rms gave 100% of clean. We also did asymmetry calculations described below in the section on central gas fill.

The largest capsule considered for this study, at 600 kJ and scale 1.5, would optimally be driven with a power pulse that is about 26 ns long. There will be a limit on how long a pulse NIF can deliver, around this length. In the results shown in

Figure 3, at the larger scales the pulse shape was changed from a pure scale, in order to keep the pulse length under 22 ns (see Figure 4). We also considered a direct scale, with a longer pulse length. Figure 5 shows the R-T sensitivity for these more optimally scaled targets. The price paid for keeping the pulse length fixed is about 140 kJ out of 600 kJ.

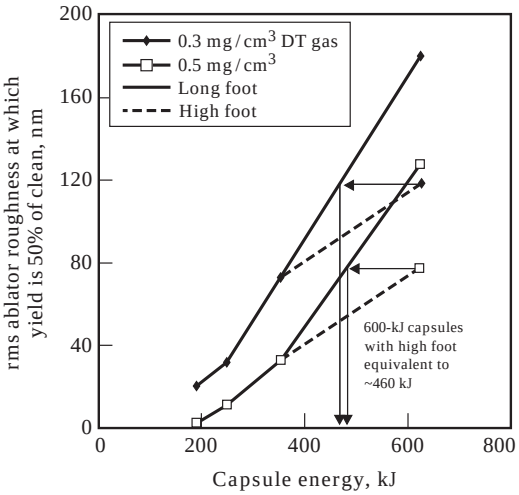

FIGURE 5. Effect on stability of the pulse-shape variations shown in Figure 4. At 600 kJ, the shorter pulse with the higher foot produces an implosion with robustness similar to a scale at about 460 kJ, as shown by the black arrows. (NIF-0602-05237)

Doped Polystyrene as an Ablator Material

Most of the work done on ignition target designs recently has used ablators of beryllium or polyimide. A third material, polystyrene doped with Br or Ge, was examined years ago. A comparison published in 1998 indicated that the other two materials were superior to polystyrene.[2] However, polystyrene is probably the easiest material from which to fabricate the capsules. Recent work on hohlraum coupling efficiency suggested the possibility of increased energy available to the capsule, making polystyrene possibly more attractive as an ablator material. Hence work was begun on redesigning the polystyrene targets, to do a full comparison of polystyrene, polyimide, and beryllium.

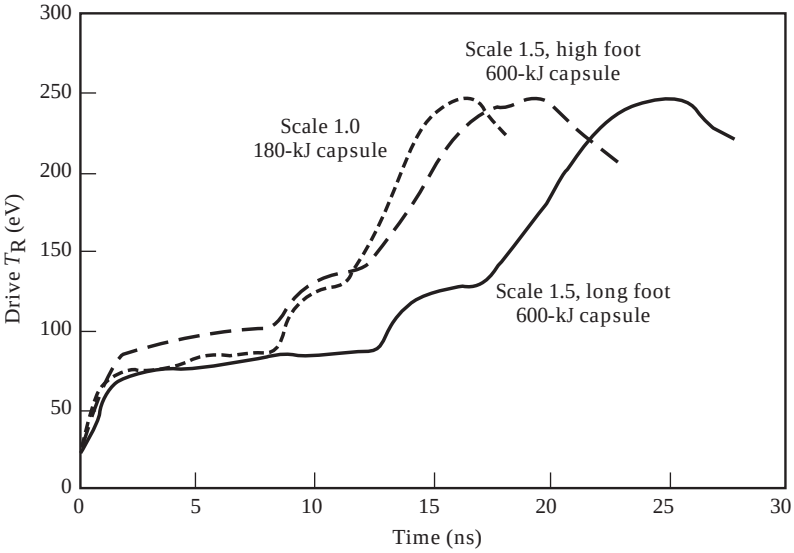

FIGURE 4. Pulse shapes used for study of pulse-length effect in 250-eV Be(Cu) capsules. The curve labeled "Scale 1.5, high foot 600-kJ capsule" has the foot raised in order to keep the total laser pulse length below about 22 ns. For the curve labeled "Scale 1.5, long foot 600-kJ capsule," this constraint was relaxed and the profile is an exact scale of the profiles driving the other size capsules. (NIF-0602-05236)

Using a cocktail wall mixture, the target scale can be increased to 1.1, increasing the absorbed energy from 150 kJ to 180 kJ, for the previous baseline laser energy and power of 1.3 MJ and 400 TW. Integrated simulations confirmed that scale 1.1 targets can be driven with this much power and energy, and that the symmetry is acceptable. The symmetry is actually better because of the increased albedo of the cocktail wall. The capsule dimensions were approximately optimized, and 2D R-T simulations were done for the optimal target, shown in Figure 1. These simulations used the x-ray drive spectrum calculated in the integrated simulation with the cocktail wall. Results of these simulations are included in Figure 3. It is clear that polystyrene targets can be made as robust as the baseline polyimide, provided that a cocktail wall can be used to increase the energy delivered to the capsule. Figure 3 shows the original polystyrene target (PT) at

somewhat poor performance at 20-nm maximum tolerated roughness, absorbing 150 kJ. The new design can tolerate 35-nm roughness, both because it is somewhat bigger (180 kJ) and because it is better optimized. Future work will reexamine the optimization of these capsules, using both ablator materials.

For the plastic capsules, it is possible that the beta-layering of the solid DT layer will be enhanced with infrared radiation at a frequency absorbed by the DT and transmitted by the ablator. To facilitate this, it may be necessary to use deuterium in place of ordinary hydrogen in the plastic ablators—the absorption lines of deuterated plastic are better differentiated from the DT absorption than are those of the plastics made with ordinary hydrogen. This makes little difference to the behavior of these plastics as ablators; the only effect is a small increase in density, which generally makes the ablator perform better. This is true for both polystyrene and polyimide, and current design simulations with both materials generally use deuterated material. We will continue to do so until or unless target fabrication issues suggest otherwise.

not such a severe impact that the lower density is unequivocally necessary. The impact is equivalent to a 30–40% loss in absorbed energy; how important this is depends on how much margin we have in the final targets. Note that it is equivalent in impact to about 30–40% reduction in laser energy, so it is not a minor issue.

A related issue is contamination of the central gas. The DT in the center of the capsule will be contaminated both with atomic hydrogen ^{1}H and with ^{3}He produced by decay of the tritium. Since making a good layer will probably require melt and refreeze, and since both of these contaminants have lower condensation temperatures than DT, all of the contaminant in the fuel will end up in the central gas.

It is necessary to consider R-T instability growth to evaluate the impact of these contaminants. The contamination can actually increase the 1D performance, since it delays ignition and the target burns at higher column density. However, additional R-T instability growth during the time delay before ignition means that the surface roughness specifications are tighter. Specifications will be proportionately tighter for both the ice roughness and the ablator roughness.

Impact of Central Gas Density

A key parameter is the cryogenic temperature at which the capsule is held prior to the shot. This determines the density of the central gas, in equilibrium with the solid fuel layer. It also affects the quality of the ice roughness in a way that is still being determined by surface characterization experiments.

For a baseline polyimide design, a 350-eV beryllium design, and the subscale designs, we see a significant but acceptable tightening of surface roughness specifications when the gas fill is increased. These results are shown in Figure 3.

Asymmetry requirements for three targets are shown in Figure 6. It is evident that increasing the central DT density from 0.3 mg/cm^3 to 0.5 mg/cm^3 decreases the robustness of the target significantly, but is

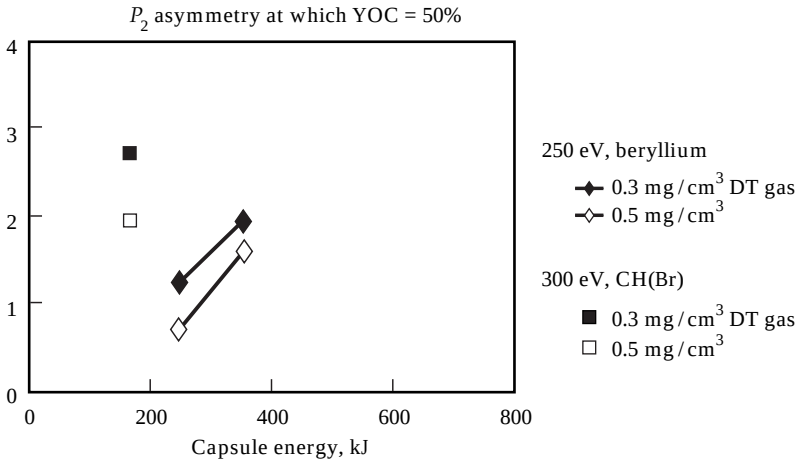

FIGURE 6. Dependence of asymmetry specifications on capsule-absorbed energy, peak drive temperature, and central gas density. The quantity plotted is the asymmetry at which the simulated yield is 50% of the clean 1D yield (YOC); a sensible requirement for the asymmetry would be about ⅓ of the value plotted here. More simulations need to be done to bring this plot to the level of completeness represented by Figure 3. (NIF-0602-05235)

Figure 7 shows how the ablator roughness specification tightens as either ^{1}H or ^{3}He is added to the central gas. Atom-for-atom, ^{3}He has more impact because it increases conductive and radiative losses, but gram-for-gram the two contaminants have about the same impact.

Impact of Radiation Drive Spectrum

Other parts of the program are exploring the possible advantages of a cocktail material mixture in the hohlraum wall. A possible concern with the use of a cocktail wall is how the x-ray drive spectrum will affect the R-T growth. We have not yet had the opportunity to explore this systematically, but a few pieces of information have been assembled.

First, we note that the scale 1.1 300-eV CH(Ge) target described above was driven with a cocktail spectrum, for the 2D simulations used to plot this point in Figure 3. Thus we know that the cocktail spectrum does not have a devastating impact on the R-T performance. This is the only ignition capsule for which a cocktail spectrum has been calculated so far.

As a beginning of systematic work to understand this issue, we ran simulations of the baseline polyimide capsule driven with a Planckian spectrum and a simulated cocktail spectrum. This capsule was designed with the gold spectrum, and for this work all that was changed was the spectrum. The three spectra are progressively softer: during the main part of the pulse, when the spectrum is probably the most important, the gold spectrum we have been using has 15% of the x-ray energy above 2 keV, while the cocktail spectrum has 11% and a Planckian has 9%.

With the three spectra, the R-T growth shows somewhat different evolution; with the softer spectra the perturbations grow almost twice as much during the first part of the acceleration, while the perturbations are growing on the ablation front. Then, when the perturbations are growing mostly on the now unstable accelerating interface between the ablator and the fuel, they grow most rapidly with the harder gold spectrum. At peak velocity there is little difference between the three cases. Finally, when the perturbations couple to the inside and grow during deceleration, they end up being bigger with the softer spectra, presumably because a softer spectrum allows for better compression. The net effect is that there is 85% more growth with the Planckian spectrum and 40% more with the cocktail spectrum. This would translate directly into 40% tighter surface roughness specifications, except that we may be able to reoptimize the target for the cocktail spectrum and recover some or all of this difference. Ultimately we need to systematically optimize targets with both spectra, and then see how the optimal targets compare.

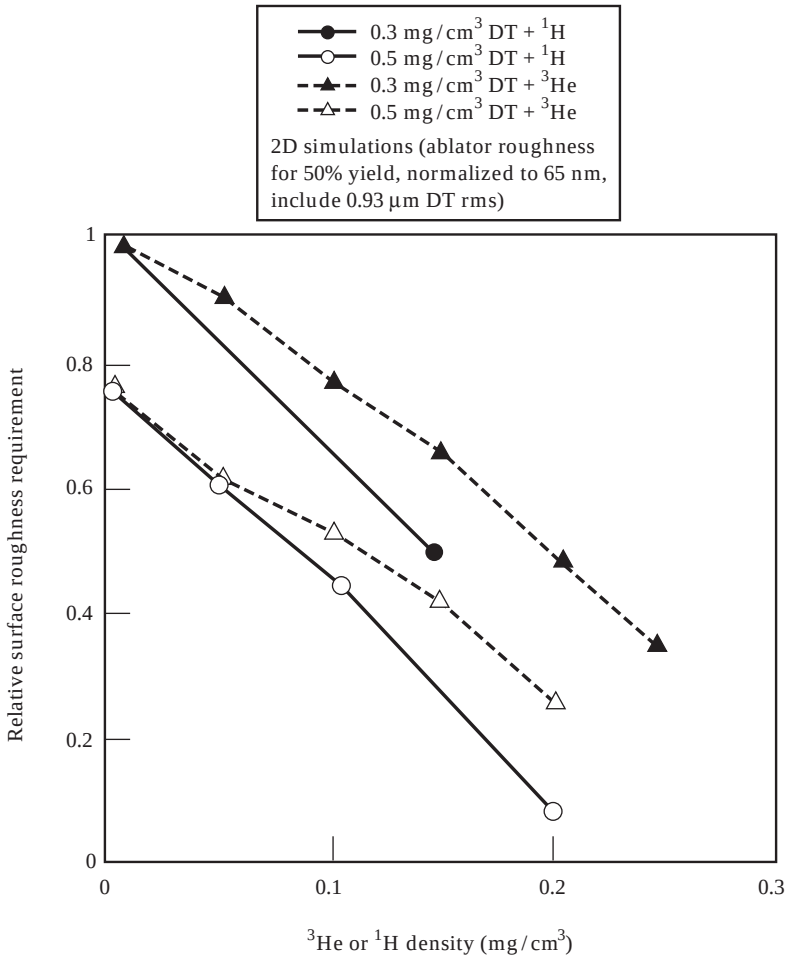

FIGURE 7. Contaminants in the gas core tighten surface roughness specifications. (NIF-0602-05238)

Fill Holes for 300-eV Be Target

Most ICF capsules historically have been filled via diffusion through the ablator shell. This appears to be viable for polymer ignition capsules, but may not be for beryllium ablators. One possible fill scenario for beryllium is the use of a thin hole through the ablator. Design calculations were done to provide guidance as to the acceptable dimensions of such a hole, and the desirability of filling the hole with some other material after it is used for the DT fill.

Significant effort went into developing the computational capability for these simulations, which are very challenging because the fill hole is much smaller than the other dimensions, and because the hydrodynamics is very far from being a small perturbation from sphericity. New semi-Eulerian rezoning techniques have been developed and were tested in preliminary fill-tube simulations.

A new rezoning scheme was developed for these simulations that uses a continuous rezoner rather than the discrete rezoner that had been used previously. Both options are now available for all capsule instability simulations, and we examined the accuracy of each. They give very similar instability growth and yield for baseline R-T simulations initiated by surface roughness, enhancing our confidence in the accuracy of these simulations. Application of these schemes to the very difficult fill-hole simulations was then appropriate.

If the fill hole is simply filled with solid DT, 2D simulations indicate that it should be less than 5 µm in diameter for a baseline beryllium capsule absorbing 175 kJ. Even at 2.5-µm diameter, the tube causes a significant perturbation on the ablation front around peak velocity: 25-µm amplitude in mode 80, with more than 10% variations in column density. This is significantly larger than we expect from the specified surface roughness. On the other hand, perturbations seeded by roughness are throughout the surface, while the fill-tube perturbation is localized. The mass involved in the fill-hole perturbation with a 5-µm hole is large enough to pollute the hot spot and is close to being enough to prevent ignition. We also explored two other possible fill-hole scenarios—filling the hole with epoxy or copper; both are significantly worse than the DT-fill case. The epoxy holds the hole open while radiation penetrates it and blows it out, and the copper causes a lag that becomes an R-T spike and grows to large amplitude. Density isocontours for these simulations are shown in Figure 8.

Low-Mode Out-of-Round

Modes below about 10 are not properly accounted for in our usual multimode simulations, but can be analyzed accurately via linear analysis. Their presence in the target results in an ignition-time perturbation that is linearly related to the initial perturbation,

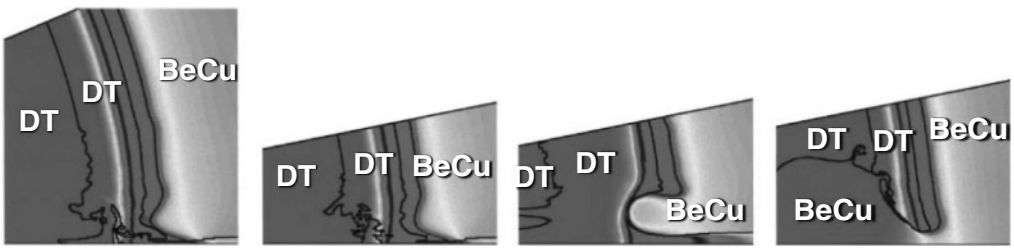

FIGURE 8. Configuration of fuel and ablator, on axis, for several fill-tube simulations. The geometry shown is when the shell is ⅔ of the way imploded, for the indicated hole sizes and materials filling the hole.
(NIF-0602-05239)

and their impact on ignition can be effectively estimated simply by calculating the bang-time rms. Some small corrections to linear analysis were included to estimate the variation with mode number of nonlinear saturation and of the maximum tolerable ignition-time amplitude.

The three surfaces (gas / ice, ice / ablator, and ablator / outside) can be described by various sets of three numbers. That is, we have three functions $R_g(\theta,\varphi)$, $R_i(\theta,\varphi)$, and $R_a(\theta,\varphi)$ for the outer surface of the gas, ice, and ablator respectively. These can also be determined from the set $R_a(\theta,\varphi)$, $T_a(\theta,\varphi) = R_a(\theta,\varphi) - R_i(\theta,\varphi)$, and $T_i(\theta,\varphi) = R_i(\theta,\varphi) - R_g(\theta,\varphi)$ where T_a is the thickness of the ablator and T_i is the thickness of the ice. The advantage of using the latter set is that the performance is most sensitive to the ablator thickness and least sensitive to perturbations that represent variations in radius at constant thickness (such as could occur if the mandrel is out-of-round, and both the coated ablator and the ice followed the perturbed mandrel). Describing the surface perturbations in terms of $R_a(\theta,\varphi)$, $T_a(\theta,\varphi)$, and $T_i(\theta,\varphi)$ makes these contrasting sensitivities as evident as possible.

Another issue encountered in describing the low-mode sensitivity is the wide variety of possible modal structures to the deviations. What really matters is the rms at bang time, and there are various initial conditions that can result in the same final rms. The way we have represented this trade-off is to make a table of "specifications" (Table 1). These numbers, which are for the baseline 150-kJ absorbed energy 300-eV polyimide capsule, are normalized so that if a capsule had exactly these deviations it would have a 2-μm ignition-time rms on the hot-spot perimeter. (The choice of 2 μm leaves margin for surface roughness and radiation asymmetry.) Some modes on some surfaces are allowed to be worse than these specs, as long as other modes, possibly on other surfaces, are better. An arbitrary actual configuration can be evaluated by forming a quadrature sum weighted with the numbers from the table as denominators. As long as this quadrature sum is less than 35, the number of terms, the perturbations are acceptable. All 35 numbers can be traded off in this way, with identical simulated impact on the capsule performance. It is also likely that we would want to separately evaluate the requirements on capsule fabrication and ice symmetry, and this can be done by dividing the allocated rms evenly between each of the three areas. So, for example, suppose we want to define a specification for the ice thickness alone. If the specification numbers from the table are designated S_l, and the actual rms per mode is A_l, then we form the sum

$$N = \sum_{l=1}^{12} (A_l / S_l)^2 \quad .$$

Since there are 12 modes, the sum N must be less than 12 for the specification to be met.

It should be emphasized that these are 3D rms deviations, and a trace does not fully determine the full deviation. Some examples suggest that this can be a more significant issue for these low modes than it typically is for surface roughness. Understanding this better is an area for future work. A possible upside is that it seems likely that several traces on a capsule, at different orientations, could be processed to give a quite good characterization of the low-mode amplitudes.

The specifications from Table 1 are quite similar to the "NIF standard" for capsule shape, indicating that the NIF standard is a

TABLE 1. Low-mode specifications for capsule out-of-round, in rms per mode. These perturbations can be traded off with each other as described in the text.

Mode	Outer radius (nm)	Ablator thickness (nm)	Fuel thickness (nm)
1	—	50	400
2	500	75	400
3	400	75	400
4	120	75	400
5	50	25	200
6	25	17	120
7	10	10	80
8	6	8	70
9	5	7	50
10	4	6	40
11	3	4.5	35
12	2.5	3	30

UCRL-LR-105820-00 / 01

good specification even at low modes. For the ice, the numbers from this table are noticeably below the characterization results. That would imply that the ice roughness in modes 4–15, according to our current understanding, is using up more than its share of the perturbation budget. Clearly this is an area that needs further attention.

3D Simulations

We have done a wide variety of simulations of the NIF ignition capsules in one, two, and three dimensions. Our 3D simulations are done with the code HYDRA.[3]

The combination of roughness and asymmetry has been done in 2D, but not yet in 3D simulations, which are most difficult. As more computer power becomes available, it is possible to do larger simulations; our next goal in this area is to do 3D simulations to verify both asymmetry and surface roughness specifications. The first step in these simulations is the definition of a baseline 3D asymmetry to be imposed on the implosions. Recent changes in hohlraum design indicate that the most likely asymmetry is somewhat better than had been assumed in previous modeling, because of increased hohlraum albedo of the cocktail-mixture hohlraum wall. We have done 2D simulations to optimize a baseline target with the new hohlraum wall and with updated spot parameters. These parameters optimize the trade-off between laser entrance hole size and laser intensity.

The new hohlraum is being designed to use 1.3 MJ of laser light in order to be at the same scale with respect to the laser as the previous point design. We keep the temperature at 300 eV, which means the power will be slightly less than the previous 400 TW.

Viewfactor simulations of various beam configurations suggest the possibility of significant asymmetry in modes $Y_{9,8}$ and $Y_{4,4}$, as well as the familiar m = 0 modes. We have also run 3D hohlraum simulations with the HYDRA code, since estimates of the 3D asymmetry depend on details of spot brightness, size, shape, and position, which are not very accurate in the viewfactor simulations.

We are doing 3D implosion simulations with various estimates of the 3D asymmetry. An example is shown in Figure 9, where we show density contours at ignition time and the density profiles on slices at various values of the azimuthal angular coordinate.

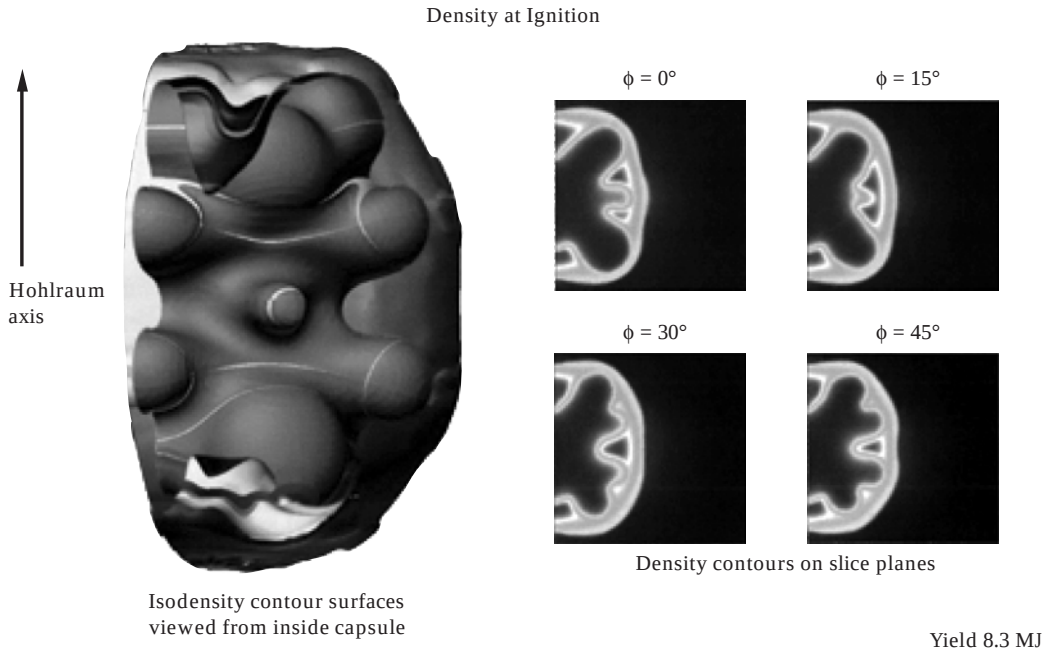

FIGURE 9. This 3D implosion simulation of a NIF ignition capsule used a preliminary estimated asymmetry that was based on viewfactor estimates and was constrained to have 45° reflection symmetry. These approximations are both known to overestimate the asymmetry, but this simulation nevertheless gave 8.3-MJ yield. Simulations are in progress with more accurate estimated asymmetry, which requires more solid angle in the simulation. (NIF-0602-05240)

This preliminary simulation, which gave 8.3-MJ yield, used an estimated asymmetry with reflection symmetry at 45° to reduce the simulation size. This increases the asymmetry in the implosion. Simulations are in progress with larger solid angle and better estimates of the asymmetry.

Simulated Output

Another important application of ignition target simulations is estimating output so that appropriate diagnostics can be designed. A suite of diagnostics is being planned so that we can ascertain as much as possible about ignition implosions, especially if they fail. Work in the period described here concentrated on the energy spectrum of the neutron output.

Calculated neutron spectra always show the same qualitative features: a down-scattered part that depends on the total capsule ρR; a primary peak the width of which depends on the burn temperature; and high-energy secondary and tertiary neutrons. A spectrum is shown in Figure 10, in which the processes responsible for the various parts of the spectrum are called out.

There are various features in these spectra that we are considering using as diagnostics of the ignition implosions.

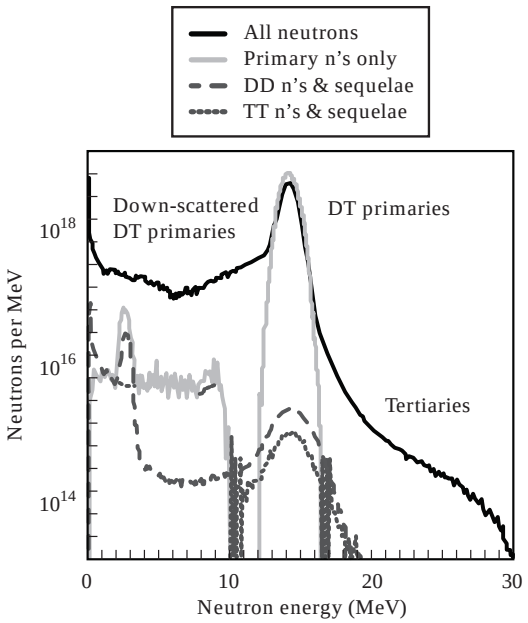

FIGURE 10. Neutron spectrum from a well-burning ignition capsule. The various processes that produce neutrons are separately indicated. (NIF-0602-05241)

First, the width of the primary peak at 14 MeV provides a measure of the burn temperature. This is a standard ICF diagnostic that has been used for years.

The high-energy neutrons (produced by an in-flight reaction of a D or T that has been up-scattered by a primary neutron) measure different aspects of the implosion in different cases. They are easiest to interpret for implosions with ρR less than 1.0 g/cm^2. For these low ρR implosions there is negligible stopping of the charged particle involved in the tertiary process, and the relative number of tertiary neutrons is directly proportional to $(\rho R)^2$. Unfortunately, ignition requires a fuel ρR somewhat greater than 1.0 g/cm^2, at least 1.2 g/cm^2 for good burn. For such cases the charged particle slows or stops before reacting and the tertiary signal depends on the fuel conditions and not just on ρR. For such cases the data will still be valuable, if more difficult to interpret.

The down-scattered neutrons will be more difficult to measure, but seem to be more robust as a direct measurement of the total ρR. Figure 11 shows the relative number of neutrons in the 4–10 MeV band for a series of simulations in which neutrons were produced in a burning core surrounded by a cold solid fuel layer at two different temperatures, as indicated. Column density was varied by varying the density. The down-scattered neutron fraction is proportional to ρR, and independent of temperature.

It could also be valuable to diagnose implosions with pure deuterium fuel (DD). The spectrum of neutrons from a DD target is shown in Figure 12. Two notions for using particles from DD targets have been investigated. In the first, a little ^{3}He would be added to the central gas so that 14.6-MeV protons are produced by a D^{3}He reaction. These protons can then react with an ambient deuteron, p(d,2p)n, to produce a continuum of neutrons at energies up to 12.3 MeV, with the possibility that the high-energy neutron signal would be proportional to the column density of the DD fuel. However, detailed simulations show that the proton is sufficiently slowed by the high column densities of the NIF targets that it appears unlikely that this idea will be useful. (It will stop in the main fuel of

full-scale targets.) The second idea we pursued appears to be more likely to be useful. In this case we propose measuring the neutrons in the 4–10 MeV band (for pure DD fuel), between the 2–3 MeV primary neutrons from the DD reaction and the 12–17 MeV neutrons produced by secondary reactions in which a triton produced by a thermonuclear DD reaction reacts with an ambient deuteron. The neutrons at intermediate energy are produced by the 12–17 MeV secondaries via elastic scattering off ambient deuterons and d(n,2n)p reactions, and the quantity of them is nicely proportional to fuel column density while being relatively independent of temperature or other details. Results of a series of test-problem simulations is shown in Figure 13. The quantity of such neutrons seems ample for detection, and they arrive before the detector is swamped by the DD thermonuclear peak. Hence this may be a valuable diagnostic for measuring column density. Work is continuing on possible noise sources (e.g., scattering and other nuclear reactions of the secondaries with other target elements and (n,gamma) reactions with various chamber elements).

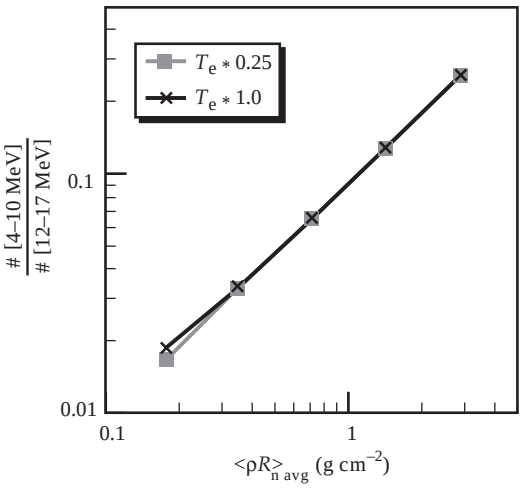

FIGURE 11. Relative number of down-scattered neutrons in the indicated bin, for a series of simulations in which the density and temperature of the DT were varied with multipliers on each. Neutrons were emitted from a central core of burning DT. (NIF-0602-05242)

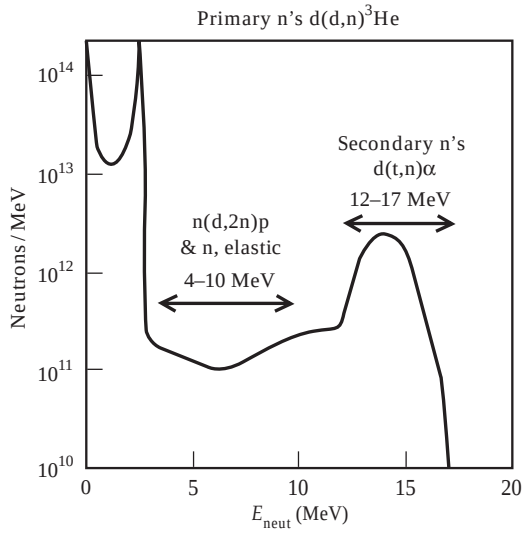

FIGURE 12. Neutron spectrum from an all-deuterium NIF-scale capsule, showing the secondary neutrons in the 12–17 MeV range and the down-scattered secondaries in 4–10 MeV. The down-scattered secondaries are proportional to column density as shown in Figure 13. (NIF-0602-05243)

Future Directions

Important work remains to be done in almost every area reported here. Our priorities for the coming year are to accomplish the following:

- Complete the optimization of the 300-eV CH(Ge) capsule by systematically exploring the parameter space of

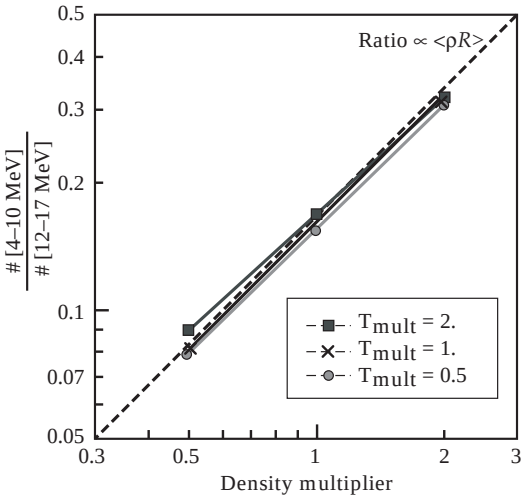

FIGURE 13. Number of down-scattered secondaries, relative to number in secondary peak, in simulations of DD targets. The ratio is proportional to column density and nearly independent of temperature. (NIF-0602-05244)

possible designs in first one and then two dimensions. This should be done with a systematic treatment of the drive radiation spectrum, so that we can quantify any possible trade-off between R-T growth and the cocktail hohlraum spectrum.
- Scale these targets, up to 400-kJ absorbed energy, to determine how rapidly the specifications loosen as the energy is increased.
- Do the same optimization and scaling for deuterated polyimide targets, with gold spectrum and cocktail spectrum.
- Do the same for 250-eV beryllium targets, with graded dopant concentration, up to 600-kJ absorbed energy.
- For each of these targets, check the sensitivity to ice roughness and radiation asymmetry.
- Continue to pursue 3D simulations, with a near-term goal of incorporating both asymmetry and short-wavelength R-T growth.

When this work is completed we will have a much better understanding of the trade-offs between the ablator materials, the x-ray drive spectra, the spectra of surface perturbations, and the available power and energy. This will be very valuable when we begin actual experiments on NIF.

Notes and References

1. P. A. Amendt et al., *Phys. Plasmas* 9, 2221 (2002).
2. M. M. Marinak et al., *Phys. Plasmas* 5, 1125 (1998).
3. M. M. Marinak et al., *Phys. Rev. Lett.* 75, 3677 (1995).

IGNITION DIAGNOSTIC DEVELOPMENT

J. A. Koch *N. Izumi* *R. A. Lerche* *M. Moran*
T. W. Phillips *G. J. Schmid* *M. A. Stoyer* *V. Glebov**
*F. Marshall** *C. Sangster** *R. Fisher*†* *S. Caldwell*‡*
J. Mack‡*

In FY00 and FY01, we made progress towards developing techniques that will allow us to diagnose ignition implosions on the NIF. This area is critical to successfully achieving ignition on the NIF since it is expected that various failure modes, undetected by other preignition ICF campaigns, may force us to tune experimental parameters based on the results of ignition experiment attempts. Reliable diagnostics of various failure modes are required, and these diagnostics will be based on particle emission (primarily neutrons) from the compressed DT fuel, x-ray emission from the compressed DT fuel, and also on post-shot analysis of materials collected from the experiment debris. Challenges include the high primary neutron yields expected from NIF implosion plasmas, the constraints imposed by the facility, and the constraints on our ability to tailor the target parameters to enhance certain signatures that might be indicative of failure modes.

*University of Rochester, Laboratory for Laser Energetics, Rochester, NY.

†General Atomics, San Diego, CA

‡Los Alamos National Laboratory, Los Alamos, NM.

Neutron Transport Calculations of Background Signals at NIF and OMEGA

Neutron spectroscopy will be a critical ignition diagnostic, providing information on fusion plasma temperature and fuel areal density through various spectroscopic techniques. These spectroscopic techniques rely on time-of-flight differences, which increase at larger distances and allow coarser time resolution to be used while providing adequate energy resolution. However, scattering and reactions between high-energy neutrons or photons and target system structures provide a background signal that can mask spectral features. It is therefore important to model the entire experimental arrangement in order to adequately estimate signal-to-noise levels expected in NIF experiments.

In FY00, we developed neutron transport models of the NIF target chamber and also the OMEGA target chamber, where we test many NIF-relevant nuclear diagnostics. We used these models to support the development of several neutron- and photon-based diagnostics. The first application of these models was to determine the feasibility of the existing neutron flight path (shielding and aperture requirements) for spectroscopy applications at the NIF. Concurrent model development for the OMEGA facility also examined the shielding and aperture requirements to extend

the capabilities of the existing Medusa neutron spectrometer for experiments with DD and DT cryogenic targets, using tertiary and down-scattered neutrons for fuel areal density measurements.

The first step in the development of the NIF model was to resurrect the original TART model used to evaluate personnel neutron exposure in the facility. Most of the primary NIF structures (concrete and metal) were included in a TART model. A number of tests using a single point source of 14.1-MeV neutrons have now been run through the model with a simplified detector at the proposed location of a time-of-flight neutron spectrometer, approximately 23 m from target chamber center. Initial results suggested that the primary neutron-induced gamma-ray background in the tertiary neutron time window is smaller than expected due to the favorable shielding configuration of the chamber gunite and the target bay wall, which effectively serve as a crude double aperture.

The neutronics modeling of the OMEGA facility now includes all of the primary structures including surrogates for the reentrant diagnostics, the brick building, the loading dock in front of and below the Medusa neutron spectrometer and the Medusa shack itself. Results of the model, based on the Monte Carlo code COG (similar to TART but with better energy resolution), were compared with neutron flux measurements throughout the target chamber using nuclear emulsion. The model results predict that the scattered neutron background should be constant throughout the target chamber, and this was verified by the measurements. The agreement between model and the measurements gives us confidence that the model can be used for predictive diagnostics development.

Down-Scattered Secondary Neutron Measurements at OMEGA Using the Medusa Time-of-Flight Array

Down-scattered (~4 to 13 MeV) primary and secondary neutrons, from DT and DD implosions respectively, have been identified as promising candidates for areal density measurements at areal densities expected for NIF ignition experiments, and possibly at areal densities achievable in OMEGA cryogenic direct-drive implosions. In preparation for OMEGA direct-drive experiments, we have begun to investigate diagnostic options for performing this measurement, and in FY00 we computationally investigated the prospects for utilizing the existing large solid-angle neutron time-of-flight spectrometer Medusa.

Using a simulated neutron spectrum generated for a nominal OMEGA cryo capsule with deuterium fill and using the COG model of the OMEGA facility, the down-scattered and background signals were calculated with a realistic response function for the individual Medusa detector elements. The initial result was that the S/N ratio is about 0.3, indicating a large background of scattered neutrons from the chamber and target bay structures. The next step was to generate simple shielding configurations within the COG model to determine whether the S/N for the down-scattered neutrons in Medusa could be increased above a value of 3 or 4, which would make such a measurement feasible with the existing detector array.

These subsequent calculations indicated that Medusa would not, in fact, be adequate for a down-scattered neutron measurement. No practical shielding

arrangement was found to improve the S/N ratio. It does appear, however, that a current mode instrument with sufficiently fast temporal response, located 20–50 cm from the OMEGA target, may be expected to record a signal from the down-scattered secondary neutrons. This option is now being pursued at the experimental level using a chemical vapor deposition (CVD) diamond detector.

Down-Scattered Neutron Measurements Using CVD Diamond Detectors

Ignition on the NIF will be achieved with DT fuel. However, important implosion diagnostic information can be obtained using DD fuels, which cannot be ignited but which retain all the physics of the implosion dynamics while providing alternative diagnostic approaches and avoiding complications from tritium contamination and high neutron yields.

In a DD implosion, two primary nuclear reactions take place: D + D → n (2.45 MeV) + ^{3}He, which gives the primary 2.45-MeV neutrons; and D + D → p (3.02 MeV) + T (1.01 MeV), which gives 1-MeV tritons. The tritons can subsequently undergo DT fusion D + T* (<0.82 MeV) → α + n (11.8–17.1 MeV), giving neutrons with 14-MeV center-of-mass-frame energy which are kinematically broadened so as to encompass the 12- to 17-MeV laboratory-frame energy range (Figure 1). The production of these secondary neutrons is related to fuel areal density. Using model-dependent assumptions about triton slowing in the fuel together with knowledge of fuel ion temperature, the areal density can be determined from the ratio of secondary neutrons to primary neutrons. Furthermore, due to the asymmetric nature of the DT cross section in the laboratory frame of reference, there is a slight correlation between the direction of the triton and the direction of the emitted secondary neutron. This allows, in principle, directional line-of-sight areal density measurements to be obtained from multiple secondary-to-primary ratio diagnostics.

One way to obtain time-of-flight neutron spectroscopy data is to use a current-mode detector placed near the target. This approach has several advantages: it can record an entire neutron spectrum before any scattered background from the chamber wall arrives; and it is small, cheap, and can be easily fielded in a standard diagnostic manipulator. To successfully implement this idea, the detector must be fast, have a large dynamic range, and be reasonably sensitive to neutrons. Diamond satisfies these criteria. It also has the additional benefit of being one of the most radiation hard materials known, and this is

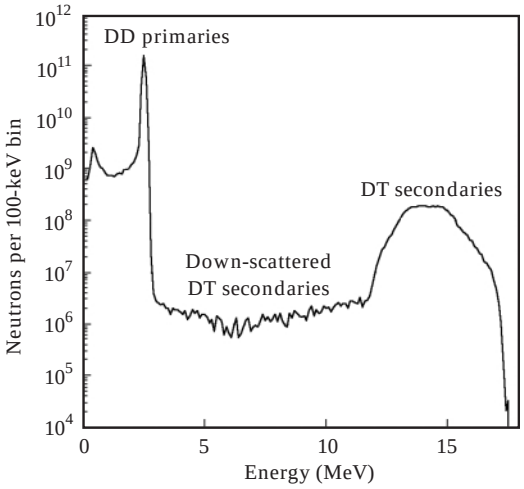

FIGURE 1. Simulated neutron spectrum from a DD implosion target. (NIF-0602-05401pb01)

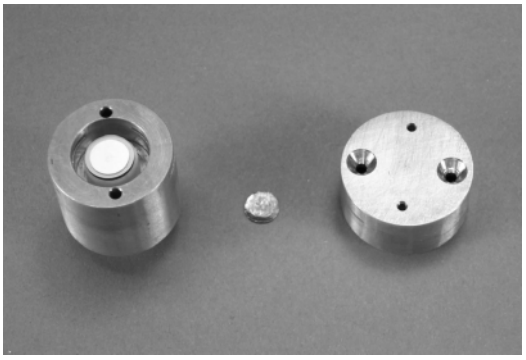

FIGURE 2. Photograph of a CVD diamond detector in its housing. (NIF-0602-05402pb01)

important for survival in the harsh NIF environment. Modern CVD diamond is larger, cheaper, and more neutron sensitive than natural diamond, and so is a better choice for neutron spectroscopy applications. We have developed CVD diamond detectors and related housings and electronics for use on OMEGA experiments (Figure 2) in order to gather experience that can later be carried over to NIF.

We have used CVD diamond-derived secondary-to-primary ratios to determine fuel areal densities in OMEGA experiments, and some of the actual oscilloscope trace data are shown in Figure 3. In Figure 3a, the full scale is shown, while in Figure 3b an expanded scale is used, which shows the small secondary peak in front of the primary peak. The areal densities obtained from these measurements are consistent with those obtained by other diagnostics. The low-energy side of the primary peak is seen to be contaminated with high-frequency electromagnetic noise. This noise will hamper later efforts to see down-scattered primary neutrons, and thus it is important to minimize this noise. We are currently working on improved detector housings and electronics that will reduce the noise level in this data.

Down-Scattered Neutron Measurements Using Gated Scintillator-Fiber Detectors

In FY00, a new concept for fuel areal density measurements was assessed based on Li-doped scintillation fibers coupled to a gated detector. This neutron spectrometer concept, named the "Palm-top Lansa," is a neutron time-of-flight system consisting of a Li-doped glass scintillation fiber bundle, a gated image intensifier, and a charge-coupled device (CCD) camera. Neutrons with energies <2.45 MeV cause $^{6}Li + n \rightarrow \alpha + T$ reactions in the core region of scintillating fiber, and the scintillation light is guided to the end of the fiber. The scintillation signal within a specific time window (corresponding to a specific energy range) is gated and amplified by the image intensifier, and each neutron signal is recorded by the CCD camera. Each fiber in the bundle functions as a single-hit-mode neutron detector if the neutron flux is appropriately small, allowing

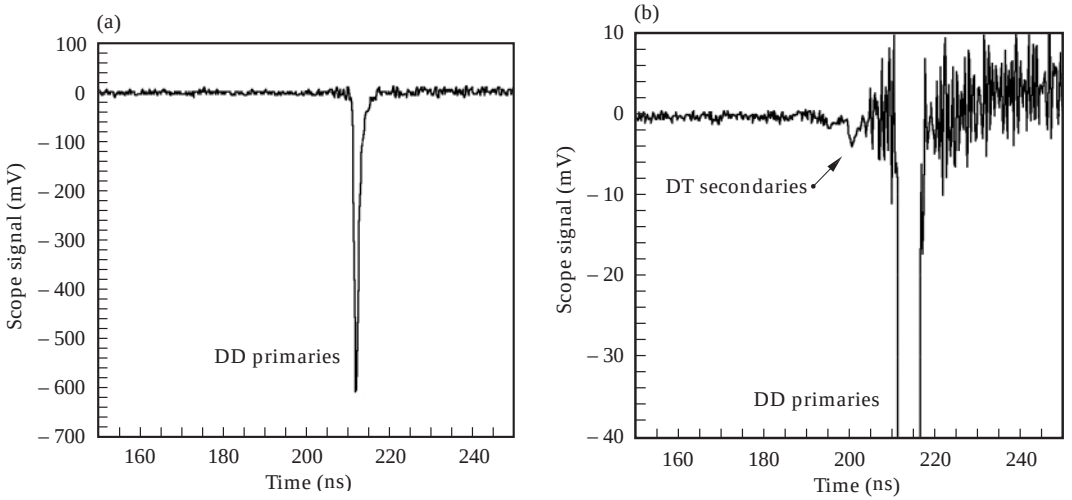

FIGURE 3. (a) Experimental CVD diamond data from a DD implosion at OMEGA. (b) Enlarged region of the spectrum in Figure 3a, showing the weak DT secondary peak. (NIF-0602-05404pb01)

down-scattered neutrons within the gated time window to be distinguished from the primary afterglow and therefore improving signal-to-noise ratio. A schematic of the Palm-top Lansa is shown in Figure 4.

The neutron flux is controlled by distance from the target; the Palm-top Lansa will be located 6 m away from the target at OMEGA, and 18 m away from the target at NIF. The Palm-top Lansa diagnostic may have certain advantages over CVD diamond current-mode detectors, principally in signal-to-noise ratio. Minimization of any low-energy neutron background is particularly important for this technique, and based on initial studies it appears that signal-to-noise ratios of 10 can be achieved with simple shielding configurations.

In the first quarter of FY00, a gated scintillation detector was rough-designed. Later progress resolved some of the final design issues for a prototype instrument, and by the end of FY00 a suitable technical design for the Palm-top Lansa was developed. Suitable commercial components for the gated detector system were identified, and we are continuing to work with outside vendors in order to obtain suitable Li-doped glass scintillator fibers.

As part of preliminary tests, we assembled the gated detector and tested it in the laboratory. The detector consists of a photocathode, a photomultiplier tube, and gating circuitry. A mesh type electrode was placed just behind the photocathode, and the potential of the mesh electrode was controlled temporally for gating. When the gate is closed, the potential of the mesh electrode is set lower than that of the cathode, and photoelectrons cannot arrive to the first dynode. When the gate is open, the potential of the mesh is set higher than that of the cathode, and the photoelectrons are guided to the electron multiplier.

Performance of the detector, including timing, transient response, extinction ratio, dynamic range, and cathode charge up, was tested using a blue light-emitting diode as a light source in place of the scintillator. The gated detector portion of the Palm-top Lansa works well, and the detector will be coupled to a conventional plastic scintillator and used for neutron measurements in high-intensity laser experiments in FY02.

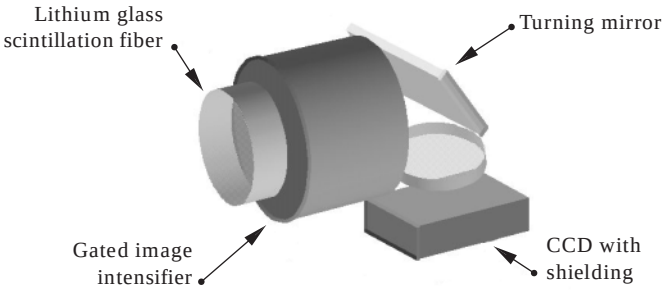

FIGURE 4. Schematic drawing of the Palm-top Lansa. (NIF-0602-05405pb01)

Gas Sampling for Radiochemistry at the OMEGA Laser Facility

Radiochemistry techniques provide a means for postshot analysis of experimental debris in order to diagnose plasma conditions during the experiment. In particular, reactions during the experiment can change isotopic abundances of trace materials introduced into the target, and these isotopic abundances can be analyzed to determine reaction rates and therefore plasma conditions. A straightforward technique is to introduce a noble gas into the implosion target fill gas and collect the gases after the experiment for isotopic analysis. A gas sampling system (OGSS) was recently installed at the OMEGA laser facility for diagnosis of OMEGA implosions and to develop gas-sampling techniques for use on NIF.

The gas sampling system hardware was assembled at Livermore and a preliminary design review was conducted with the management of LLE-OMEGA in FY00. The diagnostic utilizes a spare cryo pump (CP3) on the OMEGA target chamber to pump exclusively on the target chamber immediately after a radiochemical shot, in which nuclear reactions in the fuel and/or shell create products that can be measured using radiochemical techniques, e.g., noble gas mass spectroscopy or activation counting. The gas sampling system is mounted directly to CP3 in order to recover the gases after the cryo pump has been warmed. An identical cryo pump was

salvaged from the Nova vacuum system at Livermore to provide a development platform.

Tests during the third quarter of FY00 indicated that the original manifold design required modification to remove a mechanical diaphragm pump that backed the primary turbo-pump at the outlet of the cryo pump because the exhaust of the mechanical pump could not be sealed at the milli-Torr level as required during operation. After consulting with vacuum experts, a novel chemical sorb getter pump was built to replace the diaphragm pump. This getter pump also removes hydrogen isotopes from the gas sample, providing the added benefit of reducing tritium contamination of the mass spectroscopy counting systems at the University of Rochester and Livermore. The system was tested with the getter pump during the fourth quarter of FY00, and final system tests at LLNL have validated the operation of the system.

Tests have shown that the gas release fraction from the cryo pump is virtually 100% and that the final collection fraction from the cryo pump into a sample bottle is 42%. This collection fraction is merely the volume ratio of the sample bottle to the sum of the sample bottle plus the collection manifold. This volume ratio was measured using partial pressures of nitrogen and the known volume of the sample bottle, as well as with gas samples spiked with a known quantity of a rare isotope of neon (^{21}Ne). These samples were released into the cryo pump and then collected and analyzed. All of the test samples returned the same collection fraction to within the measurement error. The system was ready for operation at OMEGA in FY00.

Early in FY01, final tests on the OGSS were completed in Livermore; the final operational reviews with the LLE-OMEGA management were completed; and the hardware was shipped out of Livermore. Assembly and bench testing were completed in February, and the device was physically mounted on CP3 in March (Figure 5). The integrated control system was also completed and tested in the third quarter of FY01. Difficulties with a leaking gate valve on CP3 delayed initial operation of the OGSS until 2002. Background sample collection and final validation of the system is scheduled for February 2002. In these tests, background samples will be collected and analyzed to determine the amounts of various noble gases that exist in the target chamber due to air leaks and imperfect vacuum. Noble gas cocktail capsules are tentatively scheduled for April 2002. Gas samples will be collected following implosion of these capsules to determine the OGSS chamber collection efficiency.

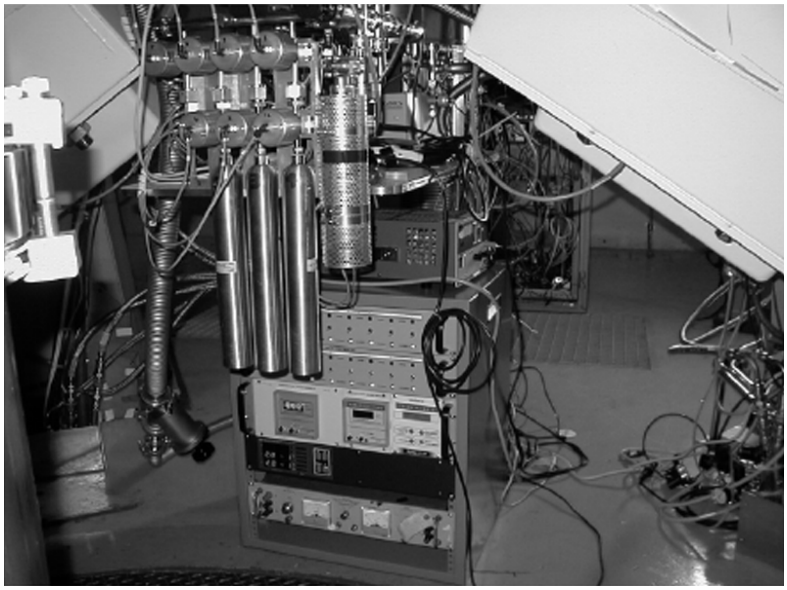

FIGURE 5. Photograph of the OGSS system at OMEGA.
(NIF-0602-05406pb01)

Monochromatic/ Multispectral X-Ray Imaging Diagnostics on OMEGA

Significantly enhanced plasma diagnostic information can be obtained by reducing the spectral content of x-ray imaging data and by utilizing multiple quasi-monochromatic x-ray images spread over a range of x-ray energies to provide spatially resolved spectroscopy data. In FY00, we developed a multiple monochromatic imager (MMI) to provide multiple monochromatic x-ray images of indirect-drive implosions at OMEGA. The MMI uses an array of pinholes coupled to a flat Bragg crystal to provide images in the 4- to 5-keV x-ray region, which corresponds to absorption by Ti doped into the capsule shell, and was designed to provide spatially resolved information on shell areal density and temperature. This diagnostic is a prototype for a technique we plan to use on NIF implosion experiments.

The experiments were conducted in October 2000. We performed four 30-beam indirect-drive implosions with different target parameters (0.2 and 0.3% Ar concentration in the 50-atm DD fuel, pulse shape 26 vs 1 ns-square, Ti vs no Ti dopant in the pusher), and obtained time-integrated data from the MMI in each case.

Typical data is shown in Figure 6, from a pulse-shape 26 implosion with 0.2% Ar dopant in the fuel and Ti dopant in the pusher layer of the shell. Energy dispersion is from left to right, with the central (4.3 keV) region corresponding to 1s-2p absorption by warm Ti that has mixed into the fuel. Each spot is an individual pinhole image, and comparison between images obtained at different x-ray energies allows spectroscopic diagnosis of Ti plasma conditions. The MMI data we obtained was not sufficiently high-quality to allow for quantitative analysis, but did provide us with experience designing the diagnostic and fielding the experiment. In particular, the graphite crystal we used to disperse the x-rays was of poor quality, and introduced spatially varying artifacts into the imaging data. A second version of the MMI (the MMI2) was then developed, which uses a multilayer mirror instead of a graphite crystal to provide dispersion, and will be fielded at OMEGA in FY02.

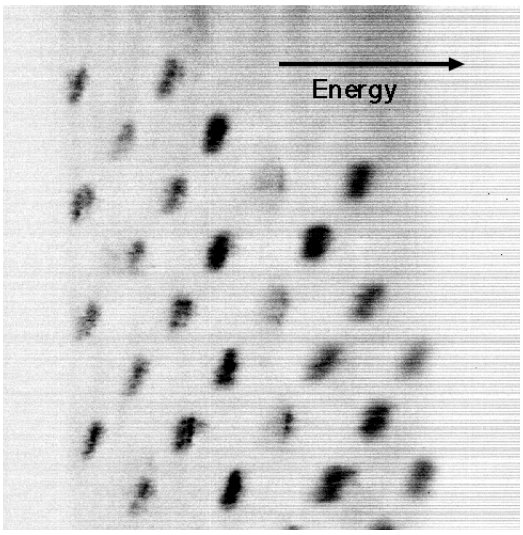

FIGURE 6. MMI data from a Ti-doped capsule implosion at OMEGA. The spots are individual core images obtained through individual pinholes. (NIF-0602-05407pb01)

Bubble Detectors for Neutron Imaging

A neutron imaging system at NIF would benefit greatly from a neutron detector with fine resolution. This would reduce the magnification required to achieve fine (~5 μm) target spatial resolution, and would allow either the detector to be moved closer to the source (increasing source flux) or the imaging aperture to be moved farther from the source (decreasing the likelihood of damage to the aperture). General Atomics has developed gel bubble detectors as an alternative to plastic scintillator arrays, and LLNL scientists have collaborated with General Atomics in this development and in testing the detectors. These detectors are composed primarily of a matrix material (99%) that holds small droplets of active bubble forming material (~1%). Neutron reactions within the active material form localized bubbles that can be counted to determine the incident neutron spatial distribution.

As a resolution test, we exposed a gel bubble detector to a neutron flux and formed a contact print of the gel onto Polaroid film. The print was scanned, and the data was analyzed to yield an image resolution consistent with the experimental setup and with the neutron statistics. The minimum bubble size for reliable optical identification was smaller than 100 μm, the limit imposed by the quality of the Polaroid film used for the print. Estimates based on the geometry of the readout setup suggest a minimum bubble size of approximately 50 μm, based on scattered light and the available film contrast. This work indicates that a bubble-based readout is feasible for a high-resolution neutron imaging system and capable of ~50-μm spatial resolution. This is far superior to the 1-mm resolution typical of current plastic scintillator arrays.

Gel-type bubble detectors lack sensitivity, however, having about 0.5% the efficiency of an equal thickness of plastic scintillator, and image system performance would be greatly enhanced by using a more efficient bubble detector. A factor of ~100 increase in efficiency is expected by switching from a gel to a liquid bubble detector, where 100% of the detector material is sensitive to neutrons. We are beginning to investigate the properties of liquid bubble detectors and techniques for recording their image information.

High-Speed Fusion Gamma-Ray Diagnostics at OMEGA

Fusion reaction history measurements can provide detailed information about the time history of shock waves within the implosion core, which locally compress and heat the fuel and alter the instantaneous reaction rate. Fusion reaction histories during the time of peak fusion yield can best be measured by observing gamma-ray emission. These gamma rays result from the primary DT reaction $D + T \rightarrow \gamma$ (16.7 MeV) + ^{5}He. Gamma rays travel at the speed of light, independent of energy, and therefore the time history of their emission faithfully reproduces the history of the primary fusion reactions independent of the distance to the diagnostic. A gamma-ray detector based on a gas Cerenkov cell (GCC) has been developed by LANL, and LLNL contributed to this effort by providing and fielding an optical streak camera detector to produce high (<15 ps) time resolution of the gamma-ray emission.

The GCC has a LANL optical relay with extended blue transmission between its output window and an LLNL S-20 optical streak camera with a UV transmitting sapphire window. The streak camera for the Cerenkov cell was assembled and tested at Livermore and delivered to the University of Rochester during FY01. Optical coating delays for the mirrors of the GCC prevented planned full system tests at OMEGA in FY01, but the LLNL streak camera was successfully operated on high-yield OMEGA shots. These tests showed high backgrounds inside the OMEGA target bay on high-yield shots.

Full system tests were conducted at the Idaho State University electron linac in late August 2001. The measured temporal response for the gas Cerenkov detector system was found to be <30 ps. Measurement speed was limited by the linac pulse width, which is also ~30 ps. We estimate true system performance to be <15 ps. LLNL is in the process of commissioning their linac with a photoinjector source, which is expected to produce 1-ps pulses; further full system tests with higher time resolution are planned.

The full GCC and streak camera system will be tested at OMEGA during the next high-yield shot opportunity, currently scheduled for March 2002. While the estimated gamma-ray and background signal levels are comparable, we are hopeful that we will be able to observe a Cerenkov gamma-ray pulse with the streak camera.

IGNITION TARGET DEVELOPMENT

T. P. Bernat *R. C. Cook* *M. Takagi* *B. W. McQuillan**
C. C. Roberts *S. A. Letts* *A. E. Nissen* *W. Shmayda*†
R. L. McEachern *P. Armstrong* *J. D. Moody* *G. W. Collins*
J. Sater‡ *B. J. Kozioziemski* *R. A. London* *D. N. Bittner*‡
J. J. Sanchez *W. Geidt* *J. W. Pipes* *N. Alexander**

In fiscal year 2000 (FY00) and 2001 (FY01), development of ignition targets for the National Ignition Facility (NIF) were focused on two broad areas: (1) developing fuel capsules corresponding to current designs and (2) developing methods to form, characterize, and control the cryogenic fuel layers on the interiors of these capsules.

Capsules for Indirect-Drive Ignition

The work of developing fuel capsules for indirect-drive ignition targets for the NIF continues to concentrate on three capsule types: (1) CH capsules with small additives of higher atomic number elements to control opacity; (2) polyimide capsules that have higher density than CH and therefore have better implosion properties in simulations; and (3) beryllium capsules, which are the best choice from a capsule physics point of view, but are the hardest to make.

*General Atomics, San Diego, CA
†Ontario Hydro, Ontario, Canada
‡Schafer Laboratories, Livermore, CA

Development of Polymer Coating Mandrels

All capsule fabrication technologies, except machined beryllium, depend upon a spherical plastic mandrel upon which the ablator is coated. The symmetry of the resulting shell, especially at the low to middle surface modes, is largely controlled by the quality of the mandrel, so producing high-quality mandrels is of the highest priority. We use microencapsulation to produce poly(α-methylstyrene) (PαMS) shells that are overcoated with 10 to 15 μm of plasma polymer and then thermally treated to decompose the PαMS to monomer gas, which diffuses through the overcoated shell. The resulting thermally stable plasma polymer shell has symmetry identical to the microencapsulated PαMS shell.[1] This conversion of the PαMS shell to a plasma polymer shell is necessary since subsequent polyimide ablator deposition and processing require a thermally stable mandrel.

For the microencapsulation process, a triple-orifice droplet generator produces water droplets encapsulated by an immiscible layer of organic solvent (fluorobenzene) containing the PαMS. (The organic phase is usually referred to as the "oil" phase in immiscible systems.) This compound droplet is suspended in an aqueous bath. The organic solvent in the oil layer then slowly diffuses into the surrounding bath leaving a solid PαMS shell. Subsequent low-temperature drying removes the inner water phase.

During this reporting period we completed development of these processes for 2-mm-diam mandrels, culminating in the production of mandrels meeting NIF specifications. To improve the low-mode sphericity of the PαMS capsules to less than 1 μm out-of-round (oor) we used polyacrylic acid (PAA) as a suspending agent in the supporting water bath.[2] This significantly increases the interfacial tension between the bath and the PαMS/fluorobenzene phases resulting in more spherical shells. The power spectra of these shells met the NIF requirements for modes 2 to 8, but roughness at somewhat higher mode numbers, particularly around mode 10 to 15, remained, as did PAA debris on the shell surface that resulted in unacceptable mid- to high-frequency roughness when the shells were overcoated with plasma polymer.

At the end of FY99, it was suggested that an organic solvent concentration gradient in the mandrel wall during curing could, if sufficiently large, drive Marangoni convection cells in the wall itself, which could lead to surface and wall perturbations. Application of the theory of Marangoni convection to spherical shells losing solvent from its outer surface provides two important results.[3]

First, convection cells are "turned on" when the Marangoni number, M, exceeds a critical value, M_c. The Marangoni number for our situation is defined as

$$M = \frac{\Delta C w (d\gamma / dC)}{\eta D} \quad , \qquad (1)$$

where ΔC is the difference in polymer concentration, C, from the inside to the outside of the fluid wall of thickness w, $(d\gamma/dC)$ is the change of the outer surface interfacial tension with respect to polymer concentration, η is the oil phase viscosity, and D is the diffusivity of fluorobenzene in the oil phase.

Second, the theory allows the prediction of the spherical harmonic mode that should characterize the lateral length scale of the convection cells. For a spherical shell there are two length scales of interest, the thickness of the oil phase wall, w, and the circumference, πD, of the oil phase shell. These two length scales give rise to a set of solutions of the hydrodynamic equations, each solution corresponding to a different spherical harmonic mode, l, characterizing the relative size of the convection cells. For each mode there is a unique critical Marangoni number. Thus the physically observed l mode will be the one that gives the minimum critical Marangoni number. Using our best estimates for our experimental process parameters, we find that this mode is approximately given by

$$l_{ob} \cong \frac{\pi D}{4w} \quad . \qquad (2)$$

The predicted mode based upon the initial encapsulation conditions is between 8 and 17, consistent with the experimental results we have seen.

These shells are not in steady state but rather are continually changing. As the solvent is removed, the interfacial tension (and probably also its gradient) is changing, the wall thickness is decreasing, the viscosity is dramatically increasing, and the diffusivity of fluorobenzene is probably decreasing. Thus, primarily because of the decrease in w and increase in η, the Marangoni number for the shell decreases during curing. Assuming M starts off above M_c, at some time later its value drops below the critical value and convection stops. If the oil phase shell is too viscous at this point to "relax out" distortions caused by the convection cells, their imprint will remain in the final dry shell.

Experimentally we find that the mode structure we see corresponds roughly with the compound droplet conditions at the time when the droplet is initially formed, when the convection is easiest due to low viscosity, rather than at some later time when M is still greater than M_c, but the calculated l_{ob} has changed due primarily to the thinning wall. The failure of the shell convection cells to "adjust" to the changing geometry by decreasing the size of its convection cells (and simultaneously increasing their number) is possibly due to an activation barrier.

We do not have quantitative values for many of the relevant terms, but the functional relationships developed clearly point to processing changes that can decrease M and thus potentially shut off

Marangoni convection while the shell is still fluid enough to relax, or perhaps prevent it entirely. We found the easiest parameter to control was the polymer concentration difference across the wall, ΔC. This was accomplished by slowing the removal of fluorobenzene during cure by providing a flow of nearly saturated fluorobenzene vapor to the space above the curing bath. As shown in Figure 1, we find that 2-mm-OD shells cured in one day (without a fluorobenzene vapor flow) have a substantial mode 10 feature compared to shells in which the curing was extended to four days using fluorobenzene vapor. By extending the drying time, we have decreased ΔC and presumably dropped the shell Marangoni number below the critical value, eliminating convection, either from the time of compound droplet formation or while the oil layer was still fluid enough to relax.

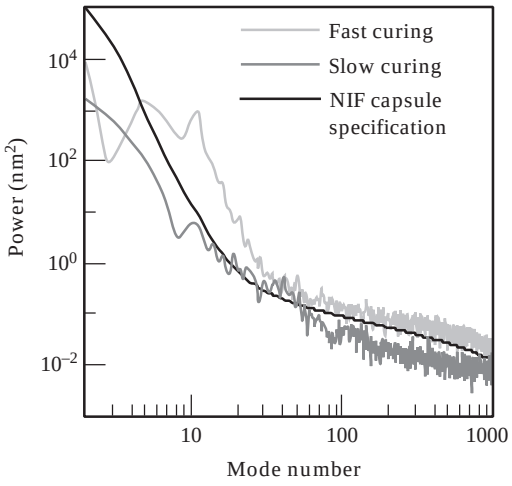

FIGURE 1. Power spectra for two shells are shown, the light-gray data for a shell cured rapidly in one day, the dark-gray data for a shell cured more slowly over four days. (NIF-0702-05363pb01)

The mandrels made using PAA as the bath additive to improve roundness were substantially rougher in the high modes than those made previously with polyvinyl alcohol (PVA) as the bath additive. Atomic force microscope (AFM) patch scans showed loosely attached "mats" of debris that we believe is PAA on the surface (Figure 2a). To address this problem we have added a NaOH washing step. The lowered pH completely ionizes the acrylic acid groups, substantially changing the chain-chain electrostatic interaction and allows them to be (mostly) washed off. The resulting surfaces are smoother (Figure 2b), but glow discharge polymer (GDP) coatings on the washed surfaces are still too rough. This is clearly shown in Figure 3 where we show the power spectra of a 2-mm PαMS shell and that of a similar shell that has been overcoated with plasma polymer. The inset shows sections of a representative AFM trace from each shell. Clearly small surface defects caused by residual PAA on the shell surface grow during the coating process resulting in unacceptably rough surfaces.

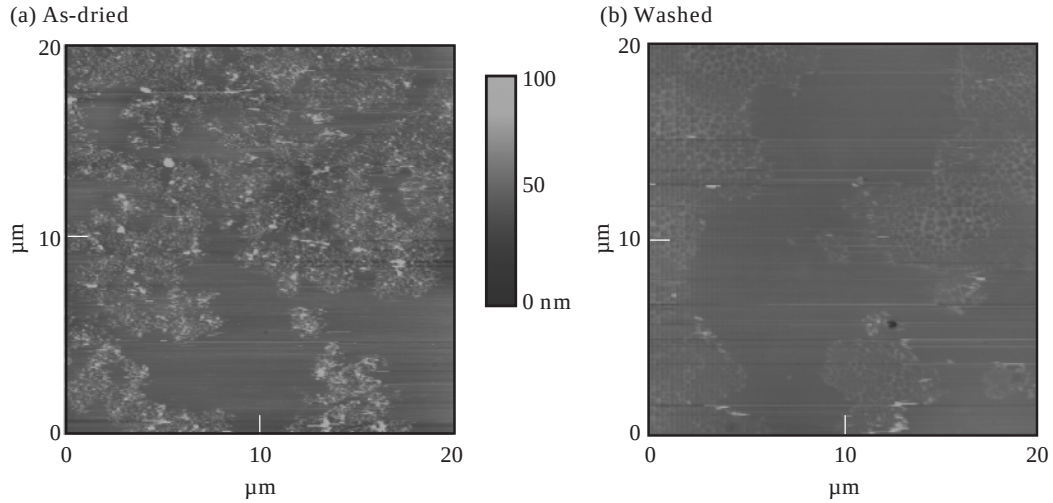

FIGURE 2. AFM patch scan of a PαMS mandrel cured in a PAA solution (a) as dried and (b) after washing in a sodium hydroxide solution. Horizontal streaks are likely the result of the interaction of surface debris (perhaps PAA) with the AFM tip. (NIF-0702-05364pb01)

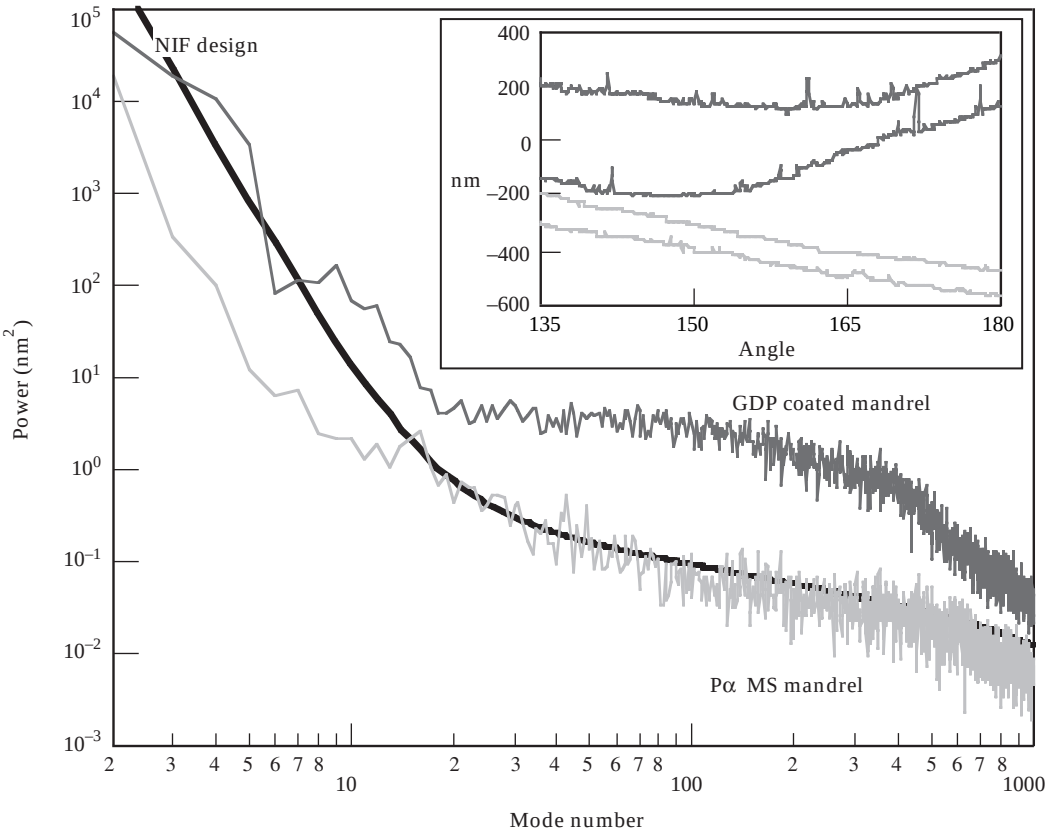

FIGURE 3. Power spectra of a 2-mm-OD PαMS mandrel (light gray) and a GDP shell (dark gray) made from the same batch. Inset shows typical profiles from the PαMS mandrel and the GDP shell, the roughness of the latter is clear. (NIF-0702-05365pb01)

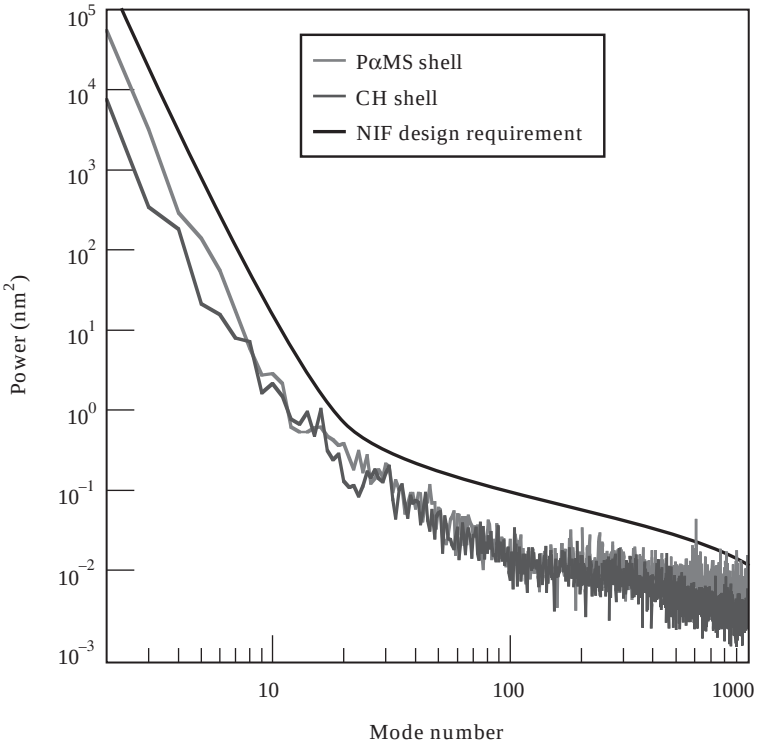

FIGURE 4. Power spectra for a PαMS mandrel and a CH shell produced from a PαMS mandrel made by the improved PAA/PVA substitution process. (NIF-0702-05366pb01)

Since we had previously demonstrated that the use of PVA in the supporting bath did not result in surface deposits, we explored ways of combining the use of PAA to promote spherical symmetry and PVA to promote clean surfaces.[4] We initially tried adding PVA solution to the bath after various cure times in PAA to fix the symmetry to see if the PVA might displace the PAA from the surface. The initial results were promising, and this led us to a procedure in which we cure the shells in PAA for 24 h and then exchange the PAA bath with a PVA bath, and continue the curing for an additional two to three days. We determined that after 24 h in PAA, the oil phase viscosity has increased to the point where the basic shell geometry is fixed, yet the PAA is not irreversibly bound to the shell surface. The removal of the shells from the PAA environment, coupled with the additional cure in PVA, results in shells that have essentially debris-free surfaces. In Figure 4 we show the power spectra of a 2-mm-diam PαMS shell made by the PAA / PVA exchange process and the

subsequent CH shell made from a PαMS shell from the same batch. The power spectra are nearly the same and both below the NIF design requirement for the final ignition capsule.

Investigation of High-Density Hydrocarbon Ablators Deposited in a Saddle-Field Plasma

Design simulations have shown that increasing the density of the ablator material while maintaining its low Z character leads to better performance due to reduced Rayleigh–Taylor (R-T) instability. The density of typical CH plasma polymer is about 1.05 g/cm^3. We have explored options to produce CH materials with higher densities and here report on work conducted by Dr. Walter Shmayda at Ontario Hydro with contractual support from LLNL.

The properties of hydrogenated amorphous carbon (C/H) films have been studied over the past decade. Plasma-based deposition systems are the preferred approach to decompose the feed gas and grow the films. In the saddle-field plasma, (see Figure 5), electrons oscillate between two electrodes and ionize the feed gas. Ions that are formed are drawn from the plasma by a gentle axial field and delivered to a substrate beyond the transparent electrodes. Both ions and neutral particles participate in the film growth process.

The underlying strength of the saddle-field plasma configuration rests in the ability to control several plasma parameters independently: the ion flux, ion energy, and the ratio of the charged to neutral particles leaving the plasma, the temperature of the substrate, and the chemical species being deposited. Adjusting these parameters alters the density of films grown, their hydrogen content, porosity, and morphology. In applying this coating technique to our problem, the microsphere to be coated is placed inside a rotating cup behind the cathode and restrained within the cup with a wire mesh cover. Flat samples, to measure the film thickness, the attenuating effects of the screen, and film stresses, are attached directly to the substrate in proximity of the rotating cup.

Previous work has shown that these techniques are capable of producing thin C/H films on flat substrates with densities as high as 1.8 or 1.9 g/cm^3. The objective of our work was to determine whether NIF-thickness films can be deposited on 2-mm spherical mandrels with adequate smoothness while maintaining densities in excess of 1.5 g/cm^3. The primary challenges are uniform deposition onto spherical substrates, the quality of the surface finish, and the control of stress in the coatings, a feature very common in plasma-deposited carbon-based films.

We coated both flat substrates and shells with mixed results. On spherical substrates we found the coating rate to be very low, typically 0.1 μm/h. Coating uniformity was excellent, with no obvious signs of stress resulting in shell deformation or coating delamination. The density was measured to be in excess of 1.5 g/cm^3 for a number of deposition conditions, and in some cases was as high as 1.9 g/cm^3. However, under these conditions the surface was degraded due to a relatively high prevalence of particulate growth on the coating surface, even for coatings of only a few microns. In Figure 6 we show power spectra obtained from 250 × 190 μm interferometrically based patch analysis that have been scaled appropriately for a 2-mm-diam shell.

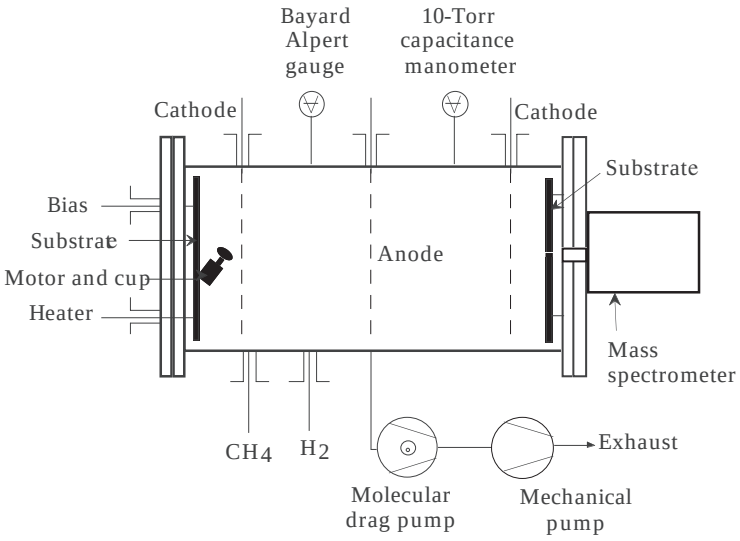

FIGURE 5. Saddle-field glow discharge apparatus. (NIF-0702-05367pb01)

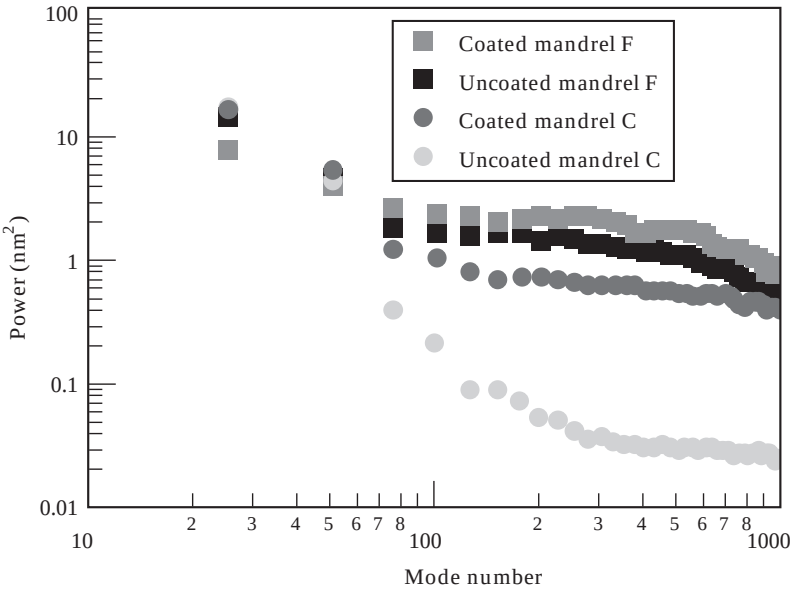

FIGURE 6. Two-mm capsule power spectra scaled from interferometrically based patch scans from two coated mandrels (light gray and dark gray). Typical power spectra for uncoated mandrels (black and very light gray) from the same batches are also shown. (NIF-0702-05368)pb01

Shown are spectra for both representative uncoated mandrels and the coated shells. We see that even for these thin coatings of a few microns, there is a significant increase in the high-frequency roughness of the shells.

In summary, the saddle-field plasma technique has been shown capable of depositing CH coating with densities up to 1.8 g/cm^3; however, the coating rate is both very slow (0.1 to 0.2 µm/h) and the surface finish of the coating is unacceptably rough. Thus we conclude that this technique for producing high-density CH ablators is not feasible for NIF ignition targets.

Notes and References

1. B. W. McQuillan, A. Nikroo, D. A. Steinman, F. H. Elsner, D. G. Czechowicz, M. L. Hoppe, M. Sixtus, and W. J. Miller, "The PαMS/GDP Process for Production of ICF Target Mandrels," *Fusion Technol*. 31, 381 (1997).
2. M. Takagi, R. Cook, R. Stephens, J. Gibson, and S. Paguio, "Decreasing Out-of-Round in Poly(α-Methylstyrene) Mandrels by Increasing Interfacial Tension," *Fusion Technol*. 38, 46 (2000).
3. The essential hydrodynamics for this analysis can be found in three papers: (a) O. Pirotte and G. Lebon, "Surface-Tension Driven Instability in Spherical Shells," *Appl. Microgravity Technol*., I(4), 175-9, (1988); (b) H. C. J. Hoefsloot, and H. W. Hoogstraten, "Marangoni Instability in Spherical Shells," *Appl. Microgravity Technol*., II(2), 106-8, (1989); and (c) O. Pirotte and G. Lebon, "Comments on the Paper 'Marangoni Instability in Spherical Shells,'" *Appl. Microgravity Technol*., II(2), 108-9, (1989). For a detailed report on the application of these ideas to microencapsulated shells, see B. W. McQuillan and M. Takagi, "Removal of Mode 10 Surface Ripples in ICF PαMS Shells," *Fusion Technol*. (2002), in press.
4. M. Takagi, R. Cook, B. McQuillan, F. Elsner, R. Stephens, A. Nikroo, J. Gibson, and S. Paguio, "Development of High Quality Poly(α-methylstyrene) Mandrels for NIF," *Fusion Technol*. (2002), in press.

Polyimide Capsules

Polyimide (PI) is one of the leading ablator designs for NIF ignition capsules.[1] At LLNL, polyimide has been developed[2] using a monomer vapor deposition technique, initially used for thin flat coatings by Salem et al.[3] Related work has been pursued at University of Rochester Laboratory for Laser Energetics;[4] however, the goal of that work is very thin layers for direct-drive capsules in contrast to the 150-µm-thick layers required for indirect drive. In addition, LLNL has supported work at Luxel Corporation to produce polyimide ablators using a polyimide precursor solution-based deposition approach.

In the FY99 *ICF Annual Report*, we detailed the basic procedures and coater equipment for the vapor deposition approach. We had previously demonstrated that 150-µm-thick layers can be deposited on GDP mandrels[5] and imidized to give uniform polyimide ablators; however, the surface finish of the capsules was poor. To remedy this, we briefly described a promising new vapor smoothing technique.

In the work presented here, we describe our progress since the last report. The vapor deposition work is divided into three parts. Following a brief background section, we discuss our efforts to improve the quality of the "as-coated" shells. This has involved both detailed studies of aspects of defect generation in the coating as well as more process-oriented modifications. Following this, we detail our work on the vapor smoothing process which has involved both empirical studies of the effects of process variations on the

effectiveness of the smoothing treatment as well as studies designed to better understand the smoothing mechanism. We also present burst strength, hydrogen permeability, density, and optical transmission results for polyimide shells. A separate section covering the solution-based polyimide effort at Luxel concludes this section.

Background

Fabrication of polyimide shells starts with the deposition of two monomeric substances, 4,4–oxydianiline (ODA) and pyromellitic dianhydride (PMDA), onto an agitated mandrel under high vacuum (10^{-6} torr). The monomers are generated in separate Knudsen cell evaporators heated to different temperatures during deposition in order to control their individual fluxes and maintain a desired 1:1 stoichiometry. Figure 7 depicts the process. As the deposition proceeds, there is some level of reaction between the two monomers on the shell surface to form polyamic acid (PAA) as shown in Figure 8.

Deposition Process Development

Contact between the shell and the shaking pan creates surface defects by either abrasion or adhesion phenomena. Hence, the deposition time is adversely correlated with the surface finish of the as-coated shell. We have found that we can increase the deposition rate from 1 or 2 µm / h to 10 µm / h, thus improving the surface finish. Typical results are shown in Figure 9. A mandrel coated with 140.9 µm at 2 µm / h shows a rougher surface finish after coating than a mandrel coated with 186.4 µm at 10 µm / h. The average rms roughness (based on three shell views) is 1400 nm at 2 µm / h and only 328 nm for the faster coating process.

To study shell coating without the effects of a bouncer pan, we mounted shells on stalks and rotated them in the center of the coating chamber in the same position they

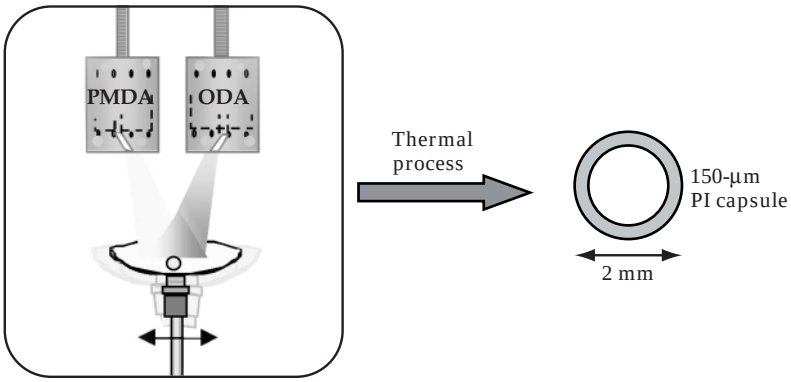

FIGURE 7. Diagram of the polyimide vapor deposition system. (NIF-0702-05369pb01)

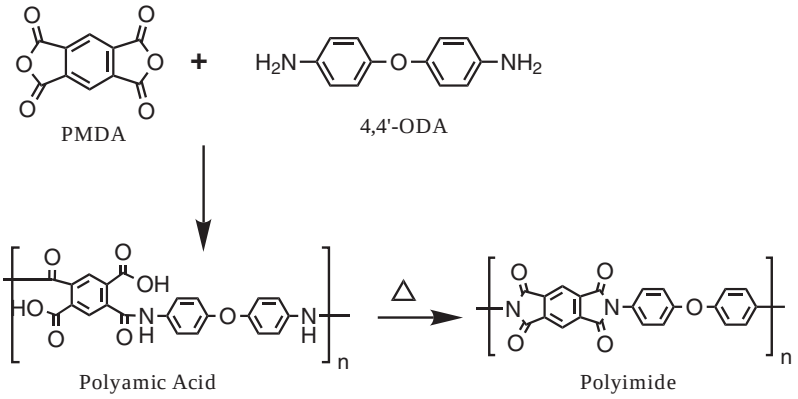

FIGURE 8. Diagram of the PMDA–ODA deposition reaction, followed by the ring closure with heat to the polyimide form. (NIF-0702-05370pb01)

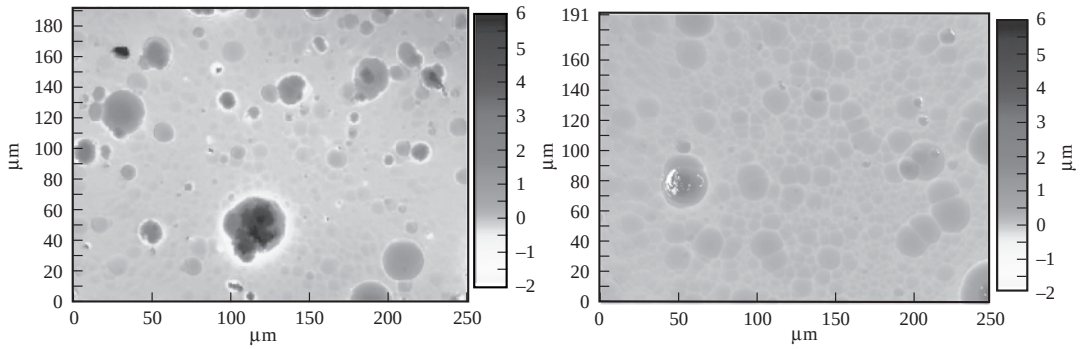

FIGURE 9. CH mandrel overcoated with 140.9 µm of PAA at 2 µm/h (left) and CH mandrel overcoated with 186.4 µm of PAA at 10 µm/h (right). Average rms surface roughnesses are 1400 nm and 328 nm respectively. (NIF-0702-05371pb01)

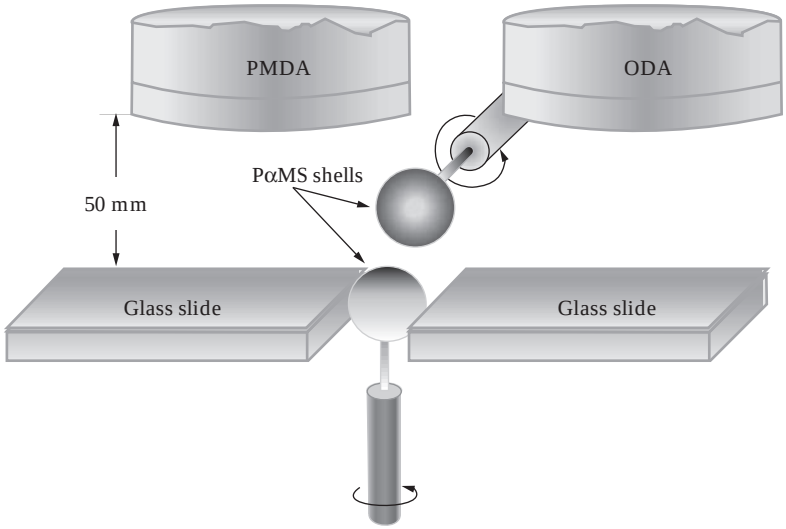

FIGURE 10. Rotated shells were coated in a vertical and horizontal orientation. Slides were placed at the side to measure the coating rate and surface roughness.
(NIF-0702-05372pb01)

would occupy if placed in a pan. During each run, two shells were held in orthogonal orientations (shown in Figure 10): one vertically, the other horizontally. It was expected that the equator of the horizontal shell would show the best surface finish obtainable without pan contact. The shells were coated at 1 to 4 μm / h rates. This resulted in a coating thickness from 15 to 60 μm on the pole of the vertical shell with the amount on the sides decreasing with angle from the vertical. On the horizontal shell the coating thickness around the equator was 10 to 40 μm.

The roughnesses of the shells were measured with a Wyko interferometer. The pole of the shell rotated on a vertical axis had a roughness of about 57 nm rms. However, the side of the vertical shell had a roughness of 350 nm rms. A rather sharp change in surface quality occurred at an angle corresponding to the limiting position where the surface was visible to both monomer sources at all times, thus insuring continuous mixed monomer deposition. We think that the increased roughness below this point may be due to momentary shadowing of the surface from one monomer source, resulting in deposition of only a single monomer and simultaneous crystallization.

The equator band of the horizontal shell had a roughness of 123 nm rms. In this case a portion of the equator was always subject to shadowing as described above. The vertical shell was rotated at 22 rpm while the horizontal shell was rotated at 80 rpm. When the rate of shell rotation was reduced by a factor of 10, the magnitude of coating roughness doubled for the horizontal orientation and was unchanged at the pole of the vertical orientation, consistent with the shadowing model.

To more carefully study the effect of stoichiometric imbalance caused by shadowing, we mounted a silicon wafer horizontally on a rotating platform under the evaporators. Each monomer was constrained to coat only on one-half of the wafer at any instant by placing a barrier between the evaporators. The substrate was rotated under the evaporators receiving alternate exposures to each of the monomers. We found that slow rotation or fast deposition conditions consistent with thicker single monomer layers produced rough surfaces that had obvious crystal inclusions. Rotating faster or depositing slower produced very smooth coatings. We determined that smooth coatings resulted if the single monomer deposition per rotation cycle was less than about 4 Å, which is less than a monolayer. Monomer layers thicker than 4 Å per rotation tend to crystallize. Thus to achieve smooth coatings on a shell held in a bouncer pan, the shell rotation must be fast enough to limit single monomer deposition in a region to less than 4 Å to prevent growth of monomer crystals.

Vapor Smoothing

As reported previously, we developed a preimidization smoothing process as shown in Figure 11. The as-coated shell is supported on a near room temperature N_2 flow that contains dimethyl sulfoxide (DMSO) vapor. The rough shell absorbs vapor from the flow, softening and perhaps fluidizing the PAA coating. After exposing the shell to smoothing vapors for a period of time, the temperature of the housing around the shell is increased to 300°C to imidize the smoothed layer in situ.

The surface finish of the final smoothed shell depends upon the roughness present on the as-coated shell. The top left of

Figure 12 is a Wyko interferometric surface image of a 70-µm-thick coating on a 2-mm mandrel. The surface finish of this as-coated shell has a large number of small bumps, with diameters less than 15 µm and heights less than 1 µm. This type of surface morphology is affected strongly by the smoothing process, and the final PI surface is quite smooth as shown at the top right.

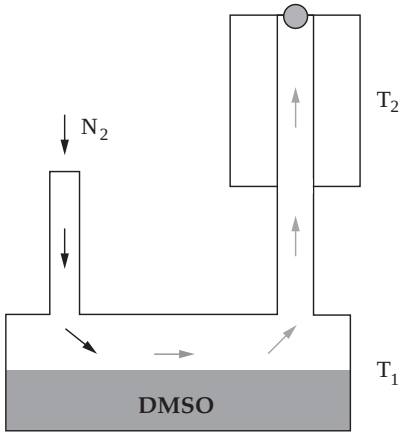

FIGURE 11. Diagram of the smoothing apparatus. (NIF-0702-05373pb01)

At the bottom left is a patch scan from a 155-µm-thick as-coated shell surface, which shows a much rougher surface with bumps as large as 20 µm in diameter and 3 µm in height. As shown at the bottom right, this surface is also smoothed by solvent exposure, but some texture remains.

Spheremap analysis shows more quantitatively the effect of smoothing as a function of mode number. In Figure 13 for two shells we show the power spectra for the mandrels, the as-coated shells, and the shells after smoothing. For both we see that up to modes between 15 and 20, the power spectra follow those of the mandrels. Above mode 20, the power spectra of the as-coated shells is dominated by the numerous bumps on the surface and the power spectra remains high out to mode 300 to 500, corresponding roughly to the width of the bumps, and then drops off more rapidly. In each case, the power spectrum of the smoothed shell begins to deviate from the as-coated shell between mode 20 and 30 and at higher modes actually drops below that of the underlying mandrel, indicating a very smooth high-frequency surface.

Experiments were conducted to investigate the effect of solvent exposure time

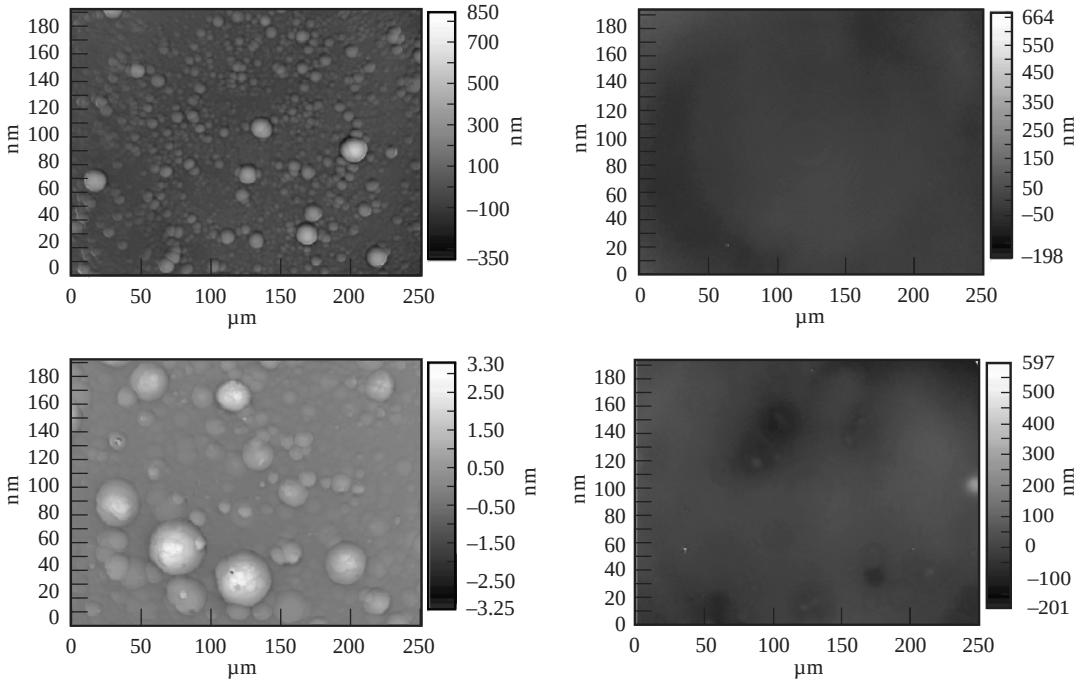

FIGURE 12. Wyko images (251 × 190 µm) for coated shells, before (left) and after (right) smoothing. Average rms values are top: 73 nm and 22 nm; bottom: 457 nm, and 32 nm. (NIF-0702-05374pb01)

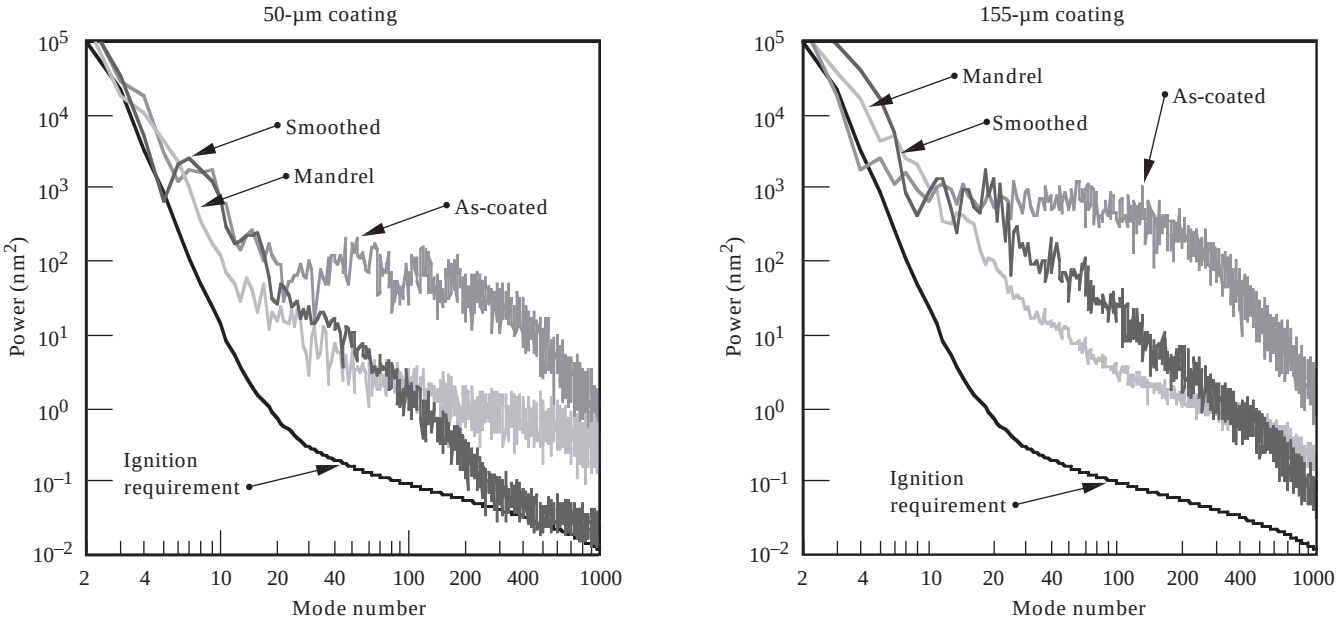

FIGURE 13. Shown are power spectra of two shells both before (light gray) and after (dark gray) smoothing. The power spectra of the mandrels used (very light gray) are also shown. (NIF-0702-05375pb01)

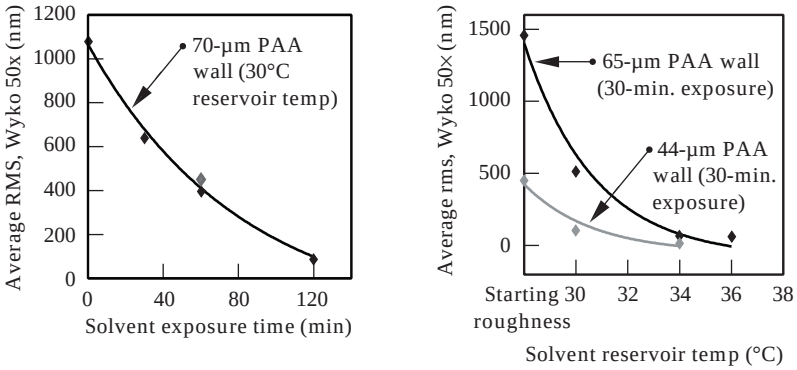

FIGURE 14. Change in rms roughness, as measured by Wyko, on PAA shells as a function of solvent exposure time (left) and solvent reservoir temperature (right). (NIF-0702-05376pb01)

and solvent vapor concentration on the smoothing effectiveness. Shells from the same PAA coating batch were treated with the smoothing process, varying either the time of solvent exposure from 30 to 120 minutes, or varying the solvent vapor concentration by the temperature of the solvent. As shown in Figure 14, both longer times and higher concentrations lower the rms roughness due to the increased solvent and more flow of the fluidized surface layer.

To further explore the time dependence of the smoothing process, we used a Wyko objective to monitor the surface of a shell exposed to organic vapor. The solvent vapor pressure was controlled by mixing saturated vapor with dry nitrogen gas. In Figure 15 the time dependence of a single line out from the Wyko data clearly shows the smoothing process. From the full Wyko images, we have also extracted the surface power spectra for shell modes 25 and above, and these are shown in Figure 16. We see that the higher modes are reduced first as the smallest defects are smoothed; the lower modes take much longer to begin smoothing and are only partially reduced after 2 hours of solvent exposure. The changes in surface morphology suggest surface tension-driven flow, as evidenced by the more rapid decrease in the higher modes of the power spectrum, where the defects with the highest amount of curvature are found. Efforts to exploit this surface tension effect are in progress.

Properties of Polyimide Shells

a. Burst Strength. Burst strength measurements were made on a selection of shells by filling to a known pressure and then rapidly (though controllably) decreasing the external pressure and recording the

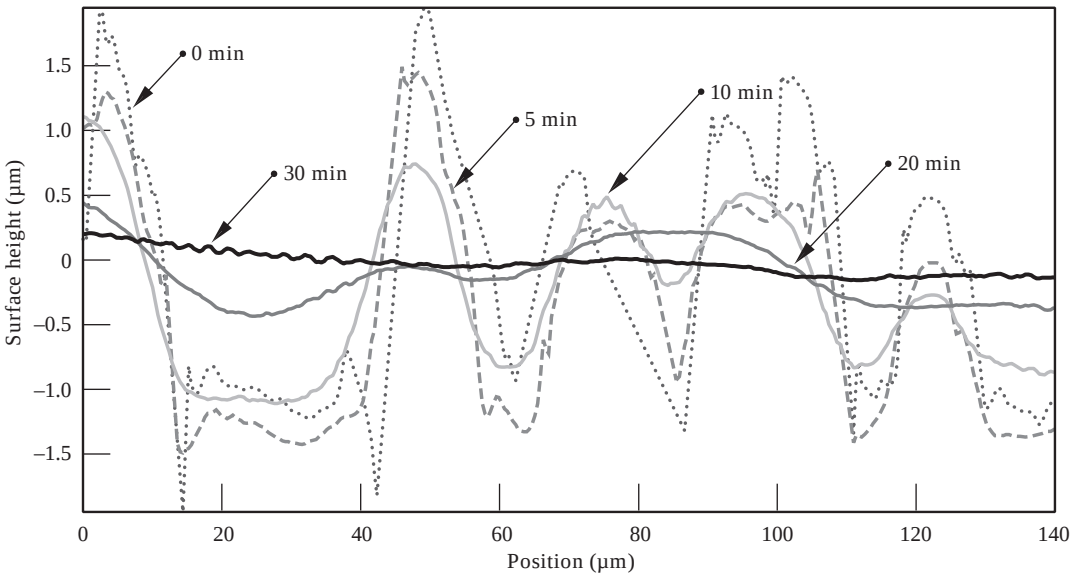

FIGURE 15. Line profile for smoothing of PAA surface over time, under Wyko analysis. Note the waves in the data at later times, which is due to an artifact of the interferometric method. (NIF-0702-05377)

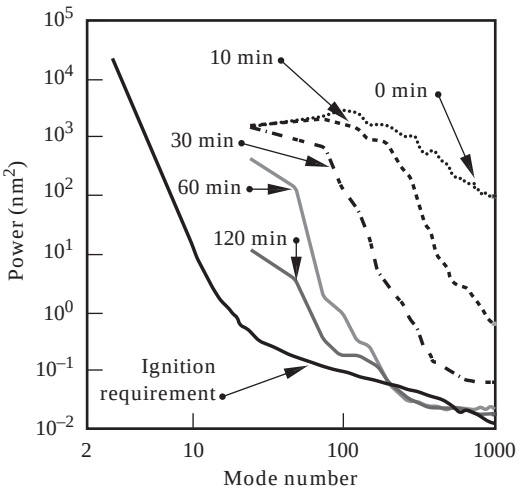

FIGURE 16. Change in Wyko power spectra as a function of solvent exposure time. (NIF-0702-05378pb01)

TABLE 1. Summary of burst strength measurements on polymide shells.

Shell ID	Vapor Smoothed	Polymide wall (μm)	Mandrel wall (μm)	Burst P (atm)	Tensile strength
A	Yes	20	14	45.7	117
B	Yes	40	14	85.9	114
C	Yes	75	15	128.0	90
D	No	24.5	11.8	46.8	105
E	No	33.5	12.3	54.8	91
F	No	55.9	12.5	81.0	79

differential pressure at which the shell burst. Table 1 presents a representative selection data. In each case the polyimide tensile strength is computed from only the polyimide thickness, the assumption being made that the mandrel provides little strength. The stresses at failure fall short of the approximately 120 MPa minimum strength needed for room temperature transport after capsule filling. Furthermore thicker shells appear weaker, though the neglect of the inner mandrel may be in part responsible for this. The smoothing process does not appear to greatly strengthen the polyimide material.

b. Hydrogen Permeability. The permeability coefficient, *K*, was measured for a number of shells. The shells were filled with H_2 in a small vessel, which was then rapidly evacuated. We monitored the time-dependent pressure increase in the vessel due to H_2 permeation through the shell. The pressure data is fit to

$$P(t) = P(\infty)\left(1 - e^{-ct}\right) \quad ,$$

where

$$c = K\frac{6RT}{wd} \quad ,$$

w and d are the capsule wall thickness and diameter, and R and T are the gas constant and Kelvin temperature. A range of K values between 1.5×10^{-16} and 2.5×10^{-16} mol-m / Pa-s-m^2 were obtained at 25°C, and there was no dependence on the type of mandrel or whether the shells had been vapor smoothed. The literature value for commercial Kapton is about 6×10^{-16} mol-m / Pa-s-m^2, indicating that our vapor-deposited material is less permeable by about a factor of three. However, the permeability is probably still too high to allow for room-temperature target assembly of filled shells (assuming they were strong enough) into hohlraums. For a NIF shell with a 150-µm vapor-deposited polyimide wall, the fill half-life would be between 15 and 25 h for the range of permeabilities reported above.

c. Density Measurements. Polyimide shell fragments were placed in a series of organic solutions of precisely known density. The fragments sank in solutions of density up to 1.428 g / cm^3 and floated in solutions of density 1.442 g / cm^3 and higher, bracketing the density to 1.435 ± 0.007 g / cm^3, close to the literature value of 1.42 g / cm^3 for commercial polyimide. The range for individual fragments was narrower. The polyimide shell density was also measured using mass and radiographically determined shell dimensions. Calculations made on several shells gave density values in the range of 1.42 to 1.45 g / cm^3 (with a measurement uncertainty of about 0.05 g / cm^3), which are in excellent agreement with the experimentally measured value.

d. Optical Transmission Properties. Smoothed shells with PI thickness (2 walls) varying from 42 to 158 µm were measured at both IR and UV-VIS wavelengths of light. In both measurements, the shells had absorption spectra similar to those of commercial films. However, they had a somewhat greater loss in transmission, which can be attributed to both exterior scattering due to the curved surface of the shells and to their roughness, as well as interior scattering caused by material inhomogeneity. Optical pictures (Figure 17) of smoothed polyimide shells demonstrate the decrease in optical transparency with thickness in the visible region. Most of this loss is due to the strong absorption at wavelengths below about 500 nm (thus the red shell color), indicating that the use of longer wavelength light (700–1000 nm) may be necessary for layer characterization.

Solution-Based Polyimide Deposition Process Development

In the solution-based approach, droplets of polyimide precursor solution (polyamic acid plus the solvent NMP) are deposited onto acoustically levitated mandrels to form uniform fluid layers that are partially cured (soft baked) to remove the solvent before the next layer is applied. After the required thickness is obtained, the polyimide shell would then be imidized at an elevated temperature to complete the process and realize the full strength of the material. The solution-based approach could produce polyimide of very high strength (over 300 MPa) with an inherently smooth surface due to a strong surface tension effect present when the polyamic acid solution is in liquid form. By spraying a mandrel in levitation, it may be possible to produce high-quality target capsules that are defect-free, partly because they are never touched by a person or a machine.

The work described here has focused on the deposition and cure steps by coating

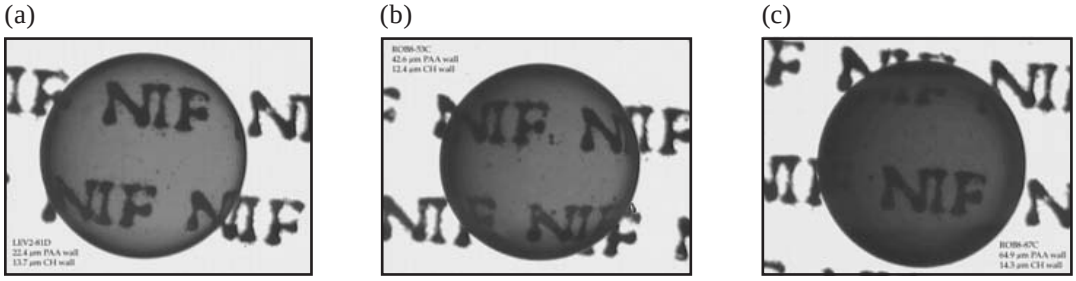

FIGURE 17. Optical pictures of PI shells of various total thicknesses: (a) 44.8 µm, (b) 85.2 µm, and (c) 129.8 µm. (NIF-0702-05379pb01)

mandrels that are mounted on stalks in order to develop processes that are adaptable to levitation. The transition to levitated mandrels would be accomplished in FY 2003.

Considerable effort has been directed at getting a uniform smooth coating using an atomizer as the spray source. A series of experiments indicated that transition to a smooth, ~100Å rms surface occurs at a liquid thickness of ~4000Å. Using this as a guideline, the work was focused on demonstrating the ability to apply multiple coatings on a spherical mandrel. It was determined that oxygen etching the mandrel before the first coat is applied helped the initial coat to wet properly. Since then it has been standard practice to oxygen etch all mandrels used by Luxel in the spray coating process.

We developed a procedure for the soft baking process required to drive off the solvent. Feedback controlled convective heating was implemented. An effective ramp and dwell temperature cycle was developed and the process was automated to run unattended. Multiple coat samples were produced with coatings as thick as 70 µm. This was accomplished by applying individual coats with a thickness of between 0.5 and 1.0 µm after soft baking.

LLNL Wyko characterization of the 70-µm-thick sample (before imidization) showed it to be very smooth locally (Figure 18); radiography showed the coatings to be very uniform with no evidence of the individual layers or delamination at the mandrel interface (Figure 19), and the radiography / shadowgraphy shows the walls to be 70 µm thick and uniform to within a few microns (Figure 19). Clearly the surface tension smoothing effect seen previously can be used to aid in fabricating a multilayer coating. However, as expected, some lower mode asymmetry was evident and this requires further effort. Subsequent imidization of the sample at 300°C resulted in no significant geometric or morphological changes.

An atomizer might not be the best device for delivering the spray in this application. The atomizer produces a spray that contains droplets with diameters varying from 1 to 100 µm with a bell curve distribution and hence is difficult to control to the extent needed. Replacement of the atomization-based delivery system with an ink-jet system capable of precise placement of individual microdrops (~50 µm in diameter) provides much greater control over the process.

Several different ink-jets that are compatible with the polyamic acid solution were found. One of the advantages of this approach is that drop-on-demand capability under computer control can be used to precisely place the spray solution droplets exactly where they are needed. After

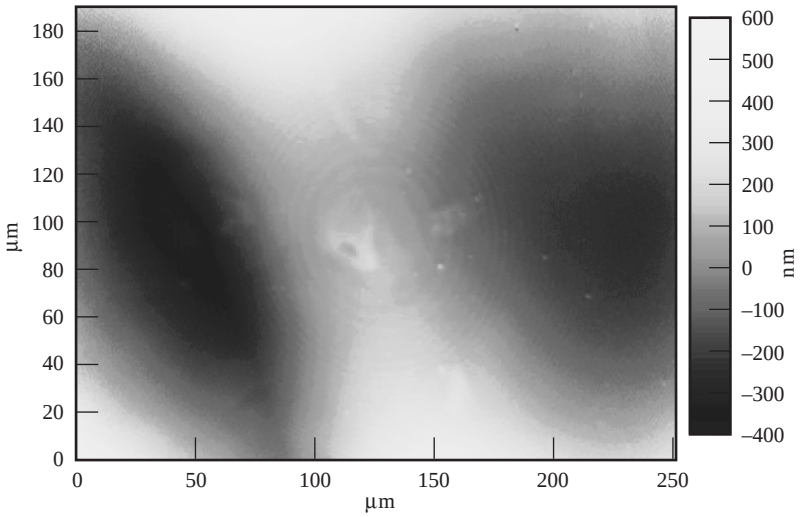

FIGURE 18. Wyko interferometric image of 250- by 190-µm patch on the 70-µm-thick coating. Note surface is locally smooth, but thickness variations of about 1 µm are present over distances of about 100 µm. (NIF-0702-05380)

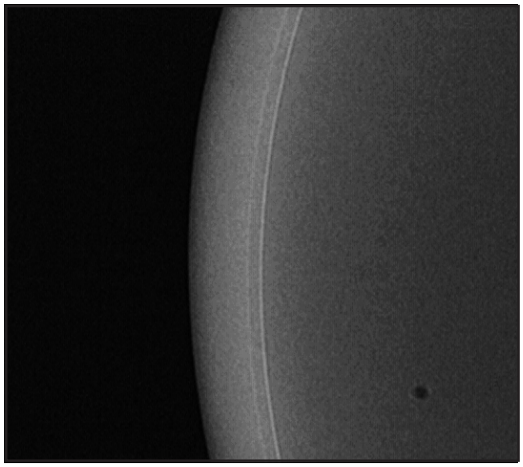

FIGURE 19. Radiograph of a portion of the 70-µm-thick coating. The bright line marks the inner wall; the fainter line near it is the outside of the initial CH mandrel. Note the coating appears very uniform, and there is no evidence of delamination at the mandrel/coating interface. Radiographs of the imidized coatings are unchanged. (NIF-0702-05381pb01)

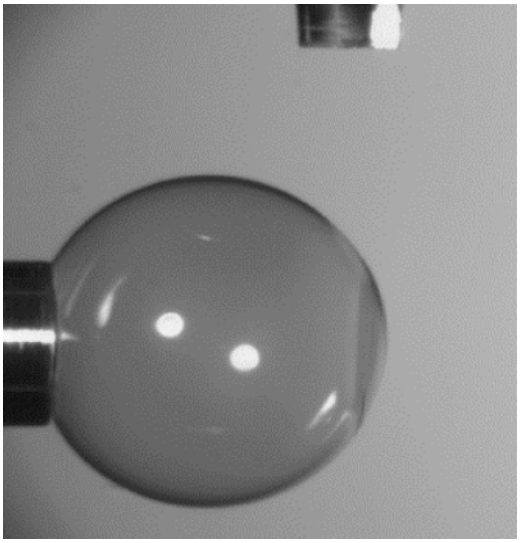

FIGURE 20. A mandrel after 9 coating cycles. Infrared cured, each bake cycle = 7 min total time @210°C, and final imidize ramp bake = 10 min total @ 325°C.
(NIF-0702-05382pb01)

considerable experimentation, this was shown to be possible by precisely laying down a continuous overlapping spiral pattern of drops on a rotating stalk-mounted mandrel. Again, the process is fully automated to take advantage of the surface tension effect to produce a uniform smooth coating over the area of the mandrel that was covered by the droplets (Figure 20).

An indication of the smoothness of the coatings is shown by the uniformity of the highlights on the sphere that come from the illuminating lights.

In an attempt to speed up the soft baking process, as well as develop a method more compatible with acoustic levitation, the heating was changed from convective heating to IR heating. The IR heating was accomplished using lamps known to provide radiation in the region where the polyamic acid is highly absorptive. It was found that with IR heating, it is possible to soft bake the inkjet-coated layers in seconds rather than minutes. However, after a coating with a total thickness of about 10 µm was accumulated, the microsphere began to become distorted. We believe the penetrating nature of the IR heating is causing significant internal heating and subsequent weakening of the shell. These unexpected and unwanted side effects need to be better understood. Further effort has shown that convective surface heating does not cause this problem.

Notes and References

1. T. R. Dittrich, S. W. Haan, S. Pollaine, and A. K. Burnham, "NIF Capsule Design Update," *Fusion Technol*., 31, 402 (1997); S. W. Haan, T. Dittrich, S. Hatchett, D. Hinkel, M. Marinak, D. Munro, O. Jones, S. Pollaine, and L. Suter, "Update on Ignition Target Fabrication Specifications," *Fusion Technol*. (2002), in press.
2. S. A. Letts, A. E. Nissen, P. J. Orthion, S. R. Buckley, E. Fearon, C. Chancellor, C. C. Roberts, B. K. Parrish, and R. C. Cook, "Vapor-Deposited Polyimide Ablators for NIF: Effects of Deposition Process Parameters and Solvent Vapor Smoothing on Capsule Surface Finish," *Fusion Technol*. (2002), in press; C. C. Roberts, P. J. Orthion, A. E. Hassel, B. K. Parrish, S. R. Buckley, E. Fearon, S. A. Letts, and R. C. Cook, "Development of Polyimide Ablators for NIF," *Fusion Technol*. 38, 94 (2000); C. C. Roberts, S. A. Letts, M. D. Saculla, E. J. Hsieh, and R. C. Cook, "Polyimide Films from Vapor Deposition: Toward High Strength NIF Capsules," *Fusion Technol*. 35, 138 (1999); see also the 1998 and 1999 *ICF Annual Reports*.
3. J. R. Salem, F. O. Sequeda, J. Duran, W. Y. Lee, and R. M. Yang, "Solventless Polyimide Films by Vapor Deposition," *J. Vac. Sci. Tech*. A4, 369 (1986).
4. F.-Y. Tsai, E. L. Alfonso, S.-H. Chen, and D. R. Harding, "Effects of Processing Conditions on the Quality and Properties of Vapor-Deposited Polyimide Shells," *Fusion Technol*. (2002), in press; F.-Y. Tsai, E. L. Alfonso, S.-H. Chen, and D. R. Harding, "Mechanical Properties and Gas Permeability of Polyimide Shells Fabricated by the Vapor Deposition Method," *Fusion Technol*. 38, 83 (2000); E. L. Alfonso, S.-H. Chen, R. Q. Gram, and D. R. Harding, "Fabrication of Polyimide Shells by Vapor Deposition for Use as ICF Targets," *Fusion Technol*. 35, 13 (1999).
5. B. W. McQuillian, A. Nikroo, D. A. Steinman, F. H. Elsner, D. G. Czechowicz, M. L. Hoppe, M. Sixtus, and W. J. Miller, "The PAMS/GDP Process for Production of ICF Target Mandrels," *Fusion Technol*. 31, 381 (1997).

Development of Beryllium Capsules by Physical Vapor Deposition

Over the past several years, we have explored sputter-coating of beryllium under a variety of conditions and with a variety of additives, or "dopants."[1, 2] While we have had success in producing very smooth and uniform coatings on flat substrates, for instance with about 15% boron-doping, in all cases coating on spherical substrates produces rough material. We conjectured that this is due to a self-shadowing instability that leads to the growth of films by physical

vapor deposition (PVD) with surface features that grow in height and width as the film becomes thicker.

The shadowing instability occurs when the coating flux arrives at the surface at an angle other than normal, a situation that exists in sputter coating on curved surfaces. To test this idea, we coated spheres with pure beryllium through masks with apertures of several sizes. We found that as the aperture size decreased, forcing the incident flux to be closer to normal to the surface, the surface features on the coating decreased in size. With an optimized apparatus that prevented debris accumulation in the coating, very fine, smooth, but thin beryllium coatings were achieved. Such a coating is seen in the scanning electron microscopy (SEM) image of Figure 21. The small and uniform grains are approximately 60 nm across, and the rms roughness is about 5 nm. Although this technique does produce the desired effect of reducing self-shadowing, it has a very low deposition rate (~0.1 μm/hour), which effectively prevents coating-through-an-aperture from being a viable production process.

We also continued to try to affect the coating morphology by varying the incoming ion energies, which can be controlled by applying a potential difference between the sputter target and the substrate. In addition we investigated "ion-enhanced" sputtering, in which a noncoating flux of ions affects the coating ions' energies once they have reached the substrate surface. To do this, we installed an electrode that is used to create a glow discharge separate from the sputter sources, which allows us to adjust the ion current independently of the ion energy during deposition. This method also increases the total current available, allowing the use of lower energy ions, which reduces Ar ion implantation and improves the behavior of the capsules in the bounce pan. Figure 22 shows the effect on the deposition of Be/1 at.% Cu of 40-V and 80-V bias, with a current density of about 0.15 mA/cm^2. The grain size and roughness are significantly reduced by the application of bias. Prior experiments at reduced currents showed little effect from 40-V bias. Varying the current also affected the microstructure, as shown in Figure 23, which compares two coatings made with the same bias voltage but a factor of 2 difference in the current density.

Using bias sputtering with ion bombardment, we tested our ability to produce Cu-doped Be ablators at a thickness close to that required for NIF capsules. Two-mm-diam CH mandrels were coated with approximately 100 μm of Be/1 at.% Cu in 12 successive coating runs. An 80-V bias was applied

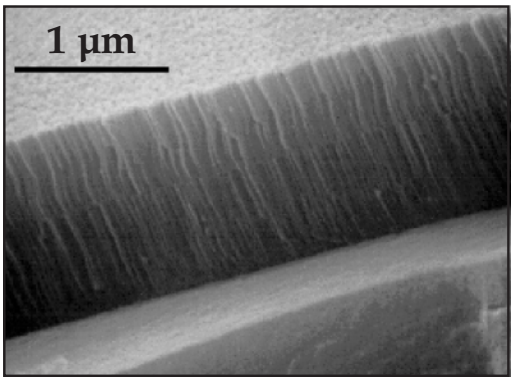

FIGURE 21. A SEM cross section showing a 2-mm-diam capsule deposited using the aperture coating method. Note the extremely fine grain structure—AFM measurements of this capsule showed a typical grain size of about 60 nm and an rms roughness of about 5 nm.
(NIF-0702-05383pb01)

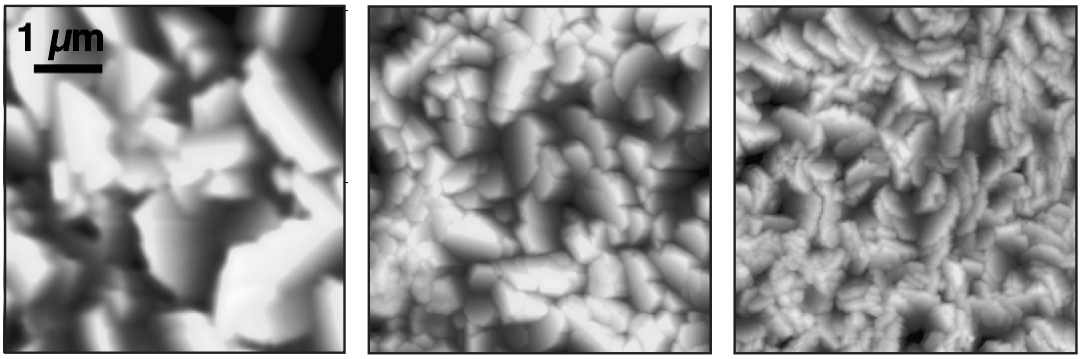

FIGURE 22. A series of AFM images of 1-mm-diam capsules with ~20-μm-thick coatings of Be/Cu showing the effect of ion bombardment during deposition. From left to right: no bias, R_q = 263 nm; 40-V bias, R_q = 130 nm; 80-V bias, R_q = 49 nm.
(NIF-0702-05384pb01)

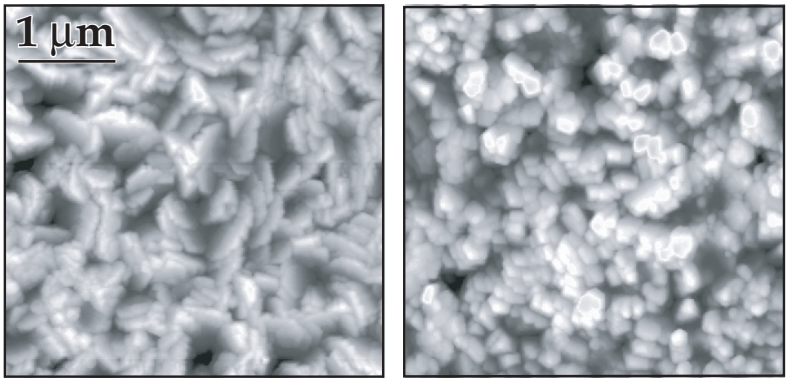

FIGURE 23. AFM images showing the effect of varying the ion current at a fixed ion energy. The image on the left is from Figure 21: 80-V bias, 0.15-mA/cm^2 current density (R_q = 49 nm). The coating on the right was made using 80-V bias, 0.3 mA/cm^2 (R_q = 33 nm). (NIF-0702-05385pb01)

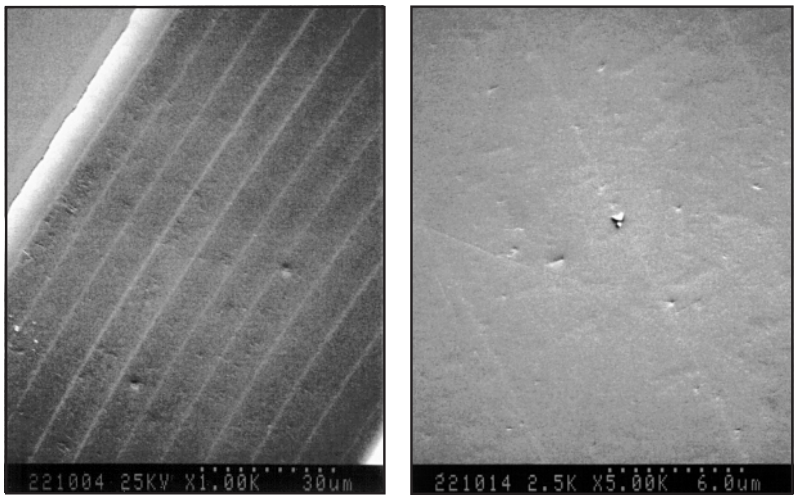

FIGURE 24. SEM images of a polished cross section of a 100-μm-thick, 2-mm-diam sputter-deposited Be/Cu capsule. The lighter bands represent the oxide layers that form after each coating run. In actual production, capsules would be sputter-etched prior to each day's run to remove the oxide. (NIF-0702-05386pb01)

during deposition to ensure a dense, fine-grained microstructure. Figure 24 shows SEM images of a polished cross section from one of the resulting capsules. The oxide layers that form when the deposition is interrupted show as light-colored bands in the images. There is no evidence of a pervasive void structure in the bulk of the coating, although transmission electron microscopy (TEM) measurements, discussed below, are much more definitive. Among the improvements that are necessary are sputter-cleaning prior to each coating run to remove the oxide layer and redesign of the bias electrode to prevent arcing as it accumulates a thick coating of Be.

We have used TEM to examine the distribution of copper in sputter-deposited Cu-doped beryllium, as well as oxygen, which is a common and nearly unavoidable impurity in beryllium. Nonuniform distributions of dopants or impurities could lead to deleterious opacity variations. We also wanted to look for any tiny voids between grains. The coatings were sputtered onto 1-mm-diam mandrels, and thin TEM samples prepared from resulting capsules. We examined a capsule coated with no bias, and a second coated with an 80-V bias.

Figure 25 shows a typical image from the outer few microns of the no-bias capsule. The grain diameters range from 0.25 μm to 0.5 μm near the inner surface to 0.75 μm to 2 μm near the outer surface, which is consistent with past cross-section SEM. The 80-V bias coating was qualitatively similar, except that the grain diameters ranged from 0.15 μm to 0.23 μm near the inner surface and 0.3 μm to 0.5 μm near the outer surface.

Using energy-filtered TEM, we imaged oxygen and copper distributions for the no-bias coating over the same area shown in Figure 25. Figures 26a and 26b show the results. The oxygen clearly highlights the grain boundaries, as would be expected of a surface layer. By contrast, the copper signal is extremely uniform, showing no signs of segregation.

Micron-Scale Hole Drilling

One approach to filling sputter-deposited beryllium capsules is to drill a micron-scale hole, which is then sealed after filling. Such holes are possible with highly focused short-pulse lasers systems. The high numerical aperture focusing objective must be wavelength matched to the laser, and the best focus point on the substrate must be located to within a micron. Alignment of the laser beam in the objective is also very important.

Using an appropriate optical system with automated alignment, we were able to drill roughly 6-μm-diam holes in a 125-μm-thick stainless-steel foil (Figure 27). The laser wavelength was 405 nm (frequency

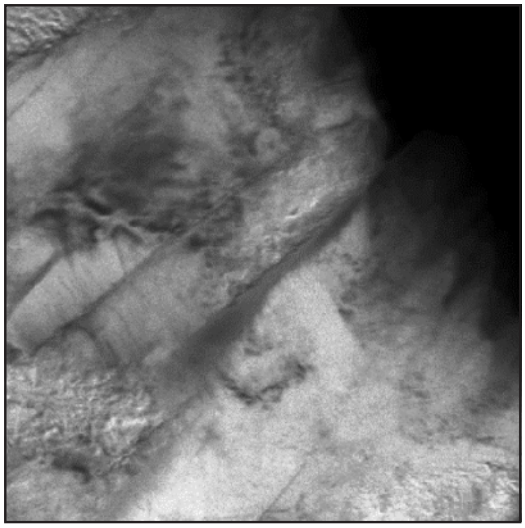

FIGURE 25. TEM image of a cross section from a Cu-doped Be coating deposited with no applied bias. The straight diagonal lines represent grain boundaries. (NIF-0702-05387pb01)

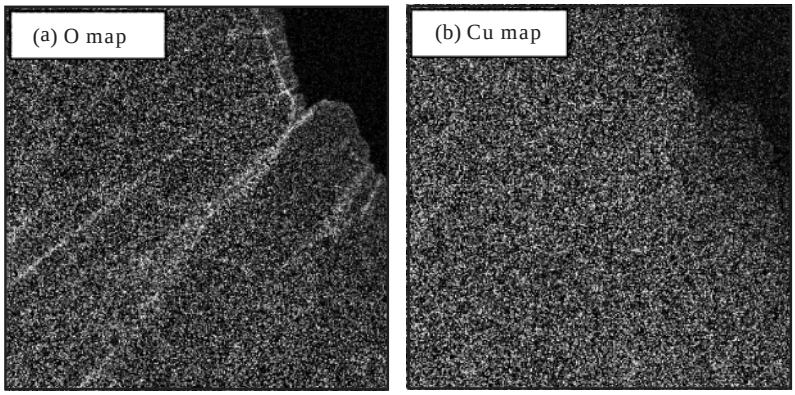

FIGURE 26. Elemental maps of (a) oxygen and (b) copper distributions in the area shown in Figure 25. Due to the highly reactive nature of a clean Be surface, some or most of the oxide could have formed during sample preparation. (NIF-0702-05388pb01)

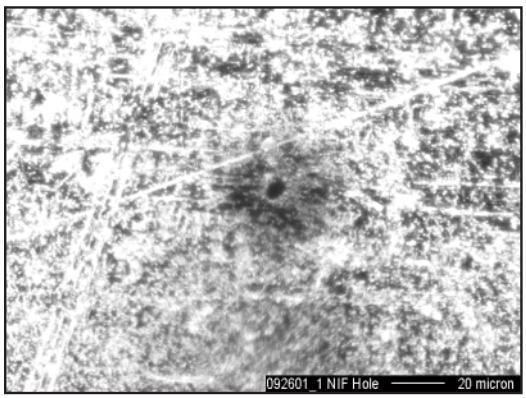

FIGURE 27. A micrograph of a hole drilled in a stainless-steel foil. Although the hole is elliptical rather than circular, it is smooth. (NIF-0702-05389pb01)

doubled from 810 nm), with pulse lengths of 120 fs and less than 1 μJ/pulse. The shape of the holes was a smooth ellipse, indicating that the laser beam had a uniform profile. A good beam profile is essential for achieving the best performance from the focusing optics. Experiments have also shown that beryllium foils can be similarly drilled.

Notes and References

1. R. L. McEachern et al., *Fusion Technol.* 31 (4), 435 (1997).
2. R. L. McEachern and C. Alford, *Fusion Technol.* 35 (2), 115 (1999).

Cryogenic Fuel Layers for Ignition

All current ignition targets contain cryogenic fuel layers inside a spherical capsule. For the case of a tritiated fuel, such as equimolar deuterium-tritium (DT), the heat from beta decay liberated in the solid drives the layer formation, a process termed "beta layering." This does not guarantee the layer thickness uniformity nor its smoothness; both of which, however, are required by target designs. We are studying ways of growing the beta layers as smoothly as possible, and characterizing them adequately. We are also studying the fundamental crystal growth morphologies of the solid layers. We have learned that coupling additional heat to the fuel by infrared radiation leads to improvements, and also allows forming nontritiated fuel layers. This has been demonstrated experimentally, and we are now implementing the infrared layering technique for capsules in hohlraums. Layer formation in hohlraums is complicated by the necessity of very carefully controlling the thermal environment inside the hohlraum, and we are working to engineer solutions. And finally, with General Atomics, we have constructed a system for integrated testing of high-pressure diffusion filling of capsules in hohlraums, and forming and characterizing the fuel layers.

Fuel Layer Formation Studies

Optimization of β Layering

We are studying the dynamics of the growth of solid DT layers from the liquid. It has long been clear that the final quality of layers formed by native β layering is sensitive to details of the initial layer formation. Cooling liquid DT rapidly through the triple point usually results in a supercooled liquid. When the liquid freezes, it does so quickly and crystals nucleate from many points, with no correlation in their orientations, sizes, etc. Where the crystals meet, a grain boundary is formed. The presence of the many randomly oriented crystal facets and their grain boundaries affect the local surface roughness and severely degrade the layer quality.[1] The β layering process does decrease the large-scale length, low-mode roughness after the initial freezing but is not able to overcome the shorter-scale effects.

To avoid the effects of supercooling and multiple crystals, the initial layer must be grown very carefully. The DT liquid is frozen and then slowly melted until a small region of solid remains at the coldest point in the capsule. (For our experiments, this is near the fill tube.) Ideally this solid region would be a single-seed crystal of DT, but we cannot directly determine or control the crystal nucleation. With a seed crystal formed, the temperature of the capsule is slowly lowered, allowing the growth / freezing front to propagate through the liquid in a controlled manner. We have determined that after the DT has all solidified, it is best to wait for several hours at a constant temperature just below the triple-point temperature of 19.73 before cooling the layer further. This allows for native ß layering to remove low-mode asymmetries.

Figures 28 and 29 are two examples of observed layer growth from a seed. These are 125-µm-thick layers in a 2-mm CD plastic capsule 40 µm thick. In Figure 28, the solid first freezes in a narrow band-like structure that originates near the fill tube

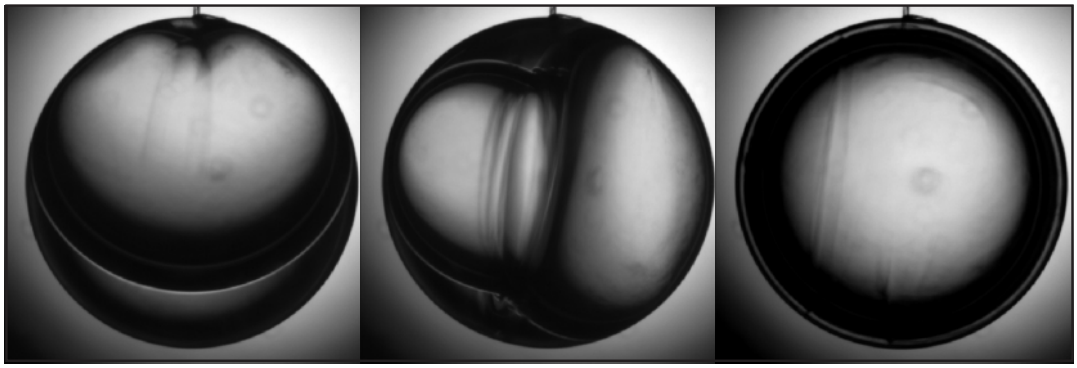

FIGURE 28. Initial growth is in a longitudinal direction as seen in first figure on the left. Later in time, a band forms almost from pole to pole and begins to thicken. Finally, the layer is complete. (The bands are slightly out of focus. The left side of the band is on the farthest side of the shell; the right is on the near side.)
(NIF-0702-05390pb01)

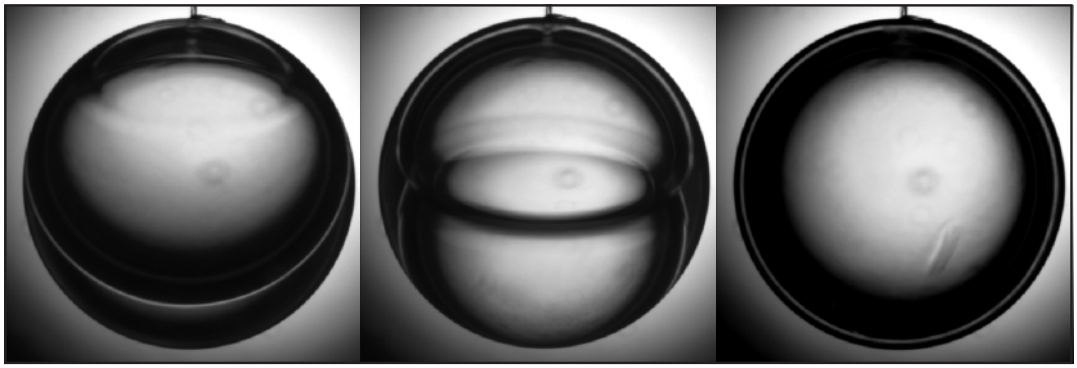

FIGURE 29. Initial growth is almost axially symmetric. As the temperature continues to decrease, the growth front moves down the shell. After completely solidifying, this capsule also forms a smooth layer.
(NIF-0702-05391pb01)

at the top of the capsule, and grows down the capsule wall. As the temperature is lowered further, the band widens, growing perpendicularly to the original growth direction. This gives a moderately smooth layer.

In Figure 29, the growth is simpler. The solid advances from the fill tube in a symmetric fashion, like a spreading cap, until it reaches the bottom of the shell. The defect observed at 5 o'clock in the last picture of Figure 29 is a remnant of the boundary formed when the growth fronts meet.

Figure 30 plots the minimum power spectral density observed for the layers formed during the runs of Figures 28 and 29. The large differences in the two sets of data, especially at the mid to high modes are largely due to the grain boundaries formed by the extra growth fronts of Figure 28. The minimum rms of the layer in Figure 28 is 2.2 μm. The minimum rms of Figure 29 is 1.1 μm. The growth mode of the layer in Figure 29 is clearly preferable. Unfortunately, layers like in Figure 28 are quite common, and so we anticipate that forming final shootable layers in actual ignition targets will require several tries.

The layer growth in Figures 28 and 29 can be related to earlier work done by Kozioziemski, Collins, and Bernat[2] on D_2 crystals on flat substrates. Figure 31 is a crystal of D_2 between the roughening temperature of the (1100) facets and the triple point. The (0001) plane is not roughened. Crystals grow most rapidly along roughened facets; therefore, this shape of crystal grows rapidly in a lateral direction and thickens slowly. This is the same behavior as exhibited in Figure 29.

Figure 32 is a D_2 crystal with its c-axis not perpendicular to the substrate. The long axis of the rectangle is the <1100> direction; the c-axis is some undetermined angle to the norm of the substrate and perpendicular to the <1100> direction. This form of crystal grows most rapidly along the <1100> direction and at an intermediate velocity in the perpendicular direction.

This is the same type of growth observed in the series of pictures in Figure 28. A long narrow structure grows in a somewhat vertical fashion in the first picture of Figure 28. In the second picture, we can see that the ends of the structure meet and that it has begun widening. With this evidence for the growth habit of hydrogen crystals, it is apparent that not only must we have a single seed for crystal growth, but that seed must be properly oriented on the capsule surface. We would then anticipate a several-try procedure for forming a good seed crystal for a shootable ignition target.

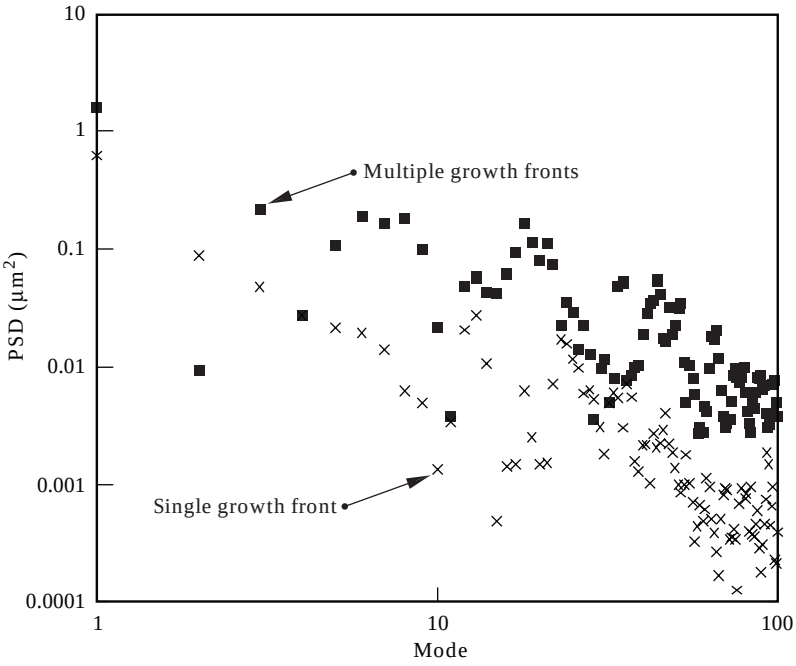

FIGURE 30. The power spectra of the finished layers from Figures 28 and 29 are very different. The power in some modes differs by an order of magnitude. The boxes are from the last image in Figure 28, the *X*s are from the last image in Figure 29.
(NIF-0702-05392pb01)

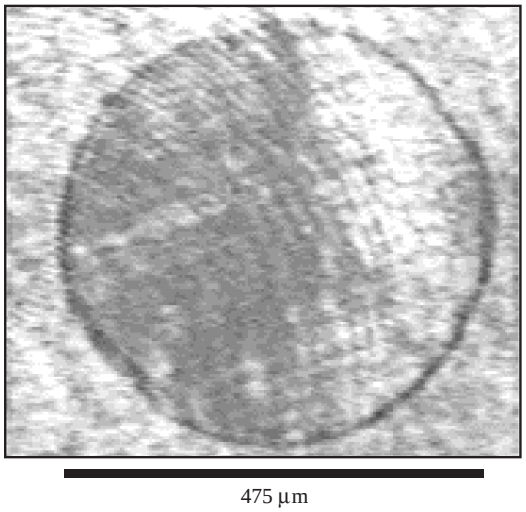

FIGURE 31. A crystallite of D_2 with the c-axis perpendicular to the substrate. The crystallite is below the triple-point temperature of D_2 but above the roughening temperature of the (1100) facet, whose directions are in the plane of the substrate.
(NIF-0702-05393pb01)

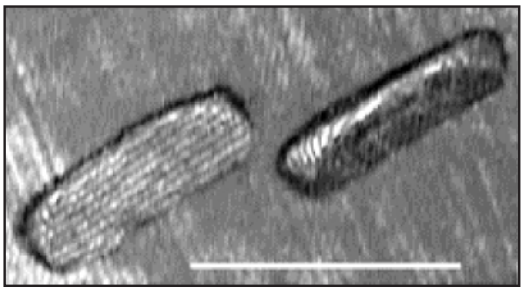

FIGURE 32. A crystallite with the c-axis oriented at some unknown angle to the norm of the page. The short sides of the rectangular shape are (1100) facets.
(NIF-0702-05394pb01)

Infrared Heating to Enhance Solid Fuel Layers

Previous work showed that, while very smooth β layers can be formed just below the triple point, as discussed above, cooling these layers more than a few tenths of a degree leads to degradation from cracking due to shrinkage and crystal faceting.[3] It has also previously been shown that infrared radiation absorbed by the solid layer increases the bulk heating rate, and can lead to layer formation even in nontritiated hydrogens.[4] Since the layer smoothness improves with higher levels of infrared, we conjectured that cooling layers while exposing them to large infrared powers could lead to good layers at the lower temperatures required by optimized designs (typically 1.5 K below the triple point, which sets the vapor density in the interior of the capsule). Indeed, as reported here, we have achieved smooth layers about 1.5 K below the triple point in HD for IR bulk absorbed power greater than 30 Q_{DT} (Q_{DT} is the bulk heating from beta decay in DT) with a 10 mK/3 min cooling rate

We performed a series of experiments to determine a bulk heating level and cooling rate that minimized layer degradation on cooling to 1.5 K below the triple point. At a fixed cooling rate of 20 mK/3 min and bulk heating from approximately 1.4 Q_{DT} to 54 Q_{DT}, we found that the layers were relatively smoother upon formation, with the smoothness improving with heating rate, but they still degraded as the temperature was lowered. At a cooling rate of 10 mK/3 min, however, and at heating levels above 30 Q_{DT}, layers remained smooth down to 1.5 K below the triple point. Figure 33a shows a layer shortly after it was formed near the triple point. Figure 33b shows the same layer after it had been cooled approximately 1.5 K. The calculated rms for both these images is 1.33 µm. The power spectra for these two images are plotted in Figure 34. Similar results were achieved at ~30 Q_{DT}.

We are attempting to reproduce the infrared enhancement of layers with DT at temperatures as cold as 18 K. The challenge is to find a DT or D_2 adsorption line that does not excessively heat the polymer capsule. This was not an issue for the IR experiments on HD. The HD adsorption lines are in a region of the IR spectrum where deuterated polymer (D-GDP) does not have appreciable absorption. The IR adsorption lines of DT and D_2 are shifted from those of HD due to the difference in nuclear masses.

The adsorption of IR energy in the capsule leads to a larger temperature difference between the capsule and the thermal boundary of the experiment, and possibly increased nonuniform cooling effects due to convection. Also, any low mode variations of the polymer thickness will imprint onto the DT layer. Finally, the excess heat limits the amount of IR that can be used to enhance the layer smoothness since the total cooling capacity is finite.

For D_2 and HD, there is one primary absorption line each that is suitable for volumetric heat generation. In the case of DT, there are several absorption lines from

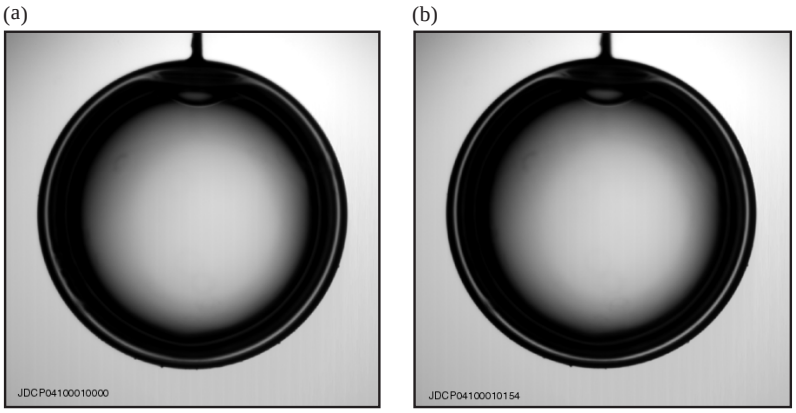

FIGURE 33. Images of a HD layer after formation near the triple point (a) and at the end of a slow cooldown (b). The volumetric heating rate in the case was about 40 Q_{DT}.
(NIF-0702-05395pb01)

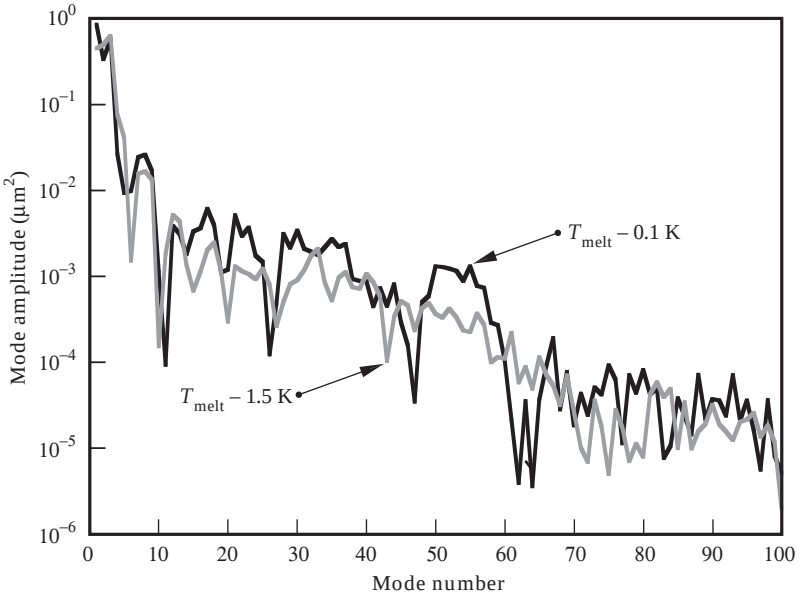

FIGURE 34. Power spectra for the two images in Figure 33. The rms for both curves is 1.33 μm. (NIF-0702-05396pb01)

which to choose. None of the lines are an obvious choice for DT. Ideal conditions require maximum ice absorption and minimum shell absorption. We made rough measurements of the shell absorption by in effect measuring the rise in the shell temperature from illumination by IR power at the various wavelengths. Using a wavelength of 3.46 μm, which should be near the peak absorption in the fuel, we attempted to form a good DT layer, with the results shown in Figure 35. The obvious nonuniformity of the layer may reflect high absorption in the shell and in the glue joint near the fill tube. Further work is needed to find the best heating line from the laser with the most heat in the fuel and least in the capsule.

Forming Fuel Layers in Capsules in Hohlraums

As already discussed, addition of infrared heating to the fuel layer improves the layer quality and makes possible the use of nontritiated (e.g., deuterium, HD) fuels. It also shortens the time to form a fuel layer, which may be very useful if it takes several tries to form a good layer. For indirect-drive targets, the infrared must be injected into a hohlraum, scattered by the hohlraum wall, and absorbed by the capsule and the fuel. The radiation must become isotropic through multiple scatterings in the hohlraum, and must uniformly bathe the capsule. Departures from isotropy will lead to nonuniform layer thicknesses. We developed a reflective optical system for injecting and positioning two cones of infrared light in the hohlraum, as shown in Figure 36. The optics also includes two different types of layer characterization—shadowgraphy and spectral interferometry. The shadowgraph provides ice surface information relative to the axial symmetry of the layer at the equator of the shell, while

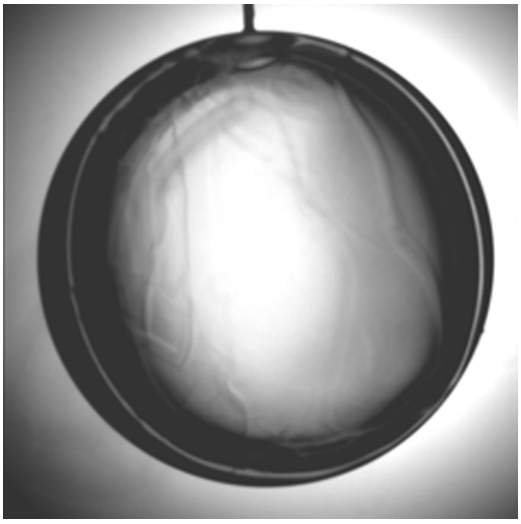

FIGURE 35. A DT layer with 44 mW of IR injected at a wavelength of 3.46 μm. This should be the peak in absorption of the DT molecule. (NIF-0503-06953pb01)

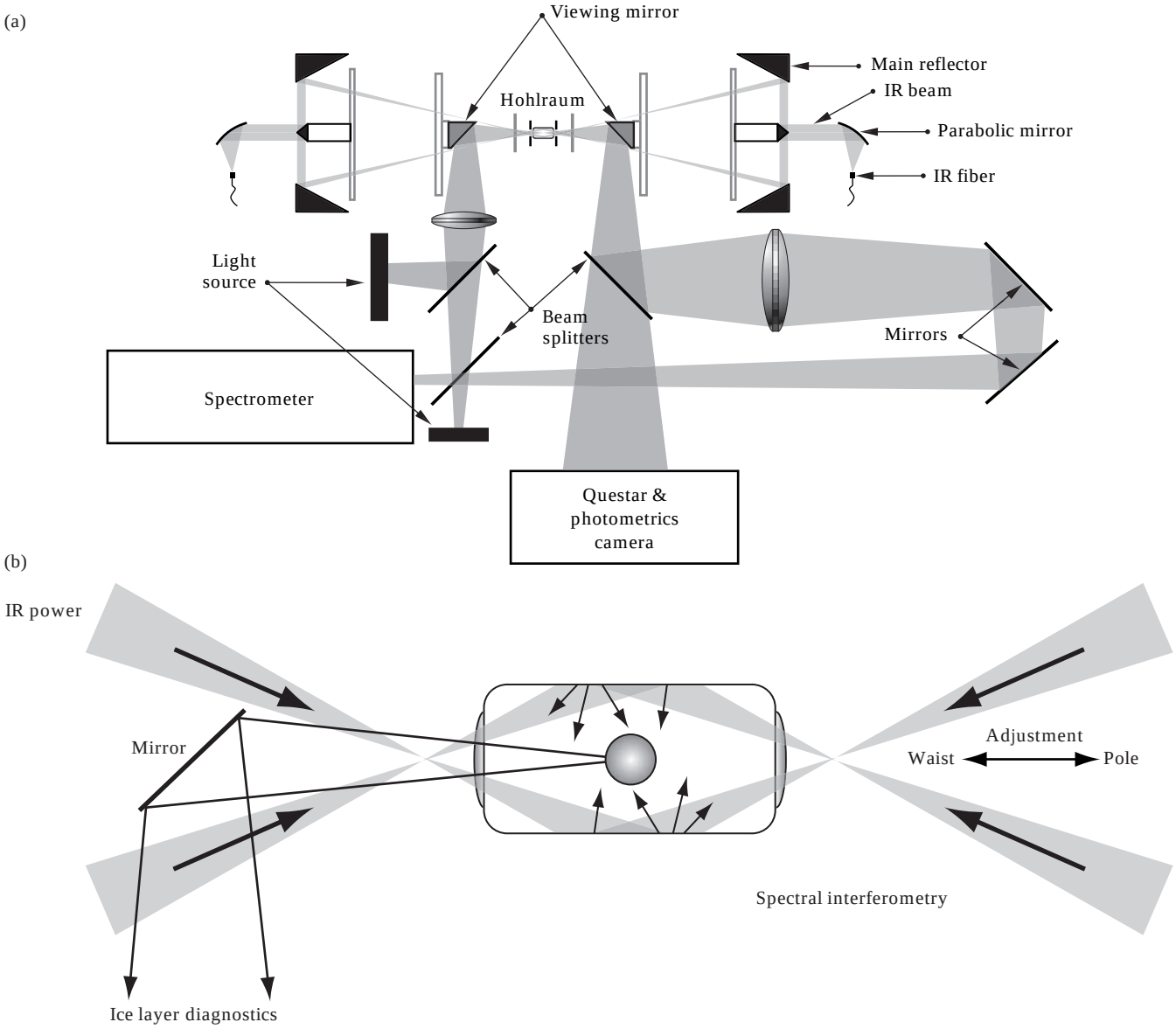

FIGURE 36. (a) Illustration of the two-sided injection IR layering experiment with shadowgraph and spectral interferometry diagnostic capabilities. The shell is backlit from the left and imaged by a telescope from the right side for shadowgraph. The spectral interferometer works in reflection mode with each path to the spectrometer alternatively blocked to measure both sides of the capsule. (b) Details of IR scattering and illumination in the hohlraum. (NIF-0503-06954pb01)

spectral interferometry provides the layer thickness at both poles of the capsule. We have begun experiments to form layers with this system. Initial results have been reported elsewhere.[5]

The IR injected into the hohlraum requires a surface that diffusely scatters the injected light (i.e., is close to Lambertian) and absorbs as little as possible. Roughened hohlraums produced by gold-coating sandblasted mandrels provide the appropriate diffuse scattering. Optimized sandblasting developed at General Atomics yields substrates as rough as 7 μm rms, which reduces specular scattering at grazing incidence angles and provides good diffuse scattering. Smaller roughnesses yield more specular scattering, making infrared isotropization more difficult in hohlraums. In addition, eliminating surface roughness at submicron length scales, which has little effect on the IR

scattering, reduces IR absorption. The submicron roughness was effectively removed by etching the sandblasted mandrels in a "bright dip" solution for 30 seconds prior to gold deposition. Without such a treatment, the rough gold surface absorbs up to 40% of the incident IR, while the absorption reduces to about 10% with the bright-dip etching.

Using the reflective optics and roughened hohlraums, we have been able to inject a ring-shaped IR beam into one of our highly scattering hohlraums and redistribute a solid to generate a cylindrically symmetric layer profile as shown in Figure 37. We have also done some preliminary sensitivity tests to see how much the layer changes shape with changes in the lateral position of the injected beam. One of the main concerns we had with the injection optics is determining how to properly align the IR beam to the hohlraum axis and shell. By copropagating visible and IR laser light through one laser entrance hole (LEH) and viewing through the opposite LEH, we have started developing a technique for using the reflected visible light exiting the hohlraum to align the injected IR beam. This technique is still being investigated to determine the sensitivity of the reflected light to the layer shape.

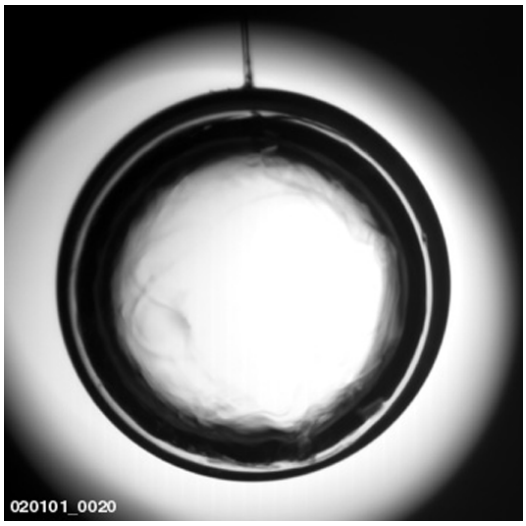

FIGURE 37. A shadowgraph of an HD ice layer formed from IR illumination, viewed through a laser entrance hole in the hohlraum. (NIF-0503-06955pb01)

Notes and References

1. G. W. Collins, T. P. Bernat, E. R. Maples, and B. J. Kozioziemski, *Phys. Rev. B*, 63, 2001.
2. B. J. Kozioziemski, G. W. Collins, and T. P. Bernat, *Fusion Technology* 31, p. 482, July 1997.
3. J. Sater et al., *Fusion Technology* 35, p. 229, March 1999.
4. D. N. Bittner, et al. *ibid*, p. 245.
5. B. J. Kozioziemski, R. L. McEachern, R. A. London, and D. N. Bittner, *Fusion Science and Technology* 41, p. 296, May 2002.

Control of Thermal Symmetry in Cryogenic Hohlraums

To produce a fuel layer with uniform thickness on the interior of a spherical capsule, the temperature of the inner surface of the capsule, i.e., the interface between the ice and the capsule, must be very uniform. For example, for an 80-μm-thick D-T layer, the capsule inner surface must be uniform to about 15 μK for a thickness uniformity of 1%. Since the capsule temperature is around 18 K, this uniformity is about one part in 10^6. To attain this for an indirect-drive target, the thermal field inside the cryogenic hohlraum must be carefully controlled. The D-T layer itself is a heat source. Indeed, this heating from beta decay is what drives the formation of a "β-layer." So two effects must be considered in attaining the required thermal symmetry in a hohlraum. First, if the hohlraum walls are isothermal, the isotherms of a spherical heat source in a cylindrical hohlraum are not spheres. Therefore the hohlraum cannot be simply isothermal. Second, current ignition designs require a fairly high density of a helium–hydrogen gas mixture in the hohlraum to control wall motion during the shot. This hohlraum gas gives rise to natural convection, which again prevents spherically symmetric cooling of the capsule. We have been addressing these problems for several years. Our initial results were published earlier.[1]

Our subsequent work has been directed at developing a self-consistent thermal model including the effects of natural convection to predict layer uniformity for various hohlraum thermal boundary conditions. We have also performed initial experiments to corroborate the thermal models. In our earlier work,[1] we showed that with the hohlraum gas in the low-pressure conduction regime, thermally shaping the hohlraum wall temperature profile

could produce isotherms close enough to spherical to yield a 1% layer uniformity. Newer modeling using the COSMOS thermal and flow code has shown that with hohlraum gas densities of 1 mg/cm^3 He-H_2 equal-atom mixtures, thermal disturbances from natural convection driven by the temperature difference between the capsule and the hohlraum result in temperature variations on the inner surface of the D-T ice of as much as 2 mK. Such a variation would lead to a D-T distribution with all the ice accumulated in the coldest parts of the capsule, and completely dry in the warmest parts.

To mitigate the deleterious effects of convection, we used our model to investigate the addition of thin baffles that act as convection barriers in the hohlraum interior. As seen in Figure 38, two such baffles, in addition to those formed by the capsule support tenting, reduce the predicted layer nonuniformity to less than 1%, essentially recovering the nonconvecting thermal conduction results. In this work, to calculate the resulting layer profile, the profile shape is iterated until the temperature on the interior surface is close to constant (to within 1%) when modeled by COSMOS.

In further work, we will explore the effects of added infrared power to the capsule, which we anticipate will worsen convection and its effects. We will also explore different hohlraum scales.

In initial experiments to corroborate our thermal models, we constructed a prototype cryogenic target assembly after the design discussed in Reference 1. That is, heaters are able to change the hohlraum wall temperatre profile, and a specially designed cooling ring assures azimuthal temperature uniformity. The capsule was filled with 100 atmospheres of deuterium, so that it was not itself a heat source. However, with a low-pressure hohlraum gas in the conduction regime (no convective effects), we were able to maniplate the thermal field inside the hohlraum to move the frozen deuterium in a predictable manner. As seen in Figure 39, we could apply a linear thermal gradient by heating the sapphire hohlraum support rods, which caused a deuterium ice boule to form in the cold direction. We could also use the

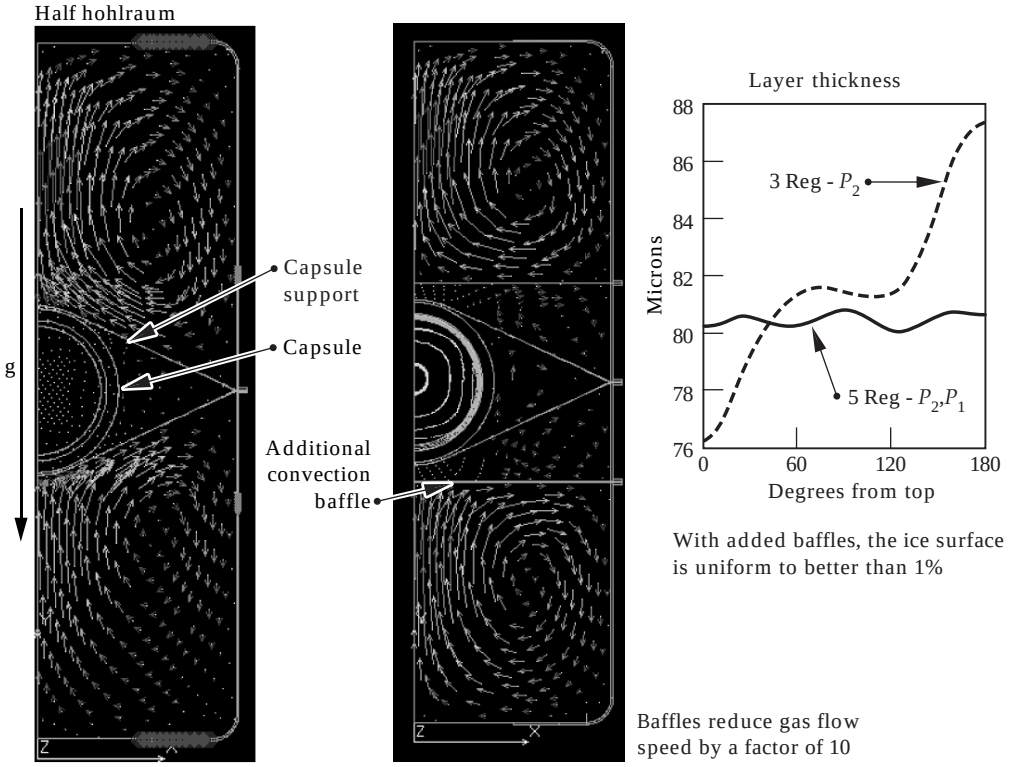

FIGURE 38. Hohlraum baffles reduce the effects of natural convection of the hohlraum gas. (NIF-0603-07064pb01)

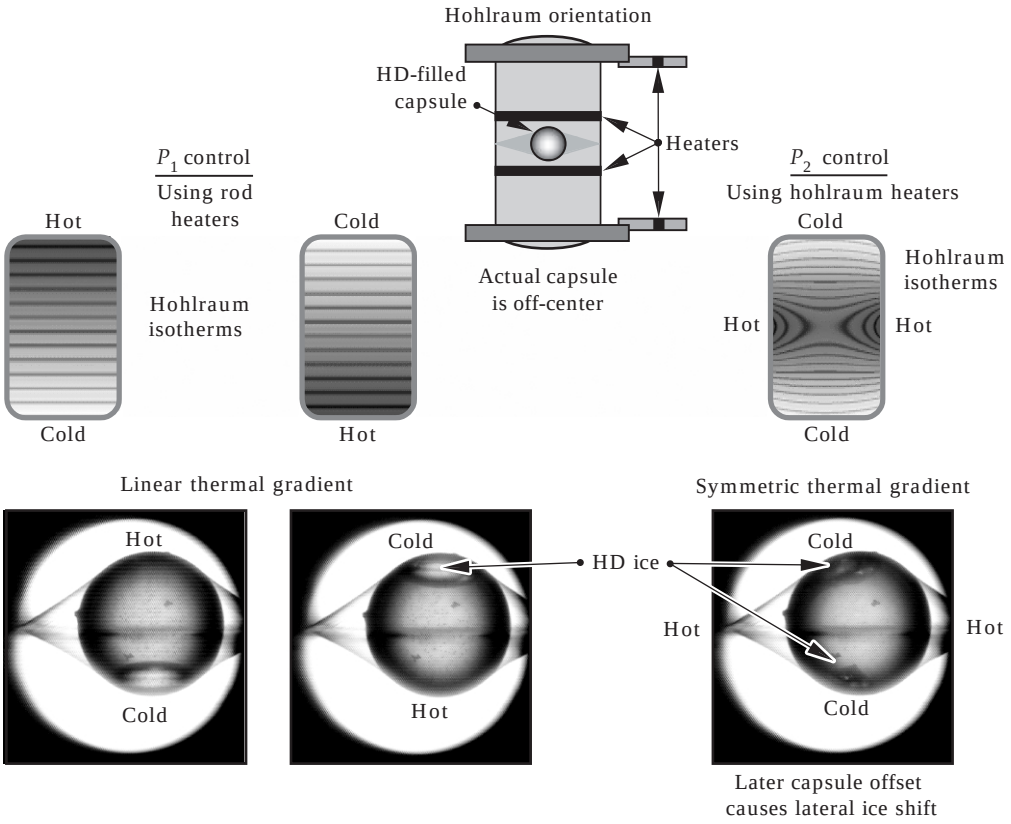

FIGURE 39. The hohlraum thermal field was controlled to move the deuterium ice in a predictable way. (NIF-0603-07062pb01)

hohlraum body heater to impress a "quadrapolar" field, resulting in migration of the deuterium to two cold spots. Additionally, for the linear gradient case, we could model the measured surface profile of the ice boule using the impressed wall temperature profile and our COSMOS code. The ice surface must be an isotherm, and we found good agreement for reasonable values of the thermal parameters of the capsule, ice, and hohlraum gas thermal conductivity. This is seen in Figure 40.

Notes and References

1. J. J. Sanchez, and W. H. Giedt, "Thermal Control of Cryogenic Cylindrical Hohlraums for Indirect-Drive Inertial Confinement Fusion," *Fusion Technology* 36, p. 346, Nov. 1999.

A New Cryogenic Apparatus to Test Filling and Layering of Indirect-Drive Ignition Targets

For all current ignition designs, the D-T fuel in the capsule is in a smooth, cryogenic, solid layer. For many target designs, the capsule is polymeric and is filled by diffusion through the capsule wall at ambient or somewhat elevated temperatures. The quantity of fuel in the layer requires that the fill pressure be in the range from approximately 400 atmospheres to as high

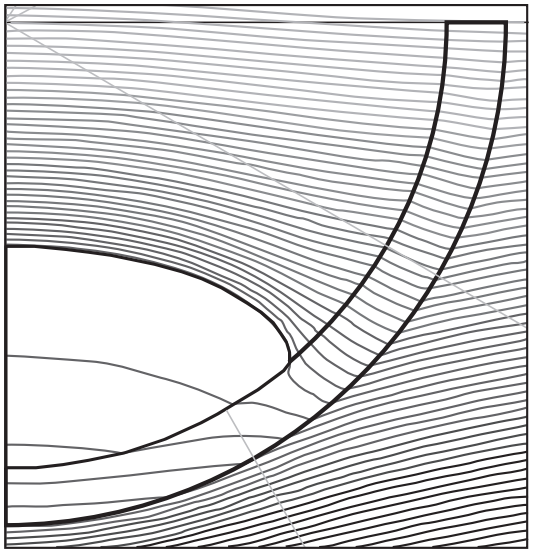

FIGURE 40. The deuterium ice boule surface profile from Figure 39 is modeled to be an isotherm. (NIF-0603-07063pb01)

as 1300 atmospheres. Such pressures would burst the capsule if handled or transported at ambient pressures and temperatures. Therefore, such targets must be handled and transported in a cryogenic state after filling. Assembled targets will be filled in independent pressurized permeation cells. Targets will be cooled to cryogenic temperatures immediately after filling, and each target then cryogenically transferred to and attached to a transport and insertion cryostat (TIC) that keeps the target cold and transports each target to the NIF building.

To test the relevant technologies for filling and maintaining indirect-drive ignition targets, we have built the Deuterium Test System (D_2TS). This will fill NIF-sized, cryogenic ignition target assemblies to full fuel density with deuterium, will allow fuel layering experiments (by the IR method and temperature shimming of the hohlraum), and will permit the transport of filled targets. A drawing of the D_2TS is shown in Figure 41. The capsule, already mounted in its hohlraum, is filled by permeation at room temperature in a high-pressure cell. After cooling to cryogenic temperature (~20 K), the cell is opened, and the D_2TS's main cryostat uses a cryogenic target gripper to remove the target assembly from the cell. The cryogenic target gripper makes mechanical, thermal, and electrical connections, and makes a gas seal to the base of the target assembly. The gas seal allows the pressure in the target assembly's hohlraum to be varied. The target can be transported cryogenically in the D_2TS's main cryostat once it is detached from the target fill system that houses the permeation cell. The main cryostat is cooled with liquid helium. The basic design concept for the D_2TS has been published elsewhere.[1]

The permeation cell ultimately may be pressurized to 20000 psi for some high-gain indirect-drive designs, as well as direct-drive designs. The cell must be designed with high-strength materials, taking into consideration the possibility of hydrogen embrittlement, and ultimately the effects of tritium radioactivity. Our first

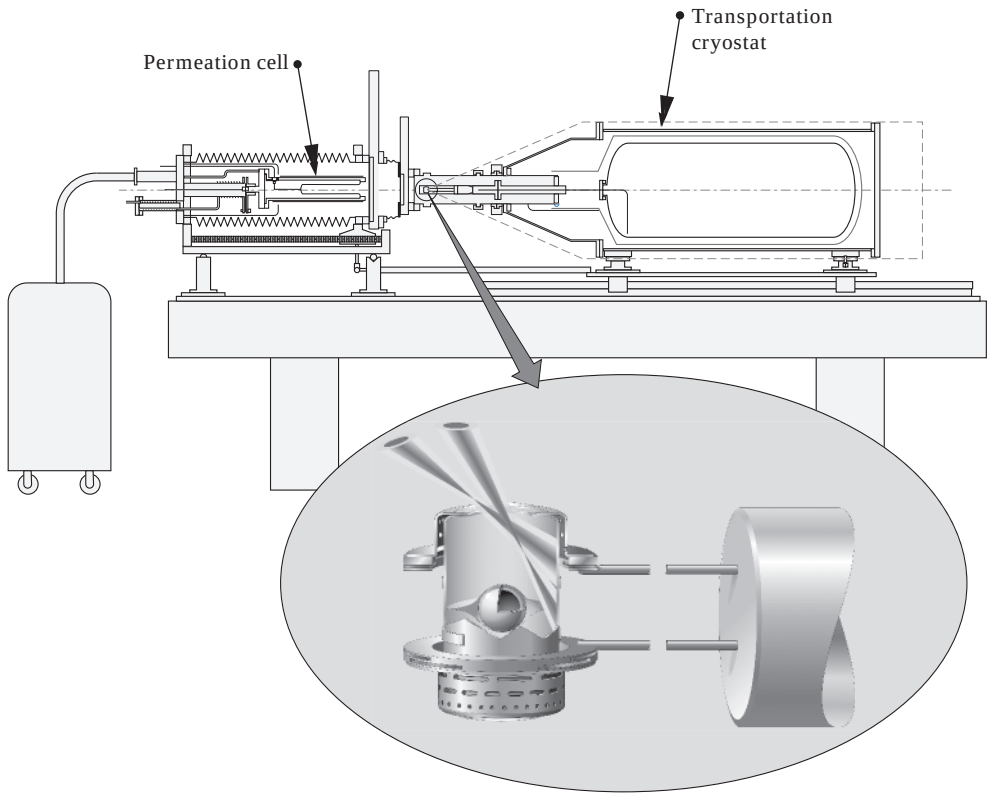

FIGURE 41. The D_2TS will prototype and test permeation filling, cooling, and transport of indirect-drive ignition targets.
(NIF-0603-07060pb01)

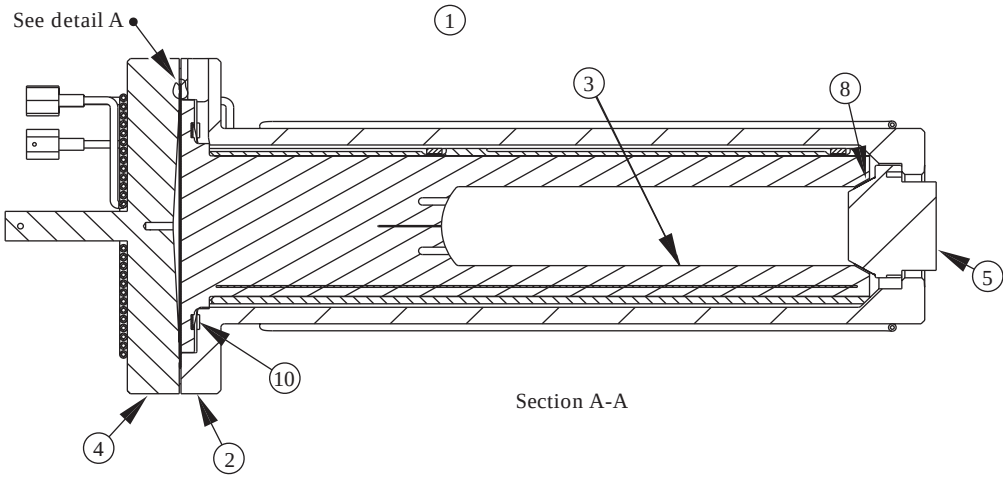

FIGURE 42. Cutaway view of the permeation cell. Tab 5 is the removable high-pressure cap, and tab 8 is the seal with the copper gasket. (NIF-0603-07061pb01)

generation permeation cell, Figure 42, has been successfully proof tested for a maximum operating pressure of 6000 psi. To be leak free at this pressure, the copper gasket that seals the demountable cap to the cell had to be carefully hydroformed to the correct shape without wrinkling the copper. With a hydroformed copper gasket, the measured leak rate at the high-pressure seal was less than 10^{-9} std cm^3 per sec.

In addition to the main cryostat and the permeation cell and its cryogenic circuitry, all of the supporting mechanical structures, the gas handling systems, the high-pressure deuterium systems, and the control systems have been constructed and are in various stages of testing. We anticipate full system operation and initial target filling tests early next year.

We contracted with General Atomics, San Diego, Calif., to serve as the D_2TS integrator, and they did much of the detailed design for the system. The main target cryostat was subcontracted to Cryogenic Technical Services, Inc., Colo.

Notes and References

1. G. E. Besenbruch et al., "Design and Testing of Cryogenic Target Systems," in *Inertial Fusion Sciences and Applications*, C. Lavaune, W. J. Hogan, and K. A. Tanaka, eds., pp. 921–926, Elsevier, Paris, 2000. See also relevant sections in the *General Atomics Inertial Confinement Fusion Annual Report*, April 2001, document GA-A23852, available from General Atomics, San Diego, CA.

SECTION 2

HIGH ENERGY DENSITY SCIENCE

High Energy Density Experimental Science

O. L. Landen *C. A. Back* *G. Dimonte* *S. G. Glendinning*
A. J. Bullock *S. Glenzer* *R. E. Turner* *W. W. Hsing*

The High Energy Density Science (HEDS) effort within the NIF Programs Directorate consists of laser experiment projects in the areas of hydrodynamics, radiation flow, implosions, material strength, and capability development that are conducted on the OMEGA, Janus, and HELEN laser facilities. This work is done in support of, and in collaboration with, the Defense and Nuclear Technologies Directorate, the Defense Threat Reduction Agency, and the Physical Database Research Program.

During the past two years, all experimental activities were conducted at the OMEGA Facility at the University of Rochester and the Janus Facility at LLNL. In addition to the science research, several new experimental capabilities were evaluated and developed on OMEGA to explore some of its unique capabilities in preparation for future NIF experiments: backlit point projection radiography, x-ray Thomson scattering, and dual-color radiography.

Measuring Hydrodynamics of Spherical OMEGA Implosions

Tests of Implosions with Emphasis on the Pushered Single-Shell Design

Work in fiscal year 2000 (FY00) concentrated on developing pushered single-shell (PSS) capsule implosions at OMEGA in support of quantifying the extent of and studying the effects of mix at the pusher-fuel interface. The purpose of these experiments is to explore the Rayleigh-Taylor (RT) instability in a converging geometry during the deceleration phase when ablative stabilization is absent. The PSS capsule consists of an 18-μm-thick SiO_2 mandrel overcoated with Ge-doped CH, driven in a scale-1 hohlraum by a 3.5-ns-long ramped, moderate peak temperature (170 eV) drive. Shots are distributed among surrogate Ar-doped plastic capsules used for core imaging of symmetry and the DT-filled PSS capsules. The principal diagnostics for the pushered shells include the x-ray drive temperature, the neutron yield (expected at 10^9 levels), the neutron burn history, and 10- to 20-μm resolution, 9-keV backlighting of the capsule's plastic-glass interface trajectory.

Five DT PSS capsules were shot. The Dante drive data is consistent with postshot simulations including a 15–25% backscatter power loss late in time (see Figure 1). The implosions gave yields between 5×10^8 and 1.1×10^9 neutrons, 10–20% fractional yield over clean (YoC) one-dimensional (1D) preshot predictions. The yields do follow the predicted strong power law with laser energy ($Y \sim E_L^5$) shown in Figure 2. A neutron burn history was also obtained on each shot using a sensitive close-in (2.1 cm) scintillator detector showing a 200-ps duration main burst of neutrons with possible earlier weaker shock-induced bursts. Backlighting of the imploding shell with 9-keV photons was also obtained (see Figure 3), yielding additional information on shell symmetry and the minimum value of the shell areal density.

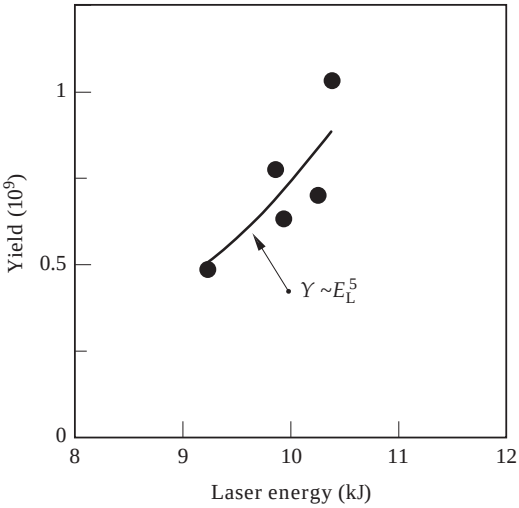

FIGURE 2. DT PSS yield vs laser energy.
(NIF-0403-06128pb01)

FIGURE 1. Measured (solid line) and calculated (dashed lines) drive temperature vs time. Upper and lower dashed lines represent 5% and 25% backscatter losses over last 1.5 ns.
(NIF-0403-06127pb01)

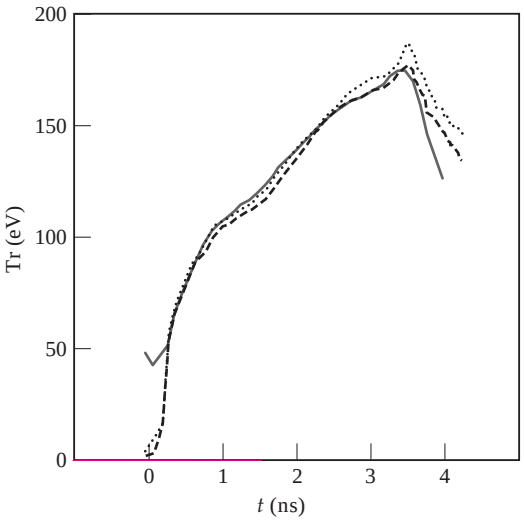

Performance of Smooth PSS Implosions with Modified Acceleration History

Shots from a two-year campaign of PSS implosions were analyzed for yield and bang time and compared with CALE calculations. The experiments averaged over all shots obtained YoC ~ 0.15, which agreed with 1D CALE simulations using reasonable mix model parameters based on Linear Electric Motor data. The measured and calculated bang times also agree within 100-ps error bars. However, two-dimensional (2D) LASNEX simulations indicate that drive asymmetry should contribute a 50% yield degradation, principally due to mode 4 and higher drive asymmetries. This

FIGURE 3. Nine-keV backlit images of glass shell midway in implosion; 10-μm pinhole on left, 20-μm pinhole on right.
(NIF-0403-06129pb01)

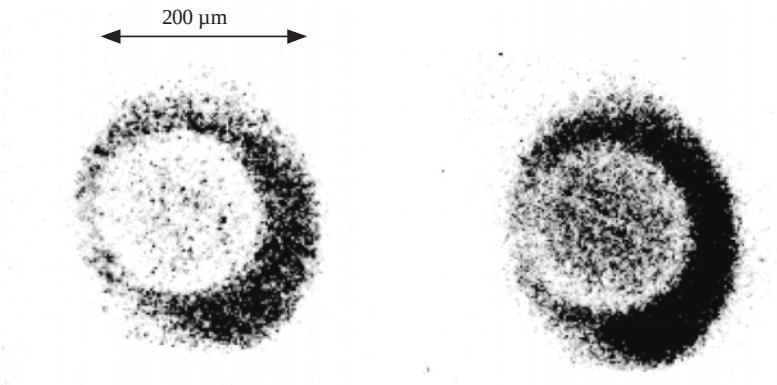

changes the inferred CALE mix model parameters by of order 20%. In order to verify LASNEX code-calculated implosion symmetry, imaging capsules doped with Ar and having similar implosion histories were fielded. An x-ray core image (see Figure 4) shows close to a round implosion, consistent with postprocessed simulations, suggesting at least that the lowest order asymmetry, P_2, is correctly predicted as being small.

The standard PSS has a CH-Glass interface 16 μm from the fuel, which is hydrodynamically unstable during the acceleration phase of the implosion. Perturbations from this interface can feedthrough to the pusher-fuel interface and cause mixing during the stagnation phase. In order to test this hypothesis, we shot all-glass capsules that have similar implosion trajectories as the standard PSS. Indeed, the all-glass capsules produced a significantly higher neutron yield of 1.2×10^9 compared to 0.8×10^9 for the standard PSS. This at first sight suggests growth and feedthrough of instabilities at an embedded interface are important and dominate the effect of greater sensitivity to ablation front instability growth for all-glass capsules. However, the predicted yield depends on the exact initial surface roughnesses, which was smoother for the all-glass capsules. Hence, we believe feedthrough at the embedded interface is not an important contributor to final deceleration phase mix.

Techniques to Measure Instabilities in Implosions

X-Ray Backlighting Techniques for Measuring Interface Mix in Spherically Convergent Geometry

Proposals for complementary experiments directly observing mix at the converged pusher-fuel interface were prepared. The first experiment proposed consisted of imaging a radiographically opaque band of the mandrel to avoid line-of-sight integration over curved surfaces and hence the need for Abel inversions. The experiment relies on new target fabrication capabilities using decomposable mandrels, and the recent success of target-mounted pinhole imaging which can provide 2-μm diffraction-limited resolution.

A second related technique requiring far less target development and fabrication effort was actually designed and demonstrated for diagnosing late-time mixing at the fuel / pusher interface. Specifically, in an implosion geometry similar to the PSS, the glass pusher is replaced with a Ge (5%) -doped CH in order to reduce the pusher opacity. Only the inner few microns of the CH are

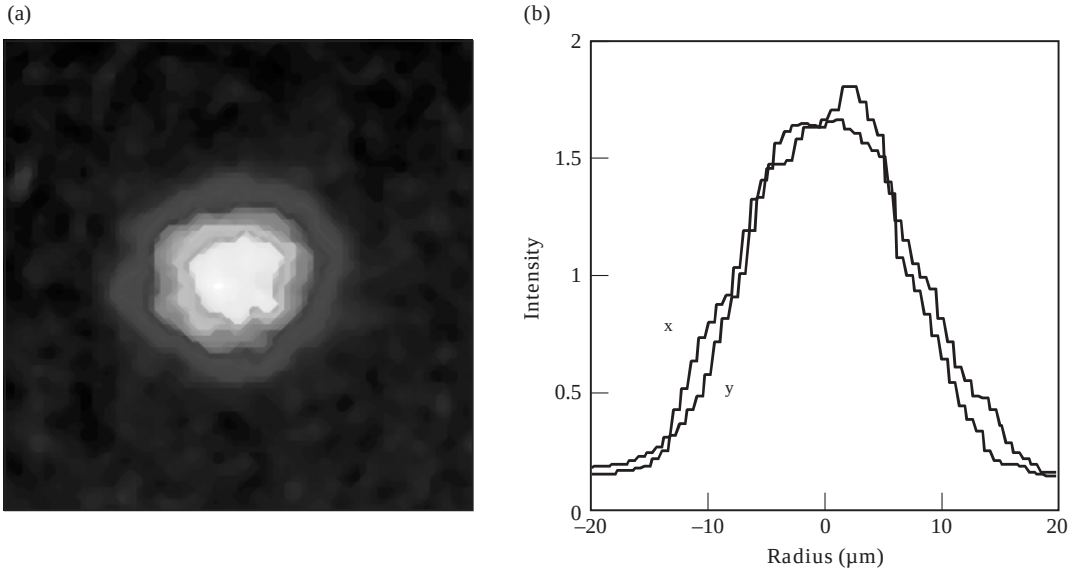

FIGURE 4. (a) X-ray core image of Ar-doped plastic shell. (b) Lineouts in horizontal and vertical plane showing symmetry. (NIF-0403-06130pb01)

doped with Ge to provide localized opacity above the Ge L edge. As more mixing of opaque Ge into the low-Z fuel occurs, the transmission through chords passing near zero radius should decrease (see Figure 5). We have demonstrated 5-μm accuracy in determining the interface position, based on analyzing the quality of backlit shell limbs in implosion data as shown in Figure 6. By using different backlighter energies between 5–8 keV, we can diagnose the shell trajectory during the implosion and explosion phase. We hope to characterize in FY02 the mixing at the fuel/pusher interface just after the minimum radius and during the explosion phase for smooth and intentionally roughened capsules.

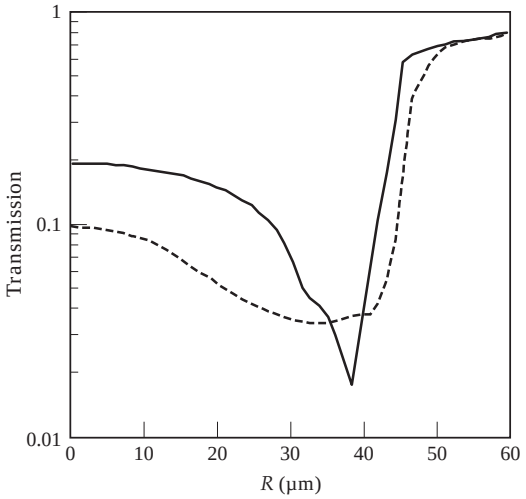

FIGURE 5. One-dimensional CALE simulation of transmission at 5 keV of re-exploding core 500 ps after minimum radius without (solid line) and with mix (dashed line). Capsule shell contains 2.5% Ge-doped tracer layer in plastic. The pusher-fuel interface is at 30 μm (12 μm) without (with) mix in calculations. (NIF-0403-06131pb01)

Diagnostic Techniques to Measure Energy Dynamics

Soft and Hard X-Ray Imaging Techniques for Energy Transport

We have completed initial experiments on the OMEGA facility extending the study of supersonic radiation energy transport to subsonic regimes. These experiments examine the behavior of heated foams, which have significant hydrodynamic motion occurring during the laser heating pulse. For these experiments, there are two main target fabrication requirements. First, the radiative source is a heated scale-1.4 halfraum that has a diameter of 2.24 mm and a 75% laser entrance hole (LEH). It has been scaled to a size larger than previous experiments in order to produce 3-ns-long stepped pulse drive that has a peak radiation temperature of approximately 160 eV.[1]

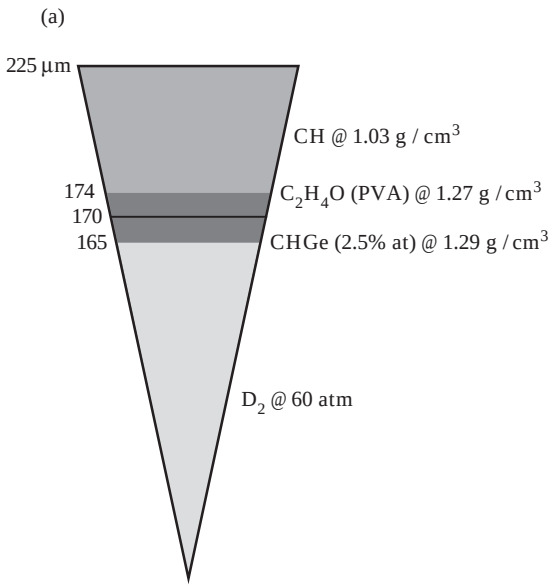

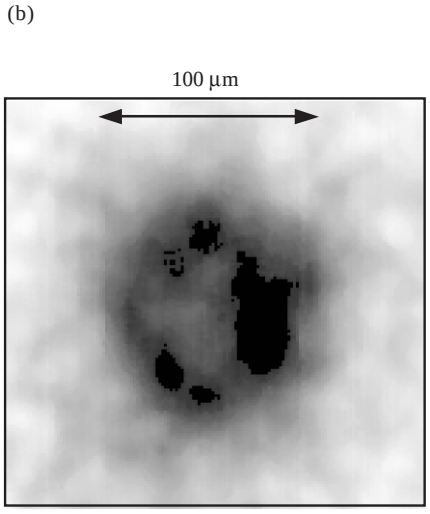

FIGURE 6. (a) Pie diagram of Ge-doped plastic shell used for backlighting imploding limb. (b) Backlit image at 4.7 keV of Ge-doped shell implosion, showing expected limb darkening. (NIF-0403-06132pb01)

Second, the heated sample is a 250-mg/cm^3 cylindrical Ta_2O_5 foam, a factor of 6.25 denser than in previous experiments. The foam has an annular opening machined in the disk that allows a clear line-of-sight to the backlighter initially.

The experiments examine radially resolved emissivity from the heated foam at 250 eV with diagnostics already employed in other radiation transport experiments (see Figure 7). In addition, we explore axial backlighting through the foam to measure its density. Exploratory shots were used to optimize contrast of the backlit image and to maximize spatial resolution. We used 14 beams to create two distinct backlight x-ray sources using a 12.5-μm-thick Ti foil. The foil is irradiated from the backside and the x-rays pass through the sample and the half-hohlraum. The transmitted photons were recorded by a streaked x-ray pinhole camera that provided a spatial resolution of ~ 20 microns. Figure 8 shows a streaked record of the backlighter. At about 1.5 ns, we note the appearance of Au stagnation emission at the halfraum axis, as well as blowoff emission from the laser plasmas. These additional sources of emission were identified by performing shots without the backlighter turned on. Hence, hohlraum filling limits the annular region available for the experiment.

Soft x-ray time-resolved measurements at hν = 250 eV were obtained at 50-μm resolution, 6.5× magnification using a transmission grating. Figure 9 shows a streaked record of the self-emission, showing the early emission through the opening

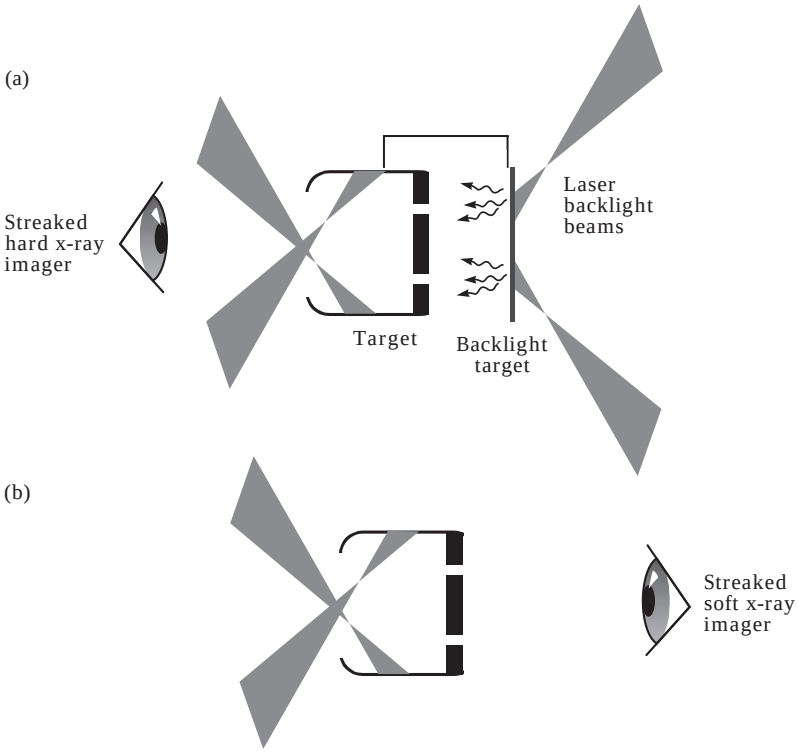

FIGURE 7. Experimental geometry for (a) hard x-ray backlighting and (b) soft x-ray imaging. (NIF-0403-06133pb01)

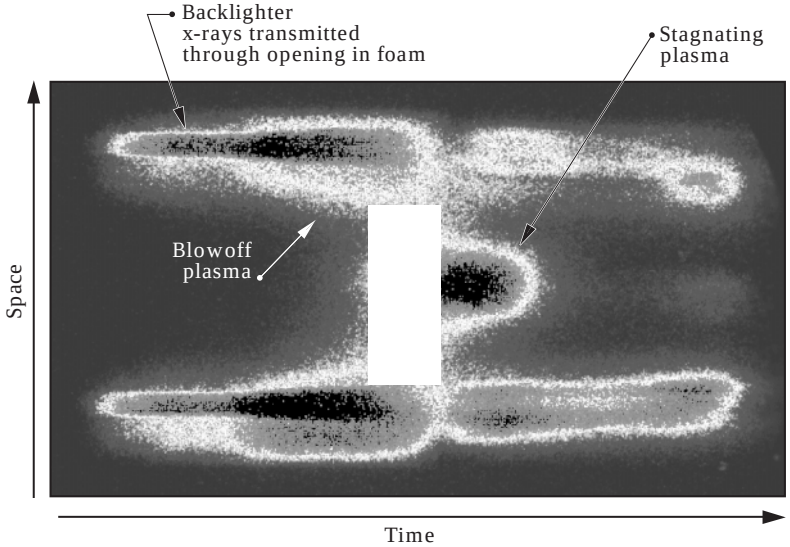

FIGURE 8. Example of streaked hard x-ray backlit data.
(NIF-0403-06134pb01)

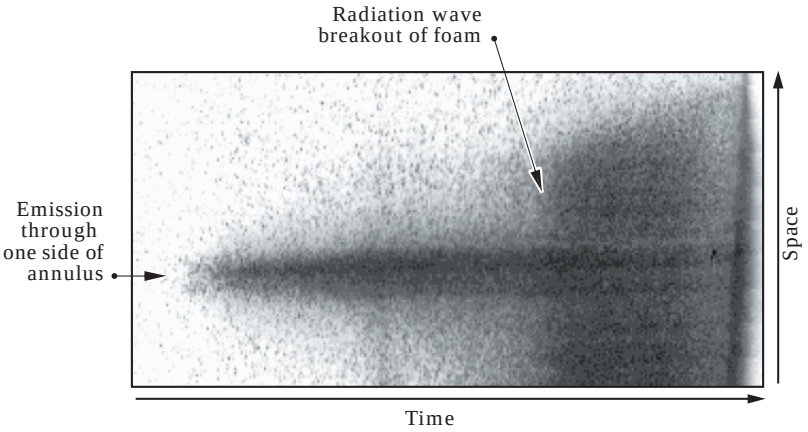

FIGURE 9. Example of streaked soft x-ray backlit data. (NIF-0403-06135pb01)

through foam. At about 2 ns, the self-emission increases throughout the field-of-view signifying burnthrough of the foam.

Developing and Characterizing Hohlraum Radiation Sources

Documenting Characteristics of $^{1}/_{2}$ Hohlraum Source

In FY00, shots concentrated on definitive drive measurements in scale-1 halfraums. The halfraums are driven by fifteen 0.5-TW 48 and 60° beams for the first 1.1 ns followed by five 0.5-TW 23° beams for the second 1.1 ns. The photoconductive detector (PCD) used for earlier drive measurements had an unacceptably slow (≈ 1 ns) rise due to a high-frequency fidelity loss in a long cable, explaining the earlier drive discrepancies. For these experiments we shot targets with no foam, Ta_2O_5 foam, SiO_2 foam, and Ta_2O_5 with a disk. The variations were to separate the effects of the foam on the drive temperature Tr and the slight temperature enhancement expected with a Au disk in the foam. We obtained absolute Dante and cross-calibrated PCD drive measurements through the LEH[2] as well as through the foam. We found that the halfraum shots oriented so that the Dante could measure the drive (see Figure 10) produced a Tr that much more closely matched the calculated drive early in time (see Figure 11). In both the Dante and P-11 PCDs, the drive temperature is 5% higher with higher-Z foams (Ta_2O_5 vs SiO_2) as expected due to the higher albedo of the higher-Z foam.

The lower than expected drive after 1.2 ns suggests that the low-angle (23°) beams, which turn on then (while all high-angle beam turn off then), are not coupling as well as predicted. This has been observed in other hohlraum shots used to drive implosions [Murphy][3] and suggests the amount of first-bounce reflected light or "glint" is underestimated in the simulations. After the end of the laser pulse, the experimental radiation pulse falls more rapidly in time than the calculations, as observed for full hohlraums. The supersonic scale-1 halfraum experiments tend to take data before this discrepancy is a problem. However, future subsonic experiments may need to investigate this further. The difference is probably due to the absence of dielectronic recombination processes in the calculations.

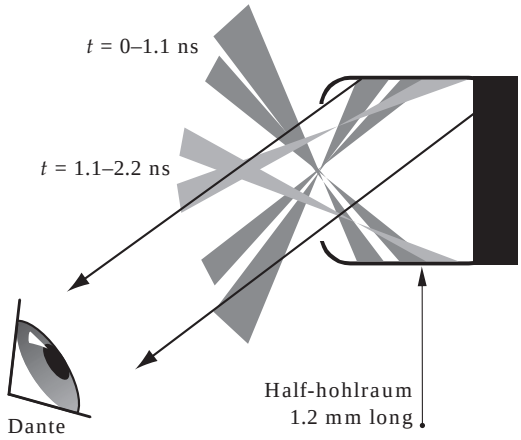

FIGURE 10. Experimental geometry showing Dante line-of-sight for shots dedicated to drive measurements. (NIF-0403-06137pb01)

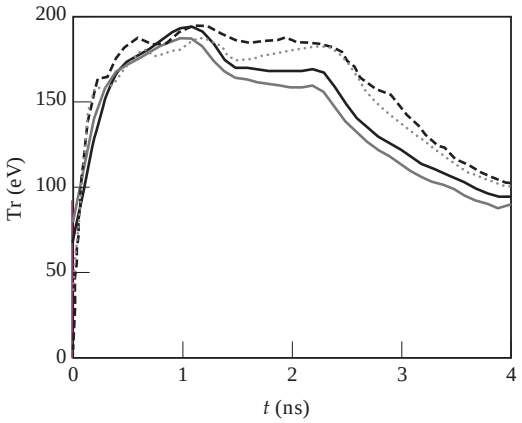

FIGURE 11. Measured (solid lines) vs postshot calculated drive (dashed lines) seen by Dante. The thicker (thinner) lines represent halfraums with Ta_2O_5 (SiO_2) foam at the ends. (NIF-0403-06137pb01)

Notes and References

1. O. L. Landen et. al., "Analytic Limits to Hohlraum Performance-U," submitted to *Defense Research Rev*. (2002).
2. C. Decker, R. E. Turner, O. L. Landen, H. N. Kornblum, P. Amendt, L. J. Suter, B. A. Hammel, T. J. Murphy, J. Wallace, A. A. Hauer, J. Knauer, F. J. Marshall, D. K. Bradley, W. Seka, and J. Soures, "Hohlraum Drive Measurements on the OMEGA Laser," *Phys. Rev. Lett*. 79, 1491 (1997) .
3. T. J. Murphy, J. M. Wallace, N. D. Delamater, C. W. Barnes, et. al., "Hohlraum Symmetry Experiments with Multiple Beam Cones on the OMEGA Laser Facility," *Phys. Rev. Lett*. 13,108 (1998).

Experiments in Simple and Complex Geometries on High-Powered Lasers or Pulsed Power Sources

Analyzing and Documenting Radiation Transport in Simple Geometries

The *Physical Review Letter* manuscript on the 12-ns, 70-eV radiation transport experiments performed at OMEGA in 1998 was submitted and published.[1] This paper describes radiation breakout in SiO_2 aerogel disks of various lengths and is the first to demonstrate the importance of wall losses on the radiation transport.

A *Physics of Plasmas* paper was published in May 2000,[2] based on an invited talk at the American Physical Society Division of Plasma Physics (DPP) Plasma Physics meeting in November 1999. The paper gives the full details on the March and July 1999 experiments in the $^1/_2$ hohlraum "halfraum" geometry. The article includes all 2.4-ns, 180-eV radiation transport results through disks of various length, demonstrating fully diffusive (3 mean-free-paths) and supersonic radiation flow (radiation Mach # = 3) in Ta_2O_5. It discusses the details of the curvature in the radiation breakout from the perspective of the number of transverse mean free paths. Furthermore, this paper gives useful analytic scalings of the optically thin and optically thick regimes for materials. A simple power loss model to estimate when 2D effects become important is also included.

A *DNT Stewardship News* article (Vol. 2, No. 8 February / March issue) was published, discussing the 1999 experiments in the $^1/_2$ hohlraum and emphasizing the advantages of this geometry over the scale-3 hohlraum geometry for radiation experiments.

An *ICF Quarterly* article (3rd quarter 1999 issue) was also written, comparing the scale-3 geometry and the $^1/_2$ hohlraum scale-1 geometry experiments. It is a summary article of the series of single-foam experiments and gives more detail on the importance of the opacity modeling for understanding the radiation transport in these foams.

Notes and References

1. C. A. Back, J. D. Bauer, O. L. Landen, B. F. Lasinski, J. H. Hammer, M. D. Rosen, L. J. Suter, and W. H. Hsing, "Detailed Measurements of a Diffusive Supersonic Wave in a Radiatively Heated Foam," *Phys. Rev. Lett*. 84, 274 (2000).
2. C. A. Back, J. D. Bauer, J. H. Hammer, B. F. Lasinski, R. E. Turner, P. W. Rambo, O. L. Landen, L. J. Suter, M. D. Rosen, and W. W. Hsing, "Diffusive, Supersonic X-Ray Transport in Radiatively-Heated Foam Cylinders," *Phys. Plasmas* 7, 2126 (2000).

Analyzing and Documenting Radiation Transport in Complex Disk Geometries

Work in FY00 and 01 completed a set of experiments studying supersonic radiation flow in the presence of solid density disks embedded in foams (see Figure 12). The Ta_2O_5 foam data is particularly useful, since, unlike the SiO_2 cases, the heated material opacity eliminates a direct view of the spatially nonuniform hohlraum source. Extensive testing on the aerogel composition has been completed. The empirical formula of the samples is $Ta_4O_{13}H_3$. This was determined by Thermal Gravimetric Analysis and C,H analysis. Figure 13 shows examples of streaked radiation breakout data in the presence of a thin Au disk embedded midway in a 500-µm-thick 40 mg/cm^3 Ta_2O_5 foam. Clear differences in the breakout time and profile are observed for different radii disks.

The measured and calculated shortest breakout times (<1.2 ns) now match as expected given the good agreement between measured and calculated drive up to 1.2 ns described in the subsection "Documenting Characteristics of $^1/_2$ Hohlraum Source." The later breakout times are progressively more delayed relative to calculations (450–700 ps), again consistent with the lower than expected drive after 1.2 ns.

Analysis of the data images has been improved by using a low-pass filter on the data. Corrections to the data related to phosphor variations have been taken into account and have improved the comparison of data to calculations. The embedded disk radiation breakout data has been compared to different radiation transport models, which predict significant differences in the radial profile of the radiation wave breakout.[1]

This data clearly and repeatably distinguishes between the models, independent of drive uncertainties. The data have been analyzed using both 2D and 3D codes. Computational results are not significantly different in 2D vs 3D, which is expected since the actual experimental geometry is 2D. Hence, we believe we have performed the first "true" AGEX radiation transport experiments. Moreover, the experiments lend themselves easily to a 3D geometry by using noncentered disks in the future.

FIGURE 12. Experimental geometry for complex radiation transport experiments.
(NIF-0403-06138pb01)

Notes and References

1. C. A. Back et. al., *a Defense Research Review* (DRR) article in preparation.

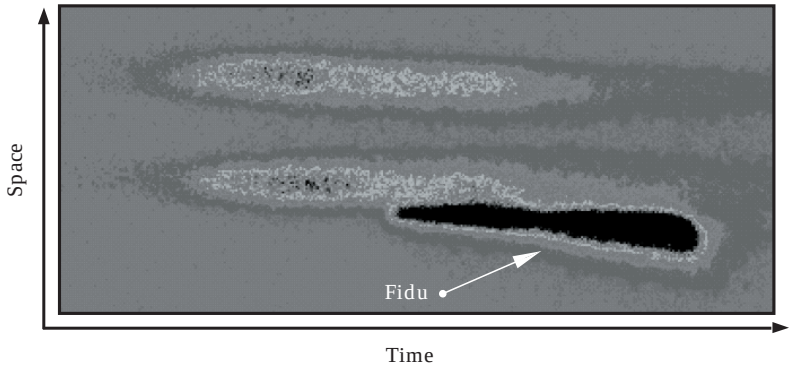

FIGURE 13. Streaked radiation breakout at hν = 250 eV around Au disk embedded in 500 µm-thick 40 mg/ cm^3 Ta_2O_5 foam.
(NIF-0403-06139pb01)

Experiments to Explore Sensitivity of Radiation Transport to Walls

Emissivity of Rippled Wall as a Function of Period, Amplitude, and Time

Roughened walls can slow radiation flow by promoting backscattering at the expense of forward scattering. We have focused on measuring the emission anisotropy of well-characterized rippled wall targets. In particular, the backside of ripples that are not directly viewing the hohlraum will be cooler and less emissive. By imaging the backside of both a rippled and nonrippled section of the foam walls (see Figure 14), one should be able to see a reduction in average emissivity for the rippled part, even if the ripples themselves could not be spatially resolved. The experiments used low-density, low-Z foams that provide tamping of the walls to avoid ripple closure while simultaneously providing an optically thin view of these walls. The results were very bright, and did show a promising as-expected reduction in the emissivity on the rippled side. A null shot was performed as well with no ripples to correct for any flat-field issue with the imaging instrument. Both the null and one of the images from a rippled target are shown in Figure 15. In Figure 16, lineouts across the area of interest for both the rippled and nonrippled cases show the reduction in intensity at the ripples. More work is required to provide quantitative comparisons with calculations under various ripple conditions.

FIGURE 14. Experimental geometry for viewing rippled wall. (NIF-0403-06140pb01)

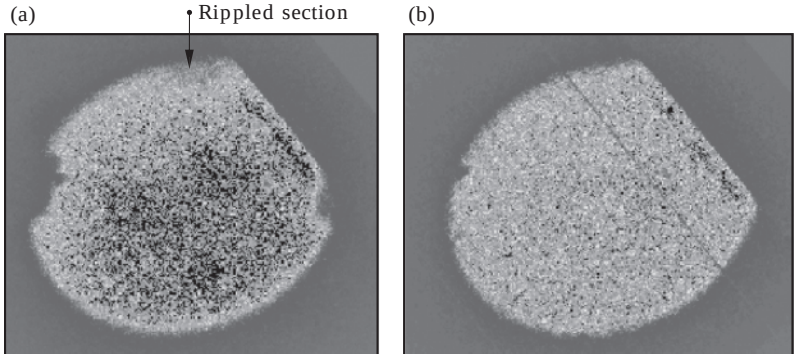

FIGURE 15. Soft x-ray (hν = 450 eV) images at 1.75 ns of Au walls (a) with and (b) without a rippled section. (NIF-0403-06141pb01)

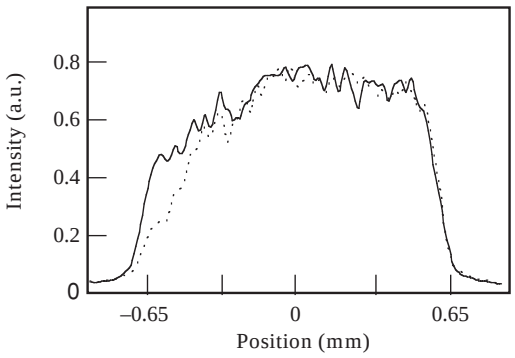

FIGURE 16. Lineouts showing significant less emission for rippled section (dashed line) in Figure 15 (a) than equivalent nonrippled section (solid line) in Figure 15 (b). (NIF-0403-06142pb01)

Measuring Wall Loss Effects by Comparing Results and Simulations of Low-Z vs High-Z Wall Experiments

The traditional high-Z, high-albedo Au foam sleeve was substituted with Be on a subset of the simple radiation transport shots in foam cylinders described in the subsection "Analyzing and Documenting Radiation Transport in Simple Geometries." The change to Be for the sleeve was motivated by two reasons: (1) Verify the importance of wall loss effects in explaining radiation breakout front curvature by obtaining radiation

breakout information with a different low-Z sleeve material, and (2) Check that a Be sleeve was an acceptable substitute for future experiments that require sidelighting perpendicular to the direction of the radiation propagation. Although the Be sleeve would seem to greatly magnify wall losses because of its low albedo, simulations show that the Be is very similar to the Au in radiation breakout time along the centerline of the foam. This lack of substantial difference is due to the fact that the total energy expended in heating the sleeve is only ~25%, in part due to the moderate aspect ratio of the targets, in part due to the the several mean free paths of isolation between the wall and foam center. Calculations of these targets show only a 10% difference in the central breakout time for equivalent drive but do show an expected weaker radiation breakout near the wall for the lower albedo Be case. This is confirmed in the experiments for both 0.5-mm and 1-mm-long foams (see Figure 17). The radiation breakout at center is only slightly delayed by switching to

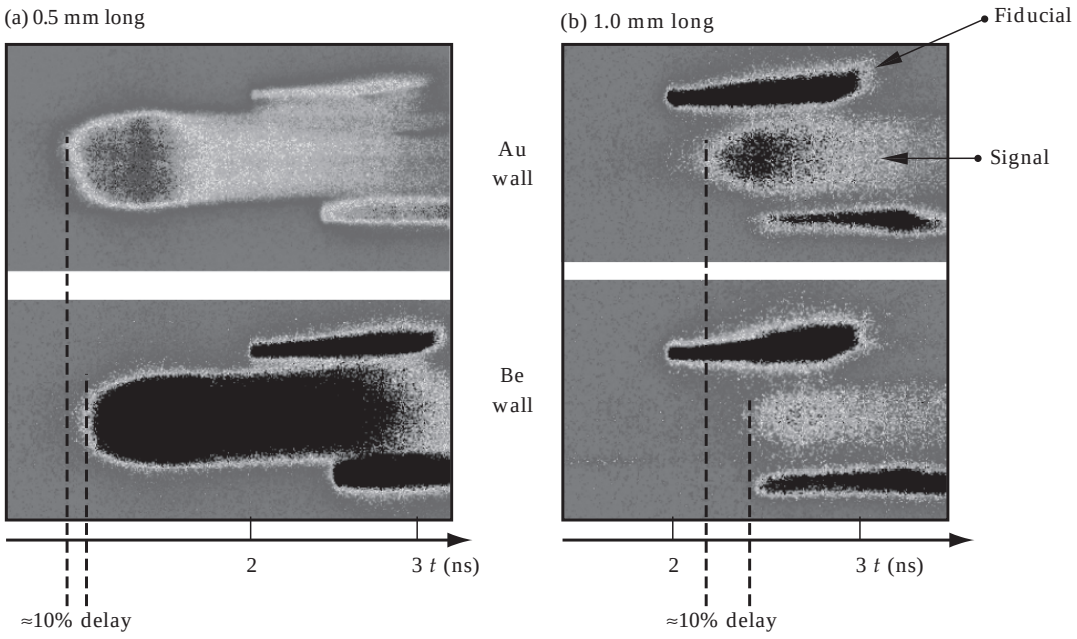

FIGURE 17. Streaked radiation breakouts in (a) 0.5-mm-long and (b) 1-mm-long 40 mg/cm^3 Ta_2O_5 at hν = 500 eV for Au (above) and Be (below) sleeves.
(NIF-0403-06143pb01)

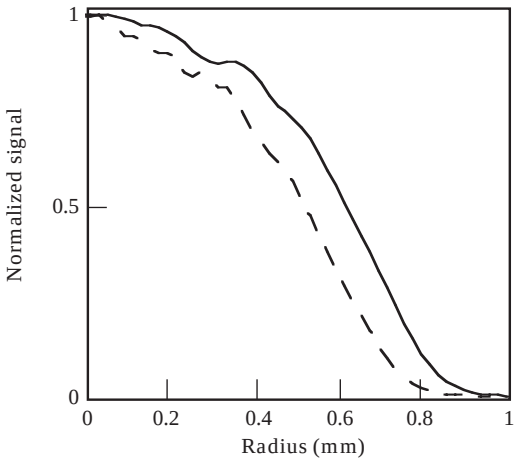

FIGURE 18. Radial emissivity 200 ps after radiation breakout in 0.5-mm-long 40 mg/cm^3 Ta_2O_5 foams for Au (solid curve) and Be (dashed curve) sleeves.
(NIF-0403-06144pb01)

the lossier, lower-albedo Be wall as expected from simulations. In addition, the increased curvature in the radial emissivity profile with the lossier Be has been confirmed (see Figure 18).

Backlighting Capabilities Required for NIF Hydrodynamics Experiments

Demonstrating 10- to 20-μm Backlit Pinhole Backlighting for High Field-of-View Imaging

The backlit pinhole backlighting technique had been successfully used at 25- to 35-μm resolution.[1-3] The current experiments were designed to extend the technique to 5- to 10-μm resolution as well as study the limits imposed by x-ray driven pinhole ablation and closure.[4] As shown in Figure 19, a Ti backlighter irradiated by a P_L = 0.5 TW, 5×10^{14} W/cm^2 OMEGA laser irradiation is placed a small distance d (0.45–1.0 mm) from a 5- or 10-μm pinhole, and a streak camera is placed behind the pinhole to capture the transmitted backlighter x-rays. The small distances chosen between backlighter source and pinhole is dictated by the need to maintain an adequate field-of-view when extrapolating this technique to NIF. Specifically, we expect timescales for pinhole closure to scale as the x-ray flux at the pinhole ~ $\eta P_L / d^2$, where η is the conversion efficiency. For the future NIF with a single beam (single quad of beams) with power 4(16) × greater than current experiments at OMEGA [2.4(9.6) TW vs 0.6 TW], the pinhole standoff distance for fixed η and closure time should hence be 2(4) × greater, 2–4 mm. Given the predicted minimum spot sizeof 0.3 mm on NIF, this should provide an acceptable field-of-view of 0.1 radians.

Placed in between the pinhole and the streak camera are three 25-μm-wide tungsten wires whose streaked backlit 100× magnification images provide additional information on backlighter resolution and background emission vs time. A second arm using a larger, more distant 25-μm pinhole serves as a reference arm for normalizing out the source emissivity vs time.

For the 10-μm pinholes at either distance, wire images are clearly visible even 500 ps after arrival of the backlighter laser pulse (see Figure 20). An increase in background

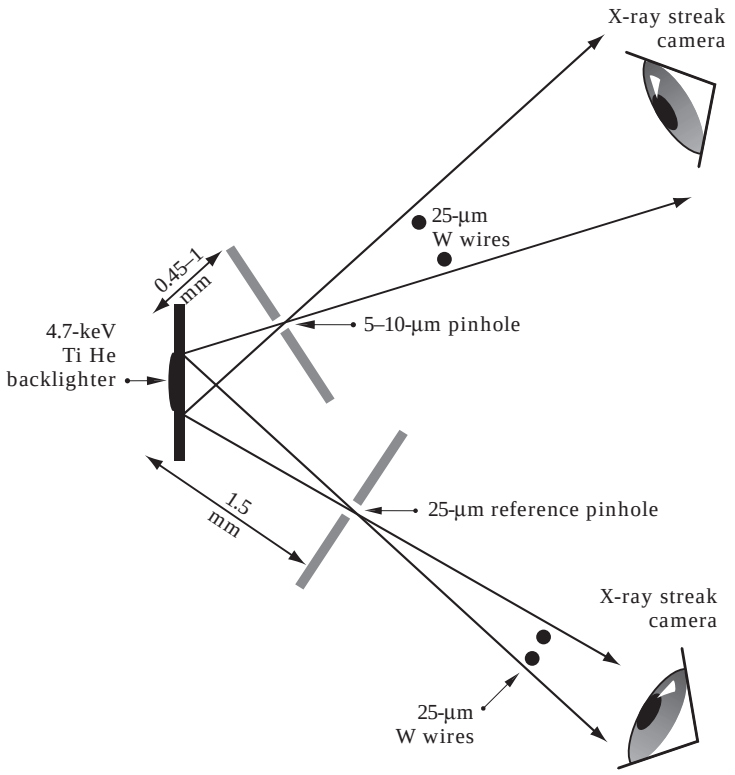

FIGURE 19. The backlit pinhole backlighting technique experimental setup. (NIF-0403-06147pb01)

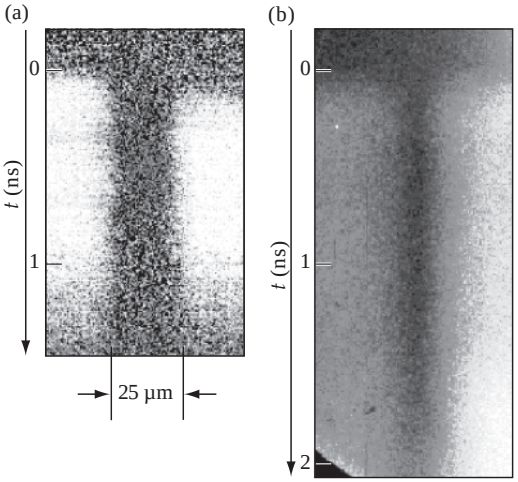

FIGURE 20. Streaked record of backlit 25-μm wire to (a) 10-μm pinhole and (b) 25-μm pinhole. (NIF-0403-06148pb01)

after 0.5 ns is ascribed to backlighter x-rays leaking around the Ti foil and pinhole substrate. After removing background and normalizing (see Figure 21), the timescale for pinhole closure can be extracted, 0.8 and 1.3 ns at 50% transmission for the 0.4-mm and 1-mm distant pinholes respectively. Figure 22 plots the transmission of a 5-μm pinhole placed 0.45 mm away from the Ti backlighter. The 50% transmission point has now been shortened to 400 ps, just sufficiently long for recording snapshots in a real experiment.

An analysis of the backlit wire image profiles (see Figure 23) shows for example that the 1D wire image resolution taken with an 11-μm pinhole remains at ≈ 10 μm over 1 ns (see Figure 21). This implies that pinhole ablation fills the center regions with low-density substrate material, thereby attenuating pinhole transmission in all regions of the pinhole, rather than closing due to a hard aperture.

Detailed computer simulations of the pinhole closure experimental data began with the goal of eventually providing a pinhole closure modeling capability. HYADES, a 1D Lagrangian hydrodynamics and energy transport code, was chosen to provide the simulations. The first step was to simulate the laser interaction with the backlighter foil. HYADES predicts the thin backlighter foil emits an x-ray spectrum with high-intensity soft x-ray (0.1–1 keV) and medium photon energy (1–4 keV) components in addition to the 4.7-keV Heα line emission. The second step was to include all three sources when calculating the ablation at the Ta pinhole substrate. The calculated pinhole transmission agreed well with the data for pinholes placed both 0.45 mm and 1 mm away from the backlighter (see Figure 21). In addition, the calculations now match the data in predicting that the resolution is barely affected as the pinhole transmission drops (see top of Figure 21). This is in sharp contrast with a simple analytic isothermal expansion model, which suggested incorrectly that decreased transmission would be accompanied by improved resolution.

Since the soft and medium x-ray emission were predicted to dominate the pinhole closure process, adding Be between the backlighter and pinhole substrate in the simulation should greatly reduce closure. This hypothesis was tested later as discussed in the subsection "Reduced Pinhole Closure for Pinhole-Assisted Backlighting on OMEGA."

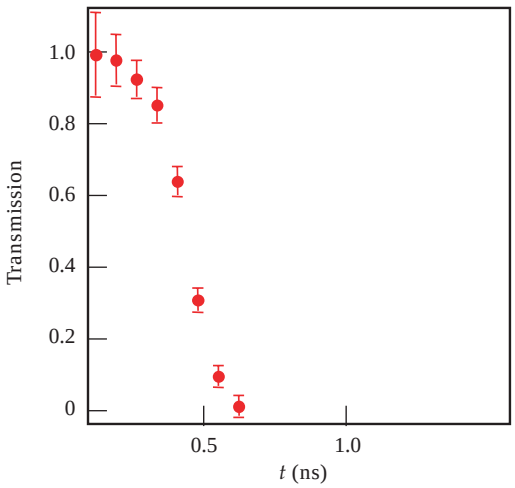

FIGURE 22. Measured transmission for 5-μm pinhole at 0.45 mm from 0.5-TW Ti backlighter.
(NIF-0403-06150pb01)

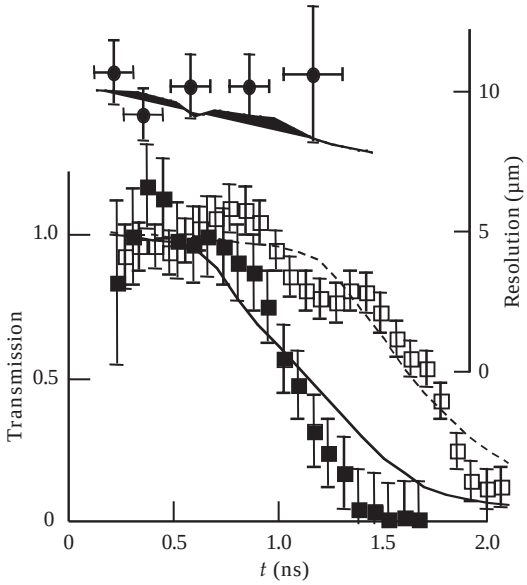

FIGURE 21. Measured and HYADES-simulated transmission and resolution for 10-μm pinhole at 0.45 mm (solid squares) and 1 mm (open squares) from 0.5-TW Ti backlighter. Circles are measured resolution for 10-μm pinhole images. All lines are HYADES simulations.
(NIF-0403-06149pb01)

Notes and References

1. O. L. Landen, D. R. Farley, S. G. Glendinning, et al.,"X-ray Backlighting for the National Ignition Facility," *Rev. Sci. Instrum.* 72, 627 (2001).
2. S. M. Pollaine, D. K. Bradley, O. L. Landen, R. J. Wallace, O. S. Jones, P. A. Amendt, L. J. Suter, and R. E. Turner, "National Ignition Facility-scale Hohlraum Asymmetry Studies by Thin Shell Radiography," *Phys. Plasmas* 8, 2357–2364 (2001).
3. D. K. Bradley, O. L. Landen, A. B. Bullock, S. G. Glendinning, and R. E. Turner, "Efficient 1–100 keV X-ray Radiography with High-Spatial and Temporal Resolution," *Opt. Lett.* 27 (2), 134 (2002).
4. A. B. Bullock, O. L. Landen, and D. K. Bradley, "10 and 5 μm Pinhole-Assisted Point-Projection Backlit Imaging for the National Ignition Facility," *Rev. Sci. Instrum.* 72, 690 (2001) .

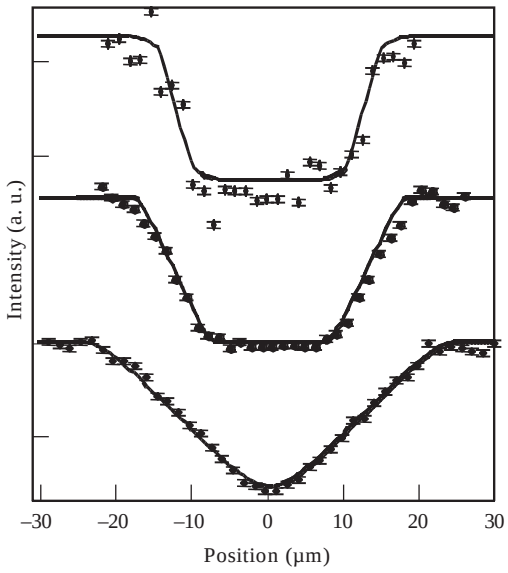

FIGURE 23. Measured lineout and fitted resolution for 5-, 10- and 23-μm pinhole images of 25-μm W wire. Data separated along y-axis. Top data taken at t = 150 ps by a 5-μm pinhole placed 1 mm away from the backlighter is best fit using a 5.1-μm pinhole resolution. Middle data taken at t = 600 ps by a 10-μm pinhole placed 0.45 mm away from the backlighter is best fit using a 10.6-μm pinhole resolution. Bottom data taken at t = 600 ps by a 23-μm pinhole 1.5 mm away is best fit using a 23.5-μm pinhole resolution.
(NIF-0403-06151pb01)

Improvements in Gated Detector SNR through Flat Fielding and Switching from Film to CCD as the Recording Medium

Framing cameras based on gated microchannel plates (MCPs) equipped with film recording media have been used for over a decade for a wide variety of x-ray-based experiments. In Table 1, the signal-to-noise ratio (SNR) contribution from these detectors and their subelements (where measured) is tabulated for a pixel size at the detector plane of 100 μm. These SNRs have been verified to be almost independent of the signal level or detector gain; they are not associated with shot noise, which should not be a concern for a well-designed experiment. The representative 100-μm-pixel size has been chosen to be large compared to the spatial resolution of the detectors but small compared to the dimensions of the detector. The SNR increases roughly linearly with pixel size between the size range of detector resolution and detector dimensions. However, it is clear from these small values of SNR that the useful spatial resolution for 2D images recorded on gated detectors has been limited by noise rather than by the intrinsic resolution (30-40 μm for MCPs).

To reduce random noise levels, the optical film used as recording medium for MCP-based framing cameras has been replaced by optical CCDs. While the SNR for film is characteristically a constant over a wide range of exposure levels, the absolute value of the CCD noise is characteristically a constant, as determined by the dark noise level. For a typical 9-μm-pixel 4000 × 4000 array optical CCD in use at OMEGA, the random dark noise is 20 counts compared to an optimized exposure level (i.e., approaching MCP saturation) of 20,000 counts. Averaged over a 100-μm spatial scale, the CCD SNR is hence ~10,000, a >500× improvement over the film SNR (see Table 1). Even at a few percent of maximum exposure level, the CCD SNR is still an order of magnitude greater than for film. Adding prompt data viewing and analysis capabilities and at least as good a dynamic range to the SNR advantage, we see CCDs as clearly desirable for replacing film in all future backlighting experiments.[1, 2]

In Table 1, we note that the SNR for MCP-based film data is smaller than the film SNR on its own. We have recently discovered that this additional noise source in photon-rich MCP-based framing camera data is repeatable on spatial scales as small as 20 μm (see Figure 24). This noise can be removed on any data by dividing, pixel by pixel, by a uniformly illuminated test image (i.e., by flat fielding). Examples of the improvement in uniformity before and after flat fielding are shown in Figures 25

TABLE 1. SNR at 100-µm scale for various detectors and subelements, with and without flat fielding, in the absence of shot noise. For CCD, signal approaching MCP saturation level of 20,000 counts is assumed.

Detector element	Raw SNR	SNR after flat field
Optical film (T3200)	17	
MCP + T3200	8	12
CCD	10,000	
MCP + CCD	9	>50

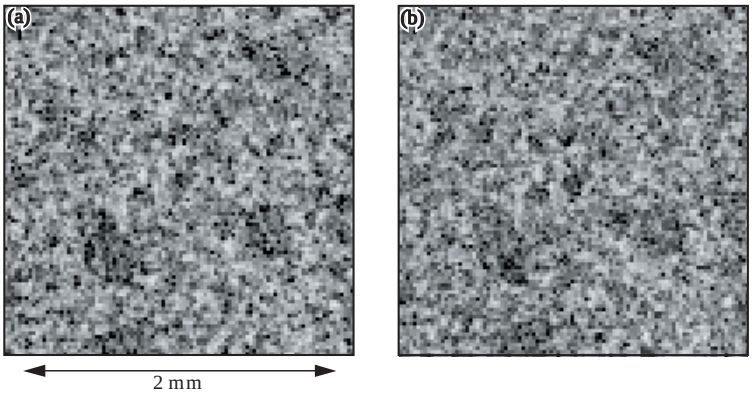

FIGURE 24. (a) and (b) are two successive film images of 2 mm × 2 mm section of uniformly x-ray illuminated microchannel plate (MCP) run in dc mode. The MCP is operated at low gain (<100) to minimize the contribution of shot noise. The two images show repeatable structure down to a 20-µm scale. (NIF-0403-06152pb01)

and 26. The noise has been traced to nonuniformities in the phosphor. The improvement in SNR accomplished so far through such flat fielding is also given in Table 1 for both film and CCD as the recording medium.

In summary, the combination of flat fielding MCP-based data and switching to CCD as recording medium can increase SNR by close to an order of magnitude. We anticipate that this will improve gated backlighting data quality for a wide variety of experiments at OMEGA and NIF. The discovery of how to provide high-SNR gated imaging also paves the way for long-pulse, point-projection, backlit-pinhole backlighting to perhaps become the backlighting method of choice for NIF.

Notes and References

1. R. E. Turner, O. L. Landen, D. K. Bradley, et al., "Comparison of Charge Coupled Device vs Film Readouts for Gated Micro-Channel Plate Cameras," *Rev. Sci. Instrum.* 72, 706 (2001).
2. O. L. Landen, D. R. Farley, S. G. Glendinning, et al., "X-ray Backlighting for the National Ignition Facility," *Rev. Sci. Instrum.* 72, 627 (2001).

FIGURE 25. (a) CCD image of uniformly illuminated section of MCP run at low gain in pulsed mode. (b) CCD image (a) divided by second uniformly illuminated image. (c) Lineout across image (a). (d) Lineout across flat-fielded image (b), demonstrating 5× improvement in SNR. (NIF-0403-06153pb01)

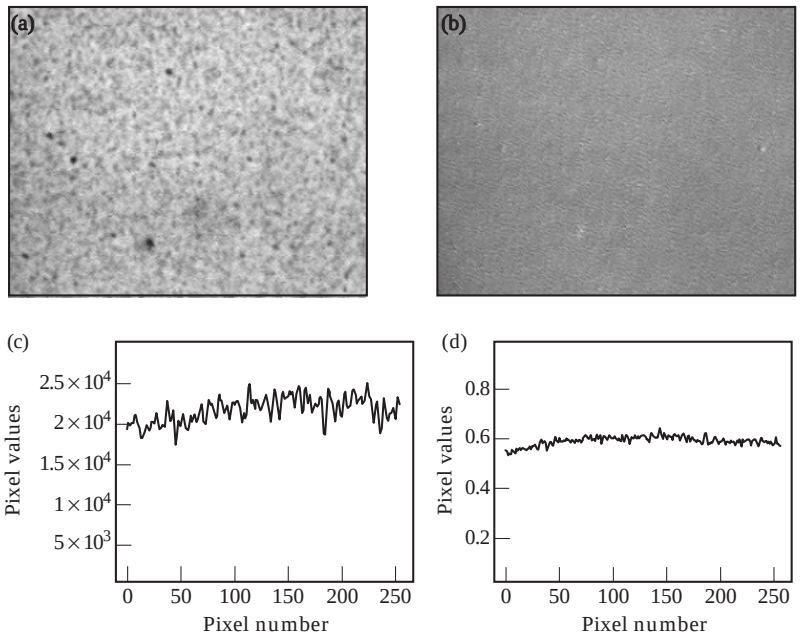

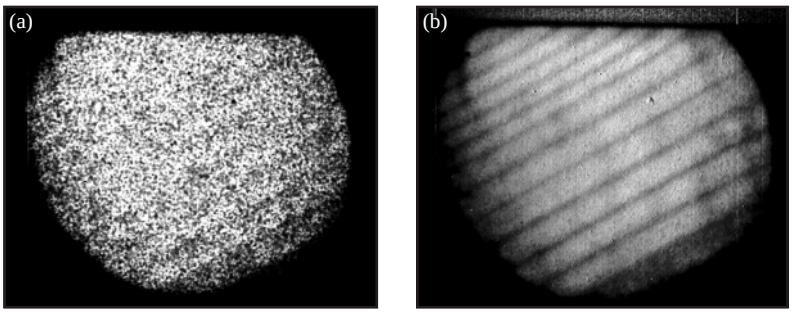

FIGURE 26. Gated image of backlit rippled package: (a) before flat field and (b) after flat field. (NIF-0403-06154pb01)

Polychromatic Backlighting (K-, L- or M-Shell Emitter)

In an effort to increase backlighter output required for NIF, one can envisage using multiple foils along a common line of sight to take advantage of many beam facilities, such as OMEGA and NIF.[1] This has the advantage of distributing laser intensity amongst many surfaces, thus avoiding saturation effects in conversion efficiency at the higher intensities present if only irradiating a single foil [Workman][2]. However, to avoid reabsorption on the He-like n = 2-1 resonance line radiation often used, a polychromatic approach may be required such that each successive foil of higher-Z material is transparent to the radiation of the previous foils (see Figure 27). The purpose of this study was to demonstrate the concept using double-sided irradiation of a single foil, both monochromatic and polychromatic. X-ray framing cameras were used to monitor the backlighter emissivity from both sides, an x-ray streak spectrometer was used to monitor x-ray spectra, and the HENWAY spectrometer was used to monitor total spectral output. The experiments were conducted at OMEGA using 1-ns, 3-TW, 10^{15}-W/cm^2 irradiation per side.[3]

Specifically, the relative efficiency of double-sided Ti backlighters and Sc/Ti backlighters were compared with the efficiency of a single-sided Ti backlighter (see Figure 28). Narrowband (4.2–4.9 keV) and broadband (4.2–6 keV) emission efficiencies were studied for both foil types. As expected, the Ti emissivity was very weak as seen from the Sc side due to reabsorption above the lower-Z Sc K edge. Figure 29 shows that the time-averaged narrowband (4.2–4.9 keV) double-sided Ti/Ti (Sc/Ti) backlighter emissivity as seen from the Ti side is 70% (50%) greater than that of the single-sided Ti backlighter.

Notes and References

1. O. L. Landen, D. R. Farley, S. G. Glendinning, et al.,"X-ray Backlighting for the National Ignition Facility," *Rev. Sci. Instrum.* 72, 627 (2001).
2. J. Workman and G. Kyrala, "X-ray yield scaling studies performed on the OMEGA laser," *Rev. Sci. Instrum.* 72, 678 (2001).
3. A. B. Bullock, O. L. Landen, and D. K. Bradley, "Relative X-Ray Backlighter Intensity Comparison of Ti and Ti/Sc Combination Foils Driven in Double-Sided and Single-Sided Laser Configuration," *Rev. Sci. Instrum.* 72, 686 (2001).

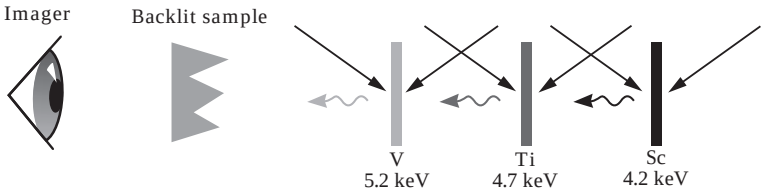

FIGURE 27. Proposed polychromatic multiple foil backlighter geometry. (NIF-0403-06155pb01)

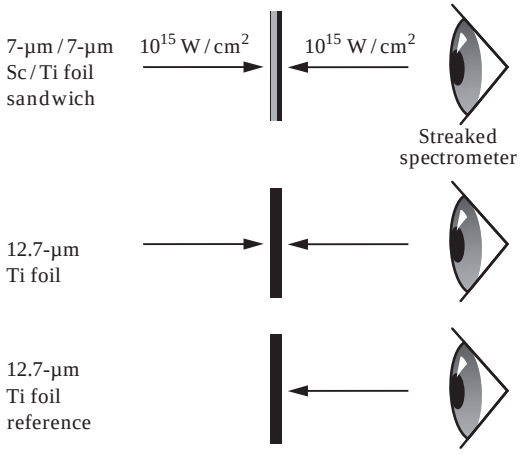

FIGURE 28. Experimental setup showing single- and double-sided backlighter target types. (NIF-0403-06156pb01)

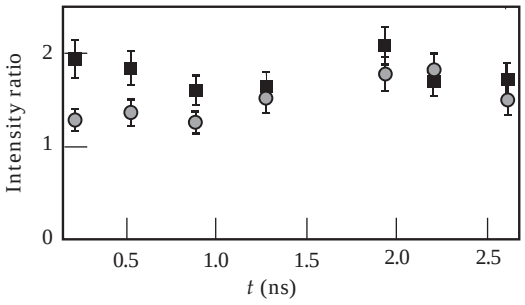

FIGURE 29. Ratio of double-sided to single-sided Ti backlighter emissivity between 4.2 and 4.9 keV for Ti/Ti (squares) and Ti/Sc (circles) foils.
(NIF-0403-06157pb01)

Reduced Pinhole Closure for Pinhole-Assisted Backlighting on OMEGA

Previous experiments described in the subsection "Demonstrating 10- to 20-μm Backlit Pinhole Backlighting for High Field-of-View Imaging" have shown that 5-μm pinholes ablate and close on the 200-ps timescale. This timescale is too short for comfort for many important applications. HYADES modeling presented in the cited subsection had shown that high-power soft x-ray ($E < 1$ keV) emission from the backlighter rear surface may be largely responsible for pinhole ablation and closure during point-projection backlit imaging. Furthermore, the modeling suggested that placing a Be soft x-ray filter between the backlighter and the pinhole would mitigate the closure.

The targets were built as in previous pinhole closure experiments described in the subsection cited in the previous paragraph, except that a 125-μm Be foil was placed at the rear surface of the backlighter on some targets. As before, an x-ray streak camera was placed 15 cm away from the pinhole substrate in order to capture the time-dependent pinhole x-ray transmission through 10-μm pinholes. In addition, a soft x-ray framing camera was used to image the soft (0.5 keV) and medium (1 keV) energy x-ray emission from the rear backlighter surface. Pinhole transmission was measured for pinholes placed both 1 mm and 0.45 μm away from the backlighter (0.6 TW in 3 ns on 250-μm spot on rear side of 12.7-μm Ti foil). Figure 30 shows a comparison of pinhole transmission for 10-μm pinholes placed 0.45 mm away from the backlighter. The addition of 125 μm of Be did not measurably decrease pinhole closure.

Furthermore, measurements of 500-eV and 1-keV emission from the rear Ti surface show that soft x-ray emission did not rise above the 10-MW level during the experiment. Since the modeling predicted 6 GW of soft x-ray emission at 1.5 ns after the start of the laser–backlighter interaction, this suggested that HYADES was overestimating soft x-ray emission from the rear surface. Hence we now believe that the hard 4.7-keV x-rays are indeed driving the closure. HYADES modeling of the Ta ablation including only the hard 4.7-keV x-ray component can now explain the rate of closure if the hard x-ray conversion efficiency is set at 0.1% (see Figure 31).[1] While the model does not fully agree with the observed pinhole transmission for both the 0.45-mm and 1-mm-distance cases, this disagreement may be explained by the vignetting effects of these large (5–10) aspect ratio pinholes. Specifically, it is possible that the high aspect ratio of the pinhole prevented the deeper regions inside the pinhole from seeing the full backlighter source. This effect would be expected to slow closure, which would explain the fact that 0.45-mm data shows a slower pinhole

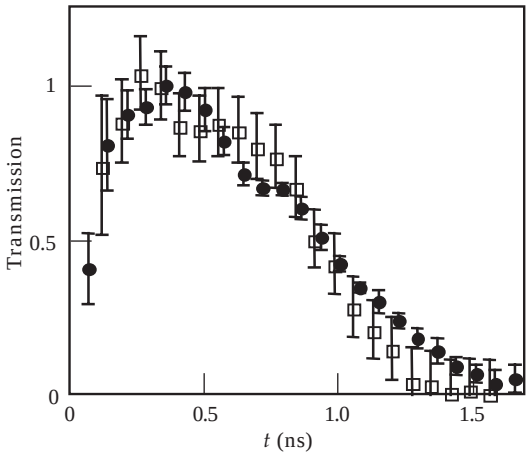

FIGURE 30. Transmission of 10-μm pinhole at 0.45-mm to backlighter, with (closed circles) and without (open squares) 125-μm Be between Ti and pinhole.
(NIF-0403-06158pb01)

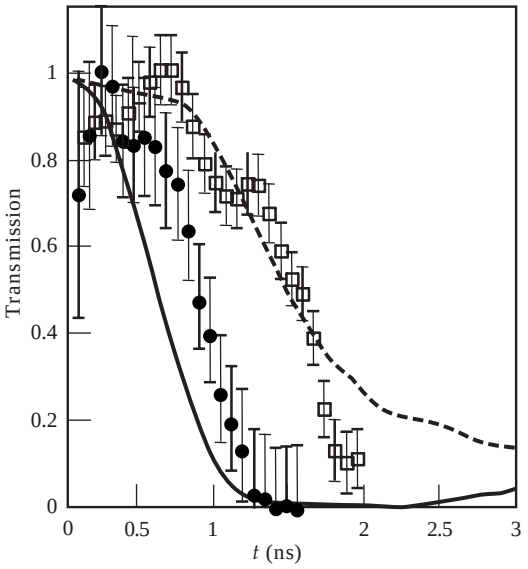

FIGURE 31. Measured and hard x-ray only HYADES simulation of transmission for 10-µm pinhole at 0.45 mm (closed circles) and 1 mm (open squares) from 0.5-TW Ti backlighter. (NIF-0403-06159pb01)

closure than the model normalized to the 1-mm data. The importance of this effect would depend strongly on the exact cross-sectional shape of the pinhole with depth, which is not well known. For example, it is clear that for tapered conical pinhole cross sections, there will be less ablation with the thin end pointed towards the backlighter plasma.

Since the simple Be overcoating did not mitigate closure, we are exploring another technique for reducing pinhole closure. Pinholes tamped with plastic or Be can potentially inhibit pinhole closure; but due to the microscopic dimensions involved, we cannot convincingly prove by characterization that conventional plastic filling techniques will fill the entire pinhole. Instead, we built tamped slits by joining two Ta substrates "edge-on" that had been initially overcoated with a thin Be layer. This produced a slit with well-understood tamping properties and slit width. If these slits strongly mitigate the closure problem, then these slits can be used to build closure-resistant pinholes by using, for example, two crossed slits.[2]

The targets were built as in previous pinhole closure experiments, except that the pinhole substrate was replaced with a slit substrate in one arm of the experiment. Figure 32 compares the slit transmission for 10- and 5-µm slits placed 0.45 mm away from the backlighter. Untamped slit transmission was roughly similar to pinhole transmission for slits and pinholes of equivalent size. Both the 10-µm pinhole and the 10-µm slit show a transmission of 50% at a time of approximately 1 ns, and both the 5-µmpinhole and the 5-µm slit show a transmission of 50% at a time of approximately 500 ps. Due to experimental problems, measurement of the tamped slit transmission has been postponed beyond FY01.

Nevertheless, the success so far has led to point projection imaging using 5- to 20-µm backlit pinholes being attempted for other LLNL, Los Alamos National Laboratory, National Laser Users' Facility, and the University of Rochester's Laboratory for Laser Energetics hydrodynamics shots as a replacement for traditional area backlighting.

Notes and References

1. A. B. Bullock, O. L. Landen, J. Edwards, and D. K. Bradley, "X-Ray Induced Pinhole Closure in Point Projection X-ray Radiography," *J. Appl. Phys.,* to be submitted.
2. O. L. Landen, P. M. Bell, R. Costa, D. H. Kalantar, and D. K. Bradley, "X-ray Framing Cameras for > 5 keV Imaging," in *Ultrahigh- and High-Speed Photography, Videography, and Photonics,* G. Kyrala, Ed. (SPIE, Bellingham, 1995) Vol. 2549, p. 38.

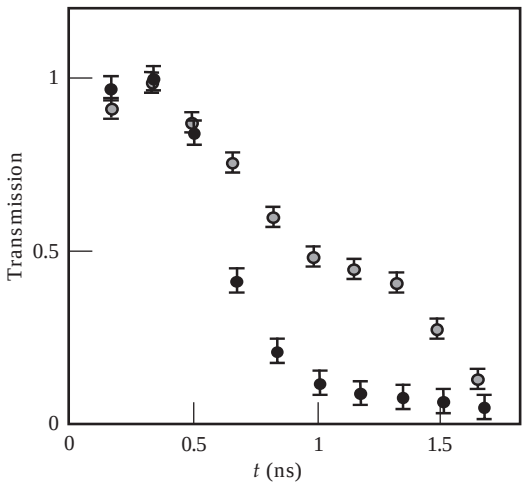

FIGURE 32. Transmission of 5-µm (closed circles) and 10-µm (open circles) untamped slits at 0.45 mm to Ti backlighter. (NIF-0403-06160pb01)

Demonstrating Dual-Color Radiography for Mix Diagnosis on OMEGA

A technique was developed to measure the density profiles of both species simultaneously across an interface between two fluids, even when the fluids are mixed. This is done by taking radiographs at two different x-ray energies, one below an absorption edge and the other above the edge of one of the materials (material 1 shown as solid-line opacity in Figure 33). Material 2 has continuum absorption in this region. The concentration of each material is adjusted so that the opacity of material 1 dominates above the edge and that of material 2 dominates below the edge. Experiments were conducted on OMEGA using a backlighter above (Ni 7.8 keV) and below (Fe 6.7 keV) the Fe edge. The targets utilize Fe-doped foam as the low-density fluid (material 1) and Br-doped plastic for the high-density fluid (material 2). They are packaged in a 1.1-mm-diameter Be cylinder with a specially designed stepped interface between the Fe-doped foam and the plastic layer. The experiment uses dual 5-μm slit-projection sidelit imaging at 15× magnification onto a wide strip (30 mm) gated MCP (see Figure 34). The use of slits allows for collecting more photons while maintaining resolution.

We were able to show that the dual-color imaging geometry will produce images of high resolution and signal-to-noise ratio; but due to data saturation, we were unable to verify that the technique will measure opacity levels accurately. Static radiographs exhibited the expected qualitative behavior for the relative transmissions of Fe and Br above and below the Fe absorption edge, as shown in Figure 35. In addition, the 1D resolution appears to be of order 3.5 μm, with very good signal-to-noise ratio attributed to using slits for better photon collection efficiency.

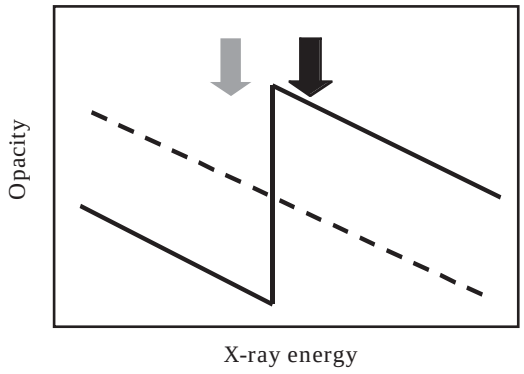

FIGURE 33. Schematic of dual-color imaging concept showing absorption vs photon energy. Material 1 is shown as solid-line opacity, material 2 as dashed-line opacity. (NIF-0403-06161pb01)

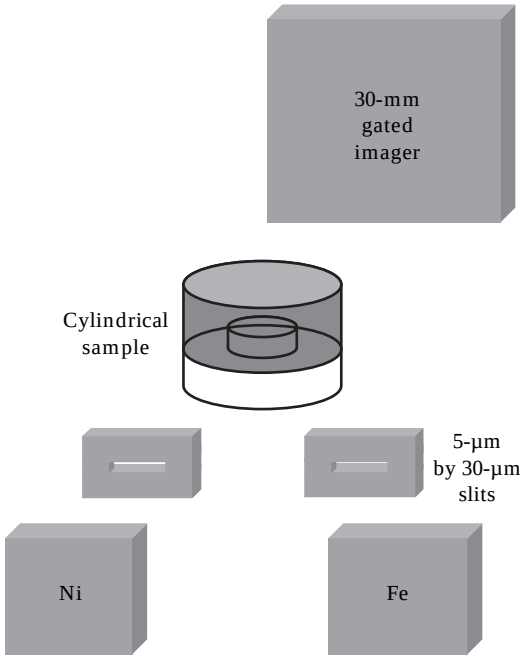

FIGURE 34. Experimental setup for demonstration of dual-color slit projection radiography. (NIF-0403-06162pb01)

Demonstrating Fluorescence Anisotropy for Inferring Micron-Scale Features

We have begun testing a new technique for resolving, by fluorescence anisotropy, submicron hydrodynamic features inaccessible to traditional pinhole or x-ray optic imaging. The technique uses the fact that any features larger than the photon mean free path will have its fluorescence in the forward or near-forward "shadowed" direction reabsorbed when pumped (see Figure 36). By contrast, the near-forward fluorescence of an atomically mixed or featureless surface will be detectable. Hence a measure of the forward fluorescence should allow one to distinguish between atomically mixed vs

chunks of material without requiring submicron imaging capabilities.

The proof-of-principle design uses pumping of the 2-keV Au M-shell fluorescence pumped by Cl He-like and H-like radiation. A photon energy of 2 keV was chosen to provide sufficient transmission for any overcoated low-Z tampers while minimizing the fluorescence mean-free-path (0.3 μm), which sets the measurement spatial resolution. At OMEGA, low-resolution (mm) framing camera x-ray images of CH-coated, Au planar targets (flat and corrugated) driven into fluorescence by a 1-ns, 10^{14}-W/cm^2 Saran backlighter (Cl Heα at 2.8 keV) were captured in both the near-forward and backward directions (≈ 30° to the target surface; see Figure 37). Examples of images at 0.9 ns of forward scattering and fluorescing from a flat Au target are shown in Figure 38. By filtering each image differently, we were able to infer the relative contributions of simple scattering at 2.8 keV to fluorescence at 2.13 keV. For targets with a Au surface machined with a small 1.1-μm amplitude, 20-μm wavelength perturbations, we did not observe a difference in scattering/fluorescence signal between the front and backward directions as normalized to the flat target data, as expected. Unfortunately, no data was obtained on the rougher targets for which an anisotropy was expected.

A downscaled experiment was performed at Janus, using a single gated x-ray imager viewing in the near-forward direction and composite targets having both smooth and intentionally roughened areas. The Janus experiments to date have shown that a Saran (CH_2Cl_2) x-ray backlighter driven by one arm of Janus (2-ω, 80 J, 1 ns) could induce 2- to 3-keV x-ray emission from a Au target placed 1 mm away from the backlighter. Furthermore, use of differential filtering in front of the MCP showed that the x-ray emission was composed of both 2.13-keV fluorescence photons and 2.77-keV scattered photons. However, no evidence for the expected anisotropy was observed when comparing signals off the smooth and preroughened areas of the gold foils. It is possible the signal was contaminated by either specular x-ray reflection or emission from a stray laser-produced plasma on the surface of the Au.

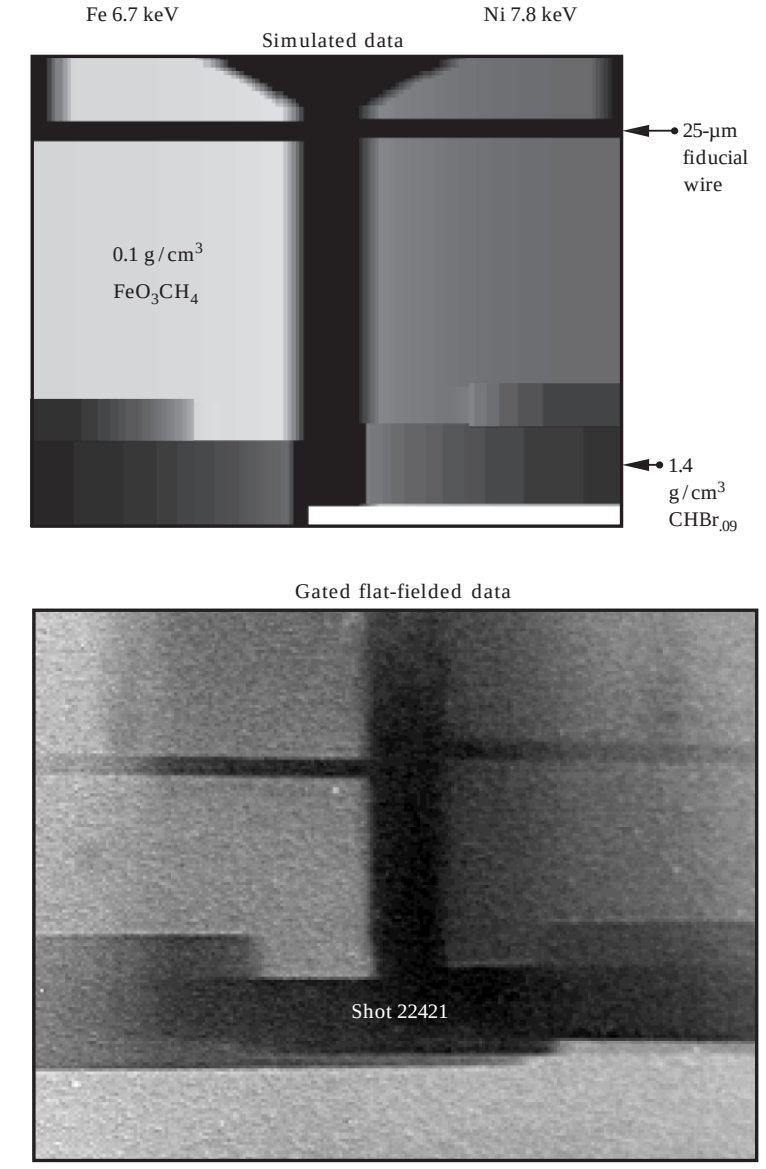

FIGURE 35. Flat-fielded radiograph of dual-color imaging of static target compared to preshot predictions. (NIF-0403-06163pb01)

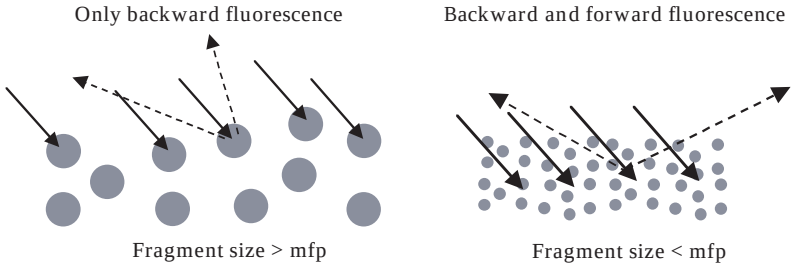

FIGURE 36. Schematic of fluorescence anisotropy technique for inferring feature size. (NIF-0403-06164pb01)

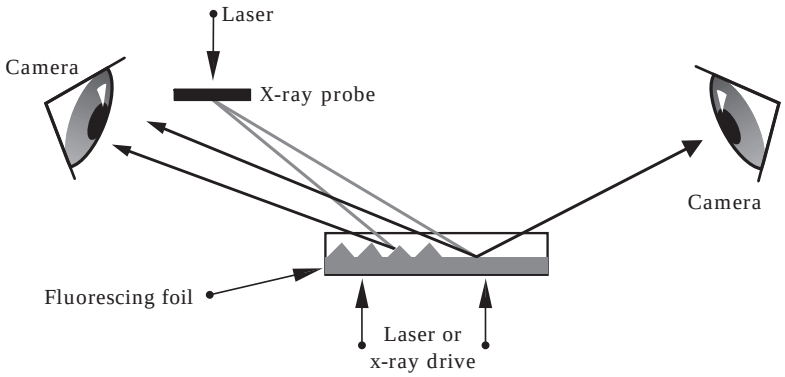

FIGURE 37. Experimental setup for demonstration of fluorescence anisotropy.
(NIF-0403-06165pb01)

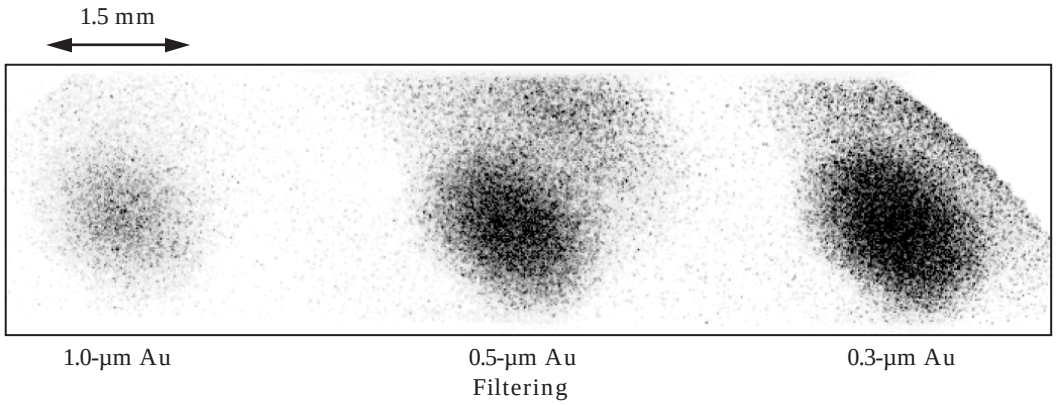

FIGURE 38. Differentially filtered data from forward imaging of fluorescence and scattering from 2-mm-square smooth Au foil.
(NIF-0403-06166pb01)

Diagnostics for EOS Measurements

X-ray Thomson Scattering as a High-Density Temperature and Density Diagnostic

The full range of plasmas, from Fermi degenerate, to strongly coupled, to high-temperature ideal gas plasmas are present at high density in a variety of laboratory and astrophysical environments. Material properties such as electrical, thermal conductivity, opacity, and equation-of-state have been measured in this regime to attempt to resolve theoretical and calculational uncertainties. However, the usefulness of such measurements has been impaired because of the lack of an independent measurement of the key plasma parameters, temperature and density. For example, surface probing of any overdense plasmas is difficult to interpret because tiny density gradient scale lengths dramatically modify observables such as optical reflectivity and phase modulation. Internal x-ray probing for plasmas at densities near solid and above has relied, so far, on continuum edge spectroscopy and extended x-ray absorption fine-structure (EXAFS), line shape spectroscopy, or nonspectrally resolved x-ray scattering. However, the interpretation of results from all such techniques relies on knowledge of the ionization balance, density, and temperature.

Such high-density plasmas are the principal state of matter in inertial confinement fusion (ICF) and high energy density physics (HEDP) research, an important component of LLNL's Stockpile Stewardship Management Program.

Specifically, this milestone developed a novel characterization technique for low-atomic-number plasmas that could be ultimately used to measure the compressed ICF fuel density and temperature and provide a noninvasive internal-temperature measurement in radiatively and shock-heated materials for HEDP. In addition, this project extends the development of transient hot laser plasmas as x-ray probes that have been a key part of the experimental expertise built up over decades at LLNL.

We are extending the plasma characterization technique of spectrally resolved optical photon scattering off free electrons (Thomson scattering) to the x-ray regime to be able to provide dense plasma data unattainable by other means.[1, 2] We used resonance line emission from laser plasmas as a narrow bandwidth transient x-ray probe that scatters from sample solid-density plasmas created by volumetric heating using other laser plasmas. The shape of the collected scattered spectra provides instantaneous information on the free electron density and temperature of the sample plasma. The form of the Thomson-scattered spectrum from individual electrons ($\alpha < 1$ scattering parameter) will in general depend on the Fermi energy T_F, hence free electron density n_e, and temperature T_e. In the limit $T_e/T_F < 1$ and $\alpha << 1$, the incoherent scattered distribution function from electrons will be dependent on T_e and T_F and is given by $f\{(\Delta\nu/\nu)/2(\upsilon_F/c)\sin(\theta/2)\} = f(\upsilon_x/\upsilon_F)$, where $f(\upsilon_x/\upsilon_F)$ is given by:

$$f\left(\frac{\nu_x}{\nu_F}\right)d\left(\frac{\nu_x}{\nu_F}\right) \propto \int_0^{\pi/2} \frac{\left(\frac{\nu_x}{\nu_F\cos\beta}\right)^2 \tan\beta d\beta}{\exp\left[\left(\left(\frac{\nu_x}{\nu_F\cos\beta}\right)^2 - 1 + \left(\frac{\pi^2}{12}\right)\left(\frac{T_e}{T_F}\right)^2\right)\Big/\left(\frac{T_e}{T_F}\right)\right] + 1} d\left(\frac{\nu_x}{\nu_F}\right)$$

and where υ_x is the component of the electron velocity in the $\bar{x} = \bar{k}_s = \bar{k}_{scat} - \bar{k}_{I/P}$ direction, υ_F is the Fermi velocity = $\sqrt{(2kT_F/m_e)}$, β is the angle between the electron velocity direction and the x axis, and $\Delta\nu$ is the frequency shift from the Compton shifted position. The term $(\pi^2/12)(T_e/T_F)^2$ accounts for the fact that the chemical potential μ in the expression for the occupation of states for fermions, $1/\{\exp[(E-\mu)/T_e] + 1\}$, has some temperature dependence at finite temperature.

Examples of calculated velocity distribution function $f(\upsilon_x/\upsilon_F)$ using the above equation are shown on Figure 39 as a function of various values of T_e/T_F (for T_F = 15 eV). In the limit of $T_e = 0$, the form of the scattered distribution function is parabolic, making a transition to the familiar Gaussian distribution in the case of Boltzmann statistics ($T_e >> T_F$). Clearly measurements on the tail of the distribution are most sensitive to the ratio T_e/T_F.

We chose and optimized designs on two proof-of-principle experiments involving volumetrically heated solid Be (see Figure 40) and shocked LiH and plastic. The designs included 2D radiation-hydrodynamic simulations of the expected test plasma conditions, which confirmed earlier analytic calculations of test plasma uniformity. Be experiments were fielded on the OMEGA laser facility (see Figure 40), providing high-quality scattered spectra on several shots. The use of a lower-Z pumps (Pd and Mo) vs CsI for volumetrically heating the Be sample did help to

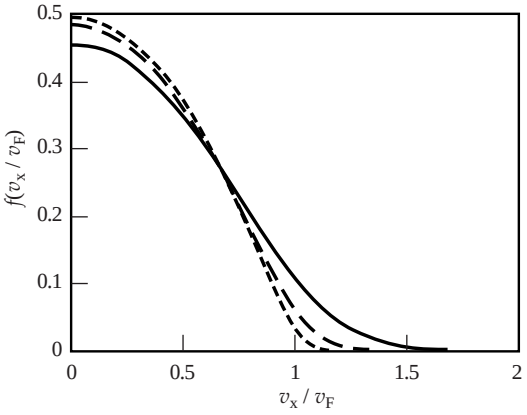

FIGURE 39. Predicted velocity distribution for red wing as a function of T_e/T_F for T_F = 15 eV. Short dashed, long dashed and solid are for T_e/T_F = 0.1, 0.2, and 0.4 respectively. (NIF-0403-06167pb01)

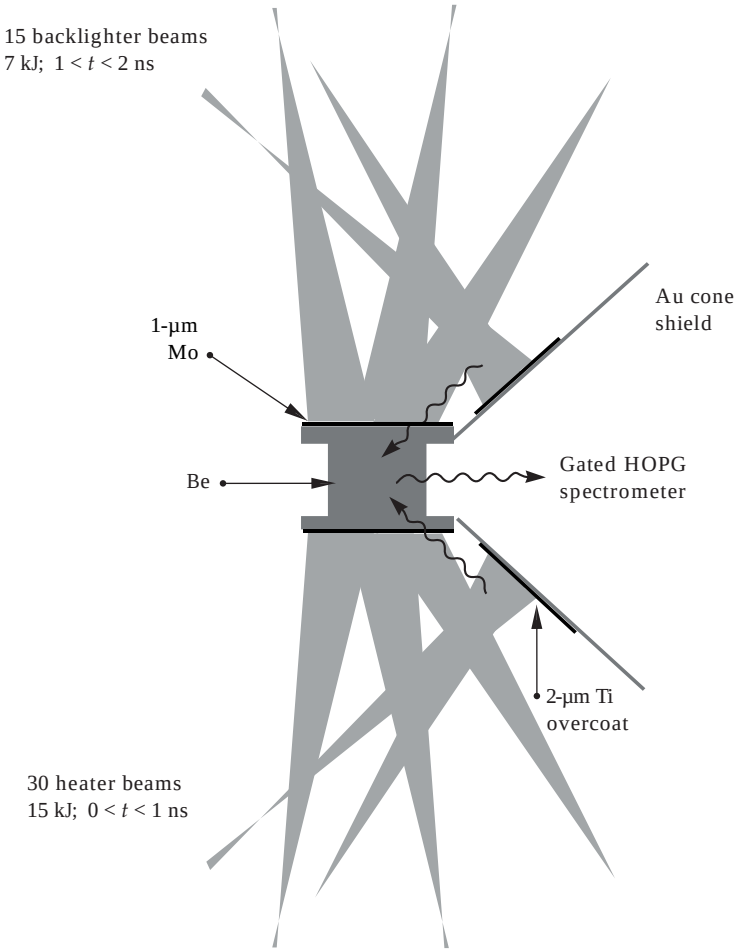

FIGURE 40. Experimental setup for demonstration of x-ray Thomson scattering.
(NIF-0403-06168pb01)

mitigate spectral contamination, as witnessed by the HOPG and Henway spectrometers. The spectra (see Figure 41) and lineouts (see Figure 42) of the scattered spectra display the expected Compton downshifted and Doppler-broadened spectral signatures. In particular, the comparison of the spectra of the heated vs cold Be sample shows increased broadening, representing the first ever demonstration of sensitivity of x-ray Thomson scattering to plasma temperature. The spectra are well fitted by calculated spectra using the expected Fermi energy of 14 eV in both cases, and including an electron temperature of 7 eV in the heated case, within a factor of 2 of simulated.

Notes and References

1. O. L. Landen, S. H. Glenzer, R. C. Cauble, R. W. Lee, M. J. Edwards, and J. S. DeGroot, "Warm Dense Plasma Characterization by X-Ray Thomson Scattering," in *ECLIM 2000 Proc.,* M. Kalal, K. Rohlena and M. Sinor, Eds. (SPIE, Bellingham, 2001) Vol. 4424, p. 112.
2. O. L. Landen, S. H. Glenzer, M. J. Edwards, R. W. Lee, G. W. Collins, R. C. Cauble, W. W. Hsing and B. A. Hammel, "Dense Matter Characterization by X-ray Thomson Scattering," *J. of Quant. Spectrosc. & Radiat. Transfer* 71, 465–478 (2001).

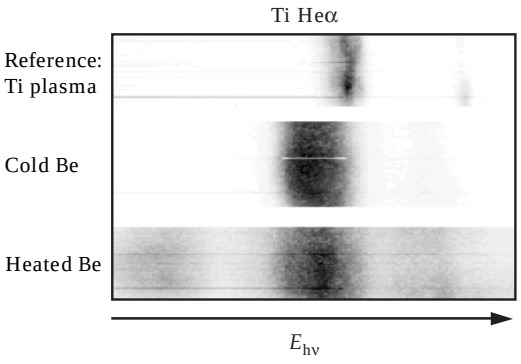

FIGURE 41. Gated spectra from (a) reference Ti disk, (b) cold Be scattering, (c) heated Be scattering. Gain increased by 10,000 for last two spectra.
(NIF-0403-06169pb01)

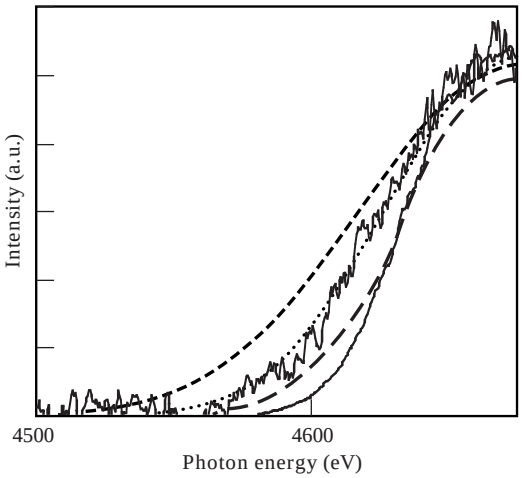

FIGURE 42. Measured (solid lines) and fitted (dashed lines) lineouts for red wing of cold and heated Be scattered spectra. The three dashed lines correspond to T_e = 0, 7 and 14 eV with T_F for solid Be held constant at 14 eV. The cold Be spectra is best fitted by T_e = 0 eV while the hot (pumped) Be spectra is best fitted by T_e = 7 eV.
(NIF-0403-06170pb01)

APPENDIX A
AWARDS, PATENTS, AND REFEREED PUBLICATIONS IN 2000 AND 2001

The *2000–2001 ICF Annual Report* uses this space to report on the Awards received by, Patents issued to, and Publications by LLNL employees in the ICF Program. The goal is to showcase the distinguished scientific and technical achievements of our employees.

This *Annual Report* is based on the Fiscal Years of 2000 and 2001, whereas the achievements listed here are based on the Calendar Years of 2000 and 2001. The reason for this disparity is the fact that a publication or award may not have a precise date other than the particular year it was given.

The awards listed are those granted by recognized organizations outside of LLNL and given to ICF Program employees.

The patents may include work that is afield from ICF but are granted to ICF Program employees. This could include work that is supported from discretionary funds.

The publications listed are those from refereed scientific journals. Therefore, conference proceedings are generally not included unless they are also published in refereed scientific journals. The work in ICF is broad-based at LLNL, and many employees who are not directly in the ICF Program publish ICF-related results; these publications are included. Furthermore, publications are included in which an ICF Program author contributes but is not the lead author.

2000 ICF Program Awards

American Physical Society Fellows
Robert C. Cauble
James H. Hammer
Joseph Nilsen

Optical Society of America Fellows
Stephen Payne
Michael Perry

APS Award for Outstanding Doctoral Dissertation in Plasma Physics
Mark Herrmann

Teller Fellowship
Mordecai Rosen

Fusion Power Associates Leadership Award
John Lindl

Fusion Power Associates Award for Education
Don Correll

Division of Plasma Physics Distinguished Lecturer
Bruce Remington
Mordecai Rosen

Federal Laboratory Consortium Award for "Excellence in Technology Transfer"
LaserShot Peening System for Treating Metal on Airplane—Lloyd Hackel, Ralph Jacobs, John Wooldridge, Curt Theisen, Daryl Gzybicki

Society for Technical Communication Awards
The Society for Technical Communication (STC), the largest organization of its type, is dedicated to advancing the arts and sciences of technical communication. Its 20,000 members include technical writers, editors, graphic designers, videographers, multimedia artists, and others whose work involves making technical information available to those who need it. The mission of the society is to improve the quality and effectiveness of technical communication for audiences worldwide.

There are four levels of awards: distinguished, excellence, merit, and achievement.

Northern California (Touchstone) Awards, 2000
Excellence Award (Technical Reports)
Inertial Confinement Fusion Quarterly Report, Vol. 9, No. 2
Jason Carpenter
Pamela Davis
Al Miguel

UCRL-LR-105820-00/01

Merit Award (Technical Reports)
Inertial Confinement Fusion Quarterly Report, Vol. 9, No. 3
Jason Carpenter
Pamela Davis
Al Miguel

Phoenix Chapter Competition Awards, 2000

Distinguished Award (Technical Communication – Art)
December 1999 NIF Status Poster
Thomas Reason

Excellence Award (Technical Communication – Art)
Rendezvous with Science
Kathy McCullough
Karen Kiernan
Bryan Quintard

Merit Award (Technical Communication – Art)
NIF Hohlraum Target
Jackie McBride
Bryan Quintard

Merit Award (Technical Communication – Art)
Inside the NIF Target Chamber
Jackie McBride
Bryan Quintard

Merit Award (Technical Communication – Art)
The National Ignition Facility, Its Mission & How It Works
Clayton Dahlen
Jason Carpenter

Kachina, N.M., Chapter Awards, 2000
Merit Award (Photograph)
Star Chamber Welding
Jacqueline McBride
Bryan Quintard

2001 ICF Program Awards

American Association for the Advancement of Science Fellows
John Lindl

American Physical Society Fellows
Siegfried Glenzer
David Munro

Optical Society of America Fellows
Howard Powell

DOE Bright Light Award
Implantable Device to Monitor Glucose Levels—Stephen Lane, Tom Peyser, Chris Darrow, Natalia Zaitseva, Joe Satcher

APS Division of Plasma Physics Distinguished Lecturer
Mordecai Rosen
Bruce Remington

Edward Teller Medal
Mordecai Rosen

Edward Teller Fellowship
Claire Max

Federal Laboratory Consortium Award for "Excellence in Technology Transfer" (2001)
Implantable Device to Monitor Glucose Levels—Stephen Lane, Tom Peyser, Chris Darrow, Natalia Zaitseva, Joe Satcher

2001 R&D 100 Awards
Lasershot Marking System—Brent Dane, Lloyd Hackel, Hao-Lin Chen, John Halpin, and John Honig

Continuous Laser Glass Melting Process—Jack Campbell, Paul Ehrmann, Michael Riley, William Steele, Tayyab Suratwala, and Charles Thorsness

Society for Technical Communication Awards

Kachina, N.M., Chapter Awards, 2001/2002

Distinguished Award (Technical Publications - Newsletters)
Laser Science & Technology Program Update
Al Miguel
Hao-Lin Chen
Cyndi Brandt

Excellence Award (Technical Publications – Newsletters)
NIF Programs Focus Newsletter
Cindy Cassady
Jason Carpenter
Sue Stephenson

Merit Award (Technical Publications – Brochures)
Fusion Energy Science: Clean, Safe, and Abundant Energy
Karen Kline
Daniel Moore
Charles Baker
Tom Reason

Merit Award (Technical Art)
Discover science in the most unusual places
Kathy McCullough
Karen Kiernan
Bryan Quintard

STC International Competition Best of Show Awards, 2001/2002

Merit Award (Technical Publications - Newsletters)
Laser Science & Technology Program Update
Al Miguel
Hao-Lin Chen
Cyndi Brandt

2000 ICF PATENTS

Vernon, Ceglio
Maskless Deposition Technique for the Physical Vapor Deposition of Thin Film and Multilayer Coatings with Subnanometer Precision and Accuracy
U.S. Patent 6,010,600
January 4, 2000

Spiller, Mirkarimi, Montcalm, Bajt, Folta
Method to Adjust Multilayer Film Stress-Induced Deformation of Optics
U.S. Patent 6,011,646
January 4, 2000

Small, Celliers
Single-Fiber Multi-Color Pyrometry
U.S. Patent 6,012,840
January 11, 2000

Shafer
Reflective Optical Imaging System
U.S. Patent 6,014,252
January 11, 2000

Sommargren
Embedded Fiducials in Optical Surfaces
U.S. Patent 6,014,264
January 11, 2000

Nathel, Cartland, Colston, Everett, Roe
Multiple-Wavelength Spectroscopic Quantitation of Light-Absorbing Species in Scattering Media
U.S. Patent 6,015,969
January 18, 2000

Vann
Bar Coded Retroreflective Target
U.S. Patent 6,017,125
January 25, 2000

Dinh, Balooch, Schildbach, Hamza, McLean
Low Work Function, Stable Compound Clusters and Generation Process
U.S. Patent 6,019,913
February 1, 2000

Celliers, Da Silva, Glinsky, London, Maitland, Matthews, Fitch
Opto-Acoustic Thrombolysis
U.S. Patent 6,022,309
February 8, 2000

Hudyma
High Numerical Aperture Ring Field Projection System for Extreme Ultraviolet Lithography
U.S. Patent 6,033,079
March 7, 2000

Hackel, Dane, Dixit, Everett, Honig
Laser Illuminator and Optical System for Disk Patterning
U.S. Patent 6,037,565
March 14, 2000

Hale
Three-Tooth Kinetic Coupling
U.S. Patent 6,065,898
March 23, 2000

Payne, Page, Schaffers, Nostrand, Krupke, Schunemann
Low-Phonon-Frequency Chalcogenide Crystalline Hosts for Rare Earth Lasers Operating beyond Three Microns
U.S. Patent 6,047,013
April 4, 2000

Hagans, Clough
Optical Key System
U.S. Patent 6,055,079
April 25, 2000

Lee, Fitch, Schumann, Da Silva, Benett, Krulevitch
Microfabricated Therapeutic Actuators and Release Mechanisms Therefor
U.S. Patent 6,059,815
May 9, 2000

Hudyma
High Numerical Aperture Projection System for Extreme Ultraviolet Projection Lithography
U.S. Patent 6,072,852
June 6, 2000

Lee, Fitch
Micro Devices Using Shape Memory Polymer Patches for Mated Connections
U.S. Patent 6,086,599
July 11, 2000

Maitland
Shape-Memory-Polymer (SMP) Gripper with a Release Sensing System
U.S. Patent 6,102,917
August 15, 2000

Lee, Northrup, Ciarlo, Krulevitch, Benett
Release Mechanism Utilizing Shape Memory Polymer Material
U.S. Patent 6,102,933
August 15, 2000

Montcalm
High-Reflectance, Low-Stress, Mo-Si Multilayer Reflective Coatings
U.S. Patent 6,110,607
August 29, 2000

Vann
Multi-Dimensional Position Sensor Using Range Detectors
U.S. Patent 6,115,128
September 5, 2000

Spiller, Mirkarimi, Montcalm, Bajt, Folta
Method to Adjust Multilayer Film Stress-Induced Deformation of Optics
U.S. Patent 6,134,049
October 17, 2000

Trebes, Bell, Robinson
Miniature X-Ray Source
U.S. Patent 6,134,300
October 17, 2000

Cohen, Jeong, Shafer
Four-Mirror Extreme Ultraviolet (EUV) Lithography Projection System
U.S. Patent 6,142,641
November 7, 2000

Lee, Lemoff
Micromachined Magnetohydrodynamic Actuators and Sensors
U.S. Patent 6,146,103
November 14, 2000

Hale, Malsbury, Hudyma, Parker
Projection Optics Box
U.S. Patent 6,147,818
November 14, 2000

Vernon
Defect Tolerant Transmission Lithography Mask
U.S. Patent 6,150,060
November 21, 2000

Perry, Stuart, Banks, Myers, Sefcik
Laser Machining of Explosives
U.S. Patent 6,150,630
November 21, 2000

Beach, Honea, Bibeau, Mitchell, Lang, Maderas, Speth, Payne
Hollow Lensing Duct
U.S. Patent 6,160,934
December 12, 2000

Dinh, McLean, Balooch, Fehring, Schildbach
Low Work Function, Stable Thin Films
U.S. Patent 6,162,707
December 19, 2000

Page, Beach
Thermal Lens Elimination by Gradient-Free Zone Coupling of Optical Beams
U.S. Patent 6,167,069
December 26, 2000

2001 ICF Patents

Colston, Everett, Da Silva, Matthews
Optical Coherence Domain Reflectometry Guidewire
U.S. Patent 6,175,669 B1
January 16, 2001

Sommargren
Inspection of Lithographic Mask Blanks for Defects
U.S. Patent 6,177,993 B1
January 23, 2001

Everett, Colston, Sathyam, Da Silva
Dental Optical Coherence Domain Reflectometry Explorer
U.S. Patent 6,179,611 B1
January 30, 2001

Hudyma
High Numerical Aperture Ring Field Projection System for Extreme Ultraviolet Lithography
U.S. Patent 6,183,095 B1
February 6, 2001

Chapman, Nugent
Condenser for Ring-Field Deep-Ultraviolet and Extreme-Ultraviolet Lithography
U.S. Patent 6,186,632 B1
February 13, 2001

Hudyma, Shafer
High Numerical Aperture Ring Field Projection System for Extreme Ultraviolet Lithography
U.S. Patent 6,188,513 B1
February 13, 2001

Hackel, Dane
Laser Beam Temporal and Spatial Tailoring for Laser Shock Processing
U.S. Patent 6,198,069
March 6, 2001

Darrow, Satcher, Lane, Lee, Wang
Implantable Medical Sensor System
U.S. Patent 6,201,980 B1
March 13, 2001

Ackler, Swierkowski, Tarte, Hicks
Method for Vacuum Fusion Bonding
U.S. Patent 6,205,819 B1
March 27, 2001

Hale, Malsbury, Patterson
Pedestal Substrate for Coated Optics
U.S. Patent 6,206,966 B1
March 27, 2001

Benett, Krulevitch
Microfluidic Interconnects
U.S. Patent 6,209,928 B1
April 3, 2001

Payne, Marshall, Powell, Krupke
Hybrid Solid State Laser System Using a Neodymium-Based Oscillator and Ytterbium-Based Amplifier
U.S. Patent 6,212,215 B1
April 3, 2001

Beach, Honea, Payne
Delivering Pump Light to a Laser Gain Element While Maintaining Access to the Laser Beam
U.S. Patent 6,222,872 B1
April 24, 2001

Hudyma
Reflective Optical Imaging Systems with Balanced Distortion
U.S. Patent 6,226,346 B1
May 1, 2001

Bajt, Wall
MoRu/Be Multilayers for Extreme Ultraviolet Applications
U.S. Patent 6,228,512 B1
May 8, 2001

Koo
Paper Area Density Measurement from Forward Transmitted Scattered Light
U.S. Patent 6,229,612 B1
May 8, 2001

Bajt, Barbee
High Reflectance and Low Stress Mo2C/Be Multilayers
U.S. Patent 6,229,652
May 8, 2001

Lee, Simon, McConaghy
Micromachined Low Frequency Rocking Accelerometer with Capacitive Pickoff
U.S. Patent 6,230,566 B1
May 15, 2001

Haddad, Trebes, Mathews
Microwave Hematoma Detector
U.S. Patent 6,233,479 B1
May 15, 2001

Dinh, McLean, Balooch, Fehring, Schildbach
Generation of Low Work Function, Stable Compound Thin Films by Laser Ablation
U.S. Patent 6,235,615 B1
May 22, 2001

Lee, Benett, Schumann, Krulevitch, Fitch
Apparatus for Loading Shape Memory Gripper Mechanisms
U.S. Patent 6,240,631 B1
June 5, 2001

Zapata, Hackel
Lamp System for Uniform Semiconductor Wafer Heating
U.S. Patent 6,252,203 B1
June 26, 2001

Yang, Moses, Hartmann-Siantar
FALCON: Automated Optimization Method for Arbitrary Assessment Criteria
U.S. Patent 6,260,005 B1
July 10, 2001

Freitas, Skidmore, Wooldridge, Emanuel, Payne
Monolithic Laser Diode Array with One Metallized Sidewall
U.S. Patent 6,266,353 B1
July 24, 2001

Benett, Krulevitch
Microfluidic Interconnects
U.S. Patent 6,273,478 B1
August 14, 2001

Barbee, Lane, Hoffman
High Efficiency Replicated X-Ray Optics and Fabrication Method
U.S. Patent 6,278,764 B1
August 21, 2001

Perry, Banks, Stuart
Method to Reduce Damage to Backing Plate
U.S. Patent 6,303,901 B1
October 16, 2001

Krupke, Payne, Marshall
Blue Diode-Pumped Solid-State Laser Based on Ytterbium-Doped Laser Crystals Operating on the Resonance Zero-Phonon Transition
U.S. Patent 6,304,584 B1
October 16, 2001

Montcalm, Mirkarimi
Process for Fabricating High Reflectance-Low Stress Mo-Si Multilayer Reflective Coatings
U.S. Patent 6,309,705 B1
October 30, 2001

Hudyma
High Numerical Aperture Ring Field Projection System for Extreme Ultraviolet Lithography
U.S. Patent 6,318,869 B1
November 20, 2001

Krulevitch, Lee, Northrup, Benett
Microfabricated Instrument for Tissue Biopsy and Analysis
U.S. Patent 6,319,474 B1
November 20, 2001

Mirkarimi, Bajt, Stearns
The Mitigation of Substrate Defects in Reticles Using Multilayer Buffer Layers
U.S. Patent 6,319,635 B1
November 20, 2001

Hale, Jensen
Highly Damped Kinematic Coupling for Precision Instruments
U.S. Patent 6,325,351 B1
December 4, 2001

2000 Refereed Publications

S. Alexiou, R. W. Lee, S. H. Glenzer, and J. I. Castor
"Analysis of Discrepancies Between Quantal and Semiclassical Calculations of Electron Impact Broadening in Plasmas"
J. Q. S. R. T. 65(1–3), 15–22 (2000)

L. Aschke, S. Depierreux, K. G. Estabrook, K. B. Fournier, J. Fuchs, S. Glenzer, R. W. Lee, W. Rozmus, R. S. Thoe, and P. E. Young
"Towards an Experimental Benchmark for Aluminum X-Ray Spectra"
J. Q. S. R. T. 65(1–3), 23–30 (2000)

C. A. Back, J. D. Bauer, J. H. Hammer, B. F. Lasinski, R. E. Turner, P. W. Rambo, O. L. Landen, L. J. Suter, M. D. Rosen, and W. W. Hsing
"Diffusive, Supersonic X-Ray Transport in Radiatively Heated Foam Cylinders"
Phys. Plasmas 7(5), 2126–2134 (2000)

C. A. Back, N. C. Woolsey, T. Missalla, O. L. Landen, S. B. Libby, L. S. Klein, and R. W. Lee
"Implosions: An Experimental Testbed for High Energy Density Physics"
Astrophys. J. 127, 227–232 (2000)

C. A. Back, J. D. Bauer, O. L. Landen, R. E. Turner, B. F. Lasinski, J. H. Hammer, M. D. Rosen, L. J. Suter, and W. H. Hsing
"Detailed Measurements of a Diffusive Supersonic Wave in a Radiatively Heated Foam"
Phys. Rev. Lett. 84(2), 274–277 (2000)

S. Bajt, A. Barty, K. A. Nugent, M. McCartney, M. Walll, and D. Paganin
"Quantitative Phase-Sensitive Imaging in a Transmission Electron Microscope"
Ultramicroscopy 83(1–2), 67–73 (2000)

S. Bajt
"Molybdenum-Ruthenium/Beryllium Multilayer Coatings"
J. Vac. Sci. Tech. A18(2), 557–559 (2000)

I. M. Barton, S. N. Dixit, L. J. Summers, C. A. Thompson, K. Avicola, and J. Wilhelmsen
"A Diffractive Alvarez Lens"
Opt. Lett. 25(1), 1–3 (2000)

A. J. Bayramian, C. Bibeau, R. J. Beach, C. D. Marshall, and S. A. Payne
"Consideration of Stimulated Raman Scattering in Yb:$Sr_5(PO_4)_3F$ Laser Amplifiers"
Appl. Optics 39(21), 3746–3753 (2000)

A. J. Bayramian, C. Bibeau, R. J. Beach, C. D. Marshall, S. A. Payne, and W. F. Krupke
"Three-Level Q-Switched Laser Operation of Ytterbium-Doped $Sr_5(PO_4)_3F$ at 985 nm"
Opt. Lett. 25(9), 622–624 (2000)

A. J. Bayramian, C. Bibeau, K. I. Schaffers, C. D. Marshall, and S. A. Payne
"Gain Saturation Measurements of Ytterbium-Doped $Sr_5(PO_4)_3F$"
Appl. Opt. 39(6), 982–985 (2000)

G. R. Bennett, J. M. Wallace, T. J. Murphy, R. E. Chrien, N. D. Delamater, P. L. Gobby, A. A. Hauer, K. A. Klare, J. A. Oertel, R. G. Watt, D. C. Wilson, W. S. Varnum, R. S. Craxton, V. Yu. Glebov, J. D. Schnittman, C. Stoeckl, S. M. Pollaine, and R. E. Turner
"Moderate-Convergence Inertial Fusion Implosions in Tetrahedral Hohlraums at Omega"
Phys. Plasmas 7(6), 2594–2603 (2000)

C. Bibeau, A. Bayramian, R. J. Beach, J. C. Chanteloup, C. A. Ebbers, M. A. Emanuel, C. D. Orth, S. A. Payne, J. E. Rothenberg, H. T. Powell, K. I. Shaffers, J. A. Skidmore, S. B. Sutton, and L. E. Zapata
"Mercury and Beyond: Diode-Puimped Solid-State Lasers for Inertial Fusion Energy"
Comptes Rendus 1(6), 745–749 (2000)

M. Borghesi, A. J. MacKinnon, R. Gaillard, G. Malka, C. Vickers, O. Willi, A. A. Offenberger, B. Canaud, J. L. Miguel, N. Blanchot, J. R. Davies, A. Pukhov, and J. Meyer-Ter-Vehn
"Short Pulse Interaction Experiments for Fast Ignitor Applications"
Laser and Part. Beams 18(3), 389–397 (2000)

K. E. Branham, H. Byrd, R. Cook, J. W. Mays, and G. M. Gary
"Preparation of Soluble, Linear Titanium-Containing Copolymers by the Free Radical Copolymerization of Vinyl Titanate Monomers with Styrene"
J. Appl. Polymer Sci. 78(1), 190–199 (2000)

K. S. Budil, D. M. Gold, K. G. Estabrook, B. A. Remington, J. Kane, P. M. Bell, D. M. Pennington, C. Brown, S. P. Hatchett, J. A. Koch, M. H. Key, and M. D. Perry
"Development of a Radiative-Hydrodynamics Testbed Using the Petawatt Laser Facility"
Astrophys. J. 127, 261–265 (2000)

D. A. Callahan-Miller and M. Tabak
"Progress in Target Physics and Design for Heavy Ion Fusion"
Phys. Plasmas 7(5), 2083–2091 (2000)

R. Cauble, P. M. Celliers, G. W. Collins, L. B. Da Silva, D. M. Gold, M. E. Foord, K. S. Budil, and R. J. Wallace
"Equation of State and Material Property Measurements of Hydrogen Isotopes at the High-Pressure, High-Temperature, Insulator-Metal Transition"
Astrophys.. J. 127, 267–273 (2000)

J. H. Campbell and T. I. Suratwala
"Nd-Doped Phosphate Glasses for High-Energy / High-Peak-Power Lasers"
J. Non-Cryst. Solids 263(1–4), 318–341 (2000)

J. H. Campbell, T. I. Suratwala, C. B. Thorsness, J. S. Hayden, A. J. Thorne, J. M. Cimino, A. J. Marker, K. Takeuchi, M. Smolley, and G. F. Ficini-Dorn
"Continuous Melting of Phosphate Laser Glass"
J. Non-Cryst. Solids 263(1–4), 342–357 (2000)

P. M. Celliers and J. Conia
"Measurement of Localized Heating in the Focus of an Optical Trap"
Appl. Opt. 39(19), 3396–3407 (2000)

P. M. Celliers, G. W. Collins, L. B. Da Silva, D. M. Gold, R. Cauble, R. J. Wallace, M. E. Foord, and B. A. Hammel
"Shock-Induced Transformation of Liquid Deuterium into a Metallic Fluid"
Phys. Rev. Lett. 84(24), 5564–5567 (2000)

C. Cherfils and O. Lafitte
"Analytic Solutions of the Rayleigh Equation for Linear Density Profiles"
Phys. Rev. E62(2PtB), 2967–2970 (2000)

G. W. Collins, P. M. Celliers, L. B. Da Silva, D. M. Gold, and R. Cauble
"Laser-Shock-Driven Laboratory Measurements of the Equation of State of Hydrogen Isotopes in the Megabar Regime"
High Press. Res. 16(5–6), 281–290 (2000)

R. Cook
"Models of Polyimide Spray Coating"
Fusion Tech. 38, 74–82 (2000)

T. E. Cowan, A. W. Hunt, T. W. Phillips, S. C. Wilks, M. D. Perry, C. Brown, W. Fountain, S. Hatchett, J. Johnson, M. H. Key, T. Parnell, D. M. Pennington, R. A. Snavely, and Y. Takahashi
"Photonuclear Fission from High Energy Electrons from Ultraintense Laser-Solid Interactions"
Phys. Rev. Lett. 84(5), 903–906 (2000)

T. E. Cowan, M. Roth, J. Johnson, C. Brown, M. Christl, W. Fountain, S. Hatchett, E. A. Henry, A. W. Hunt, M. H. Key, A. MacKinnon, T. Parnell, D. M. Pennington, M. D. Perry, T. W. Phillips, T. C. Sangster, M. Singh, R. Snavely, M. Stoyer, Y. Takahashi, S. C. Wilks, and K. Yasuike
"Intense Electron and Proton Beams from Petawatt Laser-Matter Interactions"
Nucl. Inst. Meth. 455A(1), 130–139 (2000)

N. D. Delamater, E. L. Lindman, G. R. Magelssen, B. H. Failor, T. J. Murphy, A. A. Hauer, P. Gobby, J. B. Moore, V. Gomez, K. Gifford, R. L. Kauffman, O. L. Landen, B. A. Hammel, G. Glendinning, L. V. Powers, L. J. Suter, S. Dixit, R. R. Peterson, and A. L. Richard
"Observation of Reduced Beam Deflection Using Smoothed Beams in Gas-Filled Hohlraum Symmetry Experiments on Nova"
Phys. Plasmas 5(5Pt1), 1609–1613 (2000)

S. Depierreux, J. Fuchsa, C. Labaune, A. Michard, H. A. Baldis, D. Pesme, S. Huller, and G. Laval
"First Observation of Ion Acoustic Waves Produced by the Langmuir Decay Instability"
Phys. Rev. Lett. 84(13), 2869–2872 (2000)

S. Depierreux, C. Labaune, J. Fuchs, and H. A. Baldis
"Application of Thomson Scattering to Identify Ion Acoustic Waves Stimulated by the Langmuir Decay Instability"
Rev. Sci. Inst. 71(9), 3391–3401 (2000)

G. Dimonte
"Spanwise Homogeneous Buoyancy-Drag Model for Rayleigh-Taylor Mixing and Experimental Evaluation"
Phys. Plasmas 7(6) 2255–2269 (2000)

G. Dimonte and M. Schneider
"Density Ratio Dependence of Rayleigh-Taylor Mixing for Sustained and Impulsive Acceleration Histories"
Phys. Fluids 12(2), 304–321 (2000)

T. Ditmire, J. Zweiback, V. P. Yanovsky, T. E. Cowan, G. Hays, and K.B. Wharton
"Nuclear Fusion in Gases of Deuterium Clusters Heated by Femtosecond Laser"
Phys. Plasmas 7(5), 1993–1998 (2000)

T. Ditmire, A. Rubenchik, V. V. Mirnov, and D. Ucer
"Modeling of the Expansion of Ultra-Short-Pulse Laser-Produced Plasmas in Magnetic Fields"
Astrophys. J. 127, 293–297 (2000)

T. Ditmire, K. Shigemori, B. A. Remington, K. Estabrook, and R. A. Smith
"The Production of Strong Blast Waves Through Intense Laser Irradiation of Atomic Clusters"
Astrophys. J. 127, 299–304 (2000)

R. P. Drake, J. J. Carroll III, T. B. Smith, P. Keiter, S. Gail Glendinning, O. Hurricane, K. Estabrook, D. D. Ryutov, B. A. Remington, R. J. Wallace, E. Michael, and R. McCray
"Laser Experiments to Simulate Supernova Remnants"
Phys. Plasmas 7(5), 2142–2148 (2000)

R. P. Drake, T. B. Smith, J. J. Carroll III, Y. Yan, S. G. Glendinning, K. Estabrook, D. D. Ryutov, B. A. Remington, R. J. Wallace, and R. McCray
"Progress Toward the Laboratory Simulation of Young Supernova Remnants"
Astrophys. J. 127, 305–310 (2000)

J. Dunn, Y. Li, A. L. Osterheld, J. Nilsen, J. R. Hunter, and V. N. Shlyaptsev
"Gain Saturation Regime for Laser-Driven Tabletrop, Transient Ni-Like Ion X-Ray Lasers"
Phys. Rev. Lett. 84(21), 4834–4837 (2000)

D. C. Eder, G. Pretzler, E. Fill, K. Eidmann, and A. Saemann
"Spatial Characteristics of K_α Radiation from Weakly Relativistic Laser Plasmas"
Appl. Phys. B70(2), 211–217 (2000)

J. Edwards, S. G. Glendinning, L. J. Suter, B. A. Remington, O. Landen, R. E. Turner, T. J. Shepard, B. Lasinski, K. Budil, H. Robey, J. Kane, H. Louis, R. Wallace, P. Graham, M. Dunne, and B. R. Thomas
"Turbulent Hydrodynamics Experiments Using a Plasma Piston"
Phys. Plasmas 7(5), 2099–2107 (2000)

P. R. Ehrmann, J. H. Campbell, T. I. Suratwala, J. S. Hayden, D. Krashkevich, and K. Takeuchi
"Optical Loss and Nd^{3+} Non-Radiative Relaxation by Cu, Fe and Several Rare Earth Impurities in Phosphate Laser Glasses"
J. Non-Cryst. Solids 263(1–4), 251–262 (2000)

D. R. Farley and L. M. Logory
"Single-Mode, Nonlinear Mix Experiments at High Mach Number Using Nova"
Astrophys. J. Supplement Series 127(2), 311–316 (2000)

M. E. Foord, S. H. Glenzer, R. S. Thoe, K. L. Wong, K. B. Fournier, J. R. Albritton, B. G. Wilson, and P. T. Springer
"Accurate Determination of the Charge State Distribution in a Well Characterized Highly Ionized Au Plasma"
J. Q. S. R. T. 65 (1–3), 231–241 (2000)

M. E. Foord, S. H. Glenzer, R. S. Thoe, K. L. Wong, K. B. Fournier, B. G. Wilson, and P. T. Springer
"Ionization Processes and Charge-State Distribution in a Highly Ionized High-Z Laser-Produced Plasma"
Phys. Rev. Lett. 85(5), 992–995 (2000)

J. Fuchs, C. Labaune, S. Depierreux, V. T. Tikhonchuk, and H. A. Baldis
"Stimulated Brillouin and Raman Scattering from a Randomized Laser Beam in Large Inhomogeneous Plasmas. I. Experiment"
Phys. Plasmas 7(11), 4659–4668 (2000)

J. Fuchs, C. Labaune, S. Depierreux, A. Michard, H. Baldis
"Modification of Spatial and Temporal Gains of Stimulated Brillouin and Raman by Polarization Smoothing"
Phys. Rev. Lett. 84(14), 3089–3092 (2000)

F. Y. Genin, M. D. Feit, M. R. Kowzlowski, A. M. Rubenchik, A. Salleo, and J. Yoshiyama
"Rear-Surface Laser Damage on 355-nm Silica Optics Owing to Fresnel Diffraction on Front-Surface Contamination Particles"
Appl. Opt. 39(21), 3654–3663 (2000)

S. G. Glendinning, J. Colvin, S. Haan, D. H. Kalantar, O. L. Landen, M. M. Marinak, B. A. Remington, R. Wallace, C. Cherfils, N. Dague, L. Divol, D. Galmiche, and A. L. Richard
"Ablation Front Rayleigh-Taylor Growth Experiments in Spherically Convergent Geometry"
Phys. Plasmas 7(5), 2033–2039 (2000)

S. G. Glendinning, K. S. Budil, C. Cherfils, R. P. Drake, D. Farley, D. H. Kalantar, J. Kane, M. M. Marinak, B. A. Remington, A. Richard, D. Ryutov, J. Stone, R. J. Wallace, and S. V. Weber
"Experimental Measurements of Hydrodynamic Instabilities on Nova of Relevance to Astrophysics"
Astrophys. J. 127, 325–331 (2000)

S. H. Glenzer
"Thomson Scattering in Inertial Confinement Fusion Research"
Contrib. Plasma Phys. 40(1–2), 36–45 (2000)

S. H. Glenzer, K. B. Fournier, C. Decker, B. A. Hammel, R. W. Lee, L. Lours, B. J. MacGowan, and A. L. Osterheld
"Accuracy of K-Shell Spectra Modeling in High-Density Plasmas"
Phys. Rev. E62 (2PT B), 2728–2738 (2000)

S. H. Glenzer, K. G. Estabrook, R. W. Lee, B. J. MacGowan, and W. Rozmus
"Detailed Characterization of Laser Plasmas for Benchmarking of Radiation-Hydrodynamic Modeling"
J. Q. S. R. T. 65(1–3), 253–271 (2000)

S. H. Glenzer, L. J. Suter, R. L. Berger, K. G. Estabrook, B. A. Hammel, R. L. Kauffman, R. K. Kirkwood, B. J. MacGowan, J. D. Moody, J. E. Rothenberg, and R. E. Turner
"Hohlraum Energetics with Smoothed Laser Beams"
Phys. Plasmas 7(6), 2585-2593 (2000).

D. M. Gold, P. M. Celliers, G. W. Collins, K. S. Budil, R. Cauble, L. B. Da Silva, M. E. Foord, R. E. Stewart, R. J. Wallace, and D. Young
"Interferometric and Chirped Optical Probe Techniques for High-Pressure Equation-Of-State Measurements"
Astrophys. J. 127, 333–357 (2000)

S. R. Goldman, C. W. Barnes, S. E. Caldwell, D. C. Wilson, S. H. Batha, J. W. Grove, M. L. Gittings, W. W. Hsing, R. J. Kares, K. A. Klare, G. A. Kyrala, R. W. Margevicius, R. P. Weaver, M. D. Wilke, A. M. Dunne, M. J. Edwards, P. Graham, and B. R. Thomas
"Production of Enhanced Pressure Regions Due to Inhomogeneities in Inertial Fusion Targets"
Phys. Plasmas 7(5), 2007–2013 (2000)

K. Gulec, M. Abdou, R. W. Moir, N. B. Morley, and A. Ying
"Novel Liquid Blanket Configurations and Their Hydrodynamic Analyses for Innovative Confinement Concepts"
Fus. Engr. Design 49, 567–576 (2000)

F. V. Hartemann, A. L. Troha, H. A. Baldis, A. Gupta, A. K. Kerman, E. C. Lindahl, N. C. Luhman, Jr., and J. R. Van Meter
"High-Intensity Scattering Processes of Relativistic Electrons in Vacuum and Their Relevance to High-Energy Astrophysics"
Astrophys. J. 127, 347–356 (2000)

F. V. Hartemann, E. C. Landahl, D. J. Gibson, A. L. Troha, J. R. Van Meter, J. P Heritage, H. A. Baldis, N. C. Luhman, C. H. Ho, T. T. Yang, M. J. Horny, J. Y. Hwang, W. K. Lau, and M. S. Yeh
"RF Characterization of a Tunable, High-Gradient, X-Band Photoinjector"
IEEE Trans. Plasma Sci. 28(3), 898–904 (2000)

S. P. Hatchett, C. G. Brown, T. E. Cowan, E. A. Henry, J. S. Johnson, M. H. Key, J. A. Koch, A. B. Langdon, B. F. Lasinski, R. W. Lee, A. J. MacKinnon, D. M. Pennington, M. D. Perry, T. W. Phillips, M. Roth, T. C. Sangster, M. S. Singh, R. A. Snavely, M. A. Stoyer, S. C. Wilks, and Yasuike
"Electron, Photon, and Ion Beams from the Relativistic Interaction of Petawatt Laser Pulses with Solid Targets"
Phys. Plasmas 7(5), 2076–2082 (2000)

J. S. Hayden, A. J. Marker, T. I. Suratwala, and J. H. Campbell
"Surface Tensile Layer Generation during Thermal Annealing of Phosphate Glass"
J. Non-Cryst. Solids 263(1–4), 228–239 (2000)

D. G. Hicks, C. K. Li, F. H. Seguin, A. K. Ram, J. A. Frenje, R. D. Petrasso, J. M. Soures, V. Y. Glebov, D. D. Meyerhofer, S. Roberts, C. Sorce, C. Stockl. T. C. Sangster, and T. W. Phillips
"Charged-Particle Acceleration and Energy Loss in Laser-Produced Plasmas"
Phys. Plasmas 7(12), 5106–5117 (2000)

E. C. Honea, R. J. Beach, S. C. Mitchell, J. A. Skidmore, M. A. Emanuel, S. B. Sutton, S. A. Payne, P. V. Avizonis, R. S. Monroe, and D. G. Harris
"High-Power Dual-Rod Yb:YAG Laser"
Opt. Lett. 25(11), 805–807 (2000)

T. B. Kaiser
"Laser Ray Tracing and Power Deposition on an Unstructured Three-Dimensional Grid"
Phys. Rev. E61(1), 895–905 (2000)

D. H. Kalantar, B. A. Remington, J. D. Colvin, K. O. Mikaelian, S. V. Weber, L. G. Wiley, J. S. Wark, A. Loveridge, A. M. Allen, A. A. Hauer, and M. A. Meyers
"Solid-State Experiments at High Pressure and Strain Rate"
Phys. Plasmas 7(5), 1999–2006 (2000)

D. H. Kalantar, B. A. Remington, E. A. Chandler, J. D. Colvin, D. M. Gold, K. O. Mikaelian, S. V. Weber, L. G. Wiley, J. S. Wark, A. Loveridge, A. Hauer, B. H. Failor, M. A. Meyers, and G. Ravichandran
"Developing Solid-State Experiments on the Nova Laser"
Astrophys. J. 127, 357–363 (2000)

J. Kane, D. Arnett, B. A. Remington, S. G. Glendinning, G. Bazan, E. Muller, B. A. Fryxell, and R. Teyssier
"Two-Dimensional versus Three-Dimensional Supernova Hydrodynamic Instability Growth"
Astrophys. J. 528(2Pt1), 989–994 (2000)

J. Kane, D. Arnett, B. A. Remington, S. G. Glendinning, G. Bazan, R. P. Drake, and B. A. Fryxell
"Supernova Experiments on the Nova Laser"
Astrophys. J. 127, 365–369 (2000)

K. A. Keilty, E. P. Liang, T. Ditmire, B. A. Remington, K. Shigemori, and A. M. Rubenchik
"Modeling of Laser-Generated Radiative Blast Waves"
Astrophys. J. 538(2Pt1), 645–652 (2000)

K. Keilty, E. Liang, B. Remington, R. London, K. Estabrook, and J. Kane
"Numerical Simulations of Blast Waves Generated by an Impulsive Temperature Source"
Astrophys. J. 127, 375–377 (2000)

B.-K. Kim, M. D. Feit, A. M. Rubenchik, E. J. Joslin, J. Eichler, P. C. Stoller, and L. B. Da Silva
"Effects of High Repetition Rate and Beam Size on Hard Tissue Damage Due to Sub-Picosecond Laser Pulses"
Appl. Phys. Lett. 76(26), 4001–4003 (2000)

B. M. Kim, J. Eichler, K. M. Reiser, A. M. Rubenchik, and L. B. Da Silva
"Collagen Structure and Nonlinear Susceptibility: Effects of Heat, Glycation, and Enzymatic Cleavage on Second Harmonic Signal Intensity"
Laser Surg. and Med. 27(4), 329–335 (2000)

R. I. Klein, K.S. Budil, T. S. Perry, and D. R. Bach
"Interaction of Supernova Remnants with Interstellar Clouds: From the Nova Laser to the Galaxy"
Astrophys. J. 127, 379–383 (2000)

J. P. Knauer, R. Betti, D. K. Bradley, T. R. Boehly, T. J. B. Collons, V. N. Goncharov, P. W. McKenty, D. D. Meyerhofer, V. A. Smalyuk, C. P. Verdon, S. G. Glendinning, D. H. Kalantar, and R. G. Watt
"Single-Mode, Rayleigh-Taylor Growth-Rate Measurements on the OMEGA Laser System"
*Phys. Plasma*s 7(1), 338–345 (2000)

J. A. Koch, R.W. Presta, R. A. Sacks, R. A. Zacharias, E. S. Bliss, M. J. Dailey, M. Feldman, A. A. Grey, F. R. Holdener, J. T. Salmon, L. G. Seppala, J. S. Toeppen, L. Van Atta, B. M. Van Wonterghem, W. T. Whistler, S. E. Winters, and B. W. Woods
"Experimental Comparison of a Shack-Hartmann Sensor and a Phase-Shifting Interferometer for Large-Optics Metrology Applications"
Appl. Opt. 39(25), 4540–4546 (2000)

J. A. Koch, T. P. Bernat, G. W. Collins, B. A. Hammel, B. J. Kozioziemski, A. J. MacKinnon, J. D. Sater, D. N. Bittner, and Y. Lee
"Quantitative Analysis of Backlit Shadowgraphy as a Diagnostic of Hydrogen Ice Surface Quality in ICF Capsules"
Fusion Tech. 38(1), 123–131 (2000)

W. L. Kruer
"Interaction of Plasmas with Intense Lasers"
Phys. Plasmas 7(6), 2270–2278 (2000)

C. Labaune, H. A. Baldis, E. Schifano, B. S. Bauer, A. Maximov, I. Ourdev, W. Rozmus, and D. Pesme
"Enhanced Forward Scattering in the Case of Two Crossed Laser Beams Interacting with a Plasma"
Phys. Rev. Lett. 85(8), 1658–1661 (2000)

C. Labaune, J. Fuchs, S. Depierreux, H. A. Baldis, D. Pesme, J. Myatt, S. Huller, V. T. Tikhonchuk, and G. Laval
"Laser-Plasma Interaction Physics in the Context of Fusion"
Comptes Rendus 1(6), 727–735 (2000)

S. H. Langer, H. A. Scott, M. A. Marinak, and O. L. Landen
"Modeling Line Emission from ICF Capsules in 3 Dimensions"
J. Q. S. R. T. 65(1–3), 333–366 (2000)

R. H. Lehmberg and J. E. Rothenberg
"Comparison of Optical Beam Smoothing Techniques for Inertial Confinement Fusion and Improvement of Smoothing by the Use of Zero-Correlation Masks"
J. Appl. Phys. 87(3), 1012–1022 (2000)

C. K. Li, D. G. Hicks, F. H. Seguin, J. A. Frenje, R. D. Petrasso, J. M. Soures, P. B. Radha, V. Yu. Glebov, C. Stoeckl, D. R. Harding, J. P. Knauer, R. Kremens, F. J. Marshall, D. D. Meyerhofer, S. Skupsky, S. Roberts, C. Sorce, T. C. Sangster, T W Phillips, M.D. Cable, and R. J. Leeper
"D-^{3}He Proton Spectra for Diagnosing Shell ρR and Fuel T_i of Imploded Capsules at Omega"
Phys. Plasmas 7(6), 2578–2584 (2000)

Y. L. Li, J. Dunn, J. Nilsen, T. W. Barbee, A. L. Osterheld, and V. N. Shlyaptsev
Saturated Tabletop X-Ray Laser System at 19nm"
J. Opt. Soc. Am. B17(6), 1098–1101 (2000)

B. G. Logan, W. R. Meier, R. W. Moir, M. Abdou, P. F. Peterson, G. L. Kulcinski, M. S. Tillack, J. F. Latkowski, D. Petti, K. R. Schultz, and A. Nobile
"Progress and Critical Issues for IFE Blanket and Chamber Research"
Fus. Engr. Design 51–52, 1095–1101 (2000)

L. M. Logory, P. L. Miller, and P. E. Stry
"Nova High-Speed Jet Experiments"
Astrophys. J. 127, 423–428 (2000)

A. V. Maximov, R. M. Oppitz, W. Rozmus, and V. T. Tikhonchuk
"Nonlinear Stimulated Brillouin Scattering in Inhomogeneous Plasmas"
Phys. Plasmas 7(10), 4227–4237 (2000)

P. B. Mirkarimi, S. Bajt, and M. A. Wall
"Mo/Si and Mo/Be Multilayer Thin Films on Zerodur Substrates for Extreme-Ultraviolet Lithography"
Appl. Optics 39(10), 1617–1625 (2000)

R. W. Moir
"Liquid Walls for Fusion Reaction Chambers"
Comments on Mod. Phys. 2(2), C99–C111 (2000)

R. W. Moir
"Grazing Incidence Liquid Metal Mirrors (GILMM) for Radiation Hardened Final Optics for Laser Inertial Fusion Energy Power Plants"
Fus. Engr. Design 51–52, 1121–1128 (2000)

J. D. Moody, B. J. MacGowan, R. L. Berger, K. G. Estabrook, S. H. Glenzer, R. K. Kirkwood, W. L. Kruer, G. F. Stone, and D. S. Montgomery
"Experimental Study of Laser Beam Transmission and Power Accounting in a Large Scalelength Laser-Plasma"
Phys. Plasmas 7(8), 3388–3398 (2000)

J. D. Moody, B. J. MacGowan, S. H. Glenzer, R. K. Kirkwood, W. L. Kruer, D. S. Montgomery, A. J. Schmitt, E. A. Williams, and G. F. Stone
"Experimental Investigation of Short Scalelength Density Fluctuations in Laser-Produced Plasmas"
Phys. Plasmas 7(5), 2114–2125 (2000)

J. E. Murray, D. Milam, C. D. Boley, and K. G. Estabrook
"Spatial Filter Pinhole Development for the National Ignition Facility"
Appl. Opt. 39(9), 1405–1420 (2000)

J. Nilsen, J. Dunn, Y. L. Li, A. L. Osterheld, V. N. Shlyaptsev, T. W. Barbee, and J. R. Hunter
"Review of Ni-Like Ion X-Ray Laser Research at Lawrence Livermore National Laboratory"
Comptes Rendus 1(8), 1035–1044 (2000)

J. Nilsen, Y. Li, and J. Dunn
"Modeling psec-Laser-Driven Neon-Like Titanium X-Ray Laser Experiments"
J. Opt. Soc. Am. B17(6), 1084–1092 (2000)

P. K. Patel, E. Wolfrum, O. Renner, A. Loveridge, R. Allott, D. Neely, S. J. Rose, and J. S. Warek
"X-Ray Line Reabsorption in a Rapidly Expanding Plasma"
J. Q. S. R. T. 65(1–3), 429–439 (2000)

D. M. Pennington, C. G. Brown, T. E. Cowan, S. P. Hatchett, E. Henry, S. Herman, M. Kartz, M. Key, J. Koch, A. J, MacKinnon, M. D. Perry, T. W. Phillips, M. Roth, T. C. Sangster, M. Singh, R. A. Snavely, M. Stoyer, B. C. Stuart, and S. C. Wilks
"Petawatt Laser Systems and Experiments"
IEEE Sel. Topics Quant. Elect. 6(4), 676–688 (2000)

T. S. Perry, S. J. Davidson, F. J. D. Serduke, D. R. Bach, C. C. Smith, J. M. Foster, R. J. Doyas, R. A. Ward, C. A. Iglesias, F. J. Rogers, J. Abdallah, Jr., R. E. Stewart, R. J. Wallace, J. D. Kilkenny, and R. W. Lee
"Opacity Measurements in a Hot Dense Medium"
Astrophys. J. 127, 433–436 (2000)

T. S. Perry, R. I. Klein, D. R. Bach, K. S. Budil, R. Cauble, H. N. Kornblum, Jr., R. J. Wallace, and R. W. Lee
"Temperature and Density Measurements of the Collision of Two Plasmas"
Astrophys. J. 127, 437–443 (2000)

R. W. Petzoldt, D. Goodin, and N. Siegel
"Status of Target Injection and Tracking Studies for Inertial Fusion Energy"
Fusion Tech. 38(1), 22–27 (2000)

B. A. Remington, R. P. Drake, D. Arnett, and H. Takabe
"Proceeding of the Second International Workshop on Laboratory Astrophysics with Intense Lasers—Introduction"
Astrophys. J. 127(2), 211 (2000)

B. A. Remington, R. P. Drake, H. Takabe, and D. Arnett
"A Review of Astrophysics Experiments on Intense Lasers"
Phys. Plasmas 7(5), 1641–1652 (2000)

C. C. Roberts, P. J. Orthion, A. E. Hassel, B. K. Parrish, S. R. Buckley, E. Fearon, S. A. Letts, and R. C. Cook
"Development of Polyimide Ablators for NIF: Analysis of Defects on Shells, a Novel Smoothing Technique and Upilex Coatings"
Fus. Tech. 38(1), 94–107 (2000)

H. F. Robey, S. Y. Potapenko, and K. D. Summerhays
"'Bending' of Steps on Rapidly Grown KH_2PO_4 Crystals Due to an Inhomogeneous Surface Supersaturation Field"
J. Crystal Growth 213(3–4), 340–354 (2000)

H. F. Robey and S. Y. Potapenko
"Ex Situ Microscopic Observation of the Lateral Instability of Macrosteps on the Surfaces of Rapidly Grown KH_2PO_4 Crystals"
J. Crystal Growth 213(3–4), 355–367 (2000)

J. E. Rothenberg
"Polarization Beam Smoothing for Inertial Confinement Fusion"
J. Appl. Phys. 87(8), 3654–3662 (2000)

W. Rozmus, S. H. Glenzer, K. G. Estabrook, H. A. Baldis, and B. J. MacGowan
"Modeling of Thomson Scattering Spectra in High-Z, Laser-Produced Plasmas"
Astrophys. J. 127, 459–463 (2000)

D. D. Ryutov
"Radical Restructuring of the Fusion Effort"
Comments on Mod. Phys. 2(2), C139–U14 (2000)

D. D. Ryutov
"Destabilizing Effect of Thermal Conductivity on the Rayleigh-Taylor Instability in a Plasma"
Phys. Plasmas 7(12), 4797–4800 (2000)

D. D. Ryutov, R. P. Drake, and B. A. Remington
"Criteria for Scaled Laboratory Simulations of Astrophysical MHD Phenomena"
Astrophys. J. 127, 465–468 (2000)

K. Shigemori, T. Ditmire, B. A. Remington, V. Yanovsky, D. Ryutov, K. G. Estabrook, M. J. Edwards, A. M. Rubenchik, E. Liang, and K. A. Keilty
"Observation of the Transition from Hydrodynamic to Radiative Shocks"
Astrophys. J. 533(2Pt2), L159–L162 (2000)

K. Shigemori, R. Kodama, D. R. Farley, T. Koase, K. G. Estabrook, B. A. Remington, D. D. Ryutov, Y. Ochi, H. Azechi, J. Stone, and N. Turner
"Experiments on Radiative Collapse in Laser-Produced Plasmas Relevant to Astrophysical Jets"
Phys. Rev. E 62(6 PT B), 8838–8841 (2000)

R. A. Snavely, M. H. Key, S. P. Hatchett, T. E. Cowan, M. Roth, T. W. Phillips, M. A. Stoyer, E. A. Henry, T. C. Sangster, M. S. Singh, S. C. Wilks, A. MacKinnon, A. Offenberger, D. M. Pennington, K. Yasuike, A. B. Langdon, B. F. Lasinski, J. Johnson, M. D. Perry, and E. M. Campbell
"Intense High-Energy Proton Beams from Petawatt-Laser Irradiation of Solids"
Phys. Rev. Lett. 85(14), 2945–2948 (2000)

C. H. Still, R. L. Berger, A. B. Langdon, D. E. Hinkel, L. J. Suter, and E. A. Williams
"Filamentation and Forward Brillouin Scatter of Entire Smoothed and Aberrated Laser Beams"
Phys. Plasmas 7(5), 2023–2032 (2000)

J. M. Stone, N. Turner, K. Estabrook, B. Remington, D. Farley, S. G. Glendinning, and S. Glenzer
"Testing Astrophysical Radiation Hydrodynamics Codes with Hypervelocity Jet Experiments on the Nova Laser"
Astrophys. J. 127, 497–502 (2000)

T. I. Suratwala, R. A. Steele, G. D. Wilke, J. H. Campbell, and K. Takeuchi
"Effects of OH Content, Water Vapor Pressure, and Temperature on Sub-Critical Crack Growth in Phosphate Glass"
J. Non-Cryst. Solids 263(1–4), 213–227 (2000)

L. J. Suter, J. Rothenberg, D. Munro, B. Van Wonterghem, and S. Haan
"Exploring the Limits of the National Ignition Facility's Capsule Coupling"
Phys. Plasmas 7(5), 2092–2098 (2000)

M. Takagi, R. Cook, R. Stephens, J. Gibson, and S. Paguio
"Decreasing Out-Of-Round in Poly(α-Methylstyrene) Mandrels by Increasing Interfacial Tension"
Fus. Tech. 38(1), 46–49 (2000)

M. Takagi, R. Cook, R. Stephens, J. Gibson, and S. Paguio
"Stiffening of PαMS Mandrels During Curing"
Fus. Tech. 38(1), 50–53 (2000)

M. Takagi, R. Cook, R. Stephens, J. Gibson, and S. Paguio
"The Effects of Controlling Osmotic Pressure on a PαMS Microencapsulated Mandrel During Curing"
Fus. Tech. 38(1), 54–57 (2000)

K. Takahashi, R. Kodama, K. A. Tanaka, H. Hashimoto, Y. Kato, K. Mima, F. A. Weber, T. W. Barbee, and L. B. Da Silva
"Laser-Hole Boring into Overdense Plasmas Measured with Soft X-Ray Laser Probing"
Phys. Rev. Lett. 84(11), 2405–2408 (2000)

K. A. Tannaka, R. Kodama, H. Fufita, M. Heya, N. Izumi, Y. Kitagawa, K. Mima, N. Miyanaga, T. Norimatsu, A. Pukhov, A. Sunahara, K. Takahashi, M. Allen, H. Habara, T. Iwatani, T. Matusita, T. Miyakosi, M. Mori, H. Setoguchi, T. Sonomoto, M. Tanpo, S. Tohyama, H. Azuma, T. Kawasaki, T. Komeno, O. Maekawa, S. Matsuo, T. Shozaki, Ka Suzuki, H. Yoshida, T. Yamanaka, Y. Sentoku, F. Weber, T. W. Barbee, Jr., and L. Da Silva
"Studies of Ultra-Intense Laser Plasma Interactions for Fast Ignition"
Phys. Plasmas 7(5), 2014–2022 (2000)

K. A. Tanaka, R. Kodama, N. Izumi, K. Takahashi, M. Heya, H. Fujita, Y. Kato, Y. Kitagawa, K. Mima, N. Miyanaga, T. Norimatsu, Y. Sentoku, A. Sunahara, H. Takeabe, T. Yamanaka, T. Koase, T. Iwatani, F. Ohtani, T. Miyakoshi, H. Habara, M. Tanpo, S. Tohyama, F. A. Weber, T. W. Barbee, and L. B. Da Silva
"Self-Focusing and Its Related Interactions at Very High Laser Intensities for Fast Ignition at Osaka University"
Comptes Rendus-Astrophysique 1(6), 737–744 (2000)

R. Teyssier, D. Ryutov, and B. Remington
"Accelerating Shock Waves in a Laser-Produced Density Gradient"
Astrophys. J. 127, 503–508 (2000)

D. Toet, P. M. Smith, T. W. Sigmon, and M. O. Thompson
"Experimental and Numerical Investigations of a Hydrogen-Assisted Laser-Induced Materials Transfer Procedure"
J. Appl. Phys. 87(7), 3537–3546 (2000)

R. E. Turner, P. Amendt, O. L. Landen, S. G. Glendinning, P. Bell, C. Decker, B. A. Hammel, D. Kalantar, D. Lee, R. Wallace, D. Bradley, M. Cable, R. S. Craxton, R. Kremens, W. Seka, J. Schnittman, K. Thorp, T. J. Murphy, N. Delamater, C. W. Barnes, A. Hauer, G. Magelssen, and J. Wallace
"Demonstration of Time-Dependent Symmetry Control in Hohlraums by Drive-Beam Staggering"
Phys. Plasmas 7(1), 333–337 (2000)

R. Unanyan, S. Guerin, B. W. Shore, and K. Bergmann
"Efficient Population Transfer by Delayed Pulses Despite Coupling Ambiguity"
Euro. Phys. J. 8D(3), 443–449 (2000)

R. G. Unanyan, N. V. Vitanov, B. W. Shore, and K. Bergmann
"Coherent Properties of a Tripod System Coupled Via a Continuum"
Phys, Rev. A6104(4), 3408, U402–U410 (2000)

W. S. Varnum, N. D. Delamater, S. C. Evans, P. L. Gobby, J. E. Moore, J. M. Wallace, R. G. Watt, J. D. Colvin, R. Turner, V. Glebov, J. Soures, and C. Stoeckl
"Progress Toward Ignition with Noncryogenic Double-Shell Capsules"
Phys. Rev. Lett. 84(22), 5153–5155 (2000)

A. L. Velikovich, J. P. Dahlburg, A. J. Schmitt, J. H. Gardner, L. Phillips, F. L. Cochran, Y. K. Chong, G. Dimonte, and N. Metzler
"Richtmyer-Meshkov-Like Instabilities and Early-Time Perturbation Growth in Laser Targets and Z-Pinch Loads"
Phys. Plasmas 7(5), 1662–1671 (2000)

N. V. Vitanov, B. W. Shore, R. G. Unanyan, and K. Bergmann
"Measuring a Coherent Superposition"
Opt. Comm. 179(1–6), 73–83 (2000)

O. Willi, L. Barringer, A. Bell, M. Borghesi, J. Davies, R. Gaillard, A. Iwase, A. MacKinnon, G. Malka, C. Meyer, S. Nuruzzaman, R. Taylor, C. Vickers, D. Hoarty, P. Gobby, R. Johnson, R. G. Watt, N. Blanchot, B. Canaud, H. Croso, B. Meyer, J. L. Miguel, C. Reverdin, A. Pukhov, and J. Meyer-Ter-Vehn
"Inertial Confinement Fusion and Fast Ignitor Studies"
Nucl. Fusion 40(N3Y 3), 537–545 (2000)

N. C. Woolsey, C. A. Back, R. W. Lee, A. Calisti, C. Mosse, R. Stamm, B. Talin, A. Asfaw, and L. S. Klein
"Experimental Results on Line Shifts from Dense Plasmas"
J. Q. S. R. T. 65(1–3), 573–578 (2000)

J. Zweiback, T. E. Cowan, R. A. Smith, J. H. Hartley, R. Howell, C. A. Steinke, G. Hays, K. B. Wharton, J. K. Crane, and T. Ditmire
"Characterization of Fusion Burn Time in Exploding Deuterium Cluster Plasmas"
Phys. Rev. Lett. 85(17), 3640–3643 (2000)

J. Zweiback, R. A. Smith, T. E. Cowan, G. Hays, K. B. Wharton, V. P. Yanovsky, and T. Ditmire
"Nuclear Fusion Driven by Coulomb Explosions of Large Deuterium Clusters"
Phys. Rev. Lett. 84(12), 2634–2637 (2000)

2001 Refereed Publications

J. J. Adams, C. A. Ebbers. K. I. Schaffers, and S. A. Payne
"Nonlinear Optical Properties of $LaCa_4O(BO_3)_3$"
Opt. Lett. 26(4), 217–219 (2001)

P. Amendt, A. I. Shestakov, O. L. Landen, D. K. Bradley, S. M. Pollaine, L. J. Suter, and R. E. Turner
"Thinshell Symmetry Surrogates for the National Ignition Facility: A Rocket Equation Analysis"
Phys. Plasmas 8(6), 2908–2917 (2001)

P. Amendt
"Pseudomoment Fluid Modeling: Electron Landau Damping of Ion-Acoustic Waves"
Phys. Plasmas 8(4), 1437–1440 (2001)

J. M. Auerbach, P. J. Wegner, S. A. Couture, D. Eimerl, R. L. Hibbard, D. Milam, M. A. Norton, P. K. Whitman, and L. A. Hackel
"Modeling of Frequency Doubling and Tripling with Measured Crystal Spatial Refractive-Index Nonuniformities"
Appl. Opt. 40(9), 1404–1411 (2001)

C. A. Back, J. Grun, C. Decker, L. J. Suter, J. Davis, O. L. Landen, R. Wallace, W. W. Hsing, J. M. Laming, U. Feldman, M. C. Miller, and C. Wuest
"Efficient Multi-keV Underdense Laser-Produced Plasma Radiators"
Phys. Rev. Lett. 87(27), 82–84 (2001)

J. E. Bailey, D. Cohen, G. A. Chandler, M. E. Cuneo, M. E. Foord, R. F. Heeter, D. Jobe, P. Lake, D. A. Liedahl, J. J. MacFarlane, T. J. Nash, D. Nielson, R. Smelser, and W. A. Stygar
"Neon Photoionization Experiments Driven by Z-Pinch Radiation"
J.Q.S.R.T. 71(2–6), 157–168 (2001)

S. Bajt, D. G. Stearns, and P. A. Kearney
"Investigation of the Amorphous-to-Crystalline Transition in Mo/Si Multilayers"
J. Appl. Phys. 90(2), 1017–1025 (2001)

K. L. Baker, K. G. Estabrook, R. P. Drake, and B. B. Afeyan
"Alternative Mechanism for $\omega_0/2$ Emission in Laser-Produced Plasmas"
Phys. Rev. Lett. 86(17), 3787–3790 (2001)

H. A. Baldis, J. Dunn, M. E. Foord, W. Rozmus, C. Anderson, and R. Shepherd
"New Regime of Thomson Scattering: Probing Dense Plasmas with X-Ray Lasers"
J. de Physique IV 11(NPR2), 469–472 (2001)

I. M. Barton, J. A. Britten, S. N. Dixit, L. J. Summers, I. M. Thomas, M. C. Rushford, K. Lu, R. A. Hyde, and M. D. Perry
"Fabrication of Large-Aperture Lightweight Diffractive Lenses for Use in Space"
Appl. Opt. 40(4), 447–451 (2001)

R. J. Beach and B. L. Freitas
"Practical 100-kW-Class Diode Arrays Emerge"
Laser Focus World 37(2), 103–107 (2001)

R. J. Beach, S. C. Mitchell, H. E. Meissner, O. R. Meissner, W. F. Krupke, J. M. McMahan, and W. J. Bennett
"Continuous-Wave and Passively Q-Switched Cladding-Pumped Planar Waveguide Lasers"
Opt. Lett. 26(12), 881–883 (2001)

P. Bell. D. Lee, A. Wooton, B. Mascio, J. Kimbrough, N. Sewall, W. Hibbard, P. Dohoney, M. Landon, G. Christianson, and J. Celeste
"Target Area and Diagnostic Interface Issues on the National Ignition Facility"
Rev. Sci. Inst. 72(1Pt2), 492–498 (2001)

G. R. Bennett, O. L. Landen, R. F. Adams, J. L. Porter, L. E. Ruggles, W. W. Simpson, and C. Wakefield
"X-Ray Imaging Techniques on Z Using the Beamlet Laser"
Rev. Sci. Inst. 72(1Pt2), 657–662 (2001)

R. R. Berggren, S. E. Caldwell, J. R. Faulkner Jr., R. A. Lerche, J. M. Mack, K. J. Moy, J. A. Oertel, and C. S. Young
"Gamma-Ray-Based Fusion Burn Measurements"
Rev. Sci. Inst. 72(1Pt2), 873–876 (2001)

K. Bohmer, T. Halfmann, L. P. Yatsenko, B. W. Shore, and K. Bergmann
"Stimulated Hyper-Raman Adiabatic Passage, III Experiment"
Phys. Rev. A 64(2), 459–468 (2001)

M. Borghesi, A. Schiavi, D. H. Campbell, M. G. Haines, O. Willi, A. J. MacKinnon, L. A. Gizzi, M. Galimberti, R. J. Clarke, and H. Ruhl
"Proton Imaging: A Diagnostic for Inertial Confinement Fusion / Fast Ignitor Studies"
Plasma Phys. Cont. Fusion 43(Supp12A), 267–276 (2001)

J. L. Bourgade, B. Villette, J. L. Bocher, J. Y. Boutin, S. Chivhe, N. Dague, D. Gontier, J. P. Jadaud, B. Savale, R. Wrobel, and R. E. Turner
"DMX: An Absolutely Calibrated Time-Resolved Broadband Soft X-Ray Spectrometer Designed for MJ Class Laser-Produced Plasmas"
Rev. Sci. Inst. 72(1Pt2), 1173–1182 (2001)

D. K. Bradley, P. M. Bell, A. K. L. Dymoke-Bradshaw, J. D. Hares, R. E. Bahr, V. A. Smalyuk, D. R. Hargrove, and K. Piston
"Development and Characterization of a Single-Line-Of-Sight Framing Camera"
Rev. Sci. Inst. 72(1Pt2), 694–697 (2001)

N. A. Brilliant and K. Lagonik
"Thermal Effects in a Dual-Clad Ytterbium Fiber Laser"
Opt. Lett. 26(21), 1669–1671 (2001)

K. S. Budil, B. Lasinski, M. J. Edwards, A. S. Wan, B. A. Remington, S. V. Weber, S. G. Glendinning, L. Suter, and P. E. Stry
"The Ablation-Front Rayleigh-Taylor Dispersion Curve in Indirect Drive"
Phys. Plasmas 8(5Pt2), 2344–2348 (2001)

B. Bullock, O. L. Landen, and D. K. Bradley
"Relative X-Ray Backlighter Intensity Comparison of Ti and Ti / Sc Combination Foils Driven in Double-Sided and Single-Sided Laser Configuration"
Rev. Sci. Inst. 72(1Pt2), 686–689 (2001)

B. Bullock, O. L. Landen, and D. K. Bradley
"10 and 5 μm Pinhole-Assisted Point-Projection Backlit Imaging for the National Ignition Facility"
Rev. Sci. Inst. 72(1Pt2), 690–693 (2001)

A. Burger, K. Chattopadhyay, J. O. Ndap, X. Ma, S. H. Morgan, C. I. Rablau, C.-H. Su, S. Feth, R. H. Page, K. I. Shaffers, and S. A. Payne
"Preparation Conditions of Chromium Doped ZnSe and Their Infrared Luminescence Properties"
J. Crystal Growth 225(2–4), 249–256 (2001)

R. Cauble, D. K. Bradley, P. M. Celliers, G. W. Collins, L. B. Da Silva, and S. J. Moon
"Experiments Using Laser-Driven Shockwaves for EOS and Transport Measurements"
Contrib. Plasma Phys. 41(2–3), 239–242 (2001)

D. M. Chambers, S. H. Glenzer, J. Hawreliak, E. Wolfrum, A. Gouveia, R. W. Lee, R. S. Marjoribanks, O. Renner, P. Sondhauss, S. Topping, P. E. Young, P. A. Pinto, and J. S. Wark
"Detailed Hydrodynamic and X-Ray Spectroscopic Analysis of a Laser-Produced Rapidly-Expanding Aluminum Plasma"
J.Q.S.R.T. 71(2–6), 237–247 (2001)

B. I. Cohen, H. A. Baldis, R. L. Berger, K. G. Estabrook, E. A. Williams, and C. Labaune
"Modeling of the Competition of Stimulated Raman and Brillouin Scatter in Multiple Beam Experiments"
Phys. Plasmas 8(2), 571–591 (2001)

G. W. Collins, P. M. Celliers, L. B. Da Silva, R. Cauble, D. M. Gold, M. E. Foord, N. C. Holmes, B. A. Hammel, R. J. Wallace, and A. Ng
"Temperature Measurements of Shock Compressed Liquid Deuterium Up to 230 GPa"
Phys. Rev. Lett. 87(16), 165504-1, –4 (2001)

G. W. Collins, T. P. Bernat, E. R. Mapoles, B. J. Kozioziemski, and C. Duriez,
"Heat-Flux Induced Changes to Multicrystalline D_2 Surfaces"
Phys. Rev. B 63, 195416 (2001)

M. E. Cuneo, R. A. Vesey, J. L. Porter, Jr., G. A. Chandler, D. L. Fehl, T. L. Gilliland, D. L. Hanson, J. S. McGurn, P. G. Reynolds, L. E. Ruggles, H. Seaman, R. B. Soelman, K. W. Struve, W. A. Stygar, W. W. Simpson, J. A. Torres, D. F. Wenger, J. H. Hammer, P. W. Rambo, D. L. Peterson, and G. C. Idzorek
"Development and Characterization of a Z-Pinch-Driven Hohlraum High-Yield Inertial Confinement Fusion Target Concept"
Phys. Plasmas 8(5Pt2), 2257–2267 (2001)

E. Dattolo, L. Suter, M.-C. Monteil, J.-P. Jadaud, N. Dague, S. Glenzer, R. Turner, D. Juraszek, B. Lasinski, C. Decker, O. Landen, and B. MacGowan
"Status of Our Understanding and Modeling of X-Ray Coupling Efficiency in Laser Heated Hohlraums"
Phys. Plasmas 8(1), 260–265 (2001)

O. Delage, R. A. Lerche, T. C. Sangster, and H. H. Arsenault
"SIRINC: A Code for Assessing and Optimizing the Neutron Imaging Diagnostic Capabilities in Inertial Confinement Fusion Experiments"
Rev. Sci. Inst. 76(1PT2), 869–872 (2001)

J. Dunn, A. L. Osterheld, J. Nilsen, J. R. Hunter, Y. L. Li, A. Y. Faenov, T. A. Pikuz, and V. N. Shlyaptsev
"Saturated Output Tabletop X-Ray Lasers"
J. de Physique IV, 11(Pr2), 19–26 (2001)

J. Dunn, A. Y. Faenov, T. A. Pikuz, A. L. Osterheld, S. J. Moon, K. B. Fournier, J. Nilsen, I. Y. Skobelev, A. I. Magunov, and V. N. Shlyaptsev
"Spectral and Imaging Characterization of Tabletop X-Ray Lasers"
J. de Physique IV, 11(Pr2), 51–54 (2001)

M. J. Edwards, A. J. MacKinnon, J. Zwieback, K. Shigemori, D. Ryutov, A. M. Rubenchik, K. A. Kielty, E. Liang, B. A. Remington, and T. Ditmire
"Investigation of Ultrafast Laser-Driven Radiative Blast Waves"
Phys. Rev. Lett. 87(8), 72–74 (2001)

J. L. Feldman, J. H. Eggert, H. K. Mao, and R. J. Hemley
"Computations of Vibron Excitations and Raman Spectra of Solid Hydrogen"
J. Low Temp. Phys. 122(3/4), 389–399 (2001)

H. Fiedorowicz, H. Bartnik, J. Dunn, R. F. Smith, J. Hunter, J. Nilsen, A. L. Osterheld, and V. N. Shlyaptsev
"Demonstration of a Neonlike Argon Soft X-Ray Laser with a Picosecond-Laser-Irradiated Gas Puff Target"
Opt. Lett. 26(18), 1403–1405 (2001)

E. Fourkal, V. Y. Bychenkov, W. Rozmus, R. Sydora, C. Kirkby, C. E. Capjack, S. H. Glenzer, and H. A. Baldis
"Electron Distribution Function in Laser Heated Plasmas"
Phys. Plasmas 8(2), 550–556 (2001)

K. B. Fournier, B. K. F. Young, S. J. Moon, M. E. Foord, D. F. Price, R. L. Shepherd, and P. T. Springer
"Characterization of Time Resolved, Buried Layer Plasmas Produced by Ultrashort Laser Pulses"
J.Q.S.R.T. 71(2–6), 339–354 (2001)

J. A. Frenje, K. M. Green, D. G. Hicks, C. K. Li, F. H. Seguin, R. D. Petrasso, T. C. Sangster, T. W. Phillips, V. Y. Glebov, D. D. Meyerhofer, S. Roberts, J. M. Soures, C. Stoeckl, K. Fletcher, S. Paladino, and R. J. Leeper
"A Neutron Spectrometer for Precise Measurements of DT Neutrons from 10 to 18 MeV at OMEGA and the National Ignition Facility"
Rev. Sci. Inst. 72(1Pt2), 854–858 (2001)

J. Fuchs, C. Labaune, S. Depierreaux, H. A. Baldis, A. Michard, and G. James
"Experimental Evidence of Plasma-Induced Incoherrence of an Intense Laser Beam Propagating in an Underdense Plasma"
Phys. Rev. Lett. 86(3), 432–435 (2001)

N. Y. Garces, K. T. Stevens, L. E. Halliburton, M. Yan, N. P. Zaitseva, and J. J. De Yoreo
"Optical Absorption and Electron Paramagnetic Resonance of Fe Ions in KDP Crystals"
J. Crystal Growth 225(2–4), 435–439 (2001)

N. Y. Garces, K. T. Stevens, L. E. Halliburton, S. G. Demos, H. B. Radousky, and N. P. Zaitseva
"Identification of Electron and Hole Traps in KH_2PO_4 Crystals"
J. Appl. Phys. 89(1), 47–52 (2001)

R. H. Gee, L. E. Fried, and R. C. Cook
"Structure of Chlorotrifluoroethylene/Vinylidene Fluoride Random Copolymers and Homopolymers by Molecular Dynamics Simulations"
Macromolecules 34(9), 3050–3059 (2001)

F. Y. Genin, A. Allen, T. V. Pistor, and L. L. Chase
"Role of Light Intensification by Cracks in Optical Breakdown on Surfaces"
J. Opt. Soc. A 18(10), 2607–2616 (2001)

S. H. Glenzer, R. L. Berger, L. M. Divol, R. K. Kirkwood, B. J. MacGowan, J. D. Moody, A. B. Langdon, L. J. Suter, and E. A. Williams
"Reduction of Stimulated Scattering Losses from Hohlraum Plasmas with Laser Beam Smoothing"
Phys. Plasmas 8(5Pt2), 1692–1696 (2001)

S. H. Glenzer, L. M. Divol, R. L. Berger, C. Geddes, R. K. Kirkwood, J. D. Moody, E. A. Williams, and P. E. Young
"Thomson Scattering Measurements of Saturated Ion Waves in Laser Fusion Plasmas"
Phys. Rev. Lett. 86(12), 2565–2568 (2001)

S. H. Glenzer, K. B. Fournier, B. G. Wilson, R. W. Lee, and L. J. Suter
"Ionization Balance in Inertial Confinement Fusion Hohlraums Plasmas"
J. Q. S. R. T. 71, 355–363 (2001)

S. H. Glenzer, R. L. Berger, L. M. Divol, R. K. Kirkwood, B. J. MacGowan, J. D. Moody, J. E. Rothenberg, L. J. Suter, and E. A. Williams
"Laser-Plasma Interactions in Inertial Confinement Fusion Hohlraums"
Phys. Rev. Lett. 87(4), 64–66 (2001)

S. H. Glenzer, R. L. Berger, L. M. Divol, R. K. Kirkwood, B. J. MacGowan, J. D. Moody, J. E. Rothenberg, L. J. Suter, and E. A. Williams
"Laser-Plasma Interactions in Inertial Confinement Fusion Hohlraum Plasmas"
J.Q.S.R.T. 71(2–6), 355–363 (2001)

M. E. Glinsky, D. S. Bailey, R. A. London, P. A. Amendt, A. M. Rubenchik, and M. Strauss
"An Extended Rayleigh Model of Bubble Evolution"
Phys. Fluids 13(1), 20–31 (2001)

F. V. Hartemann, H. A. Baldis, A. K. Kerman, A. Le Foll, N. C. Luhman, and B. Rupp
"Three-Dimensional Theory of Emittance in Compton Scattering and X-Ray Protein Crystallography"
Phy. Rev. E 64(1Pt2), 730–754 (2001)

J. Hawreliak, D. Chambers, S. Glenzer, R. S. Marjoribanks, M. Notley, P. Pinto, O. Renner, P. Sondhauss, R. Steel, S. Topping, E. Wolfrum, P. Young, and J. S. Wark
"A Thomson Scattering Post-Processor for the MEDUSA Hydrocode"
J.Q.S.R.T. 71(2/6), 383–395 (2001)

R. F. Heeter, J. E. Bailey, M. E. Cuneo, J. Emig, M. E. Foord, P. T. Springer, and R. S. Thoe
"Plasma Diagnostics for X-Ray Driven Foils at Z"
Rev. Sci. Inst. 72(1Pt2), 1224–1227 (2001)

M. C. Herrmann, M. Tabak, and J. D. Lindl
"Ignition Scaling Laws and Their Application to Capsule Design"
Phys. Plasmas 8(5Pt2), 2296–2304 (2001)

W. J. Hibbard, M. D. Landon, M. D. Vergino, F. D. Lee, and J. A. Chael
"Design of the National Ignition Facility Diagnostic Instrument Manipulator"
Rev. Sci. Inst. 72(1Pt2), 530–532 (2001)

D. G. Hicks, C. K. Li, F. H. Seguin, J. D. Schnittman, A. K. Ram, J. A. Frenje, R. D. Petrasso, J. M. Soures, D. D. Meyerhofer, S. Roberts, C. Sorce, C. Stockl. T. C. Sangster, and T. W. Phillips
"Observations of Fast Protons Above 1 MeV Produced in Direct-Drive Laser-Fusion Experiments"
Phys. Plasmas 8(2), 606–610 (2001)

D. G. Hicks, C. K. Li, F. H. Seguin, J. A. Frenje, R. D. Petrasso, and T. C. Sangster
"Optimal Foil Shape for Neutron Time-Of-Flight Measurements Using Elastic Recoils"
Rev. Sci. Inst. 72(1Pt2), 859–862 (2001)

O. A. Hurricane, S. G. Glendinning, B. A. Remington, R. P. Drake, and K. K. Dannenberg
"Late-Time Hohlraum Pressure Dynamics in Supernova Remnant Experiments"
Phys. Plasmas 8(6), 2609–2612 (2001)

J. Jovanovic, B. J. Comaskey, and D. M. Pennington
"Angular Effects and Beam Quality in Optical Parametric Amplification"
J. Appl. Phys. 90(9), 4328–4337 (2001)

D. H. Kalantar, P. M. Bell, T. S. Perry, N. Sewall, J. Kimbrough, F. Weber, C. Diamond, and K. Piston
"Optimizing Data Recording for the NIF Core Diagnostic X-Ray Streak Camera"
Rev. Sci. Inst. 762(1Pt2), 751–754 (2001)

J. O. Kane, H. F. Robey, B. A. Remington, R. P. Drake, J. Knauer, D. D. Ryutov, H. Lewis, R. Teyssier, O. Hurricane, D. Arnett, R. Rosner, and A. Calder
"Interface Imprinting by a Rippled Shock Using an Intense Laser"
Phys. Rev. E 63(5Pt.2), 22–24 (2001)

M. H. Key
"Fast Track to Fusion Energy"
Nature 412(6849), 775–776 (2001)

B.-K. Kim, M. D. Feit, A. M. Rubenchik, E. J. Joslin, P. M. Celliers, J. Eichler, and L. B. Da Silva
"Influence of Pulse Duration on Ultrashort Laser Pulse Ablation of Biological Tissues"
J. Biomedical Opt. 6(3), 332–338 (2001)

J. R. Kimbrough, P. M. Bell, G. B. Christianson, F. D. Lee, D. H. Kalantar, T. S. Perry, N. R. Sewall, and A. J. Wootton
"National Ignition Facility Core X-Ray Streak Camera"
Rev. Sci. Inst. 72(1Pt2), 748–750 (2001)

O. L. Landen, D. R. Farley, S. G. Glendinning, L. M. Logory, P. M. Bell, J. A. Koch, F. D. Lee, D. K. Bradley, D. H. Kalantar, C. A. Back, and R. E. Turner
"X-Ray Backlighting for the National Ignition Facility"
Rev. Sci. Inst. 72(1Pt2), 627–634 (2001)

O. L. Landen, A. Lobban, T. Tutt, P. M. Bell, R. Costa, D. R. Hargrove, and F. Ze
"Angular Sensitivity of Gated Microchannel Plate Framing Cameras"
Rev. Sci. Inst. 72 (1Pt2), 709–712 (2001)

O. L. Landen, S. H. Glenzer, M. J. Edwards, R. W. Lee, G. W. Collins, R. C. Cauble, W. W. Hsing, and B. A. Hammel
"Dense Matter Characterization by X-Ray Thomson Scattering"
J.Q.S.R.T. 71(2–6), 465–478 (2001)

M. D. Landon, J. A. Koch, S. S. Alvarez, P. M. Bell, F. D. Lee, and J. D. Moody
"Design of the National Ignition Facility Static X-Ray Imager"
Rev. Sci. Inst. 72 (1Pt2), 698–700 (2001)

S. H. Langer, H. A. Scott, M. M. Marinak, and O. L. Landen
"Modeling Titanium Line Emission from ICF Capsules in Three Dimensions"
J.Q.S.R.T. 71(2/6), 479–492 (2001)

A. Loveridge-Smith, A. Allen, J. Belak, T. Boehly, A. Hauer, B. Holian, D. Kalantar, G. Kyrala, R. W. Lee, P. Lomdahl, M. A. Myers D. Paisley, S. Pollaine, B. Remington, D. C. Swift, S. Weber, and J. S. Wark
"Anomalous Elastic Response of Silicon to Uniaxial Shock Compression on Nanosecond Timescales"
Phys. Rev. Lett. 86(11), 2349–2352 (2001)

J. I. MacKenzie, S. C. Mitchell, R. J. Beach, H. E. Meissner, and D. P. Shepherd
"15 W Diode-Side-Pumped Tm: YAG Waveguide Laser at 2µm"
Elect. Lett. 37(4), 898–899 (2001)

A. J. MacKinnon, M. Borghesi, S. Hatchett, M. H. Key, P. K. Patel, H. Campbell, A. Schiavi, R. Snavely, S. C. Wilks, and O. Willi
"Effect of Plasma Scale Length on Multi-MeV Proton Production by Intense Laser Pulse"
Phys. Rev. Lett. 86(9), 1769–1772 (2001)

M. M. Marinak, G. D. Kerbel, N. A. Gentile, O. Jones, D. Munro, S. Pollaine, T. R. Dittrich, and S. W. Haan
"Three-Dimensional HYDRA Simulations of National Ignition Facility Targets"
Phys. Plasmas 8(5Pt2), 2275–2280 (2001)

W. A. Mascio, N. R. Sewall, R. Kirkwood, F. D. Lee, and W. J. Hibbard
"Near to Backscattered Light Imaging Diagnostic on the National Ignition Facility"
Rev. Sci. Inst. 72(1Pt2), 976–978 (2001)

A. V. Maximov, I. G. Ourdev, D. Pesme, W. Rozmus, V. T. Tikhonchuk, and C. E. Capjack
"Plasma Induced Smoothing of Spatially Incoherent Laser Beam and Reduction of Backward Stimulated Brillouin Scattering"
Phys. Plasmas 8(4), 1319–1328 (2001)

D. D. Meyerhofer, J. A. Delettrez, R. Epstein, V. Yu. Glebov, V. N. Goncharov, R. L. Keck, R. L. McCrory, P. W. McKenty, F. L. Marshall, P. B. Radha, S. P. Regan, S. Roberts, W. Seka, S. Skupsky, V. A. Smalyuk, C. Sorce, C. Stoeckl, J. M. Soures, R. P. J. Town, B. Yaakobi, J. D. Zuegel, J. Frenje, C. K. Li, R. D. Petrasso, F. H. Seguin, K. Fletcher, S. Padalino, C. Freeman, N. Izumi, R. Lerche, T. W. Phillips, and T. C. Sangster
"Core Performance and Mix in Direct-Drive Spherical Implosions with High Uniformity"
Phys. Plasmas 8 (5Pt2), 2251–2453 (2001)

M. C. Miller, J. R. Celeste, M. A. Stoyer, L. J. Suter, M. T. Tobin, J. Grun, J. F. Davis, C. W. Barnes, and D. C. Wilson
"Debris Characterization Diagnostic for the NIF"
Rev. Sci. Inst. 72(1Pt2), 537–539 (2001)

P. B. Mirkarimi, S. L. Baker, C. Montcalm, and J. A. Folta
"Recovery of Multilayer-Coated Zerodur and ULE Optics for Extreme-Ultraviolet Lithography by Recoating, Reactive-Ion Etching, and Wet-Chemical Processes"
Appl. Opt. 40(1), 62–70 (2001)

R. W. Moir
"Thick Liquid-Walled, Field-Reversed Configuration-Magnetic Fusion Power Plant"
Fusion Tech. 39(2Pt2), 758–767 (2001)

C. Montcalm
"Reduction of Residual Stress in Extreme Ultraviolet Mo/Si Multilayer Mirrors with Postdeposition Thermal Treatments"
Optical Engr. 40(3), 469–477 (2001)

C. Montcalm, S. Bajt, and J. F. Seely
"MoRu-Be Multilayer-Coated Grating with 10.4% Normal-Incidence Efficiency Near the 11.4-nm Wavelength"
Opt. Lett. 26(3), 125–127 (2001)

J. D. Moody, B. J. MacGowan, J. E. Rothenberg, R. L. Berger, L. Divol, S. H. Glenzer, R. K. Kirkwood, E. A. Williams, P. E. Young
"Backscatter Reduction Using Combined Spatial, Temporal, and Polarization Beam Smoothing in a Long-Scale-Length Laser Plasma"
Phys. Rev. Lett. 86(13), 2810–2813 (2001)

D. H. Munro, P. M. Celliers, G. W. Collins, D. M. Gold, L. B. Da Silva, S. W. Haan, R. C. Cauble, B. A. Hammel, and W. W. Hsing
"Shock Timing Technique for the National Ignition Facility"
Phys. Plasmas 8(5Pt2), 2245–2250 (2011)

T. J. Murphy, C. W. Barnes, R. R. Berggren, P. Bradley, S. E. Caldwell, R. E. Chrien, J. R. Faulkner, P. L. Gobby, N. Hoffman, J. L. Jimerson, K. A. Klare, C. L. Lee, J. M. Mack, G. L. Oertel, F. J. Swenson, P. J. Walsh, R. B. Walton, R. G. Watt, M. D. Wilke, D. C. Wilson, C. S. Young, S. W. Haan, R. A. Lerche, M. J. Moran, T. W. Phillips, T. C. Sangster, R. J. Leeper, C. L. Ruiz, G. W. Coopere, L. Disdier, A. Rouyer, A. Fedotoff, V. Y. Glebov, D. D. Meyerhofer, J. M. Soures, C. Stockl, J. A. Frenje, D. G. Hicks, C. K. Li, R. D. Petrasso, F. H. Seguin, K. Fletcher, S. Padalino, and R. K. Fisher
"Nuclear Diagnostics for the National Ignition Facility"
Rev. Sci. Inst. 72(1PT2), 773–779 (2001)

J. Nilsen, Y. L. Li, J. Dunn, T. W. Barbee, and A. L. Osterheld
"Modeling and Demonstration of a Saturated Ni-Like Mo X-Ray Laser"
J. de Physique IV, 11(Pr2), 67–73 (2001)

M. C. Nostrand, R. H. Page, S. A. Payne, L. I. Isaenko, and A. P. Yelisseyev
"Optical Properties of Dy^{3+}- and Nd^{3+}-Doped KPb_2Cl_5"
J. Opt. Soc. Am. B 18(3), 264–276 (2001)

D. Pesme, S. Huller, G. Laval, S. Depierreux, J. Fuchs, C. Labaune, A. Michaud, and H. Baldis
"First Observation of Ion Acoustic Waves Produced by the Langmuir Decay Instability"
Phys. Rev. Lett. 86(16), 3687 (2001)

F. D. Patel and R. J. Beach
"New Formalism for the Analysis of Passively Q-Switched Laser Systems"
IEEE J. Quant. Electr. 37(5), 707–715 (2001)

F. D. Patel, E. C. Honea, J. Speth, S. A. Payne, R. Hutcheson, and R. Equall
"Laser Demonstration of $Yb_3Al_5O_{12}$(Yb:YAG) and Materials Properties of Highly Doped Yb:YAG"
IEEE J. Quant. Electr. 37(1), 135–144 (2001)

S. M. Pollaine, D. K. Bradley, O. L. Landen, R. J. Wallace, O. S. Jones, P. A. Amendt, L. J. Suter, and R. E. Turner
"National Ignition Facility Scale Hohlraum Asymmetry Studies by Thin Shell Radiography"
Phys. Plasmas 8(5Pt2), 2357–2364 (2001)

H. F. Robey, J. O. Kane, B. A. Remington, R. P. Drake, O. A. Hurricane, H. Louis, R. J. Wallace, J. Knauer, P. Keiter, D. Arnett, and D. D. Ryutov
"An Experimental Testbed for the Study of Hydrodynamic Issues in Supernovae"
Phys. Plasmas 8 (5Pt2), 2446–2453 (2001)

H. F. Robey, and D. Maynes
"Numerical Simulation of the Hydrodynamics and Mass Transfer in the Large Scale, Rapid Growth of KDP Crystals. Part 1. Computation of the Transient, Three-Dimensional Flow Field"
J. Crystal Growth 222(1–2), 263–278 (2001)

M. Roth, T. E. Cowan, C. Brown, M. Christl, W. Fountain, S. Hatchett, J. Johnson, M. H. Key, D. M. Pennington, M. D. Perry, T. W. Phillips, T. C. Sangster, M. Singh, R. Snavely, M. Stoyer, Y. Takahashi, S. C. Wilks, and K. Yasuike
"Intense Ion Beams Accelerated by Petawatt-Class Lasers"
Nucl. Inst. & Meth. 464(1–3), 201–205 (2001)

M. Roth, T. E. Cowan, M. H. Key, S. P. Hatchett, C. Brown, W. Fountain, J. Johnson, D. M. Pennington, R. A. Snavely, S. C. Wilks, K. Yasuike, H. Ruhl, F. Pegoraro, C. V. Bulanov, E. M. Campbell, M. D. Perry, and H. Powell
"Fast Ignition by Intense Laser-Accelerated Proton Beams"
Phys. Rev. Lett. 86(3), 436–439 (2001)

D. D. Ryutov, B. A. Remington, and H. F. Robey
"Microhydrodynamic Scaling: From Astrophysics to the Laboratory"
Phys. Plasmas 8 (5Pt2), 1804–1816 (2001)

D. Sae-Lao and C. Montcalm
"Molybdenum-Strontium Multilayer Mirrors for the 8-12-nm Extreme-Ultraviolet Wavelength Region"
Opt. Lett. 26(7), 468–470 (2001)

K. I. Schaffers, J. B. Tassano, P. A. Waide, S. A. Payne, and R. C. Morris
"Progress in the Growth of Yb:S-FAP Laser Crystals"
J. Crystal Growth 225(2–4), 449–453 (2001)

J. F. Seely, C. Montcalm, S. Baker, and S. Bajt
"High-Efficiency MoRu-Be Multilayer-Coated Gratings Operating Near Normal Incidence in the 11.1-12.0-nm Wavelength Range"
Appl. Opt. 40(31), 5565–5574 (2001)

D. P. Shepherd, S. J. Hettrick, C. Li, J. I. MacKenzie, R. J. Beach, S. C. Mitchell, and H. E. Meissner
"High-Power Planar Dielectric Waveguide Lasers"
J. of Phys. D 34(16), 2420–2432 (2001)

B. W. Shore, M. A. Johnson, K. C. Kulander, and J. I. Davis
"The Livermore Experience: Contributions of J. H. Eberly to Laser Excitation Theory"
Opt. Express 8(2), 28–43 (2001)

R. Smith and M. H. Key
"A Review of Laser and Synchrotron Based X-Ray Sources"
J. de Physique IV 11(Pr2), 383–388 (2001)

M. A. Stoyer, T. C. Sangster, E. A. Henry, M. D. Cable, T. E. Cowan, S. P. Hatchett, M. H. Key, M. J. Moran, D. M. Pennington, M. D. Perry, T. W. Phillips, M. S. Singh, R. A. Snavely, M. Tabak, and S. C. Wilks
"Nuclear Diagnostics for Petawatt Experiments"
Rev. Sci. Inst. 72(1Pt2), 767–772 (2001)

V. T. Tikhonchuk, J. Fuchs, C. Labaune, S. Depierreux, S. Huller, J. Myatt, and H. A. Baldis
"Stimulated Brillouin and Raman Scattering from a Randomized Laser Beam in Large Inhomogeneous Collisional Plasmas, II. Model Description and Comparison with Experiments"
Phys. Plasmas 8(5Pt1), 1636–1649 (2001)

R. E. Turner, O. L. Landen, D. K. Bradley, S. S. Alvarez, P. M. Bell, R. Costa, J. D. Moody, and D. Lee
"Comparison of Charge Coupled Device vs Film Readouts for Gated Micro-Channel Plate Cameras"
Rev. Sci. Inst. 72(1Pt2), 706–708 (2001)

R. G. Unanyan, B. W. Shore, and K. Bergmann
"Preparation of an N-Component Maximal Coherent Superposition State Using the Stimulated Raman Adiabatic Passage Method"
Phys. Rev. A 6304(4), 3401, U517–U520 (2001)

R. G. Unanyan, B. W. Shore, and K. Bergmann
"Entangled-State Preparation Using Adiabatic Population Transfer-Art"
Phys. Rev. A 6304(4), 3405, U536–U542 (2001)

M. VanZeeland, W. Gekelman, S. Vincena, and G. Dimonte
"Production of Alfven Waves by a Rapidly Expanding Dense Plasma"
Phys. Rev. Lett. 8710(10), 55–57 (2001)

N. V. Vitanov, T. Halfmann, B. W. Shore, and K. Bergmann
"Laser-Produced Population Transfer by Adiabatic Passage Techniques"
Ann. Rev. Phys. Chem. 52, 763–809 (2001)

R. G. Watt, R. E. Chrien, K. A. Klare, T. J. Murphy, D. C. Wilson, and S. Haan
"A Sensitive Neutron Spectrometer for the National Ignition Facility"
Rev. Sci. Inst. 72(1 Pt2), 846–849 (2001)

K. B. Wharton, C. D. Boley, A. M. Komashko, A. M. Rubenchik, J. Zweiback, J. Crane, G. Hays, T. E. Cowan, and T. Ditmire
"Effects of Nonionizing Prepulses in High-Intensity Laser-Solid Interactions"
Phys. Rev. E 64(2 Pt2), 15–17 (2001)

K. Widmann, G. Guethlein, M. E. Foord, R. C. Cauble, F. G. Patterson, D. F. Price, F. J. Rogers, P. T. Springer, R. E. Stewart, A. Ng, T. Ao, and A. Forsman
"Interferometric Investigation of Femtosecond Laser-Heated Expanded States"
Phys. Plasmas 8(9), 3869–3872 (2001)

S. C. Wilks, A. B. Langdon, T. E. Cowan, M. Roth, M. Singh, S. Hatchett, M. H. Key, D. Pennington, A. MacKinnon, and R. A. Snavely
"Energetic Proton Generation in Ultra-Intense Laser-Solid Interactions"
Phys. Plasmas 8(2), 542–549 (2001)

O. Willi, D. H. Campbell, A. Schiavi, M. Borghesi, M. Galimberti, L. A. Gizzi, W. Nazorov, A. J. MacKinnon, A. J. Pukhov, and J. Meyer-Ter-Vehn
"Relativistic Laser Propagation Through Underdense and Overdense Plasmas"
Laser and Part. Beams 19(1), 5–13 (2001)

E. Wolfrum, A. M. Allen, I. Al'Miev, T. W. Barbee, P. D. S. Burnett, A. Djaoui, C. Iglesia, D. H. Kalantar, R. W. Lee, R. Keenan, M. H. Key, C. L. S. Lewis, A. M. Machacek, B. A. Remington, S. J. Rose, R. O'Rourke, and J. S. Wark
"Measurement of the XUV Mass Absorption Coefficient of an Overdense Liquid Metal"
J. of Phys. B 34(17), l565–L570 (2001)

Z. L. Wu, C. J. Stolz, S. C. Weakley, J. D. Hughes, and Q. Zhao
"Damage Threshold Prediction of Hafnia/Silica Multilayer Coatings by Nondestructive Evaluation of Fluence-Limiting Defects"
Appl. Opt. 40(12), 1897–1906 (2001)

K. Yasuike, M. H. Key, S. P. Hatchett, R. A. Snavely, and K. B. Wharton
"Hot Electron Diagnostic in a Solid Laser Target by K-Shell Lines Measurement from Ultraintense Laser–Plasma Interactions (3×10^{20} W/cm^2, $\leq$ 400 J)"
Rev. Sci. Inst. 72(1Pt2), 1236–1240 (2001)

J. A. Young and R. C. Cook
"Helix Reversal Motion in Polyisocyanates"
Micromolecules 34(11), 3646–3653 (2001)

S. J. Zweben, J. Caird, W. Davis, D. W. Johnson, and B. P. Le Blanc
"Plasma Turbulence Imaging Using High-Power Laser Thomson Scattering"
Rev. Sci. Inst. 72(1), 1151–1154 (2001)

APPENDIX B

PUBLICATIONS AND PRESENTATIONS

October 1999–September 2000

A

Adams, J. J., Bibeau, C., Page, R. H., Krol, D. M., Furu, L. H., and Payne, S. A., *4.0–4.5 μm Lasing of Fe:ZnSe below 180 K, a New Mid-Infrared Laser Material*, Lawrence Livermore National Laboratory, CA, UCRL-JC-135419; also in *Opt. Lett.* 24(23), 1720–1722 (1999).

Alexiou, S., Lee, R. W., Glenzer, S. H., and Castor, J. I., "Analysis of Discrepancies Between Quantal and Semiclassical Calculations of Electron Impact Broadening in Plasmas," *J. Quant. Spectros. Radiat. Transfer* 65(1-3), 15–22 (2000).

Amendt, P., Bradley, D. K., Collins, G., Haan, S., Landen, O., and Wallace, R., *Ablative Characterization Experiments on OMEGA in Cylindrical Hohlraums: Analysis and Improved Designs*, Lawrence Livermore National Laboratory, Livermore, CA, UCRL-JC-139501 ABS. Prepared for the *42nd Annual Mtg of the American Physical Society Div of Plasma Physics*, Quebec, Canada, Oct 23–27, 2000.

Amendt, P., Landen, O., Pollaine, S., Suter, L. J., and Hammel, B., *Implosion Target Surrogacy Studies on OMEGA for the National Ignition Facility: Backlit Foamballs and Thinshells*, Lawrence Livermore National Laboratory, Livermore, CA, UCRL-JC-138241-ABS. Prepared for *30th Annual Anomalous Absorption Conf*, Ocean City, MD, May 21–26, 2000.

Amendt, P., *Pseudomoment Fluid Modeling: Ion-Acoustic Landau Damping and Non-Equilibrium Temperature*, Lawrence Livermore National Laboratory, Livermore, CA, UCRL-JC-127254 Rev l. Submitted to *Phys. of Plasmas*.

Amendt, P., Turner, R. E., Bradley, D., Landen, O., Haan, S., Suter, L. J., Wallace, R., Morse, S., Pien, G., Seka, W., and Soures, J. M., *High-Convergence Indirect-Drive Implosions on OMEGA in the Absence of Argon Fuel-Dopant*, Lawrence Livermore National Laboratory, Livermore, CA, UCRL-JC-138240-ABS. Prepared for *30th Annual Anomalous Absorption Conf*, Ocean City, MD, May 21–26, 2000.

Aschke, L., Depierreux, S., Estabrook, K. G., Fournier, K. B., Fuchs, J., Glenzer, S., Lee, R. W., Rozmus, W., Thoe, R. S., and Young, P. E., "Towards an Experimental Benchmark for Aluminum X-Ray Spectra," *J. Quant. Spectros. Radiat. Transfer* 65(1-3), 23–30 (2000).

B

Back, C. A., Bauer, J. D., Hammer, J. H., Lasinski, B. F., Turner, R. E., Rambo, P. W., Landen, O. L., Suter, L. J., Rosen, M. D., and Hsing, W. W., *Diffusive, Supersonic X-Ray Transport in Radiatively-Heated Foam Cylinders*, Lawrence Livermore National Laboratory, Livermore, CA, UCRL-JC-136316; also in *Phys. Plasmas* 7(5), 2126–2134 (2000).

Back, C. A., Bauer, J. D., Landen, O. L., Turner, R. E., Lasinski, B. F., Hammer, J. H., Rosen, M. D., Suter, L. J., and Hsing, W. H., *Detailed Measurements of a Diffusive Supersonic Wave in a Radiatively Heated Foam*, Lawrence Livermore National Laboratory, Livermore, CA, UCRL-JC-135062; also in *Phys. Rev. Lett*. 84(2), 274–277 (2000).

Back, C. A., Golovkin, I., Mancini, R., Missalla, T., Landen, O. L., Lee, R. W., and Klein, L., *Diagnosing Plasma Gradients Using Spectral Line Shapes*, Lawrence Livermore National Laboratory, Livermore, CA, UCRL-JC-139309 ABS. Prepared for the *15th Intl Conf on Spectral Line Shapes*, Berlin, Germany, Jul l0–14, 2000.

Back, C. A., Grun, J., Decker, C. D., Davis, J., Laming, J. M., Feldman, U., Suter, L. J., Landen, O. L., Miller, M., Serduke, F., and Wuest, C., *X-Ray Sources Generated from Gas-Filled Laser-Heated Targets*, Lawrence Livermore National Laboratory, Livermore, CA, UCRL-JC-138111. Prepared for the *22th American Physical Society Topical Conf on Atomic Processes in Plasmas*, Reno, NV, Mar 19–24, 2000.

Back, C. A., Grun, J., Decker, C. D., Davis, J., Laming, M., Feldman, U., Landen, O. L., Suter, L. J., Miller, M., Serduke, F., and Wuest, C., *X-Ray Sources Generated from Gas-Filled Laser-Heated Targets*, Lawrence Livermore National Laboratory, Livermore, CA, UCRL-JC-138111-ABS. Prepared for *12th American Physical Society Topical Conf on Atomic Processes in Plasma*, Reno, NV, Mar 19–24, 2000.

Back, C. A., Woolsey, N. C., Missalla, T., Landen, O. L., Libby, S. B., Klein, L. S., and Lee, R. W., *Implosions: An Experimental Testbed for High Energy Density Physics*, Lawrence Livermore National Laboratory, Livermore, CA, UCRL-JC-129715; also in *Astrophys. J*. 127, 227–232 (2000).

Bajt, S., Barty, A., Nugent, K. A., McCartney, M., Wall, M., and Paganin, D., *Quantitative Phase-Sensitive Imaging in a Transmission Electron Microscope*, Lawrence Livermore National Laboratory, Livermore, CA, UCRL-JC-133368; also in *Ultramicroscopy* 83(1-2), 67–73 (2000).

Bajt, S., *Molybdenum-Ruthenium/Beryllium Multilayer Coatings*, Lawrence Livermore National Laboratory, Livermore, CA, UCRL-JC-136089; also in *J. Vac. Sci. Tech. A* 18(2), 557–559 (2000).

Baker, K. L., Drake, R. P., Bauer, B. S., and Estabrook, K. G., *Observation of the Langmuir Decay Instability Driven by Stimulated Raman Scattering*, Lawrence Livermore National Laboratory, Livermore, CA, UCRL-JC-138496 ABS. Submitted to *Phys. of Plasmas*.

Baker, K. L., Drake, R. P., Estabrook, K. G., Sleaford, B., Prasad, M. K., La Fontaine, B., and Villeneuve, D. M., "Measurement of the Frequency and Spectral Width of the Langmuir Wave Spectrum Driven by Stimulated Raman Scattering," *Phys. Plasmas* 6(11), 4284–4292 (1999).

Baldis, H., Kalantar, D. H., Remington, B. A., Weber, S. V., Meyers, M. A., Wark, J. S., Ravichandran, G., and Hauer, A. A., *Studies of Dynamic Properties of Shock Compressed Solids by In-Situ Transient X-Ray Diffraction*, Lawrence Livermore National Laboratory, Livermore, CA, UCRL-ID-139526.

Banks, P. S., Dinh, L., Stuart, B. C., Feit, M. D., Komashko, A. M., Rubenchik, A. M., Perry, M. D., and McLean, W., *Short-Pulse Laser Deposition of Diamond-Like Carbon Thin Films,* Lawrence Livermore National Laboratory, CA, UCRL-JC-134974; also in *Appl. Phys. A* 69(SUPPS), S347–S353.

Banks, P. S., Feit, M. D., Rubenchik, A. M., Stuart, B. C., and Perry, M. D., *Material Effects in Ultra-Short Pulse Laser Drilling of Metals,* Lawrence Livermore National Laboratory, CA, UCRL-JC-133743; also in *Appl. Phys. A* 69 (SUPPS), S377–S380 (1999).

Bayramian, A. J., Bibeau, C., Beach, R. J., Marshall, C. D., and Payne, S. A., *Consideration of Stimulated Raman Scattering in Yb:$Sr_5(PO_4)_3F$ Laser Amplifiers*, Lawrence Livermore National Laboratory, Livermore, CA, UCRL-JC-136913; also in *Appl. Opt*. 39(21), 3746–3753 (2000).

Bayramian, A. J., Bibeau, C., Beach, R. J., Marshall, C. D., Payne, S. A., and Krupke, W. F., *Three-Level Q-Switched Laser Operation of Ytterbium-Doped $Sr_5(PO_4)_3F$ at 985 nm*, Lawrence Livermore National Laboratory, Livermore, CA, UCRL-JC-136792; also in *Opt. Lett*. 25(9), 622–624 (2000).

Bayramian, A. J., Bibeau, C., Schaffers, K. I., Marshall, C. D., and Payne, S. A., *Gain Saturation Measurements of Ytterbium-Doped $Sr_5(PO_4)_3F$*, Lawrence Livermore National Laboratory, Livermore, CA, UCRL-JC-133980; also in *Appl. Optics* 39(6), 982–985 (2000).

Bennett, G. R., Wallace, J. M., Murphy, T. J., Chrien, R. E., Delamater, N. D., Gobby, P. L., Hauer, A. A., Klare, K. A., Oertel, J. A., Watt, R. G., Wilson, D. C., Varnum, W. S., Craxton, R. S., Glebov, V. Yu., Schnittman, J. D., Stoeckl, C., Pollaine, S. M., and Turner, R. E., "Moderate-Convergence Inertial Fusion Implosions in Tetrahedral Hohlraums at Omega," *Phys. Plasmas* 7(6), 2594–2603 (2000).

Berger, R. L., Divol, L., Hinkel, D. E., Kirkwood, R. K., Glenzer, S., Langdon, A. B., Moody, J. D., Still, C. H., Suter, L., Williams, E. A., and Young, P E., *Modeling the Backscatter and Transmitted Light Spectra of High Power Smoothed Beams with pF3D, a Massively Parallel Laser Plasma Interaction Code*, Lawrence Livermore National Laboratory, Livermore, CA, UCRL-JC-137900-ABS. Prepared for *26th European Conf on Laser Interaction with Matter*, Prague, Czech Republic, Jun 12–16, 2000.

Berger, R. L., Langdon, A. B., Hinkel, D. E., Still, C. H., and Williams, E. A., *Influence of Nonlocal Electron Heat Conduction on the Induced Incoherence of Light Transmitted through Plasma,* Lawrence Livermore National Laboratory, Livermore, CA, UCRL-JC-136373. Submitted to *Phys. Rev. Lett*.

Berger, R. L., Williams, E. A., Tikhonchuk, V. T., Brantov, A., Rozmus, W., Bychenkov, V., Valeo, E., and Brunner, S., *Thermal Effects on Laser Beam Interactions with Plasma: Collisional to Collisionless*, Lawrence Livermore National Laboratory, Livermore, CA, UCRL-JC-139463 ABS. Prepared for the *42nd Annual Mtg of the American Physical Society Div of Plasma Physics*, Quebec, Canada, Oct 23–27, 2000.

Bernat, T., Nobile, A., and Schultz, K., *Fabrication of Indirect Drive Ignition Targets for the NIF: Recent Developments*, Lawrence Livermore National Laboratory, Livermore, CA, UCRL-JC-138259-ABS. Prepared for *18th IAEA Fusion Energy Conf*, Sorrento, Italy, Oct 4–10, 2000.

Bibeau, C., Bayramian, A., Beach, R. J., Chanteloup, J. C., Ebbers, C. A., Emanuel, M. A., Orth, C. D., Payne, S. A., Rothenberg, J. E., Powell, H. T., Shaffers, K. I., Skidmore, J. A., Sutton, S. B., and Zapata, L. E., *Mercury and Beyond: Diode-Pumped Solid-State Lasers for Inertial Fusion Energy*, Lawrence Livermore National Laboratory, Livermore, CA, UCRL-JC-133970; also in *Comptes Rendus* 1(6), 745–749 (2000).

Boehly, T. R., Bradley, D. K., Fisher, Y., Meyerhofer, D. D., Seka, W., and Soures, J. M., *Effects of Optical Prepulse on Direct-Drive Inertial Confinement Fusion Target Performance*, Lawrence Livermore National Laboratory, Livermore, CA, UCRL-JC-137876. Submitted to *Phys. Plasmas.*

Borghesi, M., MacKinnon, A. J., Campbell, H. D., Galimberti, M., Gizzi, L. A., Nazarov, W., Schiavi, A., and Willi, O., *Propagation Issues and Fast Particle Source Characterization in Laser–Plasma Interactions at Intensities Exceeding 10^{19} W/cm^2*, Lawrence Livermore National Laboratory, Livermore, CA, UCRL-JC-138316 ABS. Prepared for the *26th European Conf on Laser Interaction with Matter*, Prague, Czech Republic, Jun 12–16, 2000.

Bradley, D. K., Bell, P. M., Dymoke-Bradshaw, A. K. L., Hares, J. D., and Bahr, R., *Development and Characterization of a Single Line of Sight Framing Camera*, Lawrence Livermore National Laboratory, Livermore, CA, UCRL-JC-138002-ABS. Prepared for *High Temperature Diagnostics Mtg*, Tucson, AZ, Jun 18–22, 2000.

Bradley, D. K., Bell, P. M., Dymoke-Bradshaw, A. K. L., Hares, J. D., Bahr, R. E., and Smalyuk, V. A., *Development and Characterization of a Single Line of Sight Framing Camera*, Lawrence Livermore National Laboratory, Livermore, CA, UCRL-JC-138002. Prepared for the *13th Topical Conf on High-Temperature Plasma Diagnostics*, Tucson, AZ, Aug 18–22, 2000.

Bradley, D. K., Collins, G. W., Celliers, P., Moon, S., Da Silva, L. B., Cauble, R., Hammel, B. A., and Wallace, R. J., *Shock Compressing Diamond into the Metallic Phase*, Lawrence Livermore National Laboratory, Livermore, CA, UCRL-JC-131400 ABS Rev l. Prepared for the *42nd Annual Mtg of the American Physical Society Div of Plasma Physics*, Quebec, Canada, Oct 23–27, 2000.

Bryant, R., *NIF ICCS Network Design and Loading Analysis*, Lawrence Livermore National Laboratory, Livermore, CA, UCRL-ID-135920.

Budil, K. S., Gold, D. M., Estabrook, K. G., Remington, B. A., Kane, J., Bell, P. M., Pennington, D. M., Brown, C., Hatchett, S. P., Koch, J. A., Key, M. H., and Perry, M. D., *Development of a Radiative-Hydrodynamics Testbed Using the Petawatt Laser Facility*, Lawrence Livermore National Laboratory, Livermore, CA, UCRL-JC-131549; also in *Astrophys. J.* 127, 261–265 (2000).

Bullock, A. B., and Bolton, P. R., *Optical Spectral Emission Picosecond Pulse Laser-Induced Back-Ablation of Aluminum Films*, Lawrence Livermore National Laboratory, Livermore, CA, UCRL-JC-138916. Submitted to *J. Appl. Phys*.

Bullock, A. B., Landen, O. L., and Bradley, D. K., *10 μm and 5 μm Pinhole-Assisted Point-Projection Backlit Imaging for NIF*, Lawrence Livermore National Laboratory, Livermore, CA, UCRL-JC-137904-ABS. Prepared for *High Temperature Diagnostics Mtg*, Tuscon, AZ, Jun 18–22, 2000.

Bullock, A. B., Landen, O. L., and Bradley, D. K., *10 μm and 5 μm Pinhole-Assisted Point-Projection Backlit Imaging for NIF*, Lawrence Livermore National Laboratory, Livermore, CA, UCRL-JC-137904. Prepared for the *13th Topical Conf on High-Temperature Plasma Diagnostics*, Tucson, AZ, Jun 18–22, 2000.

Bullock, A. B., Landen, O. L., and Bradley, D. K., *Modeling of Multi-Kilovolt X-Ray Driven Ablation and Closure of Pinholes during Point-Projection Backlit Imaging*, Lawrence Livermore National Laboratory, Livermore, CA, UCRL-JC-139589 ABS. Prepared for the *42nd Annual Mtg of the American Physical Society Div of Plasma Physics*, Quebec, Canada, Oct 23–27, 2000.

Bullock, A. B., Landen, O. L., and Bradley, D. K., *Multi-Kilovolt X-Ray Driven Ablation and Closure of 5 μm and 10 μm Pinholes During Point-Projection Backlit Imaging*, Lawrence Livermore National Laboratory, Livermore, CA, UCRL-JC-138515 ABS. Prepared for the *30th Annual Anomalous Absorption Conf*, Ocean City, MD, May 21–26, 2000.

Bullock, A. B., Landen, O. L., and Bradley, D. K., *Relative X-Ray Backlighter Intensity Comparison of Ti and Ti/Sc Combination Foils Driven in Double-Sided and Single-Sided Laser Configuration*, Lawrence Livermore National Laboratory, Livermore, CA, UCRL-JC-137906-ABS. Prepared for *High Temperature Diagnostics Mtg*, Tuscon, AZ, Jun 18–22, 2000.

Bullock, A. B., Landen, O. L., and Bradley, D. K., *Relative X-Ray Backlighter Intensity Comparison of Ti and Ti/Sc Combination Foils Driven in Double-Sided and Single-Sided Laser Configuration*, Lawrence Livermore National Laboratory, Livermore, CA, UCRL-JC-139282. Prepared for the *13th Topical Conf on High-Temperature Plasma Diagnostics*, Tucson, AZ, Jun 18–22, 2000.

Burnham, A., Runkel, M., Demos, S., Kozlowski, M., and Wegner, P., *Effect of Vacuum on the Occurrence of UV-Induced Surface Photoluminescence, Transmission Loss, and Catastrophic Surface Damage*, Lawrence Livermore National Laboratory, Livermore, CA, UCRL-JC-137123-ABS. Prepared for *Society of Photo-Optical Instrumentation Engineers 45th Annual Mtg*, San Diego, CA, Jul 30–Aug 4, 2000.

C

Callahan-Miller, D. A., and Tabak, M., *Progress in Target Physics and Design for Heavy Ion Fusion*, Lawrence Livermore National Laboratory, Livermore, CA, UCRL-JC-134746; also in *Phys. Plasmas* 7(5), 2083–2091 (2000).

Campbell, J. H., and Suratwala, T. I., *Nd-Doped Phosphate Glasses for High-Energy/High-Peak-Power Lasers*, Lawrence Livermore National Laboratory, Livermore, CA, UCRL-JC-132911 Rev 1; also in *J. Non-Cryst. Solids* 263(1-4), 318–341 (2000).

Campbell, J. H., Suratwala, T. I., Thorsness, C. B., Hayden, J. S., Thorne, A. J., Cimino, J. M., Marker, A. J., Takeuchi, K., Smolley, M., and Ficini-Dorn, G. F., *Continuous Melting of Phosphate Laser Glass*, Lawrence Livermore National Laboratory, Livermore, CA, UCRL-JC-134194; also in *J. Non-Cryst. Solids* 263(1-4), 342–357 (2000).

Cauble, R., Celliers, P. M., Collins, G. W., Da Silva, L. B., Gold, D. M., Foord, M. E., Budil, K. S., and Wallace, R. J., *Equation of State and Material Property Measurements of Hydrogen Isotopes at the High-Pressure, High-Temperature, Insulator-Metal Transition*, Lawrence Livermore National Laboratory, Livermore, CA, UCRL-JC-132210; also in *Astrophys. J.* 127(2), 267–273 (2000).

Cauble, R., Remington, B. A., and Campbell, E. M., *Laboratory Measurements of Materials in Extreme Conditions: The Use of High Energy Radiation Sources for High Pressure Studies*, Lawrence Livermore National Laboratory, CA, UCRL-JC-131079; also in *J. Impact Engr.* 23(1) Pt.1, 87–99 (1999).

Celliers, P. M., and Conia, J., *Measurement of Localized Heating in the Focus of an Optical Trap*, Lawrence Livermore National Laboratory, Livermore, CA, UCRL-JC-136479; also in *Appl. Opt.* 39(19), 3396–3407 (2000).

Celliers, P. M., Collins, G. W., Bradley, D. K., Cauble, R., Moon, S. J., Wallace, R. J., Hammel, B. A., and Hsing, W. W., *Optical Measurements of Strongly-Shocked Water*, Lawrence Livermore National Laboratory, Livermore, CA, UCRL-JC-138777 ABS. Prepared for the *1st Intl Workshop on Warm Dense Matter*, Vancouver, BC, May 28–31, 2000.

Celliers, P. M., Collins, G. W., Bradley, D. K., Cauble, R., Munro, D. H., Moon, S. J., Gold, D. M., Da Silva, L. B., Weber, F. A., Wallace, R. J., Hammel, B. A., and Hsing, W. W., *VISAR for Measuring EOS and Shock Propagation in Liquid Deuterium and Other Dielectrics*, Lawrence Livermore National Laboratory, Livermore, CA, UCRL-JC-138446 ABS. Prepared for the *13th Topical Conf on High-Temperature Plasma Diagnostics*, Tucson, AZ, Jun 19–22, 2000.

Celliers, P. M., Collins, G. W., Da Silva, L. B., Cauble, R., Moon, S. J., Wallace, B. A., Hammel, B. A., and Hsing, W. W., *Multiple-Shock Compression of Liquid Deuterium*, Lawrence Livermore National Laboratory, Livermore, CA, UCRL-JC-136861 ABS. Prepared for *American Physical Society March Mtg*, Minneapolis, MN, Mar 20, 2000.

Celliers, P. M., Collins, G. W., Da Silva, L. B., Cauble, R., Moon, S. J., Wallace, R. J., Hammel, B. A., Hsing, W. W., Masclet, I., Marchet, B., Rebec, M., Reverdin, C., Koenig, M., Benuzzi, A., and Batani, D., *Optical Measurements of Strongly-Shocked Water*, Lawrence Livermore National Laboratory, Livermore, CA, UCRL-JC-138777 ABS Rev l. Prepared for the *42nd Annual Mtg of the American Physical Society Div of Plasma Physics*, Quebec, Canada, Oct 23–27, 2000.

Celliers, P. M., Collins, G. W., Da Silva, L. B., Gold, D. M., Cauble, R., Wallace, R. J., Foord, M. E., and Hammel, B. A., *Shock-Induced Transformation of Liquid Deuterium into a Metallic Fluid*, Lawrence Livermore National Laboratory, Livermore, CA, UCRL-JC-130339 Rev 1; also in *Phys. Rev. Lett*. 84(24), 5564–5567 (2000).

Cherfils, C., and Lafitte, O., "Analytic Solutions of the Rayleigh Equation for Linear Density Profiles," *Phys. Rev E* 62(2PtB), 2967–2970 (2000).

Cherfils, C., Glendinning, S. G., Galmiche, D., Remington, B. A., Richard, A. L., Haan, S., Wallace, R., Dague, N., and Kalantar, D. H., *Convergent Rayleigh–Taylor Experiments on the Nova Laser*, Lawrence Livermore National Laboratory, CA, UCRL-JC-135371; also in *Phys. Rev. Lett*. 83 (26), 5507–5510 (1999).

Clark, D. S., Fisch, N. J., Langdon, A. B., and Valeo, E. J., *Stability of High Power Laser Pulse to Backward Raman Scattering in Plasma*, Lawrence Livermore National Laboratory, Livermore, CA, UCRL-JC-139715 ABS. Prepared for the *42nd Annual Mtg of the American Physical Society Div of Plasma Physics*, Quebec, Canada, Oct 23–27, 2000.

Collins, G. W., Bradley, D. K., Celliers, P., Silva, L. B., Cauble, R., Moon, S. J., Hammel, B. A., Wallace, R. J., Koenig, M., and Benuzzi-Mounaix, A., *Shock Compressing H_2O into an Electronic Conductor*, Lawrence Livermore National Laboratory, Livermore, CA, UCRL-JC-136738 ABS. Prepared for *American Physical Society March Mtg*, Minneapolis, MN, Mar 20, 2000.

Collins, G. W., Celliers, P. M., Da Silva, L. B., Gold, D. M., and Cauble, R., *Laser-Shock-Driven Laboratory Measurements of the Equation of State of Hydrogen Isotopes in the Megabar Regime*, Lawrence Livermore National Laboratory, Livermore, CA, UCRL-JC-135406; also in *High Press. Res*. 16(5-6), 281–290 (2000).

Collins, G. W., Celliers, P. M., Da Silva, L. B., Munro, D., Cauble, R., Wallace, R. J., Moon, S. J., Hammel, B. A., and Hsing, W., *Multiple-Shock Compression of Liquid Deuterium*, Lawrence Livermore National Laboratory, Livermore, CA, UCRL-JC-136861 ABS Rev l. Prepared for the *42nd Annual Mtg of the American Physical Society Div of Plasma Physics*, Quebec, Canada, Oct 23–27, 2000.

Colvin, J. D., Remington, B. A., Kalantar, D. H., and Weber, S. V., *Experimental Evidence for Shock Softening and Hardening of Metals at High Strain Rate,* Lawrence Livermore National Laboratory, Livermore, CA, UCRL-JC-136707. Submitted to *Phys. Rev. Lett*.

Colvin, J. D., *Summary of Vulcan Calculations*, Lawrence Livermore National Laboratory, Livermore, CA, UCRL-ID-138455.

Cook, R., *Models of Polyimide Spray Coating*, Lawrence Livermore National Laboratory, Livermore, CA, UCRL-JC-136289; also in *Fusion Tech*. 38, 74–82 (2000).

Crichton, S. N., Tomozawa, M., Hayden, J. S., Suratwala, T. I., and Campbell, J. H., *Subcritical Crack Growth in a Phosphate Laser Glass*, Lawrence Livermore National Laboratory, CA, UCRL-JC-131864; also in *J. Am. Ceramic. Soc*. 82(11), 3097–3104 (1999).

D

Dattolo, E., Suter, L., Monteil, M.-C., Jadaud, J.-P., Dague, N., Glenzer, S., Turner, R., Juraszek, D., Lasinski, B., Decker, C., Landen, O., and MacGowan, B., *Status of Our Understanding and Modeling of X-Ray Coupling Efficiency in Laser Heated Hohlraums*, Lawrence Livermore National Laboratory, Livermore, CA, UCRL-JC-137622 Rev l. Submitted to *Phys. of Plasmas*.

Delage, O., Lerche, R. A., Sangster, T. C., and Arsenault, H. H., *SIRINC: a Code for Assessing and Optimizing the Neutron Imaging Diagnostic Capabilities in ICF Experiments*, Lawrence Livermore National Laboratory, Livermore, CA, UCRL-JC-137922-ABS. Prepared for *13th Topical Conf on High-Temperature Plasma Diagnostics*, Tucson, AZ, Jun 18–22, 2000.

Depierreux, S., Labaune, C., Fuchs, J., and Baldis, H. A., "Application of Thomson Scattering to Identify Ion Acoustic Waves Stimulated by the Langmuir Decay Instability," *Rev. Sci. Inst*. 71(9), 3391–3401 (2000).

Dimonte, G., *Spanwise Homogeneous Buoyancy-Drag Model for Nonlinear Rayleigh–Taylor Instability*, Lawrence Livermore National Laboratory, Livermore, CA, UCRL-JC-139368 ABS. Prepared for the *42nd Annual Mtg of the APS Div of Plasma Physics*, Quebec City, Canada, Oct 23–27, 2000.

Dimonte, G., *Spanwise Homogeneous Buoyancy-Drag Model for Rayleigh–Taylor Mixing and Experimental Evaluation*, Lawrence Livermore National Laboratory, Livermore, CA, UCRL-JC-133936; also in *Phys. Plasmas* 7(6) 2255–2269 (2000).

Ditmire, T., Rubenchik, A., Mirnov, V. V., and Ucer, D., *Modeling of the Expansion of Ultra-Short-Pulse Laser-Produced Plasmas in Magnetic Fields*, Lawrence Livermore National Laboratory, Livermore, CA, UCRL-JC-141060; also in *Astrophys. J*. 127, 293–297 (2000).

Ditmire, T., Shigemori, K., Remington, B. A., Estabrook, K., and Smith, R. A., *The Production of Strong Blast Waves Through Intense Laser Irradiation of Atomic Clusters*, Lawrence Livermore National Laboratory, Livermore, CA, UCRL-JC-131534; also in *Astrophys. J*. 127, 299–304 (2000).

Ditmire, T., Zweiback, J., Yanovsky, V. P., Cowan, T. E., Hays, G., and Wharton, K. B., *Nuclear Fusion in Gases of Deuterium Clusters Heated by Femtosecond Laser*, Lawrence Livermore National Laboratory, Livermore, CA, UCRL-JC-136978 Rev 1; also in *Phys. Plasmas* 7(5), 1993–1998 (2000).

Dittrich, T. R., Haan, S. W., and Hinkel, D. E., *Small Scale Capsules for the National Ignition Facility*, Lawrence Livermore National Laboratory, Livermore, CA, UCRL-JC-139492 ABS. Prepared for the *42nd Annual Mtg of the American Physical Society Div of Plasma Physics*, Quebec, Canada, Oct 23–27, 2000.

Dittrich, T. R., Haan, S. W., and Strobel, G. L., *Effects of ^{3}He Buildup in the DT Gas in NIF Ignition Capsules*, Lawrence Livermore National Laboratory, Livermore, CA, UCRL-JC-139491 ABS. Prepared for the *42nd Annual Mtg of the American Physical Society Div of Plasma Physics*, Quebec, Canada, Oct 23–27, 2000.

Drake, R. P., Carroll III, J. J., Smith, T. B., Keiter, P., Glendinning, S. G., Hurricane, O., Estabrook, K., Ryutov, D. D., Remington, B. A., Wallace, R. J., Michael, E., and McCray, R., "Laser Experiments to Simulate Supernova Remnants," *Phys. Plasmas* 7(5), 2142–2148 (2000).

Drake, R. P., Robey, H. F., Hurricane, O. A., Remington, B. A., Knauer, J., Arnett, D., Ryutov, D. D., Kane, J. O., Budil, K. S., and Grove, J., *Experiments to Produce a Hydrodynamically Unstable, Spherically Diverging System of Relevance to Instabilities in Supernovae*, Lawrence Livermore National Laboratory, Livermore, CA, UCRL-JC-139077. Submitted to *Astrophys. J*.

Drake, R. P., Smith, T. B., Carroll III, J. J., Yan, Y., Glendinning, S. G., Estabrook, K., Ryutov, D. D., Remington, B. A., Wallace, R. J., and McCray, R., "Progress Toward the Laboratory Simulation of Young Supernova Remnants," *Astrophys. J*. 127, 305–310 (2000).

Dunn, J., Li, Y., Osterheld, A. L., Nilsen, J., Hunter, J. R., and Shlyaptsev, V. N., *Gain Saturation Regime for Laser-Driven Tabletop, Transient Ni-Like Ion X-Ray Lasers*, Lawrence Livermore National Laboratory, Livermore, CA, UCRL-JC-136645; also in *Phys. Rev. Lett*. 84(21), 4834–4837 (2000).

E

Eder, D. C., Pretzler, G., Fill, E., Eidmann, K., and Saemann, A., *Spatial Characteristics of K_α Radiation from Weakly Relativistic Laser Plasmas*, Lawrence Livermore National Laboratory, Livermore, CA, UCRL-JC-133236; also in *Appl. Phys. B* 70(2), 211–217 (2000).

Edwards, J., Glendinning, S. G., Suter, L. J., Remington, B. A., Landen, O., Turner, R. E., Shepard, T. J., Lasinski, B., Budil, K., Robey, H., Kane, J., Louis, H., Wallace, R., Graham, P., Dunne, M., and Thomas, B. R., *Turbulent Hydrodynamic Experiments Using a New Plasma Piston*, Lawrence Livermore National Laboratory, Livermore, CA, UCRL-JC-136317 Rev 2; also in *Phys. Plasmas* 7(5), 2099–2107 (2000).

Ehrmann, P. R., Campbell, J. H., Suratwala, T. I., Hayden, J. S., Krashkevich, D., Takeuchi, K., *Optical Loss and Nd^{3+} Non-Radiative Relaxation by Cu, Fe and Several Rare Earth Impurities in Phoshate Laser Glasses,* Lawrence Livermore National Laboratory, Livermore, CA, UCRL-JC-132910 Rev 1; also in *J. Non-Cryst. Solids* 263(1-4), 251–262 (2000).

F

Farley, D. R., and Logory, L. M., *Single-Mode, Nonlinear Mix Experiments at High Mach Number Using Nova*, Lawrence Livermore National Laboratory, Livermore, CA, UCRL-JC-139615; also in *Astrophys. J. Suppl. Ser*. 127(2), 311–316 (2000).

Foord, M. E., Glenzer, S. H., Thoe, R. S., Wong, K. L., Fournier, K. B., Wilson, B. G., and Springer, P. T., *Ionization Processes and Charge-State Distribution in a Highly Ionized High-Z Laser-Produced Plasma*, Lawrence Livermore National Laboratory, Livermore, CA, UCRL-JC-137022; also in *Phys. Rev. Lett*. 85(5), 992–995 (2000).

Foord, M. E., Glenzer, S. H., Thoe, R. S., Wong, K. L., Fournier, K. B., Albritton, J. R., Wilson, B. G., and Springer, P. T., *Accurate Determination of the Charge State Distribution in a Well Characterized Highly Ionized Au Plasma*, Lawrence Livermore National Laboratory, Livermore, CA, UCRL-JC-134388; also in *J. Quant. Spectros. Radiat. Transfer* 65(1-3), 231–241 (2000).

Frank, A. M., Lee, R. S., and Remington, B. A., *Numerical Simulations of Laser-Driven Microflyer Plates,* Lawrence Livermore National Laboratory, Livermore, CA, UCRL-JC-139603 ABS. Prepared for the *42nd Annual Mtg of the American Physical Society Div of Plasma Physics*, Quebec, Canada, Oct 23–27, 2000.

Fuchs, J., Labaune, C., Depierreux, S., Michard, A., and Baldis, H., *Modfication of Spatial and Temporal Gains of Stimulated Brillouin and Raman by Polarization Smoothing*, Lawrence Livermore National Laboratory, Livermore, CA, UCRL-JC-136786; also in *Phys. Rev. Lett*. 84(14), 3089–3092 (2000).

G

Galimberti, M., Giulietti, A., Giulietti, D., Gizzi, L. A., Borghesi, M., Campbell, H. D., MacKinnon, A. J., Schiavi, A., and Willi, O., *Gamma-Ray Measurements in Relativistic Laser Interactions with Underdense Plasmas*, Lawrence Livermore National Laboratory, Livermore, CA, UCRL-JC-138317 ABS. Prepared for the *26th European Conf on Laser Interaction with Matter,* Prague, Czech Republic, Jun 12–16, 2000.

Galmiche, D., Cherfils, C., Glendinning, S. G., Remington, B. A., and Richard, A., *Numerical Analysis of Spherically Convergent Rayleigh–Taylor Experiments*, Lawrence Livermore National Laboratory, Livermore, CA, UCRL-JC-139076. Prepared for the *26th European Conf on Laser Interaction with Matter,* Prague, Czech Republic, Jun 12–16, 2000.

Geddes, C. G. R., Kirkwood, R. K., Glenzer, S. H., Estabrook, K., Cohen, B. I., Young, P. E., Joshi, C., and Wharton, K. B., *Observation of Ion Wave Decay Products of Langmuir Waves Generated by Stimulated Raman Scattering in Ignition Scale Plasmas*, Lawrence Livermore National Laboratory, Livermore, CA, UCRL-JC-140379. Submitted to *Phys. Rev. Lett*.

Genin, F. Y., Feit, M. D., Kowzlowski, M. R., Rubenchik, A. M., Salleo, A., and Yoshiyama, J., *Rear-Surface Laser Damage on 355-nm Silica Optics Owing to Fresnel Diffraction on Front-Surface Contamination Particles*, Lawrence Livermore National Laboratory, Livermore, CA, UCRL-JC-133839; also in *Appl. Optics* 39(21), 3654–3663 (2000).

Glendinning, S. G., Bradley, D. K., Cauble, R., Edwards, J. M., Louis, H., Moreno, J., Moon, S., Remington, B. A., Turano, E., Craxton, R. S., Town, R., and Boehly, T. R., *Directly-Driven Shock Characterization in Plastics Using VISAR*, Lawrence Livermore National Laboratory, Livermore, CA, UCRL-JC-139602 ABS. Prepared for the *42nd Annual Mtg of the American Physical Society Div of Plasma Physics*, Quebec, Canada, Oct 23–27, 2000.

Glendinning, S. G., Budil, K. S., Cherfils, C., Drake, R. P., Farley, D., Kalantar, D. H., Kane, J., Marinak, M. M., Remington, B. A., Richard, A., Ryutov, D., Stone, J., Wallace, R. J., and Weber, S. V., *Experimental Measurements of Hydrodynamic Instabilities on Nova of Relevance to Astrophysics*, Lawrence Livermore National Laboratory, Livermore, CA, UCRL-JC-130104; also in *Astrophys. J.* 127, 325–331 (2000).

Glendinning, S. G., Colvin, J., Haan, S., Kalantar, D. H., Landen, O. L., Marinak, M. M., Remington, B. A., Wallace, R., Cherfils, C., Dague, N., Divol, L., Galmiche, D., and Richard, A. L., *Ablation Front Rayleigh–Taylor Growth Experiments in Spherically Convergent Geometry*, Lawrence Livermore National Laboratory, Livermore, CA, UCRL-JC-134966; also in *Phys. Plasmas* 7(5), 2033–2039 (2000).

Glenzer, S. H., Bar-Shalom, A., Fournier, K., Hammel, B., Klapisch, M., Lee, R., Suter, L., Thoe, B., and Wilson, B., *Ionization Balance in Inertial Confinement Fusion Hohlraums*, Lawrence Livermore National Laboratory, Livermore, CA, UCRL-JC-139505 ABS. Prepared for the *42nd Annual Mtg of the American Physical Society Div of Plasma Physics*, Quebec, Canada, Oct 23–27, 2000.

Glenzer, S. H., Berger, R. L., Divol, L. M., Kirkwood, R. K., MacGowan, B. J., Moody, J. D., Rothenberg, J. E., Suter, L. J., and Williams, E. A., *Laser–Plasma Interactions in Inertial Confinement Fusion Hohlraums,* Lawrence Livermore National Laboratory, Livermore, CA, UCRL-JC-136632. Submitted to *Phys. Rev. Lett*.

Glenzer, S. H., Chambers, D., Wolfrum, E., Wark, J., and Young, P. E., *Thomson Scattering on Astrophysical Plasmas*, Lawrence Livermore National Laboratory, Livermore, CA, UCRL-JC-137687-ABS. Prepared for *3rd Intl Conf on Laboratory Astrophysics with Intense Laser*, Houston, TX, Mar 30–Apr 1, 2000.

Glenzer, S. H., Estabrook, K. G., Lee, R. W., MacGowan, B. J., and Rozmus, W., *Detailed Characterization of Laser Plasmas for Benchmarking of Radiation-Hydrodynamic Modeling*, Lawrence Livermore National Laboratory, Livermore, CA, UCRL-JC-133739; also in *J. Quant. Spectros. Radiat. Transfer* 65(1-3), 253–271 (2000).

Glenzer, S. H., Fournier, K. B., Decker, C., Hammel, B. A., Lee, R. W., Lours, L., MacGowan, B. J., and Osterheld, A. L., *Accuracy of K-Shell Spectra Modeling in High-Density Plasmas*, Lawrence Livermore National Laboratory, Livermore, CA, UCRL-JC-137905; also in *Phys. Rev. E* 62 (2PT B), 2728–2738 (2000).

Glenzer, S. H., Fournier, K. B., Hammel, B. A., Lee, R. W., MacGowan, B. J., and Wilson, B. G., *Accuracy of X-Ray Spectra Modeling for Inertial Confinement Fusion Plasmas*, Lawrence Livermore National Laboratory, Livermore, CA, UCRL-JC-137557-ABS. Prepared for *12th American Physical Society Topical Conf on Atomic Processes in Plasmas,* Reno, NV, Mar 19–23, 2000.

Glenzer, S. H., Fournier, K. B., Hammel, B. A., Lee, R. W., MacGowan, B. J., and Back, C. A., *Accuracy of X-Ray Spectra Modeling of Inertial Confinement Fusion Plasmas*, Lawrence Livermore National Laboratory, Livermore, CA, UCRL-JC-137557. Prepared for the *12th American Physical Society Topical Conf on Atomic Processes in Plasmas*, Reno, NV, Mar 19–23, 2000.

Glenzer, S. H., *Observation of Saturated Brillouin Instability in Fusion Plasmas with Thomson Scattering*, Lawrence Livermore National Laboratory, Livermore, CA, UCRL-JC-139423 ABS. Prepared for *Frontier Science Research Conf and Technology of Laser–Matter Interactions*, La Jolla, CA, Jul 24–26, 2000.

Glenzer, S. H., Suter, L. J., Berger, R. L., Estabrook, K. G., Hammel, B. A., Kauffman, R. L., Kirkwood, R. K., MacGowan, B. J., Moody, J. D., and Rothenberg, J. E., *Holhraum Energetics with Smoothed Laser Beams,* Lawrence Livermore National Laboratory, Livermore, CA, UCRL-JC-136356. Submitted to *Contrib. Plasma Phys.*

Glenzer, S. H., Suter, L. J., Berger, R. L., Estabrook, K. G., Hammel, B. A., Kauffman, R. L., Kirkwood, R. K., MacGowan, B. J., Moody, J. D., Rothenberg, J. E., and Turner, R. E., *Hohlraum Energetics with Smoothed Laser Beams*, Lawrence Livermore National Laboratory, Livermore, CA, UCRL-JC-129862; also in *Phys. Plasmas* 7(6), 2585–2593 (2000).

Glenzer, S. H., Suter, L. J., Turner, R. E., Landen, O. L., Kirkwood, R. K., and Young, P. E., *Wall Losses of Soft X Rays in a Confined Hohlraum Geometry*, Lawrence Livermore National Laboratory, Livermore, CA, UCRL-JC-138516 ABS. Prepared for the *30th Annual Anomalous Absorption Conf*, Ocean City, MD, May 21–26, 2000.

Glenzer, S. H., *Thomson Scattering in Inertial Confinement Fusion Research*, Lawrence Livermore National Laboratory, Livermore, CA, UCRL-JC-135822; also in *Contrib. Plasma Phys*. 40(1-2), 36–45 (2000).

Gold, D. M., Celliers, P. M., Collins, G. W., Budil, K. S., Cauble, R., Da Silva, L. B., Foord, M. E., Stewart, R. E., Wallace, R. J., and Young, D., *Interferometric and Chirped Optical Probe Techniques for High-Pressure Equation-Of-State Measurements*, Lawrence Livermore National Laboratory, Livermore, CA, UCRL-JC-130118; also in *Astrophys. J.* 127, 333–357 (2000).

Goldman, S. R., Barnes, C. W., Caldwell, S. E., Wilson, D. C., Batha, S. H., Grove, J. W., Gittings, M. L., Hsing, W. W., Kares, R. J., Klare, K. A., Kyrala, G. A., Margevicius, R. W., Weaver, R. P., Wilke, M. D., Dunne, A. M., Edwards, M. J., Graham, P., and Thomas, B. R., *Production of Enhanced Pressure Regions Due to Inhomogeneities in Inertial Fusion Targets*, Lawrence Livermore National Laboratory, Livermore, CA, UCRL-JC-137588; also in *Phys. Plasmas* 7(5), 2007–2013 (2000).

Goldman, S. R., Caldwell, S. E., Wilke, M. D., Wilson, D. C., Barnes, C. W., Hsing, W. W., Delamater, N. D., Schappert, G. T., Grove, J. W., Lindman, E. L., Wallace, J. M., Weaver, R. P., Dunne, A. M., Edwards, M. J., Graham, P., and Thomas, B. R., *Shock Structuring due to Fabrication Joints in Targets*, Lawrence Livermore National Laboratory, Livermore, CA, UCRL-JC-137462. Submitted to *Phys. Plasmas.*

H

Haan, S. W., Dittrich, T. R., Marinak, M. M., and Hinkel, D. E., *Design of Ignition Targets for the National Ignition Facility,* Lawrence Livermore National Laboratory, Livermore, CA, UCRL-JC-133510. Prepared for *1st Intl Conf on Inertial Fusion Sciences and Applications,* Bordeaux, France, Sep 12, 1999.

Haan, S. W., Dittrich, T., Hinkel, D., Marinak, M., Munro, D., Strobel, G., Suter, L., Pollaine, S., Jones, O., and Lindl, J., *Hydrodynamic Instabilities and Thermonuclear Ignition on the National Ignition Facility*, Lawrence Livermore National Laboratory, Livermore, CA, UCRL-JC-137000-ABS. Prepared for *American Physical Society April Mtg 2000*, Long Beach, CA, Apr 29–May 2, 2000.

Haan, S. W., Glendinning, S. G., Turner, R. E., and Amendt, P. A., *Analysis of Polyimide Rayleigh-Taylor Experiments on OMEGA*, Lawrence Livermore National Laboratory, Livermore, CA, UCRL-JC-139502 ABS. Prepared for the *42nd Annual Mtg of the American Physical Society Div of Plasma Physics*, Quebec, Canada, Oct 23–27, 2000.

Haan, S. W., Strobel, G. L., Dittrich, T. R., Suter, L. J., Lindl, J. D., and Herrmann, M. C., *Absorbed Energy Dependence of Surface Roughness Requirements for 250 eV Ignition Capsules*, Lawrence Livermore National Laboratory, Livermore, CA, UCRL-JC-139504 ABS. Prepared for the *42nd Annual Mtg of the American Physical Society Div of Plasma Physics*, Quebec, Canada, Oct 23–27, 2000.

Haber, I., Callahan, D. A., Friedman, A., Grote, D. P., and Langdon, A. B., *Transverse-Longitudinal Temperature Equilibration in a Long Uniform Beam,* Lawrence Livermore National Laboratory, Livermore, CA, UCRL-JC-136630. Prepared for *Inst of Electrical and Electronics Engineers, Inc. Particle Accelerator Conf*, Dallas, TX, May 1, 1995.

Hammel, B. A., *Recent Advances in Indirect Drive ICF Target Physics*, Lawrence Livermore National Laboratory, Livermore, CA, UCRL-JC-138130-ABS. Prepared for *18th Fusion Energy Conf*, Sorrento, Italy, Oct 4–10, 2000.

Hartemann, F. V., Landahl, E. C., Troha, A. L., Van Meter, J. R., Baldis, H. A., Freeman, R. R., Luhman, N. C., Song, L., Kerman, A. K., and Yu, D. U. L., *The Chirped-Pulse Inverse Free-Electron Laser: A High-Gradient Vacuum Laser Accelerator*, Lawrence Livermore National Laboratory, CA, UCRL-JC-134073; also in *Phys. Plasmas* 6(10), 4104–4110 (1999).

Hartemann, F. V., Troha, A. L., Baldis, H. A., Gupta, A., Kerman, A. K., Lindahl, E. C., Luhman, Jr., N. C., and Van Meter, J. R.,"High-Intensity Scattering Processes of Relativistic Electrons in Vacuum and Their Relevance to High-Energy Astrophysics," *Astrophys. J*. 127, 347–356 (2000).

Hatchett, S. P., Brown, C. G., Cowan, T. E., Henry, E. A., Johnson, J. S., Key, M. H., Koch, J. A., Langdon, A. B., Lasinski, B. F., Lee, R. W., MacKinnon, A. J., Pennington, D. M., Perry, M. D., Phillips, T. W., Roth, M., Sangster, T. C., Singh, M. S., Snavely, R. A., Stoyer, M. A., Wilks, S. C., and Yasuike, K., *Electron, Photon, and Ion Beams from the Relativistic Interaction of Petawatt Laser Pulses with Solid Targets*, Lawrence Livermore National Laboratory, Livermore, CA, UCRL-JC-135029; also in *Phys. Plasmas* 7(5), 2076–2082 (2000).

Hawley-Fedder, R., Robey, H., Biesiada, T., DeHaven, M., Floyd, R., and Burnham, A., *Rapid Growth of Very Large KDP and KD*P Crystals in Support of the National Ignition Facility*, Lawrence Livermore National Laboratory, Livermore, CA, UCRL-JC-137102-ABS. Prepared for *Society of Photo-Optical Instrumentation Engineers 45th Annual Mtg*, San Diego, CA, Jul 30–Aug 4, 2000.

Hayden, J. S., Marker, A. J., Suratwala, T. I., and Campbell, J. H., *Surface Tensile Layer Generation during Thermal Annealing of Phosphate Glass*, Lawrence Livermore National Laboratory, Livermore, CA, UCRL-JC-134690; also in *J. Non-Cryst. Solids* 263(1-4), 228–239 (2000).

Hayden, J. S., Tomozawa, M., and Crichton, S., *OH Diffusion Measurements in Phosphate Laser Glasses,* Lawrence Livermore National Laboratory, Livermore, CA, UCRL-ID-136007.

Hicks, D. G., Li, C. K., Seguin, F. H., Ram , A. K., Petrasso, R. D., Soures, J. M., Meyerhofer, D. D., Roberts, S., Schnittman, J. D., and Sorce, C., *Studies of MeV Fast Protons Produced in Laser Fusion Experiments,* Lawrence Livermore National Laboratory, Livermore, CA, UCRL-JC-136746. Prepared for *Phys. Rev. Lett.*

Hinkel, D. E., Haan, S. W., Pollaine, S. M., Dittrich, T. R., Jones, O. S., Suter, L. J., and Langdon, A. B., *Scaled Targets for the National Ignition Facility*, Lawrence Livermore National Laboratory, Livermore, CA, UCRL-JC-138284-ABS. Prepared for *30th Annual Anomalous Absorption Conf*, Ocean City, MD, May 21–26, 2000.

Hinkel, D. E., Haan, S. W., Pollaine, S. M., Dittrich, T. R., Jones, O. S., Suter, L. J., and Langdon, A. B., *Scaled Targets for the National Ignition Facility*, Lawrence Livermore National Laboratory, Livermore, CA, UCRL-JC-138284 ABS Rev l. Prepared for the *42nd Annual Mtg of the American Physical Society Div of Plasma Physics*, Quebec, Canada, Oct 23–27, 2000.

Honea, E. C., Beach, R. J., Mitchell, S. C., Skidmore, J. A., Emanuel, M. A., Sutton, S. B., Payne, S. A., Avizonis, P. V., Monroe, R. S., and Harris, D. G., *High-Power Dual-Rod Yb:YAG Laser*, Lawrence Livermore National Laboratory, Livermore, CA, UCRL-JC-136413; also in *Opt. Lett*. 25(11), 805–807 (2000).

Hsing, W. W., *Stability Limit of the Ablation-Front Rayleigh–Taylor Instability*, Lawrence Livermore National Laboratory, Livermore, CA, UCRL-JC-139126 ABS. Prepared for the *42nd Annual Mtg of the American Physical Society Div of Plasma Physics*, Quebec City, Canada, Oct 23–27, 2000.

J

Jones, O. S., Suter, L. J., Glenzer, S., and Wallace, R., *Cocktail Hohlraums*, Lawrence Livermore National Laboratory, Livermore, CA, UCRL-JC-139456 ABS. Prepared for the *42nd Annual Mtg of the American Physical Society Div of Plasma Physics*, Quebec, Canada, Oct 23–27, 2000.

K

Kalantar, D. H., Belak, J., Colvin, J. D., Remington, B. A., Weber, S. V., Allen, A. M., Loveridge, A., Wark, J. S., Boehly, T. R., and Paisley, D., *Dynamic X-Ray Diffraction to Study Compression of Si and Cu beyond the Hugoniot Elastic Limit*, Lawrence Livermore National Laboratory, Livermore, CA, UCRL-JC-138108-ABS. Prepared for *High-Temperature Plasma Diagnostics Mtg*, Tucson, AZ, Jun 18–20, 2000.

Kalantar, D. H., Belak, J., Colvin, J. D., Remington, B. A., Weber, S. V., Allen, A. M., Loveridge, A., Wark, J. S., Boehly, T. R., and Paisley, D., *High Pressure, High Strain Rate Materials Experiments*, Lawrence Livermore National Laboratory, Livermore, CA, UCRL-JC-139585 ABS. Prepared for the *42nd Annual Mtg of the American Physical Society Div of Plasma Physics*, Quebec, Canada, Oct 23–27, 2000.

Kalantar, D. H., Bell, P. M., Perry, T. S., Sewall, N., Diamond, C., Piston, K., *Optimizing Data Recording for the NIF Core Diagnostic X-Ray Streak Camera*, Lawrence Livermore National Laboratory, Livermore, CA, UCRL-JC-138107-ABS. Prepared for *High Temperature Plasma Diagnostics Mtg*, Tucson, AZ, Jun 18–20, 2000.

Kalantar, D. H., Bell, P. M., Perry, T. S., Sewall, N., Diamond, C., and Piston, K., *Optimizing Data Recording for the NIF Core Diagnostic X-Ray Streak Camera*, Lawrence Livermore National Laboratory, Livermore, CA, UCRL-JC-138107. Prepared for the *13th Topical Conf on High Temperature Plasma Diagnostics*, Tucson, AZ, Jun 18–20,2000.

Kalantar, D. H., Colvin, J. D., Mikaelian, K. O., Remington, B. A., Weber, S. V., Wiley, L. G., Allen, A. M., Loveridge, A., Wark, J. S., Paisley, D., and Meyers, M. A., *Laser-Based Solid-State Experiments at High Pressure and Strain Rates*, Lawrence Livermore National Laboratory, Livermore, CA, UCRL-JC-140066 ABS. Prepared for the *Intl Conf on Shock Waves in Condensed Matter*, St. Petersburg, Russia, Oct 8–13, 2000.

Kalantar, D. H., Remington, B. A., Chandler, E. A., Colvin, J. D., Gold, D. M., Mikaelian, K. O., Weber, S. V., Wiley, L. G., Wark, J. S., Hauer, A. A., and Meyers, M. A., *High Pressure Solid State Experiments on the Nova Laser*, Lawrence Livermore National Laboratory, CA, UCRL-JC-129810; also in *J. Impact Engr*. 23(1) Pt. 1, 409–419 (1999).

Kalantar, D. H., Remington, B. A., Chandler, E. A., Colvin, J. D., Gold, D. M., Mikaelian, K. O., Weber, S. V., Wiley, L. G., Wark, J. S., Loveridge, A., Hauer, A., Failor, B. H., Meyers, M. A., and Ravichandran, G., *Developing Solid-State Experiments on the Nova Laser*, Lawrence Livermore National Laboratory, Livermore, CA, UCRL-JC-131851; also in *Astrophys. J*. 127, 357–363 (2000).

Kalantar, D. H., Remington, B. A., Colvin, J. D., Mikaelian, K. O., Weber, S. V., Wiley, L. G., Wark, J. S., Loveridge, A., Allen, A. M., Hauer, A. A., and Meyers, M. A., *Solid-State Experiments at High Pressure and Strain Rate*, Lawrence Livermore National Laboratory, Livermore, CA, UCRL-JC-136355; also in *Phys. Plasmas* 7(5), 1999–2006 (2000).

Kane, J. O., Robey, H. F., Remington, B. A., Drake, R. P., Knauer, J., Ryutov, D. D., Louis, H., Teyssier, R., Hurricane, O., Arnett, D., Rosner, R., and Calder, A., *Three-Layer Shock Imprint Experiment at the OMEGA Laser*, Lawrence Livermore National Laboratory, Livermore, CA, UCRL-JC-138940. Submitted to *Phys. Rev. Lett*.

Kane, J., Arnett, D., Remington, B. A., Glendinning, S. G., Bazan, G., Drake, R. P., and Fryxell, B. A., *Supernova Experiments on the Nova Laser*, Lawrence Livermore National Laboratory, Livermore, CA, UCRL-JC-129000; also in *Astrophys. J*. 127, 365–369 (2000).

Kauffman, R., *Inertial Confinement Fusion Monthly Highlights,* September 1999, Lawrence Livermore National Laboratory, Livermore, CA, UCRL-TB-128550-99-12.

Kauffman, R., *Inertial Confinement Fusion Monthly Highlights*, October 1999, Lawrence Livermore National Laboratory, Livermore, CA, UCRL-TB-128550-00-01.

Kauffman, R., *Inertial Confinement Fusion Monthly Highlights*, November 1999, Lawrence Livermore National Laboratory, Livermore, CA, UCRL-TB-128550-00-02.

Kauffman, R., *Inertial Confinement Fusion Monthly Highlights*, March 2000, Lawrence Livermore National Laboratory, Livermore, CA, UCRL-TB-128550-00-06.

Keilty, K. A., Liang, E. P., Ditmire, T., Remington, B. A., Shigemori, K., and Rubenchik, A. M., "Modeling of Laser-Generated Radiative Blast Waves," *Astrophys. J*. 538(2Ptl), 645–652 (2000).

Keilty, K., Liang, E., Remington, B., London, R., Estabrook, K., and Kane, J., "Numerical Simulations of Blast Waves Generated by an Impulsive Temperature Source," *Astrophys. J*. 127, 375–377 (2000).

Key, M. H., Campbell, E. M., Cowan, T. E., Hatchett, S. P., Henry, E. A., Koch, J. A., Langdon, A. B., Lasinski, B. F., Lee, R. W., and Mackinnon, A., *Studies of the Relativistic Electron Source and Related Phenomena in Petawatt Laser–Matter Interactions,* Lawrence Livermore National Laboratory, Livermore, CA, UCRL-JC-135477 Rev 1. Prepared for *1st Intl Conf on Inertial Fusion Sciences and Applications*, Bordeaux, France, Sept 12, 1999.

Kim, B.-K., Feit, M. D., Rubenchik, A. M., Joslin, E. J., Eichler, J., Stoller, P. C., and Da Silva, L. B., *Effects of High Repetition Rate and Beam Size on Hard Tissue Damage Due to Sub-Picosecond Laser Pulses*, Lawrence Livermore National Laboratory, Livermore, CA, UCRL-JC-135926; also in *Appl. Phys. Lett*. 76(26), 4001–4003 (2000).

Kirkwood, R. K., Langdon, A. B., Decker, C., Moody, J. D., Young, P. E., Suter, L. J., Glenzer, S. H., and Seka, W., *Study of the Dependence of Energy Transfer between Beams on Intensity in a Flowing Plasma*, Lawrence Livermore National Laboratory, Livermore, CA, UCRL-JC-139586 ABS. Prepared for the *42nd Annual Mtg of the American Physical Society Div of Plasma Physics*, Quebec, Canada, Oct 23–27, 2000.

Kirkwood, R. K., Montgomery, D. S., Afeyan, B. B., Moody, J. D., MacGowan, B. J., Joshi, C., Wharton, K. B., Glenzer, S. H., Williams, E. A., Young, P. E., Kruer, W. L., Estabrook, K. G., and Berger, R. L., *Observation of the Nonlinear Saturation of Langmuir Waves Driven by Ponderomotive Force in a Large Scale Plasma*, Lawrence Livermore National Laboratory, Livermore, CA, UCRL-JC-128298; also in *Phys. Rev. Lett*. 83(15), 2965–2968 (1999).

Klein, R. I., Budil, K. S., Perry, T. S., and Bach, D. R., *Interaction of Supernova Remnants with Interstellar Clouds: From the Nova Laser to the Galaxy*, Lawrence Livermore National Laboratory, Livermore, CA, UCRL-JC-135430; also in *Astrophys. J. Suppl*. 127, 379–383 (2000).

Koch, J. A., Bernat, T. P., Collins, G. W., Hammel, B. A., Kozioziemski, B. J., MacKinnon, A. J., Sater, J. D., Bittner, D. N., and Lee, Y., *Quantitative Analysis of Backlit Shadowgraphy as a Diagnostic of Hydrogen Ice Surface Quality in ICF Capsules*, Lawrence Livermore National Laboratory, Livermore, CA, UCRL-JC-135496; also in *Fusion Tech*. 38(1), 123–131 (2000).

Koch, J. A., Presta, R. W., Sacks, R. A., Zacharias, R. A., Bliss, E. S., Dailey, M. J., Feldman, M., Grey, A. A., Holdener, F. R., Salmon, J. T., Seppala, L. G., Toeppen, J. S., Van Atta, L., Van Wonterghem, B. M., Whistler, W. T., Winters, S. E., and Woods, B. W., *Experimental Comparison of a Shack-Hartmann Sensor and a Phase-Shifting Interferometer for Large-Optics Metrology Applications*, Lawrence Livermore National Laboratory, Livermore, CA, UCRL-JC-136105; also in *Appl. Opt*. 39(25), 4540–4546 (2000).

Koch, J. A., Sater, J., Bernat, T., Bittner, D., Collins, G., Hammel, B., Lee, Y., and Mackinnon, A., *Quantitative Analysis of Backlit Shadowgraphy as a Diagnostic of Hydrogen Ice Surface Quality in ICF Capsules,* Lawrence Livermore National Laboratory, Livermore, CA, UCRL-JC-136266. Prepared for *13th Target Fabrication Mtg,* Catalina Island, CA, Nov 8, 1999.

Koch, J., *X-Ray Interferometry with Spherically Bent Crystals*, Lawrence Livermore National Laboratory, Livermore, CA, UCRL-JC-138023-ABS. Prepared for *13th Topical Conf on High-Temperature Plasma Diagnostics*, Tucson, AZ, Jun 18–22, 2000.

Komashko, A. M., Feit, M. D., Rubenchik, A. M., Perry, M. D., and Banks, P. S., *Simulation of Material Removal Efficiency with Ultrashort Laser Pulses,* Lawrence Livermore National Laboratory, CA, UCRL-JC-133744; also in *Appl. Phys. A* 69(SUPPS), S95–S98 (1999).

Kozioziemski, B., *Crystal Growth and Radiation Induced Changes in Solid Molecular Hydrogens*, Lawrence Livermore National Laboratory, Livermore, CA, UCRL-LR-139310.

Kozlowski, M. R., Battersby, C. L., and Demos, S. G., *Luminescence Investigation of SiO_2 Surfaces Damaged by 0.35 mm Laser Illumination,* Lawrence Livermore National Laboratory, Livermore, CA, UCRL-JC-136870. Prepared for *31st Annual Symp on Optical Materials for High Power Lasers,* Boulder, CO, Oct 4, 1999.

Kruer, W. L., *Interaction of Plasmas with Intense Lasers*, Lawrence Livermore National Laboratory, Livermore, CA, UCRL-JC-132222; also in *Phys. Plasmas* 7(6), 2270–2278 (2000).

L

Labaune, C., Baldis, H. A., Schifano, E., Bauer, B. S., Maximov, A., Ourdev, I., Rozmus, W., and Pesme, D., *Enhanced Forward Scattering in the Case of Two Crossed Laser Beams Interacting with a Plasma*, Lawrence Livermore National Laboratory, Livermore, CA, UCRL-JC-135653; also in *Phys. Rev. Lett*. 85(8), 1658–1661 (2000).

Labaune, C., Fuchs, J., Depierreux, S., Baldis, H. A., Pesme, D., Myatt, J., Huller, S., Tikhonchuk, V. T., and Laval, G., *Laser-Plasma Interaction Physics in the Context of Fusion*, Lawrence Livermore National Laboratory, Livermore, CA, UCRL-JC-139168; also in *Comptes Rendus* 1(6),727–735 (2000).

Landahl, E. C., Hartemann, F. V., Le Sage, G. P., White, W. E., Baldis, H. A., Bennnett, C. V., Heritage, J. P., Kolner, B. H., Luhman, N. C., and Ho, C. H., *Phase Noise Reduction and Photoelectron Acceleration in a High-Q RF Gun*, Lawrence Livermore National Laboratory, CA, UCRL-JC-139029; also in *IEEE Trans. Plasma Sci.* 27(5), 1547 (1999).

Landen, O. L., Amendt, P. A., Back, C. A., Berger, R. L., Bradley, D. K., Bullock, A. B., Cauble, R. C., Chandler, G. A., Collins, G. W., Decker, C. D., Edwards, M. J., Glendinning, S. G., Glenzer, S. H., Haan, S. W., Kalantar, D. H., Kirkwoood, R. K., Moody, J. M., Munro, D. H., Olson, R. E., Perry, T. S., Pollaine, S. M., Remington, B. A., Robey, H. R., Sanchez, J., Suter, L. J., Turner, R. E., Young, P. E., Wallace, R. J., Hammel, B. A., and Hsing, W. W., *Recent Progress in ICF and High Energy Density Experiments*, Lawrence Livermore National Laboratory, Livermore, CA, UCRL-JC-138000-ABS. Prepared for *26th European Conf on Laser Interaction with Matter*, Prague, Czech Republic, Jun 12–16, 2000.

Landen, O. L., and Glenzer, S. H., *Warm, Dense Matter Characterization by X-Ray Thomson Scattering*, Lawrence Livermore National Laboratory, Livermore, CA, UCRL-JC-138258 ABS Rev l. Prepared for the *Intl Workshop on Warm Dense Matter*, Vancouver, Canada, May 29–31, 2000.

Landen, O. L., Bradley, D. K., Amendt, P. A., Pollaine, S. M., Glendinning, S. G., Bullock, A. B., Turner, R. E., Suter, L. J., Jones, O. S., Wallace, R. J., and Hammel, B. A., *Symmetry Diagnosis and Control for NIF-Scale Hohlraums*, Lawrence Livermore National Laboratory, Livermore, CA, UCRL-JC-137874-ABS. Prepared for *26th European Conf on Laser Interaction with Matter*, Prague, Czech Republic, Jun 12–16, 2000.

Landen, O. L., Bradley, D. K., Pollaine, S. M., Amendt, P. A., Glendinning, S. G., Suter, L. J., Turner, R. E., Wallace, R. J., Hammel, B. A., and Delamater, N. D., *Indirect-Drive Time-Dependent Symmetry Diagnosis at NIF-Scale,* Lawrence Livermore National Laboratory, Livermore, CA, UCRL-JC-136297. Prepared for *1st Intl Conf on Inertial Fusion Sciences and Applications,* Bordeaux, France, Sep 12, 1999.

Landen, O. L., Farley, D. R., Bradley, D. K., Bullock, A. B., Glendinning, S. G., Logory, L. M., Turner, R. E., Bell, P. M., Koch, J. A., Lee, F. D., Decker, C. D., Kalantar, D. H., Back, C. A., and Suter, L. J., *X-Ray Backlighting for the National Ignition Facility*, Lawrence Livermore National Laboratory, Livermore, CA, UCRL-JC-138318 ABS. Prepared for the *13th Topical Conf on High Temperature Plasma Diagnostics*, Tucson, AZ, Jun 18–22, 2000.

Landen, O. L., Glenzer, S. H., Cauble, R. C., Lee, R. W., Edwards, J. E., and Degroot, J. S., *Warm, Dense Plasma Characterization by X-Ray Thomson Scattering*, Lawrence Livermore National Laboratory, Livermore, CA, UCRL-JC-138941. Prepared for the *26th European Conf on Laser Interaction with Matter*, Prague, Czech Republic, Jun 12–16, 2000.

Landen, O. L., Lobban, A., Tutt, T., Bell, P. M., Costa, R., and Ze, F., *Angular Sensitivity of Gated Micro-Channel Plate Framing Cameras*, Lawrence Livermore National Laboratory, Livermore, CA, UCRL-JC-137879. Prepared for the *13th Topical Conf on High Temperature Plasma Diagnostics*, Tucson, AZ, Jun 19–23, 2000.

Landen, O. L., Ze, F., Lobban, A., Tutt, T., Bell, P. M., and Costa, R., *Angular Sensitivity of Gated Micro-Channel Plate Framing Cameras*, Lawrence Livermore National Laboratory, Livermore, CA, UCRL-JC-137879-ABS. Prepared for *13th Topical Conf on High-Temperature Plasma Diagnostics*, Tucson, AZ, Jun 18–22, 2000.

Langdon, A. B., Berger, R. L., Cohen, B. I., Decker, C. D., Hinkel, D. E., Kirkwood, R. K., Still, C. H., and Williams, E. A., *Power Transfer between Smoothed Laser Beams*, Lawrence Livermore National Laboratory, Livermore, CA, UCRL-JC-138282-ABS. Prepared for *30th Annual Anomalous Absorption Conf*, Ocean City, MD, May 21–26, 2000.

Langer, S. H., Scott, H. A., Marinak, M. A., and Landen, O. L., *Modeling Line Emission from ICF Capsules in 3 Dimensions*, Lawrence Livermore National Laboratory, Livermore, CA, UCRL-JC-131240; also in *J. Quant. Spectros. Radiat. Transfer* 65(1-3), 333–366 (2000).

Legrand, M., Schurtz, G., Weber, S. V., Remington, B. A., and Colvin, J. D., *Laser Driven Hydrodynamic Instabilites in the Solid State and Sensitivity to Nature of Flow*, Lawrence Livermore National Laboratory, Livermore, CA, UCRL-JC-138312 ABS. Prepared for the *30th Annual Anomalous Absorption Conf,* Ocean City, MD, May 21–26, 2000.

Lehmberg, R. H., and Rothenberg, J. E., "Comparison of Optical Beam Smoothing Techniques for Inertial Confinement Fusion and Improvement of Smoothing by the Use of Zero-Correlation Masks," *J. Appl. Phys*. 87(3), 1012–1022 (2000).

Li, C. K., Hicks, D. G., Seguin, F. H., Frenje, J. A., Petrasso, R. D., Soures, J. M., Radha, P. B., Glebov, V. Yu., Stoeckl, C., Harding, D. R., Knauer, J. P., Kremens, R., Marshall, F. J., Meyerhofer, D. D., Skupsky, S., Roberts, S., Sorce, C., Sangster, T. C., Phillips, T. W., Cable, M. D., and Leeper, R. J., *D-^{3}He Proton Spectra for Diagnosing Shell ρR and Fuel T_i of Imploded Capsules at Omega*, Lawrence Livermore National Laboratory, Livermore, CA, UCRL-JC-136808; also in *Phys. Plasmas* 7(6), 2578–2584 (2000).

Li, Y. L., Dunn, J., Nilsen, J., Barbee, T. W., Osterheld, A. L., and Shlyaptsev, V. N., *Saturated Tabletop X-Ray Laser System at 19 nm*, Lawrence Livermore National Laboratory, Livermore, CA, UCRL-JC-134716; also in *J. Opt. Soc. Am. B* 17(6), 1098–1101 (2000).

Logory, L. M., Miller, P. L., and Stry, P. E., *Nova High-Speed Jet Experiments*, Lawrence Livermore National Laboratory, Livermore, CA, UCRL-JC-130188; also in *Astrophys. J.* 127(2), 423–428 (2000).

Lukasheva, N. V., Niemela, S., Neelov, I. M., Darinskii, A. A., Sundholm, F., and Cook, R., *Conformational Variability of Helix Sense Reversals in Poly(Methyl Isocyanates)*, Lawrence Livermore National Laboratory, Livermore, CA, UCRL-JC-137206. Submitted to *Macromolecules.*

M

McCallen, D., *Acceleration Amplifications in NIF Structures Subjected to Earthquake Base Motions,* Lawrence Livermore National Laboratory, Livermore, CA, UCRL-ID-136812.

MacKinnon, A. J., Borghesi, M., Patel, P., Hatchett, S., Key, M. H., Lasinski, B., Langdon, B., Snavely, R., Wilks, S. C., Willi, O., Schiavi, A., Campbell, H., Gizzi, L., and Galimberti, M., *Effect of Plasma Scalelength on MeV Proton Production in Short Pulse High Intensity Laser Plasma Interactions*, Lawrence Livermore National Laboratory, Livermore, CA, UCRL-JC-139604 ABS. Prepared for the *42nd Annual Mtg of the American Physical Society Div of Plasma Physics*, Quebec, Canada, Oct 23–27, 2000.

MacKinnon, A. J., Patel, P., Snavely, R., Wilks, S. C., Hatchett, S., Key, M. H., Borghesi, M., Schiavi, A., Campbell, H., Willi, O., Gizzi, L., and Galimberti, M., *Effect of Plasma Scale Length on Multi MeV Proton Production by Ultra Short Laser Pulses*, Lawrence Livermore National Laboratory, Livermore, CA, UCRL-JC-139273. Submitted to *Phys. Rev. Lett*.

McKinnon, A., Shigemori, K., Ditmire, T., Remington, B. A., Yanovsky, V., Ryutov, D., Estabrook, K. G., Edwards, M. J., Keilty, K. A., and Liang, E., *Radiative Shock Experiments Relevant to Astrophysics*, Lawrence Livermore National Laboratory, Livermore, CA, UCRL-JC-137569-ABS. Prepared for *3rd Intl Conf on Laboratory Astrophysics on Intense Lasers,* Houston, TX, Mar 29–Apr 1, 2000.

Mirkarimi, P. B., Bajt, S., and Wall, M. A., *Mo/Si and MO/Be Multilayer Thin Films on Zerodur Substrates for Extreme-Ultraviolet Lithography*, Lawrence Livermore National Laboratory, Livermore, CA, UCRL-JC-135398; also in *Appl. Optics* 39(10), 1617–1625 (2000).

Moir, R. W., *Liquid Walls for Fusion Reaction Chambers*, Lawrence Livermore National Laboratory, Livermore, CA, UCRL-JC-135743; also in *Comments on Mod. Phys*. 2(2), C99–Cl11 (2000).

Montgomery, D. S., Johnson, R. P., Cobble, J. A., Fernandez, J. C., Lindman, E. L., Rose, H. A., and Estabrook, K. G., "Characterization of Plasma and Laser Conditions for Single Hot Spot Experiments," *Laser and Particle Beams* 17(3), 349–359 (1999).

Moody, J. D., MacGowan, B. J., Berger, R. L., Estabrook, K. G., Glenzer, S. H., Kirkwood, R. K., Kruer, W. L., Stone, G. F., and Montgomery, D. S., *Experimental Study of Laser Beam Transmission and Power Accounting in a Large Scalelength Laser–Plasma*, Lawrence Livermore National Laboratory, Livermore, CA, UCRL-JC-135564; also in *Phys. Plasmas* 7(8), 3388–3398 (2000).

Moody, J. D., MacGowan, B. J., Glenzer, S. H., Kirkwood, R. K., Kruer, W. L., Montgomery, D. S., Schmitt, A. J., Williams, E. A., and Stone, G. F., *Experimental Investigation of Short Scalelength Density Fluctuations in Laser-Produced Plasmas*, Lawrence Livermore National Laboratory, Livermore, CA, UCRL-JC-136401; also in *Phys. Plasmas* 7(5), 2114–2125 (2000).

Moody, J. D., MacGowan, B. J., Rothenberg, J. E., Berger, R. L., Divol, L., Glenzer, S. H., Kirkwood, R. K., Williams, E. A., and Young, P. E., *Backscatter Reduction Using Combined Spatial, Temporal, and Polarization Beam Smoothing in a Long Scalelength Laser–Plasma*, Lawrence Livermore National Laboratory, Livermore, CA, UCRL-JC-139843. Submitted to *Phys. Rev. Lett*.

Moody, J. D., Young, P. E., Chambers, D. M., Hawreliak, J., Sondhauss, P., Wark, J. S., Berger, R. L., Divol, L., Langdon, A. B., and Williams, E. A., *Observation of Laser Self-Smoothing in an Exploding Foil Plasma*, Lawrence Livermore National Laboratory, Livermore, CA, UCRL-JC-139587 ABS. Prepared for the *42nd Annual Mtg of the American Physical Society Div of Plasma Physics*, Quebec, Canada, Oct 23–27, 2000.

Munro, D. H., *Shock Timing Technique for the NIF*, Lawrence Livermore National Laboratory, Livermore, CA, UCRL-JC-139319 ABS. Prepared for the *42nd Annual Mtg of the APS Div of Plasma Physics*, Quebec City, Canada, Oct 23–27, 2000.

Murray, J. E., Milam, D., Boley, C. D., and Estabrook, K. G., *Spatial Filter Pinhole Development for the National Ignition Facility,* Lawrence Livermore National Laboratory, Livermore, CA, UCRL-JC-134647; also in *Appl. Optics* 39(9), 1405–1420 (2000).

N

Nilsen, J., Li, Y., and Dunn, J., *Modeling psec-Laser-Driven Neon-Like Titanium X-Ray Laser Experiments*, Lawrence Livermore National Laboratory, Livermore, CA, UCRL-JC-135817; also in *J. Opt. Soc. Am. B* 17(6), 1084–1092 (2000).

Noble, C. R., Hoehler, M. S., and Sommer, S. C., *NIF Ambient Vibration Measurements,* Lawrence Livermore National Laboratory, Livermore, CA, UCRL-ID-136914.

P

Patel, P. K., Wolfrum, E., Renner, O., Loveridge, A., Allott, R., Neely, D., Rose, S. J., and Warek, J. S., "X-Ray Line Reabsorption in a Rapidly Expanding Plasma," *J. Quant. Spectros. Radiat. Transfer* 65(1-3), 429–439 (2000).

Pennington, D. M., Brown, C. G., Cowan, T. E., Hatchett, S. P., Henry, E., Herman, S., Kartz, M., Key, M., Koch, J., MacKinnon, A. J., Perry, M. D., Phillips, T. W., Roth, M., Sangster, T. C., Singh, M., Snavely, R. A., Stoyer, M., Stuart, B. C., and Wilks, S. C., *Petawatt Laser Systems and Experiments*, Lawrence Livermore National Laboratory, Livermore, CA, UCRL-JC-140019; also in *IEEE Sel. Topics Quant. Elect*. 6(4), 676–688 (2000).

Perry, M. D., and Shore, B. W., *Petawatt Laser Report,* Lawrence Livermore National Laboratory, Livermore, CA, UCRL-ID-124933.

Perry, T. S., Davidson, S. J., Serduke, F. J. D., Bach, D. R., Smith, C. C., Foster, J. M., Doyas, R. J., Ward, R. A., Iglesias, C. A., Rogers, F. J., Abdallah, Jr., J., Stewart, R. E., Wallace, R. J., Kilkenny, J. D., and Lee, R. W., *Opacity Measurements in a Hot Dense Medium*, Lawrence Livermore National Laboratory, Livermore, CA, UCRL-JC-138912; also in *Astrophys J*. 127, 433–436(2000).

Perry, T. S., Klein, R. I., Bach, D. R., Budil, K. S., Cauble, R., Kornblum, Jr., H. N., Wallace, R. J., and Lee, R. W., *Temperature and Density Measurements of the Collision of Two Plasmas*, Lawrence Livermore National Laboratory, Livermore, CA, UCRL-JC-135705; also in *Astrophys. J. Suppl*. 127, 437–443 (2000).

Petzoldt, R. W., Goodin, D., and Siegel, N., "Status of Target Injection and Tracking Studies for Inertial Fusion Energy," *Fusion Tech.* 38(1), 22–27 (2000).

Pollaine, S. M., and Nellis, W. J., *Metallic Hydrogen Generated by High Shock Pressures*, Lawrence Livermore National Laboratory, Livermore, CA, UCRL-JC-138603 ABS. Prepared for the *11th Advanced Space Propulsion Research Workshop*, Pasadena, CA, May 31–Jun 2, 2000.

Pollaine, S. M., *Radiation Transport between Two Concentric Spheres*, Lawrence Livermore National Laboratory, Livermore, CA, UCRL-JC-137279 Rev l. Submitted to *Nucl. Fusion*.

Pollaine, S., Bradley, D., Landen, O., Amendt, P., Jones, O., Wallace, R., Glendinning, G., Turner, R., and Suter, L., *P6 and P8 Modes in NIF Hohlraums*, Lawrence Livermore National Laboratory, Livermore, CA, UCRL-JC-133888-ABS. - REV-2. Prepared for *30th Annual Anomalous Absorption Conf*, Ocean City, MD, May 21–26, 2000.

Pollaine, S., Bradley, D., Landen, O., Amendt, P., Wallace, R., Jones, O., Glendinning, G., Turner, R., and Suter, L., *NIF-Scale Hohlraum Asymmetry Studies Using Point-Projection Radiography of Thin Shells*, Lawrence Livermore National Laboratory, Livermore, CA, UCRL-JC-139459 ABS. Prepared for the *42nd Annual Mtg of the American Physical Society Div of Plasma Physics*, Quebec, Canada, Oct 23–27, 2000.

R

Regan, S. P., Delettrez, J. A., Yaakobi, B., Bradley, D. K., Bahr, R., Millecchia, M., Meyerhofer, D. D., and Seka, W., *Spectroscopic Analysis of Electron Temperature in Laser Driven Burnthrough Experiments*, Lawrence Livermore National Laboratory, Livermore, CA, UCRL-JC-137875-ABS. Prepared for *12th Topical Conf on Atomic Processes in Plasmas*, Reno, NV, Mar 19–23, 2000.

Regan, S. P., Delettrez, J. A., Yaakobi, B., Epstein, R., Bradley, D. K., Meyerhofer, D. D., and Seka, W., *Laser-Driven Burnthrough Experiments on OMEGA*, Lawrence Livermore National Laboratory, Livermore, CA, UCRL-JC-138442 ABS. Prepared for the *30th Annual Anomalous Absorption Conf*, Ocean City, MD, May 21–26, 2000.

Remington, B. A., Drake, R. P., Arnett, D., and Takabe, H., *Introduction to the Proceedings of the 2nd Intl Workshop of Laboratory Astrophysics with Intense Lasers*, Lawrence Livermore National Laboratory, Livermore, CA, UCRL-JC-138712 SUM. Prepared for the *2nd Intl Workshop of Laboratory Astrophysics with Intense Lasers*, Tucson, AZ, Mar 17–21, 1999.

Remington, B. A., Drake, R. P., Takabe, H., and Arnett, D., *A Review of Astrophysics Experiments on Intense Lasers*, Lawrence Livermore National Laboratory, Livermore, CA, UCRL-JC-134961; also in *Phys. Plasmas* 7(5), 1641–1652 (2000).

Remington, B. A., Kalantar, D. H., Weber, S. V., and Colvin, J. D., *Experimental Path to Deep Earth Interior Physics and Hypervelocity Micro-Flier Plates*, Lawrence Livermore National Laboratory, Livermore, CA, UCRL-JC-138109-ABS. Prepared for *3rd Intl Workshop on Laboratory Astrophysics on Intense Lasers*, Houston, TX, Mar 31–Apr 2, 2000.

Remington, B. A., *Overview of Astrophysics Experiments on Intense Lasers*, Lawrence Livermore National Laboratory, Livermore, CA, UCRL-JC-137570-ABS. Prepared for *3rd Intl Conf on Laboratory Astrophysics on Intense Lasers,* Houston, TX, Mar 29–Apr 1, 2000.

Remington, B. A., *Scaling Supernovae into the Lab: Experiments on Intense Lasers*, Lawrence Livermore National Laboratory, Livermore, CA, UCRL-JC-138713 ABS. Prepared for *Nuclei in the Cosmos 2000*, Ahrus, Denmark, Jun 27–Jul 1, 2000.

Richard, A. L., Jadaud, J. P., Dague, N., Monteil, M. C., Turner, R. E., Bradley, D., Wallace, R. J., Landen, O. L., Soures, J. M., Morse, S., and Pien, G., *Symmetry Experiments on OMEGA with LMJ Like Multiple Beam Cones Irradiation*, Lawrence Livermore National Laboratory, Livermore, CA, UCRL-JC-137873. Prepared for the *26th European Conf on Laser Interaction with Matter*, Prague, Czech Republic, Jun 12–16, 2000.

Roberts, C. C., Orthion, P. J., Hassel, A. E., Parrish, B. K., Buckley, S. R., Fearon, E., Letts, S. A., and Cook, R. C., *Development of Polymide Ablators for NIF: Analysis of Defects on Shells, a Novel Smoothing Technique and Upilex Coatings*, Lawrence Livermore National Laboratory, Livermore, CA, UCRL-JC-137737; also in *Fus. Tech*. 38(1), 94–107 (2000).

Robey, H. F., Kane, J. O., Drake, R. P., Remington, B. A., Louis, H., Wallace, R. J., Hurricane, O. A., and Calder, A., *Experimental Testbed for the Study of Hydrodynamic Issues in Supernovae*, Lawrence Livermore National Laboratory, Livermore, CA, UCRL-JC-139454 ABS. Prepared for the *42nd Annual Mtg of the American Physical Society Div of Plasma Physics*, Quebec, Canada, Oct 23–27,2000.

Robey, H. F., Kane, J., Remington, B. A., Hurricane, O., Drake, R. P., and Knauer, J., *Astrophysics Experiments on the OMEGA Laser: Interface Coupling in Supernovae Caused by Rippled Shock Imprinting*, Lawrence Livermore National Laboratory, Livermore, CA, UCRL-JC-137443-ABS. Prepared for *3rd Intl Conf on Laboratory Astrophysics with Intense Lasers*, Houston, TX, Mar 30–Apr 1, 2000.

Roth, M., Cowan, T. E., Brown, C., Christl, M., Fountain, W., Hatchett, S., Johnson, J., Key, M. H., Pennington, D. M., and Perry, M. D., *Intense Ion Beams Accelerated by Petawatt-Class Lasers,* Lawrence Livermore National Laboratory, Livermore, CA, UCRL-JC-136218-ABS. Prepared for *13th Intl Symp on Heavy Ion Inertial Fusion*, San Diego, CA, Mar 13, 2000.

Rothenberg, J. E., *Polarization Beam Smoothing for Inertial Confinement Fusion*, Lawrence Livermore National Laboratory, Livermore, CA, UCRL-JC-134521; also in *J. Appl. Phys*. 87(8), 3654–3662 (2000).

Rozmus, W., Bychenkov, V., Brantov, A. V., Glenzer, S., Estabrook, K., and Baldis, H. A., *Return Current Instability and Its Effect on the Thomson Scattering Spectra in Laser Produced Plasmas*, Lawrence Livermore National Laboratory, Livermore, CA, UCRL-JC-138514 ABS. Prepared for the *30th Annual Anomalous Absorption Conf*, Ocean City, MD, May 21–26, 2000.

Rozmus, W., Glenzer, S. H., Estabrook, K. G., Baldis, H. A., and MacGowan, B. J., *Modeling of Thomson Scattering Spectra in High-Z, Laser-Produced Plasmas*, Lawrence Livermore National Laboratory, Livermore, CA, UCRL-JC-130646; also in *Astrophys. J.* 127, 459–463 (2000).

Ryutov, D. D., and Remington, B. A., *Destabilizing Effect of Thermal Conductivity on the Rayleigh–Taylor Instability*, Lawrence Livermore National Laboratory, Livermore, CA, UCRL-JC-137568-ABS. Prepared for *3rd Intl Conf on Laboratory Astrophysics with Intense Lasers*, Houston, TX, Mar 30–Apr 1, 2000.

Ryutov, D. D., Drake, R. P., and Remington, B. A., *Criteria for Scaled Laboratory Simulations of Astrophysical MHD Phenomena*, Lawrence Livermore National Laboratory, Livermore, CA, UCRL-JC-133092; also in *Astrophys. J.* 127, 465–468 (2000).

Ryutov, D. D., *Radical Restructuring of the Fusion Effort*, Lawrence Livermore National Laboratory, Livermore, CA, UCRL-JC-136143; also in *Comments on Mod. Phys.* 2(2), C139–U14 (2000).

Ryutov, D., Ditmire, T., Edwards, J., Glendinning, G., Remington, B., and Shigemori, K., *Simple Description of the Blast Wave in the Medium with Y Close to 1*, Lawrence Livermore National Laboratory, Livermore, CA, UCRL-JC-137567-ABS. Prepared for *3rd Intl Conf on Laboratory Astrophysics with Intense Lasers,* Houston, TX, Mar 30–Apr 1, 2000.

S

Sangster, T. C., Ahle, L. A., Halaxa, E. F., Karpenko, V. P., Olddaker, M. E., Thompson, J., Beck, D. N., Bieniosek, F. M., Henestroza, E., and Kwan, J. W., *New 500-keV Ion Source Test Stand for HIF,* Lawrence Livermore National Laboratory, Livermore, CA, UCRL-JC-136744-ABS. Prepared for *13th Intl Symp on Heavy Ion Inertial Fusion,* San Diego, CA, Mar 13, 2000.

Sangster, T. C., Glebov, V., Lerche, R. A., Phillips, T. W., Stoekl, C., Padalino, S. J., Olliver, H., and Thompson, S., *Calibration of the Medusa Neutron Spectrometer at the OMEGA Laser*, Lawrence Livermore National Laboratory, Livermore, CA, UCRL-JC-137923-ABS. Prepared for *13th Topical Conf on High-Temperature Plasma Diagnostics*, Tucson, AZ, Jun 18–22, 2000.

Schmid, G. J., Izumi, N., Lerche, R. A., Phillips, T. W., Sangster, T. C., and Stoyer, M. A., *Neutronics Calculations for Diagnostics Development at NIF and OMEGA*, Lawrence Livermore National Laboratory, Livermore, CA, UCRL-JC-139588 ABS. Prepared for the *42nd Annual Mtg of the American Physical Society Div of Plasma Physics*, Quebec, Canada, Oct 23–27, 2000.

Sharp, R., and Runkel, M., *Automated Damage Onset Analysis Techniques Applied to KDP Damage and the Zeus Small Area Damage Test Facility*, Lawrence Livermore National Laboratory, Livermore, CA, UCRL-JC-134765. Prepared for *31st Boulder Damage Symposium: Annual Symposium on Optical Materials for High Power Lasers*, Boulder, CO, Oct 4–7, 1999.

Shigemori, K., Ditmire, T., Remington, B. A., Yanovsky, V., Ryutov, D., Estabrook, K. G., Edwards, M. J., Rubenchik, A. M., Liang, E., and Keilty, K. A., *Observation of the Transition from Hydrodynamic to Radiative Shocks*, Lawrence Livermore National Laboratory, Livermore, CA, UCRL-JC-134470; also in *Astrophys. J.* 533(2Pt2), L159–L162 (2000).

Still, C. H., Berger, R. L., and Langdon, A. B., *pF3D, version 2.0*, Lawrence Livermore National Laboratory, Livermore, CA, UCRL-CODE-2000-019.

Still, C. H., Berger, R. L., Langdon, A. B., Hinkel, D. E., and Williams, E. A., *Laser Plasma Simulations Using Entire Smoothed and Aberrated Laser Beams*, Lawrence Livermore National Laboratory, Livermore, CA, UCRL-JC-138283-ABS. Prepared for *30th Annual Anomalous Absorption Conf*, Ocean City, MD, May 21–26, 2000.

Still, C. H., Berger, R. L., Langdon, A. B., Hinkel, D. E., Suter, L. J., and Williams, E. A., *Filamentation and Forward Brillouin Scatter of Entire Smoothed and Aberrated Laser Beams*, Lawrence Livermore National Laboratory, Livermore, CA, UCRL-JC-135006; also in *Phys. Plasmas* 7(5), 2023–2032 (2000).

Stone, J. M., Turner, N., Estabrook, K., Remington, B., Farley, D., Glendinning, S. G., and Glenzer, S., *Testing Astrophysical Radiation Hydrodynamics Codes with Hypervelocity Jet Experiments on the Nova Laser*, Lawrence Livermore National Laboratory, Livermore, CA, UCRL-JC-135789; also in *Astrophys. J.* 127, 497–502 (2000).

Stoyer, M. A., Hudson, G. B., Lougheed, R. W., Sangster, T. C., Freeman, C., Schwartz, B., and Olsen, M. L., *OMEGA Gas Sampling System and Radiochemical Diagnostics for NIF*, Lawrence Livermore National Laboratory, Livermore, CA, UCRL-JC-133562 ABS Rev l. Prepared for the *42nd Annual Mtg of the American Physical Society Div of Plasma Physics*, Quebec, Canada, Oct 23–27, 2000.

Strobel, G. L., *M Dependence of Surface Expansion Coefficients*, Lawrence Livermore National Laboratory, Livermore, CA, UCRL-JC-137516-ABS. Prepared for *Sherwood 2000*, Los Angeles, CA, Mar 27–29, 2000.

Suratwala, T. I., Steele, R. A., Wilke, G. D., Campbell, J. H., and Takeuchi, K., *Effects of OH Content, Water Vapor Pressure, and Temperature on Sub-Critical Crack Growth in Phosphate Glass*, Lawrence Livermore National Laboratory, Livermore, CA, UCRL-JC-132912; also in *J. Non-Cryst. Solids* 263(1-4), 213–227 (2000).

Suter, L. J., Rothenberg, J., Munro, D., Van Wonterghem, B., and Haan, S., *Exploring the Limits of the National Ignition Facility's Capsule Coupling*, Lawrence Livermore National Laboratory, Livermore, CA, UCRL-JC-136319 Rev 1; also in *Phys. Plasmas* 7(5), 2092–2098 (2000).

Suter, L., Haan, S., Lindl, J., Dittrich, T., Hammel, B. A., Hinkel, D., Jones, O., Pollaine, S., and Rothenberg, J., *Recent Developments in Ignition Target Designs for the National Ignition Facility*, Lawrence Livermore National Laboratory, Livermore, CA, UCRL-JC-138309. Prepared for the *18th Intl Atomic Energy Agency Fusion Energy Conf,* Sorrento, Italy, Oct 4–8,2000.

Suter, L., Rothenberg, J., Munro, D., Van Wonterghem, B., Haan, S., and Lindl, J., *Feasibility of High Yield/High Gain NIF Capsules,* Lawrence Livermore National Laboratory, Livermore, CA, UCRL-JC-136784. Prepared for *1st Intl Conf on Inertial Fusion Sciences and Applications,* Bordeaux, France, Sep 18, 1999.

T

Takagi, M., Cook, R., Stephens, R., Gibson, J., and Paguio, S., *Decreasing Out-Of-Round in Poly(α-Methylstyrene) Mandrels by Increasing Interfacial Tension*, Lawrence Livermore National Laboratory, Livermore, CA, UCRL-JC-135539; also in *Fus. Tech.* 38(1), 46–49 (2000).

Takagi, M., Cook, R., Stephens, R., Gibson, J., and Paguio, S., *Stiffening of PαMS Mandrels During Curing*, Lawrence Livermore National Laboratory, Livermore, CA, UCRL-JC-135545; also in *Fus. Tech.* 38(1), 50–53 (2000).

Takagi, M., Cook, R., Stephens, R., Gibson, J., and Paguio, S., *The Effects of Controlling Osmotic Pressure on a PαMS Microencapsulated Mandrel During Curing*, Lawrence Livermore National Laboratory, Livermore, CA, UCRL-JC-135540; also in *Fus. Tech.* 38(1), 54–57 (2000).

Tannaka, K. A., Kodama, R., Fufita, H., Heya, M., Izumi, N., Kitagawa, Y., Mima, K., Miyanaga, N., Norimatsu, T., Pukhov, A., Sunahara, A., Takahashi, K., Allen, M., Habara, H., Iwatani, T., Matusita, T., Miyakosi, T., Mori, M., Setoguchi, H., Sonomoto, T., Tanpo, M., Tohyama, S., Azuma, H., Kawasaki, T., Komeno, T., Maekawa, O., Matsuo, S., Shozaki, T., Suzuki, Ka, Yoshida, H., Yamanaka, T., Sentoku, Y., Weber, F., Barbee, Jr., T. W., and Da Silva, L., "Studies of Ultra-Intense Laser Plasma Interactions for Fast Ignition," *Phys. Plasmas* 7(5), 2014–2022 (2000).

Teyssier, R., Ryutov, D., and Remington, B., "Accelerating Shock Waves in a Laser-Produced Density Gradient," *Astrophys. J*. 127, 503–508 (2000).

Toet, D., Smith, P. M., Sigmon, T. W., and Thompson, M. O., *Experimental and Numerical Investigations of a Hydrogen-Assisted Laser-Induced Materials Transfer Procedure*, Lawrence Livermore National Laboratory, Livermore, CA, UCRL-JC-136660; also in *J. Appl. Phys*. 87(7), 3537–3546 (2000).

Turner, R. E., Amendt, P. A., Landen, O. L., Bradley, D., and Wallace, R. J., *Effect of Ar Dopant on ICF Implosions*, Lawrence Livermore National Laboratory, Livermore, CA, UCRL-JC-139590 ABS. Prepared for the *42nd Annual Mtg of the American Physical Society Div of Plasma Physics*, Quebec, Canada, Oct 23–27, 2000.

Turner, R. E., Landen, O. L., Bradley, D. K., Bell, P. M., Costa, R., Moody, J. D., and Lee, D., *Comparison of CCD vs Film Readouts for Gated MCP Cameras*, Lawrence Livermore National Laboratory, Livermore, CA, UCRL-JC-138003-ABS. Prepared for *High-Temperature Diagnostics Mtg,* Tucson, AZ, Jun 18–22, 2000.

U

Unanyan, R. G., Vitanov, N. V., Shore, B. W., and Bergmann, K., *Coherent Properties of a Tripod System Coupled Via a Continuum*, Lawrence Livermore National Laboratory, Livermore, CA, UCRL-JC-136151; also in *Phys. Rev. A* 6104(4), 3408, U402–U410 (2000).

V

Varnum, W. S., Delamater, N. D., Evans, S. C., Gobby, P. L., Moore, J. E., Wallace, J. M., Watt, R. G., Colvin, J. D., Turner, R., Glebov, V., Soures, J., and Stoeckl, C., "Progress Toward Ignition with Noncryogenic Double-Shell Capsules," *Phys. Rev. Lett*. 84(22), 5153–5155 (2000).

Velikovich, A. L., Dahlburg, J. P., Schmitt, A. J., Gardner, J. H., Phillips, L., Cochran, F. L., Chong, Y. K., Dimonte, G., and Metzler, N., "Richtmyer–Meshkov-Like Instabilities and Early-Time Perturbation Growth in Laser Targets and Z-Pinch Loads," *Phys. Plasmas* 7(5), 1662–1671 (2000).

Vitanov, N. V., Shore, B. W., Unanyan, R. G., and Bergmann, K., "Measuring a Coherent Superposition," *Opt. Comm*. 179(1-6), 73–83 (2000).

W

Warwick, P. J., Demir, A., Kalantar, D. H., Key, M. H., Kim, N. S., Lewis, C. L. S., Lin, J., MacPhee, A. G., Neely, D., and Remington, B. A., *Radiography Measurements of Direct Drive Imprint in Thin Al Foils Using a Bright XUV Laser,* Lawrence Livermore National Laboratory, Livermore, CA, UCRL-JC-136395. Prepared for *5th Intl Conf on X-Ray Lasers,* Lund, Sweden, Jun 10, 1996.

Williams, E. A., Berger, R. L., Decker, C. D., Divol, L., Glenzer, S. H., Langdon, A. B., Moody, J. D., Still, C. H., Young, P. E., and Lours, L., *Modeling of Beam Propagation Experiments on Nova and Vulcan with Parallel F3D*, Lawrence Livermore National Laboratory, Livermore, CA, UCRL-JC-139461 ABS. Prepared for the *42nd Annual Mtg of the American Physical Society Div of Plasma Physics*, Quebec, Canada, Oct 23–27, 2000.

Williams, W., *NIF Large Optics Metrology Software; Description and Algorithms*, Lawrence Livermore National Laboratory, Livermore, CA, UCRL-MA-137950.

Wolfrum, E., Allen, A., Barbee, Jr., T. W., Burnett, P., Djaoui, A., Kalantar, D., Keenan, R., Key, M. H., Lewis, C. L. S., Machacek, A., Remington, B., Rose, S. J., O'Rourke, R., and Wark, J. S., *Measurements of the XUV Opacity of a Strongly-Coupled Aluminum Plasma*, Lawrence Livermore National Laboratory, Livermore, CA, UCRL-JC-137262. Submitted to *Phys. Rev. Lett*.

Woolsey, N. C., Back, C. A., Lee, R. W., Calisti, A., Mosse, C., Stamm, R., Talin, B., Asfaw, A., and Klein, L. S., "Experimental Results on Line Shifts from Dense Plasmas," *J. Quant. Spectros. Radiat. Transfer* 65(1-3), 573–578 (2000).

Wu, Z. L., Stolz, C. J., Weakley, S. C., Hughes, J. D., and Zhao, Q., *Damage Threshold Prediction of Hafnia/Silica Multilayer Coatings by Nondestructive Evaluation of Fluence-Limiting Defects*, Lawrence Livermore National Laboratory, Livermore, CA, UCRL-JC-137089. Submitted to *Appl. Opt*.

Y

Yatsenko, L. P., Shore, B. W., Halfmann, T., Bergmann, K., and Vardi, A., "Source of Metastable H(2*s*) Atoms Using the Stark Chirped Rapid-Adiabatic-Passage Technique," *Phys. Rev. A* 60(6), R4237–4240 (1999).

Young, J. A., and Cook, R. C., *Helix Reversal Motion in Polyisocyanates*, Lawrence Livermore National Laboratory, Livermore, CA, UCRL-JC-140380. Submitted to *Macromolecules*.

Young, P. E., Suter, L. J., and Williams, E. A., *Dependence of Laser–Plasma Instability Growth on Laser Wavelength*, Lawrence Livermore National Laboratory, Livermore, CA, UCRL-JC-139591 ABS. Prepared for the *42nd Annual Mtg of the American Physical Society Div of Plasma Physics*, Quebec, Canada, Oct 23–27, 2000.

October 2000–September 2001

A

Adams, J. J., Ebbers, C. A., Schaffers, K. I., and Payne, S. A., *Nonlinear Optical Properties of $LaCa_4O(BO_3)_3$*, Lawrence Livermore National Laboratory, Livermore, CA, UCRL-JC-139794; also in *Opt. Lett*. 26(4), 217–219 (2001).

Afeyan, B., Montgomery, D. S., LeGalloudec, N., Seka, W., Meyerhofer, D., Schmitt, A. J., Hammer, J., and Kirkwood, R., *Optical Mixing Controlled Stimulated Scattering Instabilities in Beryllium Targets: The Weak Ion Acoustic Wave Damping Regime*, Lawrence Livermore National Laboratory, Livermore, CA, UCRL-JC-143598 ABS. Prepared for *31st Anomalous Absorption Conf*, Sedona, AZ, Jun 3–8, 2001.

Amendt, P., *Pseudomoment Fluid Modeling: Electron Landau Damping of Ion-Acoustic Waves*, Lawrence Livermore National Laboratory, Livermore, CA, UCRL-JC-127254 Rev 1; also in *Phys. Plasmas* 8(4), 1437–1440 (2001).

Amendt, P., Shestakov, A. I., Landen, O. L., Bradley, D. K., Pollaine, S. M., Suter, L. J., and Turner, R. E., "Thinshell Symmetry Surrogates for the National Ignition Facility: A Rocket Equation Analysis," *Phys. Plasmas* 8(6), 2908–2917 (2001).

Amendt, P., Shestakov, A. I., Landen, O., Pollaine, S., Bradley, D. K., and Suter, L., *Implosion Target Surrogacy Studies on OMEGA for the National Ignition Facility: Backlit Thinshells*, Lawrence Livermore National Laboratory, Livermore, CA, UCRL-JC-140743. Submitted to *Phys. of Plasmas*.

Auerbach, J. M., Wegner, P. J., Couture, S. A., Eimerl, D., Hibbard, R. L., Milam, D., Norton, M. A., Whitman, P. K., and Hackel, L. A., *Modeling of Frequency Doubling and Tripling with Measured Crystal Spatial Refractive-Index Nonuniformities*, Lawrence Livermore National Laboratory, Livermore, CA, UCRL-JC-139333; also in *Appl. Opt*. 40(9), 1404–1411 (2001).

B

Back, C. A., Davis, J. L., Grun, J., Landen, O. L., Miller, M. C., and Suter, L. J., *Multi-kilovolt X-Ray Conversion Efficiencies*, Lawrence Livermore National Laboratory, Livermore, CA, UCRL-JC-145192. Prepared for *Intl Symp on Optical Science and Technology*, San Diego, CA, Jul 29–Aug 4, 200l.

Back, C. A., Davis, J. L., Grun, J., Landen, O. L., Suter, L. J., Slark, G., and Oades, K., *Multi-Kilovolt X-Ray Conversion Efficiency*, Lawrence Livermore National Laboratory, Livermore, CA, UCRL-JC-142018 ABS. Prepared for *Society of Photo-Optical Instrumentation Engineers Conf*, San Diego, CA, Jul 29–Aug 3, 2001.

Back, C. A., Golovkin, I., Mancini, R., Missalla, T., Landen, O. L., Lee, R. W., and Klein, L., *Diagnosing Plasma Gradients Using Spectral Line Shapes*, Lawrence Livermore National Laboratory, Livermore, CA, UCRL-JC-139309. Prepared for *15th Intl Conf on Spectral Line Shapes*, Berlin, Germany, Jul 10–14, 2000.

Back, C. A., Miller, M. C., Davis, J. F., Grun, J., Landen, O. L., Hsing, W. W., Suter, L. J., Slark, G., Oades, K., and Stevenson, R. M., *Multikilovolt X-ray Source Development for NIF*, Lawrence Livermore National Laboratory, Livermore, CA, UCRL-JC-144683 ABS. Prepared for *43rd Annual Mtg of the American Physical Society Div of Plasma Physics*, Long Beach, CA, Oct 29–Nov 2, 200l.

Back, C. A., Suter, L. J., Davis, J., Grun, J., Decker, C. D., Landen, O. L., Hsing, W., Miller, M., and Wuest, C., *Multi-keV X-Ray Emission Produced by Supersonic Laser Heating*, Lawrence Livermore National Laboratory, Livermore, CA, UCRL-JC-140630 ABS. Prepared for *9th Intl Workshop on Radiative Properties of Hot Dense Matter*, Santa Barbara, CA, Oct 30–Nov 3, 2000.

Bajt, S., Stearns, D. G., and Kearney, P. A., "Investigation of the Amorphous-to-Crystalline Transition in Mo/Si Multilayers," *J. Appl. Phys*. 90(2), 1017–1025 (2001).

Baker, K. L., Estabrook, K. G., Drake, R. P., and Afeyan, B. B., "Alternative Mechanism for $\omega_0/2$ Emission in Laser-Produced Plasmas," *Phys. Rev. Lett*. 86(17), 3787–3790 (2001).

Baldis, H. A., Dunn, J., Foord, M. E., Rozmus, W., Anderson, C., and Shepherd, R., "New Regime of Thomson Scattering: Probing Dense Plasmas with X-Ray Lasers," *J. De Physique IV* 11(Pr2), 469–472 (2001).

Barton, I. M., Britten, J. A., Dixit, S. N., Summers, L. J., Thomas, I. M., Rushford, M. C., Lu, K., Hyde, R. A., and Perry, M. D., *Fabrication of Large-Aperture Lightweight Diffractive Lenses for Use in Space*, Lawrence Livermore National Laboratory, Livermore, CA, UCRL-JC-137928; also in *Appl. Opt*. 40(4), 447–451 (2001).

Beach, R. J., Mitchell, S. C., Meissner, H. E., Meissner, O. R., Krupke, W. F., McMahan, J. M., and Bennett, W. J., "Continuous-Wave and Passively Q-Switched Cladding-Pumped Planar Waveguide Lasers," *Optics Lett*. 26(12), 881–883 (2001).

Bell, P., Lee, D., Wooton, A., Mascio, B., Kimbrough, J., Sewall, N., Hibbard, W., Dohoney, P., Landon, M., Christianson, G., and Celeste, J., *Target Area and Diagnostic Interface Issues on the National Ignition Facility*, Lawrence Livermore National Laboratory, Livermore, CA, UCRL-JC-138387; also in *Rev. Sci. Inst*. 72(1Pt2), 492–498 (2001).

Bennett, G. R., Landen, O. L., Adams, R. F., Porter, J. L., Ruggles, L. E., Simpson, W. W., and Wakefield, C., "X-Ray Imaging Techniques on Z Using the Beamlet Laser," *Rev. Sci. Inst*. 72(1Pt2), 657–662 (2001).

Berger, R. L., Divol, L. M., Geddes, C. G., Glenzer, S. H., and Kirkwood, R. K., *Modeling Stimulated Raman Backscatter*, Lawrence Livermore National Laboratory, Livermore, CA, UCRL-PRES-143529. Prepared for *31st Anomalous Absorption Conf*, Sedona, AZ, Jun 3–8, 2001.

Berger, R. L., Divol, L. M., Geddes, C., Glenzer, S., and Kirkwood, R., *Do the Nonlinear Theories Really Explain the Saturation of SRS and SBS Observed in Experiments?* Lawrence Livermore National Laboratory, Livermore, CA, UCRL-JC-142067 ABS. Prepared for *4th Intl Workshop on Laser–Plasma Interaction Physics*, Banff, Alberta, Canada, Feb 21–24, 200l.

Berger, R. L., Kirkwood, R., Still, C. H., and Williams, E. A., *Modeling Stimulated Raman Backscatter*, Lawrence Livermore National Laboratory, Livermore, CA, UCRL-JC-143529 ABS. Prepared for *31st Anomalous Absorption Conf*, Sedona, AZ, Jun 3–8, 2001.

Berger, R. L., *Stimulated Forward and Backward Raman Scatter*, Lawrence Livermore National Laboratory, Livermore, CA, UCRL-PRES-143543. Prepared for *31st Anomalous Absorption Conf*, Sedona, AZ, Jun 3–8, 2001.

Berggren, R. R., Caldwell, S. E., Faulkner Jr., J. R., Lerche, R. A., Mack, J. M., Moy, K. J., Oertel, J. A., and Young, C. S., "Gamma-Ray-Based Fusion Burn Measurements," *Rev. Sci. Inst*. 72(1Pt2), 873–876 (2001).

Bittner, D., Burmann, J., Collins, G., Sater, J., and Unites, W., *Generating Low Temperature Layers with IR Heating*, Lawrence Livermore National Laboratory, Livermore, CA, UCRL-JC-143446 ABS. Prepared for *14th Target Fabrication Mtg*, West Point, NY, Jul 15–19, 2001.

Bohmer, K., Halfmann, T., Yatsenko, L. P., Shore, B. W., and Bergmann, K., "Stimulated Hyper-Raman Adiabatic Passage, III Experiment," *Phys. Rev. A* 64(2), 459–468 (2001).

Bourgade, J. L., Villette, B., Bocher, J. L., Boutin, J. Y., Chiche, S., Dague, N., Gontier, D., Jadaud, J. P., Savale, B., Wrobel, R., and Turner, R. E., "DMX: An Absolutely Calibrated Time-Resolved Broadband Soft X-Ray Spectrometer Designed for MJ Class Laser-Produced Plasmas," *Rev. Sci. Inst*. 72(1Pt2), 1173–1182 (2001).

Bradley, D. K., Bell, P. M., Dymoke-Bradshaw, A. K. L., Hares, J. D., Bahr, R. E., Smalyuk, V. A., Hargrove, D. R., and Piston, K., *Development and Characterization of a Single-Line-Of-Sight Framing Camera*, Lawrence Livermore National Laboratory, Livermore, CA, UCRL-JC-138002; also in *Rev. Sci. Inst*. 72(1Pt2), 694–697 (2001).

Bradley, D. K., Collins, G. W., Braun, D. G., Cauble, R. C., Celliers, P., MacKinnon, A. J., Moon, S., and Wallace, R., *Generation of High Pressure, Steady Shocks in Metals Using High Power Laser Systems*, Lawrence Livermore National Laboratory, Livermore, CA, UCRL-JC-144680 ABS. Prepared for *43rd Annual Mtg of the American Physical Society Div of Plasma Physics*, Long Beach, CA, Oct 29–Nov 2, 200l.

Bradley, D. K., Collins, G. W., Celliers, P., Hicks, D., Da Silva, L. B., MacKinnon, A., Cauble, R., Moon, S. J., Wallace, R., Hammel, B., Hsing, W., Koenig, M., Benuzzi, A., Huser, G., Henry, E., Batani, D., Willi, O., Pasley, J., Henning, G., Loubeyre, P., Jeanloz, R., Lee, K. M., Benedetti, L. R., Neely, D., Notley, M., and Danson, C., *Equation of State Measurements in Singly Shocked Diamond*, Lawrence Livermore National Laboratory, Livermore, CA, UCRL-PRES-142143. Prepared for *12 Biennial Intl Conf of the American Physical Society Topical Group on Shock Compression of Condensed Matter*, Atlanta, GA, Jun 24–29, 200l.

Branham, K. E., Byrd, H., Cook, R., Mays, J. W., and Gary, G. M., *Preparation of Soluble, Linear Titanium-Containing Copolymers, by the Free Radical Copolymerization of Vinyl Titanate Monomers with Styrene*, Lawrence Livermore National Laboratory, Livermore, CA, UCRL-JC-134776; also in *J. Appl. Polymer Sci*. 78(l), 190–199 (2000).

Buckley, S. R., Fearon, E., Hassel, A. E., Chancellor, C., Ross, T., Orthion, P. J., Letts, S. A., and Cook, R. C., *Developments in Polyimide Coating and Characterization for NIF Capsules*, Lawrence Livermore National Laboratory, Livermore, CA, UCRL-JC-143739 ABS. Prepared for *14th Target Fabrication Mtg*, West Point, NY, Jul 15–19, 2001.

Budil, K. S., Lasinski, B., Edwards, M. J., Wan, A. S., Remington, B. A., Weber, S. V., Glendinning, S. G., Suter, L., and Stry, P. E., *The Ablation-Front Rayleigh–Taylor Dispersion Curve in Indirect Drive*, Lawrence Livermore National Laboratory, Livermore, CA, UCRL-JC-139581; also in *Phys. Plasmas* 8(5Pt2), 2344–2348 (2001).

Bullock, A. B., Landen, O. L., and Bradley, D. K., *10 and 5 μm Pinhole-Assisted Point-Projection Backlit Imaging for the National Ignition Facility*, Lawrence Livermore National Laboratory, Livermore, CA, UCRL-JC-137904; also in *Rev. Sci. Inst*. 72(1Pt2), 690–693 (2001).

Bullock, A. B., Landen, O. L., and Bradley, D. K., *Relative X-Ray Backlighter Intensity Comparison of Ti and Ti/Sc Combination Foils Driven in Double-Sided and Single-Sided Laser Configuration,* Lawrence Livermore National Laboratory, Livermore, CA, UCRL-JC-139282; also in *Rev. Sci. Inst*. 72(1Pt2), 686–689 (2001).

Burger, A., Chattopadhyay, K., Ndap, J. O., Ma, X., Morgan, S. H., Rablau, C. I., Su, C.-H., Feth, S., Page, R. H., Shaffers, K. I., and Payne, S. A., "Preparation Conditions of Chromium Doped ZnSe and Their Infrared Luminescence Properties," *J. Crystal Growth* 225(2-4), 249–256 (2001).

Burmann, J., Bittner, D., Jones, R., Moody, J., Pipes, J., and Sanchez, J., *Assembly Techniques for Cryo Hohlraums*, Lawrence Livermore National Laboratory, Livermore, CA, UCRL-JC-143419 ABS. Prepared for *14th Target Fabrication Mtg*, West Point, NY, Jul 15–19, 2001.

C

Cauble, R., Bradley, D. K., Celliers, P. M., Collins, G. W., Da Silva, L. B., and Moon, S. J., "Experiments Using Laser-Driven Shockwaves for EOS and Transport Measurements," *Contrib. Plasma Phys*. 41(2-3), 239–242 (2001).

Celliers, P. M., Amendt, P. A., Wallace, R. J., Collins, G. W., Bradley, D. K., Landen, O. L., and Hammel, B. A., *Streaked Radiography for NIF Shock Timing Studies*, Lawrence Livermore National Laboratory, Livermore, CA, UCRL-JC-144819 ABS. Prepared for *43rd Annual Mtg of the American Physical Society Div of Plasma Physics*, Long Beach, CA, Oct 29–Nov 2, 2001.

Celliers, P. M., Collins, G. W., Hicks, D., Da Silva, L. B., MacKinnon, A., Cauble, R., Moon, S. J., Wallace, R. J., Hammel, B. A., Hsing, W. W., Koenig, M., Benuzzi, A., Huser, G., Henry, E., Batani, D., Loubeyre, P., Willi, O., Pasley, J., Gessner, H., Jeanloz, R., Lee, K. M., Benedetti, L. R., Neely, D., Notley, M., and Danson, C., *Reflected Shock States in Water*, Lawrence Livermore National Laboratory, Livermore, CA, UCRL-PRES-142250. Prepared for *American Physical Society 2001 Mtg on Shock Compression of Condensed Matter*, Atlanta, GA, Jun 25–29, 200l.

Celliers, P. M., Collins, G. W., Hicks, D., Da Silva, L. B., McKinnon, A., Cauble, R., Moon, S. J., Wallace, R. J., Hammel, B. A., Koenig, M., Benuzzi, A., Huser, G., Henry, E., Batani, D., Masclet, I., Marchet, B., Rebec, M., Reverdin, C., Dague, N., Willi, O., Pasley, J., Gessner, H., Neely, D., Notley, M., and Danson, C., *Shock Hugoniot and Optical Measurements of Strongly Shocked Water*, Lawrence Livermore National Laboratory, Livermore, CA, UCRL-JC-144829 ABS. Prepared for *2nd Intl Conf on Fusion Sciences and Applications*, Kyoto, Japan, Sep 9–14, 2001.

Cohen, B. I., Baldis, H. A., Berger, R. L., Estabrook, K. G., Williams, E. A., and Labaune, C., *Modeling of the Competition of Stimulated Raman and Brillouin Scatter in Multiple Beam Experiments*, Lawrence Livermore National Laboratory, Livermore, CA, UCRL-JC-134924; also in *Phys. Plasmas* 8(2), 571–591 (2001).

Collins, G. W., Celliers, P. M., Hicks, D. G., MacKinnon, A. J., Moon, S. J., Cauble, R., Da Silva, L. B., Koenig, M., Benuzzi-Mounaix, A., Huser, G., Jeanloz, R., Lee, K. M., Benedetti, L. R., Henry, E., Batani, D., Willi, O., Pasley, J., Gessner, H., Neely, D., Notley, M., and Danson, C., *Using Vulcan to Recreate Planetary Cores*, Lawrence Livermore National Laboratory, Livermore, CA, UCRL-ID-145157.

Collins, G. W., Celliers, P. M., Hicks, D., Da Silva, L. B., MacKinnon, A., Cauble, R., Moon, S. J., Wallace, R., Hammel, B., Hsing, W., Koenig, M., Benuzzi, A., Huser, G., Henry, E., Batani, D., Willi, O., Pasley, J., Henning, G., Loubeyre, P., Jeanloz, R., Lee, K. M., Benedetti, L. R., Neely, D., Notley, M., and Danson, C., *Optical Properties of Simple Shock Compressed Fluids*, Lawrence Livermore National Laboratory, Livermore, CA, UCRL-JC-142028 ABS. Prepared for *American Physical Society Topical Conf*, Atlanta, GA, Jun 25–29, 2001.

Colvin, J. D., Legrand, M., Remington, B. A., Schurtz, G., and Weber, S. V., *A Model for Instability Growth in Accelerated Solid Metals*, Lawrence Livermore National Laboratory, Livermore, CA, UCRL-JC-143792 ABS. Prepared for *8th Intl Workshop on the Physics of Compressible Turbulent Mixing*, Pasadena, CA, Dec 9–14, 2001.

Cook, R. C., *A Model Study of the Possible Effect of Beryllium Grain Sound Speed Anisotropy on ICF Capsule*, Lawrence Livermore National Laboratory, Livermore, CA, UCRL-JC-143758 ABS. Prepared for *14th Target Fabrication Mtg*, West Point, NY, Jul 15–19, 2001.

Cowan, T. E., Roth, M., Johnson, J., Brown, C., Christl, M., Fountain, W., Hatchett, S., Henry, E. A., Hunt, A. W., Key, M. H., MacKinnon, A., Parnell, T., Pennington, D. M., Perry, M. D., Phillips, T. W., Sangster, T. C., Singh, M., Snavely, R., Stoyer, M., Takahashi, Y., Wilks, S. C., and Yasuike, K., "Intense Electron and Proton Beams from Petawatt Laser–Matter Interactions," *Nucl. Instrum. Meth*ods 455A(1), 130–139 (2000).

Cuneo, M. E., Vesey, R. A., Porter Jr., J. L., Chandler, G. A., Fehl, D. L., Gilliland, T. L., Hanson, D. L., McGurn, J. S., Reynolds, P. G., Ruggles, L. E., Seamen, H., Spielman, R. B., Struve, K. W., Stygar, W. A., Simpson, W. W., Torres, J. A., Wenger, D. F., Hammer, J. H., Rambo, P. W., Peterson, D. L., and Idzorek, G. C., "Development and Characterization of a Z-Pinch-Driven Hohlraum High-Yield Inertial Confinement Fusion Target Concept," *Phys. Plasmas* 8(5Pt2), 2257–2267 (2001).

D

Dattolo, E., Suter, L., Monteil, M.-C., Jadaud, J.-P., Dague, N., Glenzer, S., Turner, R., Juraszek, D., Lasinski, B., Decker, C., Landen, O., and MacGowan, B., *Status of Our Understanding and Modeling of X-Ray Coupling Efficiency in Laser Heated Hohlraums*, Lawrence Livermore National Laboratory, Livermore, CA, UCRL-JC-137622; also in *Phys. Plasmas* 8(1), 260–265 (2001).

Debeling, G., Brugman, V. P., Dalder, E., and Riddle, R., *Structural Analysis of the D_2 TS High Pressure Cell Assembly*, Lawrence Livermore National Laboratory, Livermore, CA, UCRL-JC-143686 ABS. Prepared for *14th Target Fabrication Mtg*, West Point, NY, Jul 15–19, 2001.

Delage, O., Dague, N., Le, T., Lerche, R. A., Sangster, T. C., Izumi, N., Jaanimagi, P. A., and Fisher, R. K., *High Spatial Resolution Imaging System for High Energy Neutrons in Inertial Confinement Fusion Experiments*, Lawrence Livermore National Laboratory, Livermore, CA, UCRL-JC-142031 ABS. Prepared for *Intl Symp on Optical Science and Technology*, San Diego, CA, Jul 29–Aug 3, 2001.

Delage, O., Lerche, R. A., Sangster, T. C., and Arsenault, H. H., *SIRINC: A Code for Assessing and Optimizing the Neutron Imaging Diagnostic Capabilities in Inertial Confinement Fusion Experiments*, Lawrence Livermore National Laboratory, Livermore, CA, UCRL-JC-137922 ABS; also in *Rev. Sci. Inst*. 76(1PT2), 869–872 (2001).

Demos, S. G., Kozlowski, M. R., Staggs, M., Chase, L. L., Burnham, A., and Radousky, H. B., *Mechanisms to Explain Damage Growth in Optical Materials*, Lawrence Livermore National Laboratory, Livermore, CA, UCRL-JC-139771. Prepared for *Annual Symp on Optical Materials for High Power Lasers*, Boulder, CO, Oct 15–18, 2000.

Depierreux, S., Labaune, C., Fuchs, J., and Baldis, H. A., "Application of Thomson Scattering to Identify Ion Acoustic Waves Stimulated by the Langmuir Decay Instability," *Rev. Sci. Inst*. 71(9), 3391–3401 (2000).

Dimonte, G., Dimits, A., Weber, S., Youngs, D., Calder, A., Fryxell, B., Biello, J., Dursi, L., MacNeice, P., Olson, K., Ricker, P., Rosner, R., Timmes, F., Tufo, H., Young, Y. N., Zingale, M., Andrews, M., Ramaprabhu, P., Wunsch, S., Garasi, C., and Robinson, A., *A Comparison of High-Resolution 3D Numerical Simulations of Turbulent Rayleigh–Taylor (RT) Instability: Alpha-Group Collaboration*, Lawrence Livermore National Laboratory, Livermore, CA, UCRL-JC-143796 ABS. Prepared for *8th Intl Workshop on the Physics of Compressible Turbulent Mixing*, Pasadena, CA, Dec 9–14, 2001.

Dimonte, G., Turner, R., Landen, O., Tipton, R., Amendt, P., Colvin, J., Mikaelian, K., Jones, O., and Wallace, R., *Multi-Shell Implosions on the Omega Laser*, Lawrence Livermore National Laboratory, Livermore,

CA, UCRL-JC-144684 ABS. Prepared for *43rd Annual Mtg of the American Physical Society Div of Plasma Physics*, Long Beach, CA, Oct 29–Nov 2, 2001.

Dipeso, G., Dimonte, G., Hewett, D., VanZeeland, M., and Gekelman, W., *Alfven Wave Generation by Exploding Plasma*, Lawrence Livermore National Laboratory, Livermore, CA, UCRL-JC-144686 ABS. Prepared for *43rd Annual Mtg of the American Physical Society Div of Plasma Physics*, Long Beach, CA, Oct 29–Nov 2, 2001.

Dunn, J., Faenov, A. Y., Pikuz, T. A., Osterheld, A. L., Moon, S. J., Fournier, K. B., Nilsen, J., Skobelev, I. Y., Magunov, A. I., and Shlyaptsev, V. N., "Spectral and Imaging Characterization of Tabletop X-Ray Lasers," *J. De Physique IV*, 11(Pr2), 51–54 (2001).

Dunn, J., Osterheld, A. L., Nilsen, J., Hunter, J. R., Li, Y. L., Faenov, A. Y., Pikuz, T. A., and Shlyaptsev, V. N., "Saturated Output Tabletop X-Ray Lasers," *J. De Physique IV*, 11(Pr2), 19–26 (2001).

E

Edwards, J., Lorenz, T., Kalantar, D., Remington, B., Colvin, J., and Greenough, J., *Shockless Acceleration and Compression of Aluminum Foils Using a Laser Driven Plasma Reservoir*, Lawrence Livermore National Laboratory, Livermore, CA, UCRL-JC-144685 ABS. Prepared for *43rd Annual Mtg of the American Physical Society Div of Plasma Physics*, Long Beach, CA, Oct 29–Nov 2, 2001.

Edwards, M. J., MacKinnon, A. J., Zwieback, J., Shigemori, K., Ryutov, D., Rubenchik, A. M., Kielty, K. A., Liang, E., Remington, B. A., and Ditmire, T., "Investigation of Ultrafast Laser-Driven Radiative Blast Waves," *Phys. Rev. Lett*. 87(8), 72–74 (2001).

F

Feldman, J. L., Eggert, J. H., Mao, H. K., and Hemley, R. J., "Computations of Vibron Excitations and Raman Spectra of Solid Hydrogen," *J. Low Temp. Phys*. 122(3/4), 389–399 (2001).

Fiedorowicz, H., Bartnik, H., Dunn, J., Smith, R. F., Hunter, J., Nilsen, J., Osterheld, A. L., and Shlyaptsev, V. N., "Demonstration of a Neonlike Argon Soft X-Ray Laser with a Picosecond-Laser-Irradiated Gas Puff Target," *Opt. Lett*. 26(18), 1403–1405 (2001).

Fourkal, E., Bychenkov, V. Y., Rozmus, W., Sydora, R., Kirkby, C., Capjack, C. E., Glenzer, S. H., and Baldis, H. A., *Electron Distribution Function in Laser Heated Plasmas*, Lawrence Livermore National Laboratory, Livermore, CA, UCRL-JC-139494; also in *Phys. Plasmas* 8(2), 550–556 (2001).

Frenje, J. A., Green, K. M., Hicks, D. G., Li, C. K., Seguin, F. H., Petrasso, R. D., Sangster, T. C., Phillips, T. W., Glebov, V. Y., Meyerhofer, D. D., Roberts, S., Soures, J. M., Stoeckl, C., Fletcher, K., Paladino, S., and Leeper, R. J., "A Neutron Spectrometer for Precise Measurements of DT Neutrons from 10 to 18 MeV at OMEGA and the National Ignition Facility," *Rev. Sci. Inst*. 72(1Pt2), 854–858 (2001).

Froula, D. H., and Glenzer, S. H., *Growth of Ion Acoustic Waves in Two Species Plasmas*, Lawrence Livermore National Laboratory, Livermore, CA, UCRL-JC-144575 ABS. Prepared for *43rd Annual Mtg of the American Physical Society Div of Plasma Physics*, Long Beach, CA, Oct 29–Nov 2, 2001.

Fuchs, J., Labaune, C., Depierreaux, S., Baldis, H. A., Michard, A., and James, G., *Experimental Evidence of Plasma-Induced Incoherrence of an Intense Laser Beam Propagating in an Underdense Plasma*, Lawrence Livermore National Laboratory, Livermore, CA, UCRL-JC-139495; also in *Phys. Rev. Lett*. 86(3), 432–435 (2001).

Fuchs, J., Labaune, C., Depierreux, S., Tikhonchuk, V. T., and Baldis, H. A., *Stimulated Brillouin and Raman Scattering from a Randomized Laser Beam in Large Inhomogeneous Plasmas. Experiment*, Lawrence Livermore National Laboratory, Livermore, CA, UCRL-JC-139507-PT-1; also in *Phys. Plasmas* 7(11), 4659–4668 (2000).

G

Garces, N. Y., Stevens, K. T., Halliburton, L. E., Demos, S. G., Radousky, H. B., and Zaitseva, N. P., *Identification of Electron and Hole Traps in KH_2PO_4 Crystals*, Lawrence Livermore National Laboratory, Livermore, CA, UCRL-JC-139770; also in *J. Appl. Phys*. 89(l), 47–52 (2001).

Garces, N. Y., Stevens, K. T., Halliburton, L. E., Yan, M., Zaitseva, N.P., and De Yoreo, J. J., "Optical Absorption and Electron Paramagnetic Resonance of Fe Ions in KDP Crystals," *J. Crystal Growth* 225(2-4), 435–439 (2001).

Gee, R. H., Fried, L. E., and Cook, R. C., *Structure of Chlorotrifluoroethylene/Vinylidene Fluoride Random Copolymers and Homopolymers by Molecular Dynamics Simulations*, Lawrence Livermore National Laboratory, Livermore, CA, UCRL-JC-141025; also in *Macromolecules* 34(9), 3050–3059 (2001).

Glendinning, S. G., Braun, D. G., Edwards, M. J., Hsing, W. W., Lasinski, B. F., Louis, H., Moreno, J., Peyser, T. A., Remington, B. A., Robey, H. F., Turano, E. J., Verdon, C. P., and Zhou, Y., *An Experimental Study of the Effect of Shock Proximity on the Richtmyer–Meshkov Instability at High Mach Number*, Lawrence Livermore National Laboratory, Livermore, CA, UCRL-JC-143806 ABS Rev 1. Prepared for *43rd Annual Mtg of the American Physical Society Div of Plasma Physics*, Long Beach, CA, Oct 29–Nov 2, 2001.

Glenzer, S. H., Berger, R. L., Divol, L. M., Kirkwood, R. K., MacGowan, B. J., Moody, J. D., Langdon, A. B., Suter, L. J., and Williams, E. A., *Reduction of Stimulated Scattering Losses from Hohlraum Plasmas with Laser Beam Smoothing*, Lawrence Livermore National Laboratory, Livermore, CA, UCRL-JC-141689; also in *Phys. Plasmas* 8(5Pt1), 1692–1696 (2001).

Glenzer, S. H., Berger, R. L., Divol, L. M., Kirkwood, R. K., MacGowan, B. J., Moody, J. D., Rothenberg, J. E., Suter, L. J., and Williams, E. A., "Laser-Plasma Interactions in Inertial Confinement Fusion Hohlraums," *Phys. Rev. Lett*. 87(4), 64–66 (2001).

Glenzer, S. H., *Dense Plasma Characterization by X-Ray Thomson Scattering*, Lawrence Livermore National Laboratory, Livermore, CA, UCRL-JC-144574 ABS. Prepared for *43rd Annual Mtg of the American Physical Society Div of Plasma Physics*, Long Beach, CA, Oct 29–Nov 2, 2001.

Glenzer, S. H., Divol, L. M., Berger, R. L., Geddes, C., Kirkwood, R. K., Moody, J. D., Williams, E. A., and Young, P. E., *Thomson Scattering Measurements of Saturated Ion Waves in Laser Fusion Plasmas*, Lawrence Livermore National Laboratory, Livermore, CA, UCRL-JC-140588; also in *Phys. Rev. Lett*. 86(12), 2565–2568 (2001).

Glenzer, S. H., Fournier, K. B., Wilson, B. G., Lee, R. W., and Suter, L. J., *Ionization Balance in Inertial Confinement Fusion Hohlraums*, Lawrence Livermore National Laboratory, Livermore, CA, UCRL-JC-139505. Submitted to *Phys. Rev. Lett*.

Glenzer, S. H., Fournier, K. B., Wilson, B. G., Lee, R. W., Suter, L. J., and Young, P. E., *Ionization Balance in Inertial Confinement Fusion Hohlraum Plasmas*, Lawrence Livermore National Laboratory, Livermore, CA, UCRL-JC-141095 ABS. Prepared for *9th Intl Workshop on Radiative Properties of Hot Dense Matter*, Santa Barbara, CA, Oct 30–Nov 3, 2000.

Glenzer, S. H., *Thomson Scattering in Inertial Confinement Fusion Research*, Lawrence Livermore National Laboratory, Livermore, CA, UCRL-JC-135822; also in *Contrib. Plasma Phys*. 40(1-2), 36–45 (2000).

Glenzer, S., Jones, O., Speck, D. R., Munro, D., Lerche, R., Salmon, T., Bliss, E., Gates, A., Boyd, B., Auerbach, J., Williams, W., Saroyan, A., Kalantar, D., MacGowan, B., Zacharias, R., Hayman, C., and Sacks, R., *3ω Power Balance Procedure on the NIF*, Lawrence Livermore National Laboratory, Livermore, CA, UCRL-ID-142777.

Glinsky, M. E., Bailey, D. S., London, R. A., Amendt, P. A., Rubenchik, A. M., and Strauss, M., *An Extended Rayleigh Model of Bubble Evolution*, Lawrence Livermore National Laboratory, Livermore, CA, UCRL-JC-130969 Rev 2; also in *Phys. Fluids* 13(l), 20–31 (2001).

Gulec, K., Abdou, M., Moir, R. W., Morley, N. B., and Ying, A., "Novel Liquid Blanket Configurations and Their Hydrodynamic Analyses for Innovative Confinement Concepts," *Fus. Engr. Design* 49, 567–576 (2000).

H

Haan, S. W., Dittrich, T., Hatchett, S., Hinkel, D., Marinak, M., Munro, D., Jones, O., Pollaine, S., and Suter, L., *Update on Instability Modeling for the NIF Ignition Targets*, Lawrence Livermore National Laboratory, Livermore, CA, UCRL-JC-143897 ABS. Prepared for *8th Intl Workshop on the Physics of Compressible Turbulent Mixing*, Pasadena, CA, Dec 9–14, 2001.

Haan, S. W., Dittrich, T., Hatchett, S., Hinkel, D., Marinak, M., Munro, D., Jones, O., Pollaine, S., and Suter, L., *Update on Ignition Target Fabrication Specification*, Lawrence Livermore National Laboratory, Livermore, CA, UCRL-JR-143218 ABS. Prepared for *14th Target Fabrication Mtg*, West Point, NY, Jul 15–19, 2001.

Haan, S. W., Dittrich, T., Hinkel, D., Strobel, G., Suter, L., Marinak, M., and Amendt, P., *Update on NIF Indirect Drive Ignition Target Fabrication Specifications*, Lawrence Livermore National Laboratory, Livermore, CA, UCRL-PRES-144266. Prepared for *14th Target Fabrication Mtg*, West Point, NY, Jul 15–19, 200l.

Haan, S. W., *Update on NIF Indirect Drive Ignition Target Design*, Lawrence Livermore National Laboratory, Livermore, CA, UCRL-JC-144267. Prepared for *2nd Intl Conf on Inertial Fusion Science and Applications*, Kyoto, Japan, Sep 7–15, 200l.

Hartemann, F. V., Baldis, H. A., Kerman, A. K., Le Foll, A., Luhman, N. C., and Rupp, B., "Three-Dimensional Theory of Emittance in Compton Scattering and X-Ray Protein Crystallography," *Phys. Rev. E* 64(1,Pt2), 730–754 (2001).

Hassel, A. E., Chancellor, C., Letts, S. A., Parrish, B., Orthion, P., Fearon, E., Buckley, S., and Cook, R. C., *Development of the Smoothing Technique for Polyimide NIF Capsules*, Lawrence Livermore National Laboratory, Livermore, CA, UCRL-JC-143417 ABS. Prepared for *14th Target Fabrication Mtg*, West Point, NY, Jul 15–19, 2001.

Heeter, R. F., Bailey, J. E., Cuneo, M. E., Emig, J., Foord, M. E., Springer, P. T., and Thoe, R. S., *Plasma Diagnostics for X-Ray Driven Foils at Z*, Lawrence Livermore National Laboratory, Livermore, CA, UCRL-JC-138708; also in *Rev. Sci. Inst*. 72(1Pt2), 1224–1227 (2001).

Herrmann, M. C., Tabak, M., and Lindl, J. D., *Ignition Scaling Laws and Their Application to Capsule Design*, Lawrence Livermore National Laboratory, Livermore, CA, UCRL-JC-141036; also in *Phys. Plasmas* 8(5Pt2), 2296–2304 (2001).

Hibbard, W. J., Landon, M. D., Vergino, M. D., Lee, F. D., and Chael, J. A., *Design of the National Ignition Facility Diagnostic Instrument Manipulator*, Lawrence Livermore National Laboratory, Livermore, CA, UCRL-JC-137910; also in *Rev. Sci. Inst*. 72(1Pt2), 530–532 (2001).

Hicks, D. G., Celliers, P. M., Collins, G. W., Da Silva, L. B., Mackinnon, A., Cauble, R., Moon, S. J., Wallace, R. J., Hammel, B. A., Koenig, M., Benuzzi, A., Huser, G., Henry, E., Batani, D., Loubeyre, P., Willi, O., Pasley, J., Gessner, H., Jeanloz, R., Lee, K. M., Benedetti, L. R., Neely, D., Bitketm N., and Danson, C., *Generating Extreme Densities in Water Using Laser-Driven Shocks in Diamond Anvil Cells*, Lawrence Livermore National Laboratory, Livermore, CA, UCRL-JC-142027 ABS. Prepared for *American Physical Society Topical Conf*, Atlanta, GA, Jun 25–29, 2001.

Hicks, D. G., Celliers, P. M., Collins, G. W., Da Silva, L. B., Mackinnon, A. J., Cauble, R., Moon, S. J., Wallace, R. J., Hammel, B. A., Koenig, M., Benuzzi, A., Huser, G., Henry, E., Batani, D., Loubeyre, P., Willi, O., Pasley, J., Gessner, H., Jeanloz, R., Lee, K. M., Benedetti, L. R., Neely, D., Notley, M., and Danson, C., *Laser-Driven Shocks in Water Pre-Compressed by Diamond Anvil Cells*, Lawrence Livermore National Laboratory, Livermore, CA, UCRL-JC-144666 ABS. Prepared for *43rd Annual Mtg of the American Physical Society Div of Plasma Physics*, Long Beach, CA, Oct 29–Nov 2, 2001.

Hicks, D. G., Li, C. K., Seguin, F. H., Frenje, J. A., Petrasso, R. D., and Sangster, T. C., "Optimal Foil Shape for Neutron Time-Of-Flight Measurements Using Elastic Recoils," *Rev. Sci. Inst*. 72(1Pt2), 859–862 (2001).

Hicks, D. G., Li, C. K., Seguin, F. H., Ram, A. K., Frenje, J. A., Petrasso, R. D., Soures, J. M., Glebov, V. Y., Meyerhofer, D. D., Roberts, S., Sorce, C., Stockl, C., Sangster, T. C., and Phillips, T. W., *Charged-Particle Acceleration and Energy Loss in Laser-Produced Plasmas*, Lawrence Livermore National Laboratory, Livermore, CA, UCRL-MI-140997; also in *Phys. Plasmas* 7(12), 5106–5117 (2000).

Hicks, D. G., Li, C. K., Seguin, F. H., Schnittman, J. D., Ram, A. K., Frenje, J. A., Petrasso, R. D., Soures, J. M., Meyerhofer, D. D., Roberts, S., Sorce, C., Stockl, C., Sangster, T. C., and Phillips, T. W., *Observations of Fast Protons Above 1 MeV Produced in Direct-Drive Laser-Fusion Experiments*, Lawrence Livermore National Laboratory, Livermore, CA, UCRL-JC-136746; also in *Phys. Plasmas* 8(2), 606–610 (2001).

Hinkel, D. E., Langdon, A. B., and Suter, L. J., *Filamentation and Backscatter in High Temperature Hohlraums*, Lawrence Livermore National Laboratory, Livermore, CA, UCRL-JC-142065 ABS. Prepared for *4th Intl Workshop on Laser–Plasma Interaction Physics*, Banff, Alberta, Canada, Feb 21–24, 2001.

Hsing, W. W., *High Energy Density Experimental Capabilities*, Lawrence Livermore National Laboratory, Livermore, CA, UCRL-JC-144682 ABS. Prepared for *43rd Annual Mtg of the American Physical Society Div of Plasma Physics*, Long Beach, CA, Oct 29–Nov 2, 2001.

Hsing, W., *Accurate Phase Diagrams for Simple Molecular Fluids (H_2, H_2O, NH_3, and CH_4) and Their Constituent Elements Are Important for Constructing Planetary Models of the Gas Giant Planets (Jupiter, Saturn, Uranus, and Neptune)*, Lawrence Livermore National Laboratory, Livermore, CA, UCRL-JC-144103 ABS. Prepared for *43rd Annual Mtg of the Div of Plasma Physics*, Long Beach, CA, Oct 29–Nov 2, 2001.

Hurricane, O.A., Glendinning, S. G., Remington, B. A., Drake, R. P., and Dannenberg, K. K., "Late-Time Hohlraum Pressure Dynamics in Supernova Remnant Experiments," *Phys. Plasmas* 8(6), 2609–2612 (2001).

I

Izumi, N., Lerche, R. A., Moran, M. J., Phillips, T. W., Sangster, T. C., Schmid, G. J., and Stoyer, M. A., *Nuclear Diagnostics of ICF*, Lawrence Livermore National Laboratory, Livermore, CA, UCRL-PRES-144322. Prepared for *6th Intl Conf on Advanced Diagnostics for Magnetic and Inertial Fusion*, Villa Monastero, Varenna, Italy, Sep 3–7, 200l.

Izumi, N., Lerche, R. A., Phillips, T. W., Schmid, G. J., Moran, M. J., and Sangster, T. C., *Development of Lower Energy Neutron Spectroscopy for Areal Density Measurement in Implosion Experiment at NIF and Omega*, Lawrence Livermore National Laboratory, Livermore, CA, UCRL-JC-142032. Prepared for *46th Annual Mtg of The Intl Symp on Optical Science and Technology*, San Diego, CA, Jul 29–Aug 3, 200l.

Izumi, N., Lerche, R. A., Phillips, T. W., Schmid, G. J., Moran, M. J., Hatchett, S. P., and Sangster, T. C., *Conceptual Design of a Scintillation Fiber Neutron Detector ρR Measurements in ICF*, Lawrence Livermore National Laboratory, Livermore, CA, UCRL-JC-144668 ABS. Prepared for *43rd Annual Mtg of the American Physical Society Div of Plasma Physics*, Long Beach, CA, Oct 29–Nov 2, 2001.

J

Jones, R. L., and Burmann, J., *Characterization and Assembly Techniques for 2mm CD Shells for Cryogenic Targets*, Lawrence Livermore National Laboratory, Livermore, CA, UCRL-JC-143420 ABS. Prepared for *14th Target Fabrication Mtg*, West Point, NY, Jul 15–19, 2001.

K

Kalantar, D. H., Allen, A. M., Gregori, F., Kad, B., Kumar, M., Lorenz, K. T., Loveridge, A., Meyers, M. A., Pollaine, S., Remington, B. A., and Wark, J. S., *Laser Driven High Pressure, High Strain-Rate Materials Experiments*, Lawrence Livermore National Laboratory, Livermore, CA, UCRL-JC-141824. Prepared for *12th Biennial Intl Conf of the American Physical Society Topical Group on Shock Compression of Condensed Matter*, Atlanta, GA, Jun 24–29, 200l.

Kalantar, D. H., Belak, J. F., Colvin, J. D., Edwards, M. J., Lasinski, B. F., Pollaine, S., Remington, B. A., Shay, H. D., and Weber, S. V., *High Pressure, Solid-State Strength Experiments for NIF*, Lawrence Livermore National Laboratory, Livermore, CA, UCRL-JC-144681 ABS. Prepared for *13th Biennial Nuclear Explosives Design Physics Conf*, Livermore, CA, Oct 15–19, 200l.

Kalantar, D. H., Belak, J., Colvin, J. D., Kumar, M., Lorenz, K. T., Mikaelian, K. O., Pollaine, S., Remington, B. A., Weber, S. V., Wiley, L. G., Allen, A. M., Loveridge, A., Wark, J. S., and Meyers, M. A., *Laser-Based High Pressure, High-Strain Solid-State Experiments*, Lawrence Livermore National Laboratory, Livermore, CA, UCRL-JC-143749 ABS. Prepared for *American Chemical Society Mtg*, Chicago, IL, Aug 25–30, 2001.

Kalantar, D. H., Belak, J., Colvin, J. D., Kumar, M., Lorenz, K. T., Mikaelian, K. O., Pollaine, S., Remington, B. A., Weber, S. V., Wiley, L. G., Allen, A. M., Loveridge-Smith, A., Wark, J. S., and Meyers, M. A., *Laser-Based High Pressure, High Strain-Rate Solid-State Experiments*, Lawrence Livermore National Laboratory, Livermore, CA, UCRL-JC-143823 ABS Rev 1. Prepared for *8th Intl Workshop on the Physics of Compressible Turbulent Mixing*, Pasadena, CA, Dec 9–14, 2001.

Kalantar, D. H., Belak, J., Lorenz, K. T., Lubcke, A., Pollaine, S., Remington, B. A., Allen, A. M., Wark, J. S., Meyers, M., and Boehly, T. R., *Laser Driven High Pressure, High Strain Rate Materials Experiments*, Lawrence Livermore National Laboratory, Livermore, CA, UCRL-JC-141824 ABS Rev 1. Prepared for *43rd Annual Mtg of the American Physical Society Div of Plasma Physics*, Long Beach, CA, Oct 29–Nov 2, 2001.

Kalantar, D. H., Bell, P. M., Perry, T. S., Sewall, N., Kimbrough, J., Weber, F., Diamond, C., and Piston, K., *Optimizing Data Recording for the NIF Core Diagnostic X-Ray Streak Camera*, Lawrence Livermore National Laboratory, Livermore, CA, UCRL-JC-138107; also in *Rev. Sci. Inst*. 762(1Pt2), 751–754 (2001).

Kalantar, D., and Meyers, M., *2000 NLUF Program: Dynamic X-Ray Diffraction*, Lawrence Livermore National Laboratory, Livermore, CA, UCRL-JC-141396 SUM.

Kane, J. O., Robey, H. F., Remington, B. A., Drake, R. P., Knauer, J., Ryutov, D. D., Lewis, H., Teyssier, R., Hurricane, O., Arnett, D., Rosner, R., and Calder, A., "Interface Imprinting by a Rippled Shock Using an Intense Laser," *Phys. Rev. E* 63(5Pt2), 22–24 (2001).

Kauffman, R., *Inertial Confinement Fusion Annual Report 1999*, Lawrence Livermore National Laboratory, Livermore, CA, UCRL-LR-105820-99.

Kauffman, R., *Inertial Confinement Fusion Monthly Highlights*, April 2000, Lawrence Livermore National Laboratory, Livermore, CA, UCRL-TB-128550-00-07.

Kauffman, R., *Inertial Confinement Fusion Monthly Highlights*, May / June 2000, Lawrence Livermore National Laboratory, Livermore, CA, UCRL-TB-128550-00-08-09.

Kauffman, R., *Inertial Confinement Fusion Monthly Highlights*, July / August 2000, Lawrence Livermore National Laboratory, Livermore, CA, UCRL-TB-128550-00-10-11.

Kauffman, R., *Inertial Confinement Fusion Monthly Highlights*, September 2000, Lawrence Livermore National Laboratory, Livermore, CA, UCRL-TB-128550-00-12.

Kauffman, R., *Inertial Confinement Fusion Monthly Highlights*, October 2000, Lawrence Livermore National Laboratory, Livermore, CA, UCRL-TB-128550-01-01.

Kauffman, R., *Inertial Confinement Fusion Monthly Highlights*, November / December 2000, Lawrence Livermore National Laboratory, Livermore, CA, UCRL-TB-128550-01-02 / 03.

Key, M. H., Amiranoff, F., Anderson, C., Batani, D., Baton, S. D., Cowan, T., Fisch, N., Freeman, R., Gremillet, L., Hall, T., Hatchett, S., Hill, J., King, J., Koch, J., Koenig, M., Lasinski, B., Langdon, B., MacKinnon, A., Martinolli, E., Norreys, P., Parks, P., Perelli-Cippo, E., Rabec Le Gloahec, M., Rosenbluth, M., Rousseaux, C., Santon, J. J., Scianitti, F., Snavely, R., and Stephens, R., *Studies of Energy Transport by Relativistic Electrons in the Context of Fast Ignition*, Lawrence Livermore National Laboratory, Livermore, CA, UCRL-JC-143454 ABS. Prepared for *2nd Intl Conf on Inertial Fusion Science and Applications*, Kyoto, Japan, Sep 9–14, 2001.

Key, M. H., Andersen, C., Cowan, T., Fisch, N., Freeman, R., Hatchett, S., Henry, E. A., Hill, J. M., Koch, J., Langdon, B., Lasinski, B., MacKinnon, A., Parks, P., Pennington, D. M., Perry, M. D., Phillips, T. W., Rosenbluth, M., Roth, M., Sangster, T. C., Singh, M., Snavely, R., Stephens, R., Stoyer, M. A., Wilks, S. C., and Yasuike, K., *Laser Generated Relativistic Electrons—the Key to Fast Ignition and Hard X-ray Sources*, Lawrence Livermore National Laboratory, Livermore, CA, UCRL-JC-144821 ABS SUM. Prepared for *Applications of High Field and Short Wavelength Sources IX Topical Mtg*, Palm Springs, CA, Oct 21–24, 200l.

Key, M. H., *Fast Ignition*, Lawrence Livermore National Laboratory, Livermore, CA, UCRL-JC-134953 ABS. Prepared for *4th Symp on Current Trends in Intl Fusion Research: A Review*, Washington, D.C., Mar 12–16, 2001.

Key, M. H., *Fast Ignition*, Lawrence Livermore National Laboratory, Livermore, CA, UCRL-JC-143402 ABS Rev 1. Prepared for *Univ of San Diego Student Seminar*, San Diego, CA, Apr 9, 2001.

Key, M. H., *Magnetically Collimated Energy Transport by Laser Generated Relativistic Electrons*, Lawrence Livermore National Laboratory, Livermore, CA, UCRL-ID-142488.

Kim, B.-K., Feit, M. D., Rubenchik, A. M., Joslin, E. J., Celliers, P. M., Eichler, J., and Da Silva, L. B., "Influence of Pulse Duration on Ultrashort Laser Pulse Ablation of Biological Tissues," *J. Biomed. Opt*. 6(3), 332–338 (2001).

Kimbrough, J. R., Bell, P. M., Christianson, G. B., Lee, F. D., Kalantar, D. H., Perry, T. S., Sewall, N. R., and Wooten, A. J., *National Ignition Facility Core X-Ray Streak Camera*, Lawrence Livermore National Laboratory, Livermore, CA, UCRL-JC-137908; also in *Rev. Sci. Inst.* 72(1Pt2), 748–750 (2001).

Kirkwood, R. K., Froula, D., Glenzer, S. H., Kachinski, R., Langdon, A. B., Kruer, W. L., Baldis, H. A., Fisch, N., and Shvets, G., *Experiment to Study Pulse Compression of a Laser by Raman Scattering in a Plasma*, Lawrence Livermore National Laboratory, Livermore, CA, UCRL-JC-144576 ABS. Prepared for *43rd Annual Mtg of the American Physical Society Div of Plasma Physics*, Long Beach, CA, Oct 29–Nov 2, 2001.

Kirkwood, R. K., Young, P. E., Langdon, A. B., Moody, J. D., Cohen, B. I., Decker, C., Glenzer, S. H., Suter, L. J., and Seka, W., *Scaling of Energy Transfer Between Crossing Laser Beams with Beam Intensity and Plasma Size and Density*, Lawrence Livermore National Laboratory, Livermore, CA, UCRL-PRES-143599. Prepared for *31st Anomalous Absorption Conf*, Sedona, AZ, Jun 3–8, 2001.

Koch, J. A., Presta, R. W., Sacks, R. A., Zacharias, R. A., Bliss, E. S., Dailey, M. J., Feldman, M., Grey, A. A., Holdener, F. R., Salmon, J. T., Seppala, L. G., Toeppen, J. S., Van Atta, L., Van Wonterghem, B. M., Whistler, W. T., Winters, S. E., and Woods, B. W., *Experimental Comparison of a Shack-Hartmann Sensor and a Phase-Shifting Interferometer for Large-Optics Metrology Applications*, Lawrence Livermore National Laboratory, Livermore, CA, UCRL-JC-136743 and 136105; also in *Appl. Opt*. 39(25), 4540–4546 (2000).

Koch, J. A., Sater, J. D., Mackinnon, A. J., Bernat, T. P., Bittner, D. N., Collins, G. W., Hammel, B. A., and Still, C. H., *Numerical Raytrace Verification of Optical Diagnostics of Ice Surface Roughness for Inertial Confinement Fusion Experiments*, Lawrence Livermore National Laboratory, Livermore, CA, UCRL-JC-142757. Submitted to *Appl Opt*.

Kozioziemski, B. J., Collins, G. W., and Bernat, T. P., *Raman Spectrum of Deuterium-Tritium*, Lawrence Livermore National Laboratory, Livermore, CA, UCRL-JC-143756 ABS. Prepared for *14th Target Fabrication Mtg*, West Point, NY, Jul 15–19, 2001.

Kozioziemski, B. J., McEachern, R. L., London, R. A., and Bittner, D. N., *Infrared Heating of Hydrogen Layers in Hohlraums*, Lawrence Livermore National Laboratory, Livermore, CA, UCRL-JC-145172. Prepared for *14th Target Fabrication Mtg*, West Point, NY, Jul 15–19, 200l.

Kozioziemski, B. J., McEachern, R. L., London, R. A., Collins, G. W., and Bittner, D. N., *Infrared Layering of HD in Hohlraums*, Lawrence Livermore National Laboratory, Livermore, CA, UCRL-JC-143447 ABS. Prepared for *14th Target Fabrication Mtg*, West Point, NY, Jul 15–19, 2001.

L

Laming, J. M., Back, C. A., Decker, C. D., Grun, J., Feldman, U., Seely, J. F., and Davis, J. F., *Modeling and Interpretation of Spectra from Kr/Xe Filled Low Z Enclosures*, Lawrence Livermore National Laboratory, Livermore, CA, UCRL-JC-141345. Submitted to *Phys. Rev. E*.

Landen, O. L., Farley, D. R., Glendinning, S. G., Logory, L. M., Bell, P. M., Koch, J. A., Lee, F. D., Bradley, D. K., Kalantar, D. H., Back, C. A., and Turner, R. E., *X-Ray Backlighting for the National Ignition Facility*, Lawrence Livermore National Laboratory, Livermore, CA, UCRL-JC-139367; also in *Rev. Sci. Inst*. 72(1PT2), 627–634 (2001).

Landen, O. L., Glenzer, S. H., Edwards, M. J., Lee, R. W., Collins, G. W., Cauble, R. C., Hsing, W. W., and Hammel, B. A., *Dense Matter Characterization by X-Ray Thomson Scattering*, Lawrence Livermore National Laboratory, Livermore, CA, UCRL-JC-141055. Prepared for *9th Intl Workshop on Radiative Properties of Hot Dense Matter*, Santa Barbara, CA, Oct 30–Nov 2, 2000.

Landen, O. L., Lobban, A., Tutt, T., Bell, P. M., Costa, R., Hargrove, D. R., and Ze, F., *Angular Sensitivity of Gated Microchannel Plate Framing Cameras*, Lawrence Livermore National Laboratory, Livermore, CA, UCRL-JC-137879; also in *Rev. Sci. Inst*. 72(1Pt2), 709–712 (2001).

Landen, O. L., Pollaine, S. M., Bradley, D. K., Amendt, P. A., Turner, R. E., Suter, L. J., Jones, O. S., Wallace, R. J., and Hammel, B. A., *Higher Order Asymmetry Diagnosis for NIF-Scale Hohlraums*, Lawrence Livermore National Laboratory, Livermore, CA, UCRL-JC-143449 ABS. Prepared for *2nd Intl Conf on Inertial Fusion Sciences and Applications*, Kyoto, Japan, Sep 9–14, 2001.

Landon, M. D., Koch, J. A., Alvarez, S. S., Bell, P. M., Lee, F. D., and Moody, J. D., *Design of the National Ignition Facility Static X-Ray Imager*, Lawrence Livermore National Laboratory, Livermore, CA, UCRL-JC-137911; also in *Rev. Sci. Inst*. 72(1PT2), 698–700 (2001).

Langdon, A. B., and Lasinski, B. F., *Zohar, Version 2.0*, Lawrence Livermore National Laboratory, Livermore, CA, UCRL-CODE-2001-009.

Langdon, B., Berger, R. L., Cohen, B. I., Hinkel, D. E., Kirkwood, R. K., Still, C. H., Suter, L. J., Williams, E. A., and Young, P. E., *Laser–Plasma Interactions in Overlapping Laser Beams*, Lawrence Livermore National Laboratory, Livermore, CA, UCRL-JC-142068 ABS. Prepared for *4th Intl Workshop on Laser–Plasma Interaction Physics*, Banff, Alberta, Canada, Feb 21–24, 2001.

Lerche, R. A., Coutts, G. W., Lagin, L. J., Nyholm, R. A., Stever, R. D., Wiedwald, J. D., Larkin, J., Stein, S., and Martin, R., *The NIF Integrated Timing System—Design and Performance*, Lawrence Livermore National Laboratory, Livermore, CA, UCRL-JC-143371 ABS. Prepared for *8th Intl Conf on Accelerator and Large Experimental Physics and Control Systems*, San Jose, CA, Nov 27–30, 2001.

Letts, S. A., Orthion, P. J., Hassel, A. E., Buckley, S., Fearon, E., and Cook, R. C., *Fabrication of Polyimide Capsules for NIF: An Overview of the Recent Progress at LLNL*, Lawrence Livermore National Laboratory, Livermore, CA, UCRL-JC-143738 ABS. Prepared for *14th Target Fabrication Mtg*, West Point, NY, Jul 15–19, 2001.

Lindl, J., *Review of the National Ignition Facility Target Designs and the Nova Technical Contract on the Indirect-Drive, Inertial Confinement Fusion (Including Recent Extensions to the Omega Laser*, Lawrence Livermore National Laboratory, Livermore, CA, UCRL-JC-143413. Submitted to *Phys. of Plasmas*.

Logan, B. G., Meier, W. R., Moir, R. W., Abdou, M., Peterson, P. F., Kulcinski, G. L., Tillack, M. S., Latkowski, J. F., Petti, D., Schultz, K. R., and Nobile, A., *Progress and Critical Issues for IFE Blanket and Chamber Research*, Lawrence Livermore National Laboratory, Livermore, CA, UCRL-JC-134976; also in *Fus. Engr. Design* 51-2, 1095–1101 (2000).

Lorenz, K. T., Kalantar, D., Edwards, J., Colvin, J. D., Reisman, D. B., and Remington, B., *Laser-Driven Near Isentropic Compression of an Aluminum Flyer Plate*, Lawrence Livermore National Laboratory, Livermore, CA, UCRL-JC-143949 ABS Rev 1. Prepared for *43rd Annual Mtg of the American Physical Society Div of Plasma Physics*, Long Beach, CA, Oct 29–Nov 2, 2001.

Loveridge-Smith, A., Allen, A., Belak, J., Boehly, T., Hauer, A., Holian, B., Kalantar, D., Kyrala, G., Lee, R. W., Lomdahl, P., Meyers, M. A., Paisley, D., Polaine S., Remington, B., Swift, D. C., Weber, S., and Wark, J. S., *Anomalous Elastic Response of Silicon to Uniaxial Shock Compression on Nanosecond Timescales*, Lawrence Livermore National Laboratory, Livermore, CA, UCRL-JC-140746; also in *Phys. Rev. Lett*. 86(11), 2349–2352 (2001).

Lukasheva, N. V., Niemela, S., Neelov, I. M., Darinskii, A. A., Sundholm, F., and Cook, R., *Computer Modeling of Helical Conformations and Helix Sense Reversals in Poly (alkylisocyanates). New Types of Reversals*, Lawrence Livermore National Laboratory, Livermore, CA, UCRL-JC-144094. Submitted to *American Chemical Society Polymeric Material*.

M

MacKenzie, J. I., Mitchell, S. C., Beach, R. J., Meissner, H. E., and Shepherd, D. P., "15 W Diode-Side-Pumped Tm: YAG Waveguide Laser at 2µm," *Elect. Lett*. 37(4), 898–899 (2001).

MacKinnon, A. J., Borghesi, M., Hatchett, S., Key, M. H., Patel, P. K., Campbell, H., Schiavi, A., Snavely, R., Wilks, S. C., and Willi, O., *Effect of Plasma Scale Length on Multi-MeV Proton Production by Intense Laser Pulse*, Lawrence Livermore National Laboratory, Livermore, CA, UCRL-JC-139273; also in *Phys. Rev. Lett*. 86(9), 1769–1772 (2001).

MacKinnon, A. J., Patel, P. K., Sentoku, Y., Andersen, C., Hatchett, S., Key, M. H., Lasinski, B., Langdon, B., Snavely, R., and Freeman, R. R., *Electron Time of Flight Effects on Proton Production in Short Pulse High Intensity Laser Plasma Interactions*, Lawrence Livermore National Laboratory, Livermore, CA, UCRL-JC-144669 ABS. Prepared for *43rd Annual Mtg of the American Physical Society Div of Plasma Physics*, Long Beach, CA, Oct 29–Nov 2, 2001.

MacKinnon, A., *Recreating Planetary Cores in the Laboratory*, Lawrence Livermore National Laboratory, Livermore, CA, UCRL-JC-142029 ABS. Prepared for *12th American Physical Society Topical Conf on Shock Compression of Condensed Matter*, Atlanta, GA, Jun 24–29, 2001.

Marinak, M. M., Kerbel, G. D., Gentile, N. A., Jones, O., Munro, D., Pollaine, S., Dittrich, T. R., and Haan, S. W., *Three-Dimensional HYDRA Simulations of National Ignition Facility Targets*, Lawrence Livermore National Laboratory, Livermore, CA, UCRL-JC-141084; also in *Phys. Plasmas* 8(5Pt2), 2275–2280 (2001).

Mascio, W. A., Sewall, N. R., Kirkwood, R., Lee, F. D., and Hibbard, W. J., *Near to Backscattered Light Imaging Diagnostic on the National Ignition Facility*, Lawrence Livermore National Laboratory, Livermore, CA, UCRL-JC-137912; also in *Rev. Sci. Inst*. 72(lPt2), 976–978 (2001).

Maximov, A. V., Oppitz, R. M., Rozmus, W., and Tikhonchuk, V. T., "Nonlinear Stimulated Brillouin Scattering in Inhomogeneous Plasmas," *Phys. Plasmas* 7(10), 4227–4237 (2000).

Maximov, A. V., Ourdev, I. G., Pesme, D., Rozmus, W., Tikhonchuk, V. T., and Capjack, C. E., *Plasma Induced Smoothing of Spatially Incoherent Laser Beam and Reduction of Backward Stimulated Brillouin Scattering*, Lawrence Livermore National Laboratory, Livermore, CA, UCRL-JC-135620; also in *Phys. Plasmas* 8(4), 1319–1328 (2001).

Maximov, A. V., Rozmus, W., Capjack, C. E., Berger, R. L., Tikhonchuk, V. T., and Pesme, D., *Evolution of Nonlinear Laser Filaments in Plasmas*, Lawrence Livermore National Laboratory, Livermore, CA, UCRL-JC-142437 ABS. Prepared for *4th Intl Workshop on Laser–Plasma Interaction Physics*, Banff, Alberta, Canada, Feb 21–24, 2001.

McEachern, R., Alford, C., and McKernan, M., *Sputter-Deposited Be for NIF Capsule Ablators*, Lawrence Livermore National Laboratory, Livermore, CA, UCRL-JC-143587 ABS. Prepared for *14th Target Fabrication Mtg*, West Point, NY, Jul 15–19, 2001.

McEachern, R., *Anomalous Roughness Measurements on Capsules Using a WYKO NT-2000 Surface Profiler*, Lawrence Livermore National Laboratory, Livermore, CA, UCRL-JC-143588 ABS. Prepared for *14th Target Fabrication Mtg*, West Point, NY, Jul 15–19, 2001.

McEachern, R., Bittner, D., Kozioziemski, B., and London, R., *Modeling IR Layering of Capsules in Hohlraums*, Lawrence Livermore National Laboratory, Livermore, CA, UCRL-JC-143590 ABS. Prepared for *14th Target Fabrication Mtg*, West Point, NY, Jul 15–19, 2001.

Meyerhofer, D. D., Delettrez, J. A., Epstein, R., Glebov, V. Yu., Goncharov, V. N., Keck, R. L., McCrory, R. L., McKenty, P. W., Marshall, F. L., Radha, P. B., Regan, S. P., Roberts, S., Seka, W., Skupsky, S., Smalyuk, V. A., Sorce, C., Stoeckl, C., Soures, J. M., Town, R. P. J., Yaakobi, B., Zuegel, J. D., Frenje, J., Li, C. K., Petrasso, R. D., Seguin, F. H., Fletcher, K., Padalino, S., Freeman, C., Izumi, N., Lerche, R., Phillips, T. W., and Sangster, T. C., "Core Performance and Mix in Direct-Drive Spherical Implosions with High Uniformity," *Phys. Plasmas* 8(5Pt2), 2251–2453 (2001).

Milam, D., *Comment: Two-Photon Photography*, Lawrence Livermore National Laboratory, Livermore, CA, UCRL-JC-141860 COM. Submitted to the *J. Opt. Soc. Am. B*.

Miller, M. C., Celeste, J. R., Stoyer, M. A., Suter, L. J., Tobin, M. T., Grun, J., Davis, J. F., Barnes, C. W., and Wilson, D. C., *Debris Characterization Diagnostic for the NIF*, Lawrence Livermore National Laboratory, Livermore, CA, UCRL-JC-137945; also in *Rev. Sci. Inst*. 72(1Pt2), 537–539 (2001).

Mirkarimi, P. B., Baker, S. L., Montcalm, C., and Folta, J. A., *Recovery of Multilayer-Coated Zerodur and ULE Optics for Extreme-Ultraviolet Lithography by Recoating, Reactive-Ion Etching, and Wet-Chemical Processes*, Lawrence Livermore National Laboratory, Livermore, CA, UCRL-JC-138380; also in *Appl. Opt*. 40(l), 62–70 (2001).

Moir, R. W., *Grazing Incidence Liquid Metal Mirrors (GILMM) for Radiation Hardened Final Optics for Laser Inertial Fusion Energy Power Plants*, Lawrence Livermore National Laboratory, Livermore, CA, UCRL-JC-133027; also in *Fus. Engr. Design* 51-2, 1121–1128 (2000).

Moir, R. W., *Liquid Walls for Fusion Reaction Chambers*, Lawrence Livermore National Laboratory, Livermore, CA, UCRL-JC-135743; also in *Comments on Modern Phys*. 2(2), C99–C111 (2000).

Moir, R. W., *Thick Liquid-Walled, Field-Reversed Configuration-Magnetic Fusion Power Plant*, Lawrence Livermore National Laboratory, Livermore, CA, UCRL-JC-139086 Rev 1; also in *Fusion Tech*. 39(2Pt2), 758–767 (2001).

Montcalm, C., Bajt, S., and Seely, J. F., *MoRu-Be Multilayer-Coated Grating with 10.4% Normal-Incidence Efficiency Near the 11.4-nm Wavelength*, Lawrence Livermore National Laboratory, Livermore, CA, UCRL-JC-140269; also in *Opt. Lett*. 26(3), 125–127 (2001).

Montcalm, C., *Reduction of Residual Stress in Extreme Ultraviolet Mo/Si Multilayer Mirrors with Postdeposition Thermal Treatments*, Lawrence Livermore National Laboratory, Livermore, CA, UCRL-JC-136174; also in *Opt. Engr*. 40(3), 469–477 (2001).

Moody, J. D., Glenzer, S. H., Williams, E. A., Berger, R. L., Chambers, D. M., Hawreliak, J., and Wark, J. S., *Experimental Study of the Onset and Development of Forward Scattering in an Exploding Foil Plasma*, Lawrence Livermore National Laboratory, Livermore, CA, UCRL-JC-144670 ABS. Prepared for *43rd Annual Mtg of the American Physical Society Div of Plasma Physics*, Long Beach, CA, Oct 29–Nov 2, 2001.

Moody, J. D., MacGowan, B. J., Rothenberg, J. E., Berger, R. L., Divol, L., Glenzer, S. H., Kirkwood, R. K., Williams, E. A., and Young, P. E., *Backscatter Reduction Using Combined Spatial, Temporal, and Polarization Beam Smoothing in a Long-Scale-Length Laser Plasma*, Lawrence Livermore National Laboratory, Livermore, CA, UCRL-JC-139843; also in *Phys. Rev. Lett*. 86(13), 2810–2813 (2001).

Moody, J. D., Sanchez, J. J., Collins, G. W., Giedt, W. H., Pipes, J. W., Burmann, J. A., Jones, R. L., Unites, W. G., and London, R. A., *Development of a Temperature Shimmed Hohlraum for the National Ignition Facility*, Lawrence Livermore National Laboratory, Livermore, CA, UCRL-JC-143416 ABS. Prepared for *14th Target Fabrication Mtg*, West Point, NY, Jul 15–19, 2001.

Moody, J. D., Williams, E. A., Chambers, D. M., Hawreliak, J., Sondhauss, P., Wark, J. S., Berger, R. L., and Young, P. E., *Characterization of Plasma-Induced Laser Smoothing Underdense Plasmas*, Lawrence Livermore National Laboratory, Livermore, CA, UCRL-JC-142048. Submitted to *Phys. Rev. Lett*.

Munro, D. H., Celliers, P. M., Collins, G. W., Gold, D. M., Da Silva, L. B., Haan, S. W., Cauble, R. C., Hammel, B. A., and Hsing, W. W., *Shock Timing Technique for the National Ignition Facility*, Lawrence Livermore National Laboratory, Livermore, CA, UCRL-JC-139319; also in *Phys. Plasmas* 8(5Pt2), 2245–2250 (2001).

Murphy, T. J., Barnes, C. W., Berggren, R. R., Bradley, P., Caldwell, S. E., Chrien, R. E., Faulkner, J. R., Gobby, P. L., Hoffman, N., Jimerson, J. L., Klare, K. A., Lee, C. L., Mack, J. M., Oertel, G. L., Swenson, F. J., Walsh, P. J., Walton, R. B., Watt, R. G., Wilke, M. D., Wilson, D. C., Young, C. S., Haan, S. W., Lerche, R. A., Moran, M. J., Phillips, T. W., Sangster, T. C., Leeper, R. J., Ruiz, C. L., Coopere, G. W., Disdier, L., Rouyer, A., Fedotoff, A., Glebov, V. Y., Meyerhofer, D. D., Soures, J. M., Stockl, C., Frenje, J. A., Hicks, D. G., Li, C. K., Petrasso, R. D., Seguin, F. H., Fletcher, K., Padalino, S., and Fisher, R. K., "Nuclear Diagnostics for the National Ignition Facility," *Rev. Sci. Inst*. 72(1PT2), 773–779 (2001).

N

Nguyen, H. T., Bryan, S. R., Britten, J. A., and Perry, M. D., *Fabrication of Efficient, Large Aperture Transmission Diffraction Gratings by Ion-Beam Etching*, Lawrence Livermore National Laboratory, Livermore, CA, UCRL-ID-140249 Rev l.

Nilsen, J., Dunn, J., Li, Y. L., Osterheld, A. L., Shlyaptsev, V. N., Barbee, T. W., and Hunter, J. R., *Review of Ni-Like Ion X-Ray Laser Research at Lawrence Livermore National Laboratory*, Lawrence Livermore National Laboratory, Livermore, CA, UCRL-JC-140228; also in *Comptes Rendus* 1(8), 1035–1044 (2000).

Nilsen, J., Li, Y. L., Dunn, J., Barbee, T. W., and Osterheld, A. L., "Modeling and Demonstration of a Saturated Ni-Like Mo X-Ray Laser," *J. De Physique IV*, 11(Pr2), 67–73 (2001).

Nostrand, M. C., Page, R. H., Payne, S. A., Isaenko, L. I., and Yelisseyev, A. P., *Optical Properties of Dy^{3+}- and Nd^{3+}-Doped KPb_2Cl_5*, Lawrence Livermore National Laboratory, Livermore, CA, UCRL-JC-137803; also in *J. Opt. Soc. Am. B* 18(3), 264–276 (2001).

P

Patel F. D., and Beach, R. J., "New Formalism for the Analysis of Passively Q-Switched Laser Systems," *IEEE J. Q. E.* 37(5), 707–715 (2001).

Patel, F. D., Honea, E. C., Speth, J., Payne, S. A., Hutcheson, R., and Equall, R., *Laser Demonstration of $Yb_3Al_5O_{12}$(YbAG) and Materials Properties of Highly Doped Yb:YAG*, Lawrence Livermore National Laboratory, Livermore, CA, UCRL-JC-139625; also in *IEEE J. Quant. Electr*. 37(l), 135–144 (2001).

Pesme, D., Huller, S., Laval, G., Depierreux, S., Fuchs, J., Labaune, C., Michaud, A., and Baldis, H., "First Observation of Ion Acoustic Waves Produced by the Langmuir Decay Instability," *Phys. Rev. Lett*. 86(16), 3687 (2001).

Pipes, J., Ross, T., and Sater, J., *High Pressure Fill Station for the Deuterium Test System*, Lawrence Livermore National Laboratory, Livermore, CA, UCRL-JC-143415 ABS. Prepared for *14th Target Fabrication Mtg*, West Point, NY, Jul 15–19, 2001.

Pollaine, S. M., Bradley, D. K., Landen, O. L., Wallace, R. J., Jones, O. S., Amendt, P. A., Suter, L. J., and Turner, R. E., *National Ignition Facility Scale Hohlraum Asymmetry Studies by Thin Shell Radiography*, Lawrence Livermore National Laboratory, Livermore, CA, UCRL-JC-139459; also in *Phys. Plasmas* 8(5Pt2), 2357–2364 (2001).

Pollaine, S., Kalantar, D., Remington, B., Belak, J., Colvin, J. D., Edwards, J., Minich, R., Mikaelian, K. O., Lorenz, T., Weber, S. V., Wiley, L. G., Paisley, D., Hauer, A., Wark, J. S., Loveridge, A., Allen, A. M., Boehly, T. R., and Meyers, M. A., *Modeling Laser Material Strength Experiments*, Lawrence Livermore National Laboratory, Livermore, CA, UCRL-PRES-143513 Rev l. Prepared for *31st Anomalous Absorption Conf*, Sedona, AZ, Jun 3–8, 2001.

R

Remington, B. A., Belak, J. F., Colvin, J., Edwards, J., Kalantar, D. H., Lasinski, B. F., Lorenz, K. T., Pollaine, S. M., Shay, H. D., Weber, S. V., and Wolfer, W. G., *Solid State Physics at Ultrahigh Pressure and Strain Rate—a Plan for NIF*, Lawrence Livermore National Laboratory, Livermore, CA, UCRL-JC-143794 ABS. Prepared for *8th Intl Workshop on the Physics of Compressible Turbulent Mixing*, Pasadena, CA, Dec 9–14, 2001.

Remington, B. A., Belak, J. F., Colvin, J., Edwards, J., Kalantar, D. H., Lasinski, B. F., Lorenz, K. T., Pollaine, S. M., Weber, S. V., and Wolfer, W. G., *Solid State Physics at Ultrahigh Pressure and Strain Rate on NIF*, Lawrence Livermore National Laboratory, Livermore, CA, UCRL-JC-144756 ABS. Prepared for *43rd Annual Mtg of the American Physical Society Div of Plasma Physics*, Long Beach, CA, Oct 29–Nov 2, 2001.

Remington, B. A., *Dyamics of Supernovae and Supernova Remnants*, Lawrence Livermore National Laboratory, Livermore, CA, UCRL-PROP-143643.

Remington, B. A., Edwards, M. J., Perry, T. S., Wilde, B. H., Foster, J. M., Rosen, P. A., Shigemori, K., Stone, J. M., and Turner, N. J., *Jets in Astrophysics and in Laser Experiments*, Lawrence Livermore National Laboratory, Livermore, CA, UCRL-PRES-144101. Prepared for *98th Mtg of the American Astronomical Society*, Pasadena, CA, Jun 3–7, 2001.

Remington, B. A., *Experimental Science at the Extremes: From Supernovae to Supersolids, and Most Everything in Between*, Lawrence Livermore National Laboratory, Livermore, CA, UCRL-JC-143421 ABS. Prepared for *2nd Intl Conf on Inertial Fusion Sciences and Applications*, Kyoto, Japan, Sep 9–14, 2001.

Remington, B. A., Ryutov, D. D., and Paul, R., *Laboratory Astrophysics Using Intense Lasers*, Lawrence Livermore National Laboratory, Livermore, CA, UCRL-JC-145125. Submitted to *Rev. Mod. Phys*.

Remington, B., Belak, J., Colvin, J., Edwards, J., Kalantar, D., Lasinski, B., Pollaine, S., Shay, H., Weber, S., and Wolfer, B., *High-Pressure, Solid-State Experiments for NIF*, Lawrence Livermore National Laboratory, Livermore, CA, UCRL-ID-142676.

Remington, B., *HED in Laboratory Plasmas*, Lawrence Livermore National Laboratory, Livermore, CA, UCRL-PRES-144102. Prepared for *Natl Research Council Committee on the Physics of the Universe*, Pasadena, CA, Jun 6–7, 2001.

Remington, B., Ryutov, D., Edwards, J., Wilde, B., Perlmutter, S., Nugent, P., and Woosley, S., *A New Paradigm for Supernova Studies*, Lawrence Livermore National Laboratory, Livermore, CA, UCRL-PROP-143571.

Robey, H. F., and Glendinning, S. G., *A Vortex Model for Studying the Effect of Shock Proximity on Richtmyer–Meshkov Instability at High Mach Number*, Lawrence Livermore National Laboratory, Livermore, CA, UCRL-JC-143797 ABS. Prepared for *8th Intl Workshop on the Physics of Compressible Turbulent Mixing*, Pasadena, CA, Dec 9–14, 2001.

Robey, H. F., Kane, J. O., Remington, B. A., Drake, R. P., Hurricane, O. A., Louis, H., Wallace, R. J., Knauer, J., Keiter, P., Arnett, D., and Ryutov, D. D., *An Experimental Testbed for the Study of Hydrodynamic Issues in Supernovae*, Lawrence Livermore National Laboratory, Livermore, CA, UCRL-JC-139454; also in *Phys. Plasmas* 8(5Pt2), 2446–2453 (2001).

Robey, H. F., Kane, J., Remington, B. A., Hurricane, O., Louis, H., Wallace, R. J., Drake, R. P., Keiter, P., Arnett, D., and Knauer, J., *Laser Experiments for the Study of Hydrodynamic Issues in Supernovae*, Lawrence Livermore National Laboratory, Livermore, CA, UCRL-JC-143243 ABS. Prepared for *198th Mtg of the American Astronomical Society*, Pasadena, CA, Jun 3–7, 2001.

Robey, H. F., Perry, T. S., Klein, R. I., Greenough, J. A., Kane, J. O., and Boehly, T. R., *Experimental Study of the Interaction of a Strong Shock with a Spherical Density Inhomogeneity*, Lawrence Livermore National Laboratory, Livermore, CA, UCRL-JC-143805 ABS Rev 1. Prepared for *43rd Annual Mtg of the American Physical Society Div of Plasma Physics*, Long Beach, CA, Oct 29–Nov 2, 2001.

Robey, H. F., Perry, T. S., Klein, R. I., Kane, J. O., Greenough, J. A., and Boehly, T. R., *Experimental Investigation of the Three-Dimensional Interaction of a Strong Shock with a Spherical Density Inhomogeneity*, Lawrence Livermore National Laboratory, Livermore, CA, UCRL-JC-143642 DR. Submitted to *Phys. Rev. Lett*.

Robey, H. F., Zhou, Y. K., Buckingham, A. C., Keiter, P., Remington, B. A., and Drake, R. P., *Turbulent Transition in a High Reynolds Number, Rayleigh-Taylor Unstable Plasma Flow*, Lawrence Livermore National Laboratory, Livermore, CA, UCRL-JC-143793 ABS. Prepared for *8th Intl Workshop on the Physics of Compressible Turbulent Mixing*, Pasadena, CA, Dec 9–14, 2001.

Robey, H. F., Zhou, Y., Buckingham, A. C., Keiter, P., Remington, B. A., and Drake, R. P., *The Onset of Turbulence in High Reynolds Number, Accelerated Flows. Part II Experiment*, Lawrence Livermore National Laboratory, Livermore, CA, UCRL-JC-144078-PT-2. Submitted to *Phys. of Fluids*.

Roth, M., Cowan, T. E., Brown, C., Christl, M., Fountain, W., Hatchett, S., Johnson, J., Key, M. H., Pennington, D. M., Perry, M. D., Phillips, T. W., Sangster, T. C., Singh, M., Snavely, R., Stoyer, M., Takahashi, Y., Wilks, S. C., and Yasuike, K., "Intense Ion Beams Accelerated by Petawatt-Class Lasers," *Nucl. Inst. & Meth.* 464(1-3), 201–205 (2001).

Roth, M., Cowan, T. E., Key, M. H., Hatchett, S. P., Brown, C., Fountain, W., Johnson, J., Pennington, D. M., Snavely, R. A., Wilks, S. C., Yasuike, K., Ruhl, H., Pegoraro, F., Bulanov, C. V., Campbell, E. M., Perry, M. D., and Powell, H., "Fast Ignition by Intense Laser-Accelerated Proton Beams," *Phys. Rev. Lett*. 86(3), 436–439 (2001).

Rushford, M. C., Britten, J. A., Hoaglan, C., and Summers, L. J., *Surface Contouring by Controlled Application of Etchant Solution Using the Marangoni Effect*, Lawrence Livermore National Laboratory, Livermore, CA, UCRL-JC-141812 ABS. Prepared for *46th Annual Mtg of the Society of Photo-Optical Instrumentation Engineers*, San Diego, CA, Jul 29–Aug 3, 2001.

Ryutov, D. D., *Destabilizing Effect of Thermal Conductivity on the Rayleigh–Taylor Instability in a Plasma*, Lawrence Livermore National Laboratory, Livermore, CA, UCRL-JC-138745; also in *Phys. Plasmas* 7(12), 4797–4800 (2000).

Ryutov, D. D., *Radical Restructuring of the Fusion Effort*, Lawrence Livermore National Laboratory, Livermore, CA, UCRL-JC-136143; also in *Comments on Mod. Phys*. 2(2), C139–154 (2000).

Ryutov, D. D., Remington, B. A., and Robey, H. F., *Micro Hydrodynamic Driven Scaling: From Astrophysics to the Laboratory*, Lawrence Livermore National Laboratory, Livermore, CA, UCRL-JC-139357; also in *Phys. Plasmas*, 8(5Pt2), 1804–1806 (2001).

Ryutov, D., and Remington, B., *Compressible MHD Turbulence in Strongly Radiating Molecular Clouds in Astrophysics*, Lawrence Livermore National Laboratory, Livermore, CA, UCRL-JC-143795 ABS. Prepared for *8th Intl Workshop on the Physics of Compressible Turbulent Mixing*, Pasadena, CA, Dec 9–14, 2001.

S

Sae-Lao, B., and Montcalm, C., *Molybdenum-Strontium Multilayer Mirrors for the 8–12-nm Extreme-Ultraviolet Wavelength Region*, Lawrence Livermore National Laboratory, Livermore, CA, UCRL-JC-139096; also in *Opt. Lett*. 26(7), 468–470 (2001).

Sanchez, J. J., and Giedt, W. H., *Multi-Region Hohlraums for Reducing Convection Induced Fuel Layer Thickness Variation*, Lawrence Livermore National Laboratory, Livermore, CA, UCRL-JC-143372 ABS. Prepared for *14th Target Fabrication Mtg*, West Point, NY, Jul 15–19, 2001.

Sater, J. D., Bittner, D., Burmann, J., Collins, G. W., Kozioziemski, B., and Pipes, J., *D-T Layering*, Lawrence Livermore National Laboratory, Livermore, CA, UCRL-JC-143418 ABS. Prepared for *14th Target Fabrication Mtg*, West Point, NY, Jul 15–19, 2001.

Schaffers, K. I., Tassano, J. B., Waide, P. A., Payne, S. A., and Morris, R. C., "Progress in the Growth of Yb:S-FAP Laser Crystals," *J. Crystal Growth* 225(2-4) 449–453 (2001).

Schmid, G. J., Glebov, V. Y., Hatchett, S. P., Izumi, N., Lerche, R. A., Moran, M. J., Phillips, T. W., Sangster, T. C., and Stoeckl, C., *CVD Diamond Detector for DD rho-r Measurement at Omega/NIF*, Lawrence Livermore National Laboratory, Livermore, CA, UCRL-JC-144667 ABS. Prepared for *43rd Annual Mtg of the American Physical Society Div of Plasma Physics*, Long Beach, CA, Oct 29–Nov 2, 2001.

Schmid, G. J., Sangster, T. C., Lerche, R. A., Phillips, T. W., and Izumi, N., *Neutron Time-of-Flight Spectroscopy at OMEGA/NIF Using Current Mode Diamond Detectors*, Lawrence Livermore National Laboratory, Livermore, CA, UCRL-JC-142030 ABS. Prepared for *Intl Symp on Optical Science and Technology*, San Diego, CA, Jul 29–Aug 3, 200l.

Shepherd, D. P., Hettrick, S. J., Li, C., MacKenzie, J. I., Beach, R. J., Mitchell, S. C., and Meissner, H. E., "High-Power Planar Dielectric Waveguide Lasers," *J. of Phys. D* 34(16), 2420–2432 (2001).

Shigemori, K., Kodama, R., Farley, D. R., Koase, T., Estabrook, K. G., Remington, B. A., Ryutov, D. D., Ochi, Y., Azechi, H., Stone, J., and Turner, N., *Experiments on Radiative Collapse in Laser-Produced Plasmas Relevant to Astrophysical Jets*, Lawrence Livermore National Laboratory, Livermore, CA, UCRL-MI-134490; also in *Phys. Rev. E* 62(6 PT B), 8838–8841 (2000).

Shore, B. W., Johnson, M. A., Kulander, K. C., and Davis, J. I., *The Livermore Experience: Contributions of J. H. Eberly to Laser Excitation Theory*, Lawrence Livermore National Laboratory, Livermore, CA, UCRL-JC-140656; also in *Opt. Express* 8(2), 28–43 (2001).

Snavely, R. A., Freeman, R. R., Andersen, C., Hatchett, S. P., Key, M. H., Koch, J. A., MacKinnon, A., Stephens, R. B., Cowan, T. E., and Aglitskiy, Y., *Measurement of EIectron Transport and Heating from FI Relevant Plasmas*, Lawrence Livermore National Laboratory, Livermore, CA, UCRL-JC-143462 ABS. Prepared for *5th Workshop on Fast Ignition of Fusion Targets*, Madeira, Portugal, Jun 18–22, 2001.

Snavely, R. A., Key, M. H., Hatchett, S. P., Cowan, T. E., Roth, M., Phillips, T. W., Stoyer, M. A., Henry, E. A., Sangster, T. C., Singh, M. S., Wilks, S. C., MacKinnon, A., Offenberger, A., Pennington, D. M., Yasuike, K., Langdon, A. B., Lasinski, B. F., Johnson, J., Perry, M. D., and Campbell, E. M., *Intense High-Energy Proton Beams from Petawatt-Laser Irradiation of Solids*, Lawrence Livermore National Laboratory, Livermore, CA, UCRL-JC-137050; also in *Phys. Rev. Lett.* 85(14), 2945–2948 (2000).

Stewart, J., and Brugman, V., *Second Generation Target Handoff Scheme*, Lawrence Livermore National Laboratory, Livermore, CA, UCRL-JC-143414 ABS. Prepared for *14th Target Fabrication Mtg*, West Point, NY, Jul 15–19, 2001.

Still, C. H., Berger, R. L., Divol, L., Langdon, A. B., and Williams, E. A., *Comparing Partial Beam Simulations to Whole Beam Simulations with pF3D*, Lawrence Livermore National Laboratory, Livermore, CA, UCRL-JC-143618 ABS Rev 1. Prepared for *43rd Annual Mtg of the American Physical Society Div of Plasma Physics*, Long Beach, CA, Oct 29–Nov 2, 2001.

Still, C. H., Berger, R. L., Langdon, A. B., Williams, E. A., and Divol, L. M., *Large Scale LPI Simulations with pF3D*, Lawrence Livermore National Laboratory, Livermore, CA, UCRL-JC-142069 ABS. Prepared for *4th Intl Workshop on Laser–Plasma Interaction Physics*, Banff, Alberta, Canada, Feb 21–24, 2001.

Stoyer, M. A., Sangster, T. C., Henry, E. A., Cable, M. D., Cowan, T. E., Hatchett, S. P., Key, M. H., Moran, M. J., Pennington, D. M., Perry, M. D., Phillips, T. W., Singh, M. S., Snavely, R. A., Tabak, M., and Wilks, S. C., *Nuclear Diagnostics for Petawatt Experiments*, Lawrence Livermore National Laboratory, Livermore, CA, UCRL-JC-138297; also in *Rev. Sci. Inst.* 72(1Pt2), 767–772 (2001).

Suter, L. H., Widmayer, C. C., and Rothenberg, J. E., *Green Light Targets for NIF*, Lawrence Livermore National Laboratory, Livermore, CA, UCRL-JC-139457 ABS Rev l. Prepared for *31st Anomalous Absorption Conf*, Sedona, AZ, Jun 3–8, 2001.

Suter, L. J., and Langdon, A. B., *Laser–Plasma Interactions in High Temperature Hohlraums*, Lawrence Livermore National Laboratory, Livermore, CA, UCRL-JC-142589 ABS. Prepared for *Inertial Fusion Sciences and Applications 2001*, Kyoto, Japan, Sept 9–14, 2001.

Suter, L. J., *Progress Towards High Gain, High Yield NIF Targets*, Lawrence Livermore National Laboratory, Livermore, CA, UCRL-JC-142272 ABS. Prepared for *Presentation to General Atomics*, San Diego, CA, Feb 15, 2001.

Suter, L., Kruer, W., Miller, M., Kirkwood, R., Williams, E., Young, P., Stevenson, M., Oades, K., Slark, G., Foster, J., Grun, J., and Davis, J., *Green Light Laser–Plasma Interaction Experiments on Helen*, Lawrence Livermore National Laboratory, Livermore, CA, UCRL-PRES-143522. Prepared for *31st Anomalous Absorption Conf*, Sedona, AZ, Jun 3–8, 2001.

T

Takagi, M., Cook, R., McQuillan, B., Elsner, F., Stephens, R., Nikroo, A., Gibson, J., and Paguio, S., *The Use of PAA/PVA Processing of NIF Scale Microencapsulated PαMS Mandrels to Reduce High Frequency Roughness*, Lawrence Livermore National Laboratory, Livermore, CA, UCRL-JC-143359 ABS. Prepared for *14th Target Fabrication Mtg*, West Point, NY, Jul 15–19, 2001.

Takagi, M., Cook, R., McQuillan, B., Elsner, F., Stephens, R., Nikroo, A., Gibson, J., and Paguio, S., *Development of High Quality PαMS Mandrels for NIF*, Lawrence Livermore National Laboratory, Livermore, CA, UCRL-JC-143360 ABS. Prepared for *14th Target Fabrication Mtg*, West Point, NY, Jul 15–19, 2001.

Tikhonchuk, V. T., Fuchs, J., Labaune, C., Depierreux, S., Huller, S., Myatt, J., and Baldis, H. A., "Stimulated Brillouin and Raman Scattering from a Randomized Laser Beam in Large Inhomogeneous Collisional Plasmas. II. Model Description and Comparison with Experiments," *Phys. Plasmas* 8(5Pt1), 1636–1649 (2001).

Turner, R. E., Landen, O. L., Bradley, D. K., Alvarez, S. S., Bell, P. M., Costa, R., Moody, J. D., and Lee, D., "Comparison of Charge Coupled Device vs Film Readouts for Gated Micro-Channel Plate Cameras," *Rev. Sci. Inst*. 72(1PT2), 706–708 (2001).

U

Unanyan, R. G., Shore, B. W., and Bergmann, K., "Entangled-State Preparation Using Adiabatic Population Transfer-Art," *Phys. Rev. A* 6304(4), 3405, U536–U542 (2001).

Unanyan, R. G., Shore, B. W., and Bergmann, K., "Preparation of an N-Component Maximal Coherent Superposition State Using the Stimulated Raman Adiabatic Passage Method," *Phys. Rev. A* 6304(4), 3401, U517–U520 (2001).

V

VanZeeland, M. A., Gekelman, W., Dimonte, G., DiPeso, G., and Hewett, D., *Characterization of a Laser-Produced Plasma Expanding in an Ambient Background Plasma and the Possibility of Fast Wave Generation*, Lawrence Livermore National Laboratory, Livermore, CA, UCRL-JC-140953 ABS. Prepared for *42nd Annual Mtg of the Div of Plasma Physics*, Quebec City, Canada, Oct 23–27, 2000.

Vitanov, N. V., Halfmann, T., Shore, B. W., and Bergmann, K., "Laser-Induced Population Transfer by Adiabatic Passage Techniques," *Ann. Rev. Phys. Chem*. 52, 763–809 (2001).

W

Watt, R. G., Chrien, R. E., Klare, K. A., Murphy, T. J., Wilson, D. C., and Haan, S., "A Sensitive Neutron Spectrometer for the National Ignition Facility," *Rev. Sci. Inst*. 72(1Pt2), 846–849 (2001).

Wharton, K. B., Boley, C. D., Komashko, A. M., Rubenchik, A. M., Zweiback, J., Crane, J., Hays, G., Cowan, T. E., and Ditmire, T., "Effects of Nonionizing Prepulses in High-Intensity Laser-Solid Interactions," *Phys. Rev. E* 64(2Pt2), 15–17 (2001).

Widmann, K., Guethlein, G., Foord, M. E., Cauble, R. C., Patterson, F. G., Price, D. F., Rogers, F. J., Springer, P. T., Stewart, R. E., Ng, A., Ao, T., and Forsman, A., "Interferometric Investigation of Femtosecond Laser-Heated Expanded States," *Phys. Plasmas* 8(9), 3869–3872 (2001).

Willi, O., Campbell, D. H., Schiavi, A., Borghesi, M., Galimberti, M., Gizzi, L. A., Nazorov, W., MacKinnon, A. J., Pukhov, A. J., and Meyer-Ter-Vehn, J., "Relativistic Laser Propagation Through Underdense and Overdense Plasmas," *Laser and Part. Beams* 19(1), 5–13 (2001).

Williams, E. A., Cohen, B. I., Divol, L., and Langdon, A. B., *Saturation of Laser Beam Energy Transfer by Nonlinear Ion Wave Damping and Frequency Shifts*, Lawrence Livermore National Laboratory, Livermore, CA, UCRL-JC-144503 ABS. Prepared for *43rd Annual Mtg of the American Physical Society Div of Plasma Physics*, Long Beach, CA, Oct 29–Nov 2, 2001.

Williams, E. A., Moody, J. D., Young, P. E., Berger, R. L., Langdon, A. B., and Still, C. H., *Modeling the Vulcan Laser Propagation Experiments with pF3D*, Lawrence Livermore National Laboratory, Livermore, CA, UCRL-JC-142066 ABS. Prepared for *4th Intl Workshop on Laser–Plasma Interaction Physics*, Banff, Alberta, Canada, Feb 21–24, 200l.

Wolfrum, E., Allen, A. M., Al'Miev, I., Barbee, T. W., Burnett, P. D. S., Djaoui, A., Iglesias, C., Kalantar, D. H., Lee, R. W., Keenan, R., Key, M. H., Lewis, C. L. S., Machacek, A. M., Remington, B. A., Rose, S. J., O'Rourke, R., and Wark, J. S., "Measurement of the XUV Mass Absorption Coefficient of an Overdense Liquid Metal," *J. of Phys. B* 34(17), L565–L570 (2001).

Wu, Z. L., Stolz, C. J., Weakley, S. C., Hughes, J. D., and Zhao, Q., "Damage Threshold Prediction of Hafnia / Silica Multilayer Coatings by Nondestructive Evaluation of Fluence-Limiting Defects," *Appl. Opt*. 40(12), 1897–1906 (2001).

Y

Young, J. A., and Cook, R. C., "Helix Reversal Motion in Polyisocyanates," *Micromolecules* 34(11), 3646–3653 (2001).

Young, P., Baldis, H. A., Cheung, P., Rozmus, W., Kruer, W., and Wilks, S., *Critical Density Interaction Studies*, Lawrence Livermore National Laboratory, Livermore, CA, UCRL-ID-142776.

Z

Zweben, S. J., Caird, J., Davis, W., Johnson, D. W., and Le Blanc, B. P., "Plasma Turbulence Imaging Using High-Power Laser Thomson Scattering," *Rev. Sci. Inst*. 72(1), 1151–1154 (2001).

ICF/NIF and HEDES Program
Lawrence Livermore National Laboratory
P.O. Box 808, L-475
Livermore, California 94551

Address Correction Requested